Investigating Nutrient-Sensing Pathways in Ageing Human Neural Stem Cells and Age-Related Cognitive Decline

De Lucia, Chiara

Awarding institution:
King's College London

Investigating Nutrient-Sensing Pathways in Ageing Human Neural Stem Cells and Age-Related Cognitive Decline

Thesis submitted for the degree of Doctor of Philosophy in Neuroscience
at King's College London

De Lucia, Chiara

2018

Department of Basic and Clinical Neuroscience
Institute of Psychiatry, Psychology and Neuroscience
King's College London

Abstract

Ageing is associated with changes in cellular and molecular processes including the alteration of stem cell pools. In particular, biological and functional changes observed in ageing neural stem cells (NSCs), are linked to age-related cognitive decline. Recently, the systemic environment has been shown to alter both NSC regulation and age-related cognitive decline. Interestingly, a well-documented and naturally occurring way of altering the composition of the systemic environment is through diet and nutrition. Studies have found an overabundance of nutrients to be detrimental for human and animal health; the presence of specific nutrients as well as the overall increase in calorie or protein intake was shown to overstimulate conserved molecular pathways and to reduce lifespan. Conversely, dietary restriction was found to be the most efficient way of extending an organism's lifespan.

In this study, we examined nutrient sensing pathways in relation to their function in NSCs, ageing and cognition. We focus on the Sirtuin, mTOR and Insulin / Insulin like growth factor-1 pathways and employ both *in vitro* and epidemiological methods to assess their contribution to age-related phenotypes. Using a human hippocampal progenitor cell line (HPC) we modelled ageing through treatment with ageing human serum and via pharmacological interventions combined with increased passage number. A semi-automated imaging platform was used for the immunocytochemical quantification of NSC proliferation, differentiation, damage and apoptosis. Further to this, candidate gene selection was preformed through literature search and validated by qPCR to measure gene expression alterations within our ageing models. Results from the *in vitro* experiments, were used to inform the selection of 9 genes belonging to nutrient-sensing pathways as candidate genes for a role in NSC regulation. Next, we investigated the effects of lifestyle and candidate-gene genotype on cognition using 1633 participants from the adult longitudinal population-based TwinsUK cohort.

We report that treatment with human serum is able to induce changes in the HPC model that relate to both the serum-donor's hippocampal volumes and their cognitive performance. In addition, we report interesting associations between candidate-gene

expression and NSC regulation. Our data also revealed increasing passage number causes significant alterations in nutrient-sensing genes and emphasised FOXO3A, NAMPT, PTEN, GRB10 and mTOR as interesting candidates for further ageing research. Finally, epidemiological analysis showed a significant effect of lifestyle on cognition and highlighted associations between SNPs in SIRT1 and ABTB1 and cognitive performance.

The results outlined in this thesis support an important role for nutrient-sensing pathways in human NSCs ageing. In addition, we provide support for the use and further development of novel *in vitro* models to investigate NSCs ageing and to validate existing pathways, uncover new targets and test novel therapies.

Acknowledgements

I would like to begin by thanking all the incredible people who have supported me throughout my PhD. Firstly, I would like to express my gratitude to Sandrine Thuret for her unwavering support and guidance throughout this project, for encouraging me to pursue my own ideas and for being an excellent role model as a scientist, a supervisor and as a mentor. I am particularly grateful to Petroula Proitsi for guiding me through the previously unknown territory of epidemiological research. Her enthusiasm, availability and expertise were instrumental for the completion of this project. I also thank Richard Dobson for his expertise and help in designing the epidemiological study and Claire Steves and the entire TwinksUK team for providing the cohort data.

I would also like to offer a special thanks to Tytus Murphy and to Aleksandra Maruszak for their mentorship in all things cell culture and beyond. Their expertise and patience have been invaluable for my scientific development; I feel extremely lucky to have been taught by two scientists who emphasised technical precision and critical thinking so greatly.
I am grateful to everyone at the Wohl institute for their support and willingness to help and for making these years an enjoyable experience. In particular, I would like to thank Demelza Smeeth, Andrea du Preez, Curie Kim and Lucia Dutan Polit for their friendship, advice and assistance during all the ups and downs of a PhD. Edina Silajdzic and Ricky Patel also deserve special mentions for providing writing-up encouragement in the form of limitless snacks and perfectly-foamed lattes.

I am also extremely grateful to my parents for supporting through every academic decision and for always encouraging me to pursue my goals. Finally, I would like thank Daisy O'Loughlin for her help in overcoming every hurdle, for her understanding during the countless times plans had to be rearranged to accommodate cell culture and for her constant support and encouragement throughout this project.

Table of Contents

Table of Figures

4. Oxidative stress, DNA damage and passaging: An Alternative Multimodal Model to Induce Neural Stem Cell Ageing

5. Impact Of Lifestyle and Genetics on Cognition: An Epidemiological Study

8. Appendix

Table of Tables

1. General Introduction

2. Materials and Methods

3. The Systemic Milieu: A Putative Model to Induce Neural Stem Cell Ageing

5. Impact of Lifestyle and Genetics on Cognition: An Epidemiological Study

8. Appendix

List of Abbreviations

BRDU	Bromodeoxyuridine
CA	Cornu Ammonis
CC3	Cleaved Caspase 3
DAPI	4’,6-diamidino-2-phenylindole
DCX	Doublecortin
DG	Dentate Gyrus
DZ	Dizygotic
FFQ	Food Frequency Questionnaire
GxE	Gene Environment interaction
HEI	Healthy Eating Index
HPC	Hippocampal Progenitor Cell
ICC	Immunocytochemistry
iN	Induced Neuron
IPAQ	International Physical Activity Questionnaire
iPSC	Induced Pluripotent Stem Cells
LSD	Least Significant Difference
MAF	Major Allele Frequency
MAP2	Microtubule Associated Protein 2
MATOC	Middle Aged to Old Cohort
MRI	Magnetic resonance Imaging
mRNA	Messenger Ribonucleic Acid
MZ	Monozygotic
NAD	Nicotinamide adenine dinucleotide
NAM	Nicotinamide
NAMPT	Nicotinamide Phosphoribosyl Transferase
NRF2	Nuclear factor (erythroid-derived 2)-like 2
OS	Oxidative Stress
p17 /p26	passage 17 / passage 26
PAL	Paired Associates Learning
QC	Quality Control
REDOX	reduction–oxidation reaction
ROS	Reactive oxygen species
SA βgal	Senescence Associated β Galactosidase
SGL	Subgranular Layer
SNP	Single Nucleotide Polymorphism
SVZ	Subventricular Zone
YOC	Young Old Cohort

1 General Introduction

Large portions of this introduction have been published as a review entitled “Emerging Molecular Pathways Governing Dietary Regulation of Neural Stem Cells during Aging” of which I am first author (de Lucia et al., 2017).

1.1 Biogerontology

Socio-economic development and advances in medicine and healthcare over the past century have led to greatly increased life expectancies across the globe. As well as a decrease in infant mortality and developments in the treatment and prevention of midlife killers such as cancer, there has also been a decrease in the number of deaths in later life: with deaths between the age of 60 and 80 decreasing by 1.5% a year for the last 30 years (Banerjee, 2015; Mathers et al., 2015). An increase in longevity however, has resulted in an ageing population with the number of the people aged over 80 expected to triple by 2050 (United nations, 2017). This social transformation has a variety of social and economic implications, one of the most concerning being the relative shrinking of the workforce able to provide for a possible increase in healthcare costs. While deaths in later age are decreasing, ageing is still accompanied by frailty and susceptibility to disease which, if left unchanged will require adaptations to health infrastructure and will have deep economic repercussions (Maestas et al., 2016). Ageing is the number one risk factor for the majority of diseases currently affecting the developed and developing world and has therefore become one of the greatest challenges of modern medicine (Niccoli and Partridge, 2012).
The area of study addressing this issue, known as biogerontology, is committed to investigating the underlying mechanisms of ageing, to explore whether they can be intervened upon to delay or perhaps even halt the progression of age-related conditions such as cardiovascular disease, cancer and neurodegeneration (Verburgh, 2015). The field hypothesises that by delaying the biological aspects of ageing there will be a concomitant delay in age-associated chronic diseases due to the shared physiological risk factors (Schubert et al., 2018). An improved understanding of ageing mechanisms could therefore

lead to the development of strategies to increase “healthspan” - the period of time free from debilitating disease (Brandhorst et al., 2015; Franklin and Tate, 2008).

Ageing is defined as the time-dependent functional decline that affects most living organisms (López-Otín et al., 2013). It is characterised by a loss of fitness at both an organismal and cellular level and is usually attributed to a time-dependent accumulation of damage (Gems and Partridge, 2013; Kirkwood, 2005). The seminal review in the ageing field by López-Otín et al. identified and assigned the cellular and molecular hallmarks of ageing to 9 categories: genomic instability, telomere attrition, epigenetic alterations, loss of proteostasis, deregulated nutrient-sensing, mitochondrial dysfunction, cellular senescence, stem cell exhaustion and altered intercellular communication. For a hallmark to be included, it must manifest during ageing, its experimental aggravation should accelerate ageing and its experimental amelioration should delay the ageing process (López-Otín et al., 2013).

This categorisation has helped identify ageing as a biological process that, whilst dependent on the passing on time, is also greatly affected by other factors. Ageing in fact, is characterised by distinct inter-individual differences (Papenberg et al., 2015). This heterogeneity is a particularly challenging aspect of ageing research, but, at the same time, has highlighted an important role for both genetics and lifestyle in determining an individual’s ageing rate. Observations like these, have given rise to the concept of biological and chronological age: the former being the advancement of the strictly biological ageing process and the latter being the passing of time (Ries and Pöthig, 1984). A typical phenotype of ageing where the discrepancy between biological and chronological ageing is evident is cognitive decline. While some individuals retain intact cognitive performance, others of a similar age may already display drastic deterioration (Papenberg et al., 2015). Recent studies, aimed at identifying the driving mechanisms behind cognitive ageing and the phenotypic heterogeneity with which it presents have emphasised an important role for neural stem cells (NSCs) and nutrient-sensing pathways (Papenberg et al., 2015; Romine et al., 2015; Yang et al., 2015). In this literature review we outline the current knowledge on the role of the hippocampus, NSCs and nutrient-sensing pathways in age-related cognitive decline as well as the gaps in research in these areas.

1.2 The ageing brain: focus on the hippocampus

Increasing age is usually accompanied by a decline in fluid cognitive abilities but a preservation of crystallised intelligence. Fluid intelligence is the capacity to reason that is independent from past knowledge while crystallised intelligence is based on an individual's knowledge and past experiences. Accordingly, attention, executive control, reaction and processing speed all show considerable decline with age while long-term semantic memory remains intact (Ghisletta et al., 2012; Samanez-Larkin and Knutson, 2015). In addition, a decline in episodic memory, a function that requires hippocampus, is one of the most common age-related cognitive-deficits (Burgess et al., 2002). In line with this, a conserved feature of age-related cognitive decline across mammalian species is reduced spatial memory; a cognitive ability known to be highly-dependent on the hippocampus (Yankner et al., 2008). Besides these observations, other factors have highlighted the hippocampus as a structure greatly affected by ageing processes. Human fMRI studies for example, have shown altered functional activation of the hippocampus in aged adults (Logan et al., 2002; Malberg, 2004). In addition, rodent and primate studies assessing neuronal activity via fMRI and in situ hybridisation have also shown a specific susceptibility of hippocampal subregions to ageing in both species (Small, 2014). Furthermore, several imaging studies have reported that the hippocampus undergoes volumetric reductions with age (Daugherty et al., 2016; Peters, 2006; Shing et al., 2011). The hippocampus is therefore often the focus of cognitive-ageing research.

The hippocampal formation is a bilateral region found in the medial temporal lobes. As initially suggested by Ramón y Cajal in 1911, it is a circuit made up of several interconnected regions, each with distinct neuron types. It is formed of the subiculum, the dentate gyrus (DG) and the four cornu ammonis (CA) subfileds: CA1, CA2, CA3 and CA4 (See **Figure 1**).

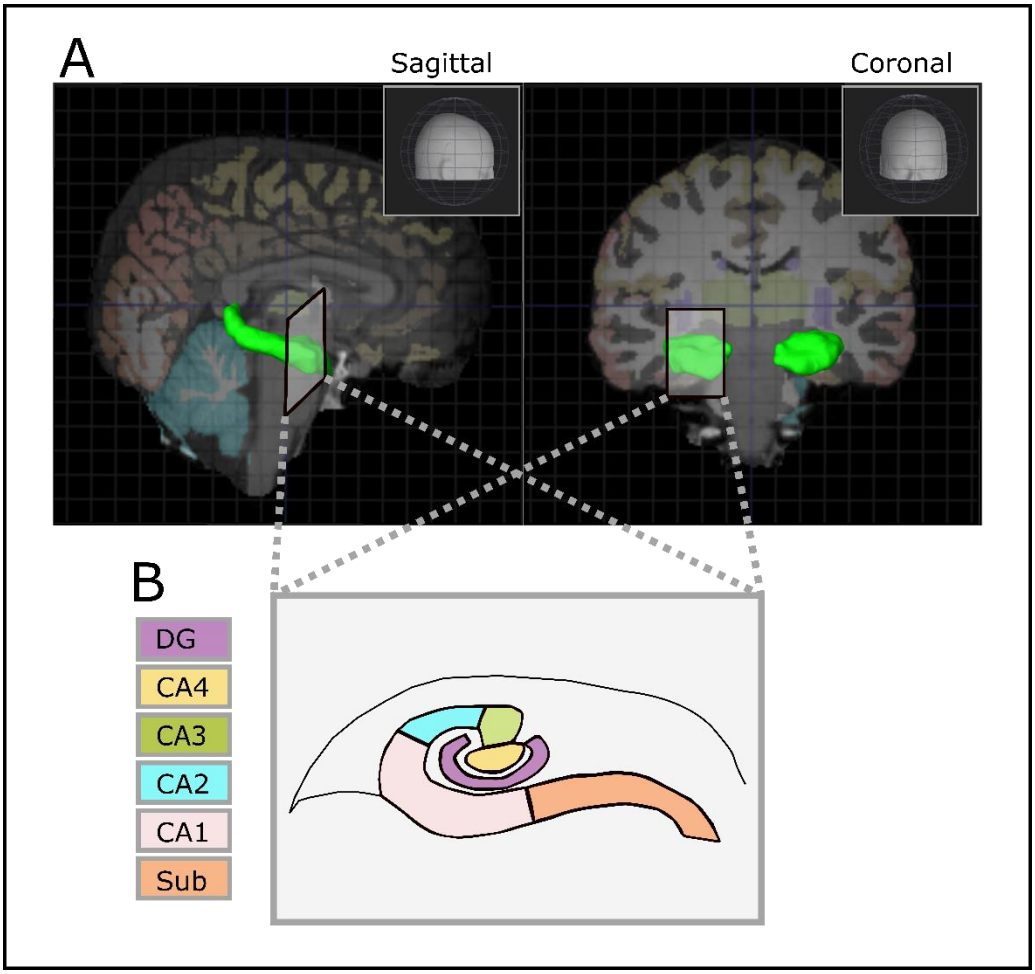

Figure 1 - The human hippocampus. Diagrams showing the location and structure of the hippocampal formation. **A**) Images created using the Allen Human Brain Atlas (2010), the hippocampus is shown in green. On the left is a sagittal section and on the right, is a coronal section. Boxes on the top right of each image show the facing direction. **B**) Shows the hippocampal subfields relative to the hippocampus orientation in A. The 6 substructures of the hippocampal formation are colour coded to the legend on the left. DG- Dentate Gyrus, CA - Cornu Ammonis, Sub – subiculum.

These subregions are connected via multi-synaptic circuits that signal to and from the entorhinal cortex; a circuitry that is thought to be responsible for the hippocampus' role in episodic memory. The entorhinal cortex also acts as an interface between the hippocampus and the neocortex. This hippocampal-neocortical network has been shown to be fundamental for the consolidation of long-term memories (Squire et al., 2004). Interestingly, the histological specialization of the hippocampal formation is indicative of highly functionally-specialised subregions. While this remains to be elucidated in humans, animal studies have demonstrated a first specialization across the anterior-posterior axis: the posterior (i.e. dorsal in rodents) hippocampus is mainly involved in memory and

cognitive processing while the anterior (i.e. ventral) hippocampus is involved in emotional processing. Further to this, subfield -specific specialisations have also been identified. Studies have suggested that the CA1 is responsible for late retrieval, recognition and consolidation while the CA3 and the DG are primarily responsible for early retrieval and encoding (Hasselmo, 2005; Hunsaker and Kesner, 2008; Mueller et al., 2011; Wan et al., 1999). Besides these functions the DG also enables pattern separation, which is the ability to differentiate between pre-existing information and similar but novel information. Interestingly, the DG is also one of the only two known regions of the adult mammalian brain capable of generating newborn neurons throughout adulthood.

1.2.1 Adult neurogenesis

Adult neurogenesis is the birth of new neurons from NSC during adulthood. Despite early neuroscientists claiming the adult brain was incapable of regeneration, this remarkable process has now been identified in several species and brain regions (Deng et al., 2010; Ramon y Cajal, 1928; Zupanc, 2001). Extensive rodent studies have demonstrated the presence of two neurogenic niches in the mammalian brain: the subventricular zone (SVZ) of the lateral ventricles and the subgranular layer (SGL) of the hippocampus (Altman and Das, 1965b; Doetsch and Hen, 2005).

In line with this, human studies in the late 90s demonstrated that new neurons are indeed born in the adult human hippocampus by using bromodeoxyuridine (BrdU) to track proliferative cells in cancer patients (Eriksson et al., 1998). More recently, elegant studies by the Frisen group provided further support for the presence of mammalian adult hippocampal neurogenesis (AHN). These studies made use of the varying levels of ^{14}C isotope in the atmosphere following above ground nuclear bomb testing to carry out carbon dating of neurons in post-mortem human tissues and demonstrated neurons in the same human brain were created at different points in time (Ernst et al., 2014; Spalding et al., 2013). Interestingly, results from this work suggested there is only a negligible level of neurogenesis in the human olfactory bulb, a surprising result given the extent of SVZ neurogenesis in rodents. This technique also provided an insight into the dynamics of adult neurogenesis allowing the authors to calculate the average total hippocampal neuron

turnover rate which was estimated at 35% and the average turnover of the DG neurons specifically, which was estimated to be close to 100%. These findings showed, for the first time, the considerable differences between human and mouse neurogenesis highlighting the need for human-based studies. Indeed, as well as the differences in olfactory bulb neurogenesis, the turnover rate of DG neurons was estimated at only 10% in rodents while the rate of AHN decline in response to age appeared far greater in mice than in humans (Bergmann et al., 2015; Imayoshi et al., 2008; Spalding et al., 2013).

In line with this, throughout the last decade, there has been an ever-growing body of evidence supporting the notion of human AHN (Boldrini et al., 2018; Galán et al., 2017; Kempermann et al., 2018; Knoth et al., 2010; Liu et al., 2008; Mathews et al., 2017). In this period, human AHN has only been contested by a limited number of publications claiming AHN falls to undetectable levels shortly after birth and the only remaining proliferating cells in the "neurogenic niches" are glial cells (Dennis et al., 2016a; Sorrells et al., 2018). Given that other studies adopting similar immunohistochemical techniques were able to show the presence of markers of adult neurogenesis in human post-mortem tissues, the most likely explanations for these discrepancies methodological differences. Recent papers have in fact suggested the lack of stereological methodology, large post-mortem delay and lenient participant inclusion criteria may explain these discrepancies (Boldrini et al., 2018; Lucassen et al., 2019). These findings however, have highlighted the need for the development of more robust techniques for assessing adult neurogenesis and for undoubtedly proving its existence throughout human lifespan (Kempermann et al., 2018; Lee and Thuret, 2018).

Such techniques would also allow the field to robustly replicate rodent studies assessing the functional relevance of AHN in humans. The animal literature in fact, has already highlighted important roles for AHN in learning and memory suggesting therapies targeting this process may prove beneficial for a number of diseases (Altman and Das, 1965a; Pencea et al., 2001; Spalding et al., 2013). The high excitability of the newborn neurons and their susceptibility to long-term potentiation (Schmidt-Hieber et al., 2004) make them perfect candidates as biological building blocks of learning and memory; the notion that the level

of AHN positively correlates with hippocampal-dependent learning tasks has been extensively proven. For example: experiments with methylazoxymethanol, a methylation agent capable of blocking neurogenesis showed rats with no neurogenesis had impaired trace-fear conditioning (Shors et al., 2002). In addition, experiments looking at co-localization of c-fos, a gene involved in memory formation, and BrdU incorporation in the hippocampus also supported this important function for newborn neurons (Tashiro et al., 2007). Furthermore, Clelland and colleagues showed newborn neurons are required for performance on pattern separation tasks showing AHN in particular is responsible for the DG's role in pattern separation (Clelland et al., 2009). Interestingly, an elaborate gene construct allowing for inducible ablation of newly generated neurons via the use of diphtheria toxin and the Cre-Lox system allowed Arruda-Carvalho and colleagues to show AHN may also be involved in destabilising existing memories (Arruda-Carvalho et al., 2011). As discussed above, the currently used techniques for detecting human AHN rely mostly on the expression of markers in post-mortem tissue thereby hindering intervention and longitudinal studies. Extensive data from animal models has identified the stages required for the maturation of NSCs to post-mitotic neuron and the pertinent markers associated to each stage. Briefly, the maturation process is believed to involve 6 stages. During the first stage, type-1 cells with unlimited regenerative capacities undergo division giving rise to transiently amplifying progenitor cells known as type-2a. These proliferate for the next 3 stages and gradually lose their proliferative capabilities while acquiring neuronal differentiation characteristics, giving rise to progenitor cell type-2b and type-3. During the 5^{th} stage, the progenitor cells differentiate into transient postmitotic cells and eventually mature into fully developed neurons during stage (Kempermann et al., 2004a). This process and the markers associated to each stage are reported in **Figure 2**.

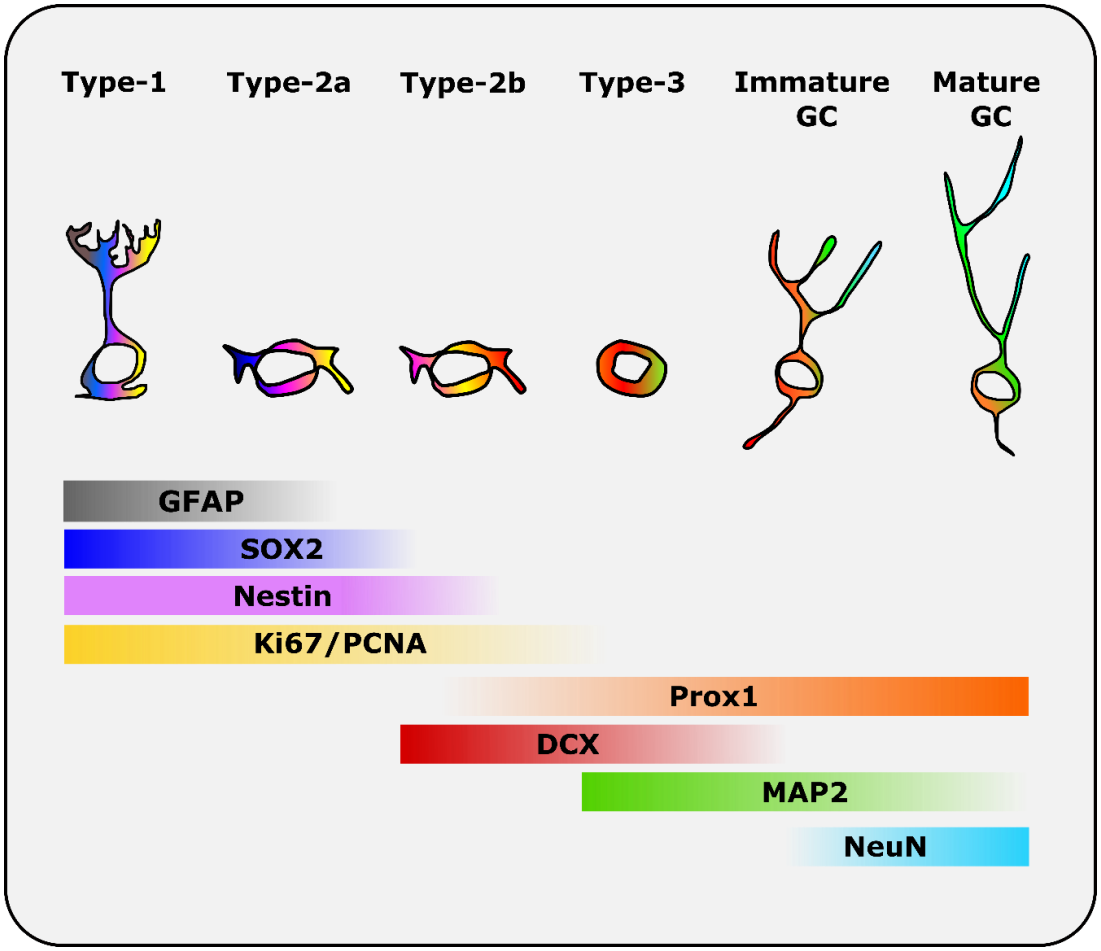

Figure 2 - Developmental stages of neural stem cell maturation The process of maturation from neural stem cell to mature granule cell (GC) can be subdivided in 6 stages each giving rise to a specific cell type (reported at the top of the image). The coloured blocks report the currently available markers to identify each cell type. Gradients represent the gradual decrease or increase in expression as the maturation process progresses. Glial Fibrillary Acidic Protein (GFAP), Proliferating Cell Nuclear Antigen (PCNA), Prospero Homeobox 1 (PROX1), Doublecortin (DCX), Microtubule Associated protein 2 (MAP2), Neuronal Nuclei (NeuN). Figure adapted from (Knoth et al., 2010).

Transplantation studies investigating AHN have shown that for NSCs to undergo the process outlined above, a uniquely permissive environment coined the 'neurogenic niche' is required (Seidenfaden et al., 2006; Shihabuddin et al., 2000). In both the human and rodent hippocampus, this is located between the granule cell layer of the DG and the CA3/CA4 region. It contains NSCs as well as their immediate progeny (type-2 and type-3 cells), immature neurons and several glial cell-types. The niche can promote neurogenesis by enabling cell to cell contact and by housing a number of astrocyte and microglia responsible for regulating the balance between gliogenesis and neurogenesis (Carpentier and Palmer, 2009). In addition, studies have shown the niche and the surrounding vasculature emanate signals able to determine the fate and differentiation rate of NSC

(Koutsakis and Kazanis, 2016). Neurogenesis is in fact considered a highly dynamic process able to respond to positive environmental stimuli such as physical exercise (Bolijn and Lucassen, 2015), enriched environments, learning (Monteiro et al., 2014) and certain dietary regimens like calorie restriction (Morgan et al., 2017) as well as to negative stimuli like sleep deprivation, social isolation and stress (Lucassen et al., 2015; Snyder et al., 2011).

The most dramatic and well-studied negative regulator of neurogenesis is ageing which has been linked to decreased proliferation, survival and differentiation of NSCs in both rodent (Ben Abdallah et al., 2010; Driscoll et al., 2006; Heine et al., 2004; Kuhn et al., 1996).and primate models (Gould et al., 1999; Ngwenya et al., 2006) In humans, the sharp age-related decline in performance in episodic memory and thereby on hippocampus-dependent tasks such as pattern separation, is highly suggestive of age-related neurogenic-impairments (Plancher et al., 2010). This has been supported by immunohistochemical studies showing a decline in the number of DCX-positive neurons and in that of proliferative markers such as Ki67 in older individuals when compared to younger individuals (Knoth et al., 2010). Though the presence of DCX positive cells is not irrefutable proof of fully integrated and functional neurons, the carbon dating experiments by Spalding and colleagues showed that the hippocampal neuron exchange rate does decline in a similar age-dependent manner to the DCX expression shown by Knoth et al. (Spalding et al., 2013).

1.2.2 Effects of ageing on neural stem cell function and neurogenesis

Stem cells in general have been closely linked to ageing owing to their reduced regenerative ability related to the decline of tissues that accompanies age (Behrens et al., 2014; Signer and Morrison, 2013). Impaired function of satellite stem cells in muscle and epidermal stem cells of the skin, for example, are key processes underlying reduced regeneration as a result of ageing in these tissues (Castilho et al., 2009; Day et al., 2010).

Similarly, NSC dysfunction is thought to be strongly associated to the cognitive impairments that accompany ageing. As introduced above, the marked decline in NSC activity in the ageing rodent DG manifests in reduced proliferation that eventually leads to the depletion of the progenitor pool (Romine et al., 2015; Yang et al., 2015). This decline partly

contributes to the age-linked decline in cognitive abilities, particularly those dependent on the hippocampus (Park et al., 2013; Romine et al., 2015; Yang et al., 2015). In the SVZ, there is a similar marked decline in NSC function which contributes to impoverished olfaction during rodent ageing (Enwere et al., 2004). Studies in model species have shown that deregulated hippocampal neurogenesis, is an important component of neurodegenerative conditions such as Alzheimer's (López-Toledano, Michael L et al., 2004; López-Toledano et al., 2007; Winner et al., 2011), further linking declines in NSC function to the deterioration of the ageing brain. Interestingly, a recent study suggested human neurogenesis remains unaffected by age in the absence of disease but that alterations in angiogenesis, quiescence and neuroplasticity may be responsible for the ageing phenotypes (Boldrini et al., 2018). Together, these studies suggest ageing exerts some of its detrimental effects in the CNS by directly interfering with multiple cellular and molecular processes that govern the regulation of the NSC population. This notion is summarized in **Figure 3**. As ageing has such severe effects on the decline of NSC and the development of neurodegenerative conditions, this prompts the field to consider whether we can target the maintenance of the NSC population to slow cognitive ageing and neurodegenerative disease progression. If so, what are the key mechanisms to target?

Interestingly, studies investigating the role of ageing on NSCs have also highlighted the possible role of the systemic milieu in regulating the neurogenic niches of the CNS; through the use of heterochronic parabiosis, Villeda and colleagues showed that the systemic environment of a young mouse was able to rescue the cognitive deficits of an aged mouse following the fusion of young-old circulatory systems (Villeda et al., 2011, 2014). This rejuvenating effect is also observed following intravenous infusion of young plasma into old mice, and was underpinned by a marked reversal of age-related decline in hippocampal neurogenesis (Villeda et al.2011) and upregulation of genes linked to synaptic plasticity (Villeda et al.2014).Villeda and colleagues however, only showed variation in proliferation and in neuroblast number using BrdU and doublecortin (DCX) respectively. Though this is strongly indicative of adult hippocampal neurogenesis, markers identifying more mature neurons as well as marker colocalization would have provided stronger evidence for the involvement of neurogenesis. For example, DCX and PSA-NCAM colocalization has been

suggested as a more reliable marker of neurogenesis (Boldrini et al., 2018; Sorrells et al., 2018). In addition, though the authors show a variation in performance in hippocampal dependent tasks such as fear conditioning and spatial awareness, the exact contribution of neurogenesis to these tasks remains to be elucidated (Merrill et al., 2003). Nevertheless, these studies were seminal in identifying the systemic environment as an important regulator of hippocampal and possibly neurogenic function.

In line with the above studies, enhanced neurogenesis in the SVZ was observed by Katsimpardi and colleagues following heterochronic parabiosis, resulting in improved odour discrimination, another task thought to rely on adult neurogenesis in rodents (Katsimpardi et al., 2014). Notably, these studies have demonstrated the role for candidate chemokines (e.g. CCL11,(Villeda et al., 2011)) and growth factors (e.g. GDF11 e.g. (Loffredo et al., 2013)) whose circulating levels fluctuate in ageing mice and appear to exert their effects, at least in part, by altering NSC function. Complementary to this, studies looking at other populations of stem cells have observed a similarly rejuvenating effect of the youthful milieu on the typical age-related declines in stem cell function throughout the body as well as vice-versa, whereby the old milieu inhibited stem cell function (Conboy and Rando, 2012). These data suggest that by altering the composition of the systemic environment, one could affect the regulation of the NSCs; a well-documented, naturally occurring way of achieving this is through diet and nutrition (Stangl and Thuret, 2009). Here, we define diet as encompassing dietary paradigms such as calorie restriction (CR), intermitted fasting (IF), dietary restriction (e.g. of specific components such as protein) (DR) and time restricted feeding (TRF) whereas nutrition involves the intake and/or supplementation of foods containing pro-neurogenic agents such as polyphenols (Valente et al., 2009), polyunsaturated fatty acids (PUFAs) (Kawakita et al., 2006; Valente et al., 2009) and vitamins/minerals (Bonnet et al., 2008; Corniola et al., 2008; Zhao et al., 2008).

As stem cells in general are designed to act in response to their environment and, and as reported above, are responsive to differing compositions of the systemic environment, it follows that diet can greatly influence their function (Murphy and Thuret, 2015). Several authors have reviewed the effect of diet on stem cells in general (Mihaylova et al., 2014;

Ochocki and Simon, 2013; Rafalski et al., 2012), for the purpose of this review we will focus on the relatively unexplored field of the effects of diet and ageing on NSCs. Nutritionists have found that an overabundance of nutrients is detrimental to several aspects of human and animal health (Keenan et al., 1994; Nagai et al., 2012). This results from an overstimulation of nutrient sensing molecular pathways, which eventually become insensitive to the stimuli (Blagosklonny, 2008; Gems and de la Guardia, 2013). CR, IF and DR have been reported to have opposite effects on these pathways and present a means to improved health and lifespan (Brandhorst et al., 2015; Fontana and Partridge, 2015; Solon-Biet et al., 2014, 2015). **Figure 3** is a schematic of how ageing, diet and the systemic environment interact to act upon these pathways. Notably, these effects are conserved across species as they have been observed in simple organisms such as yeast, C. elegans, and drosophila through to rodents and humans (Fontana et al., 2010). We will now review the impacts of dietary and nutritional regulation of NSC activity and function, with focus on the aforementioned nutrient sensing pathways and their effects on longevity.

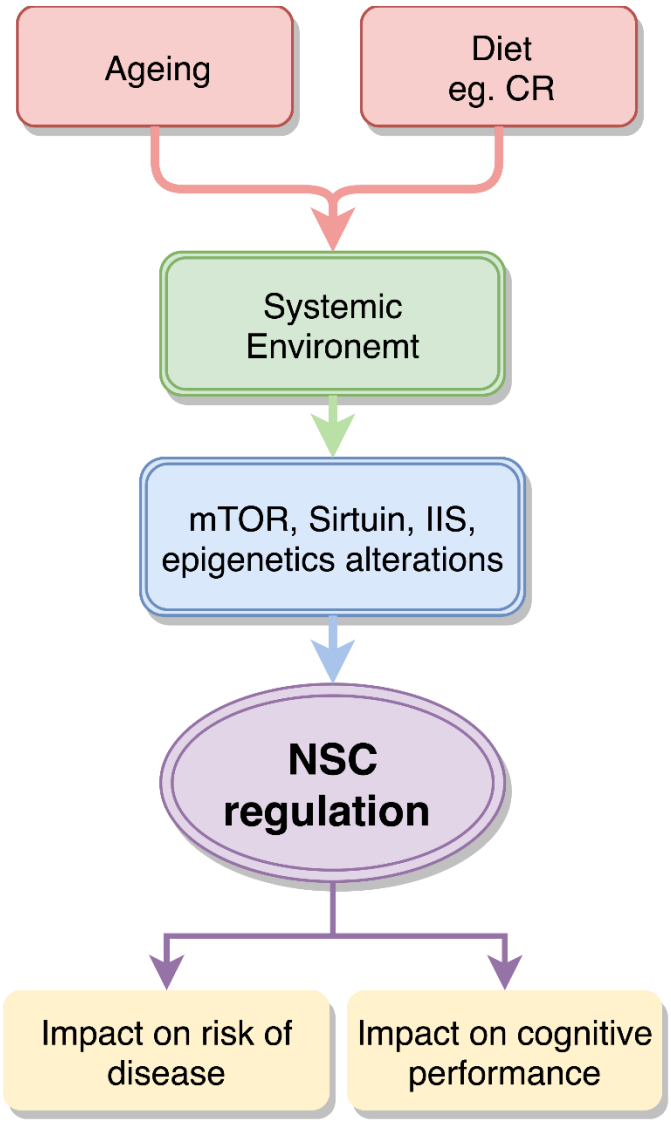

Figure 3 - Diagram summarizing the proposed relationship between ageing, nutrition and neural stem cells. Ageing and dietary modulation such as calorie restriction (CR) can alter the composition of the systemic environment, which affects epigenetic regulation and several nutrient-sensing pathways, including the mTOR, Sirtuin and Insulin and Insulin like signalling (IIS) pathways. These in turn alter neural stem cell (NSC) regulation and can predispose to disease and cognitive decline.

1.3 Impact of diet on neural stem cells

Dietary paradigms such as CR and IF are the most widely employed means of assessing the impacts of diet upon stem cell function and longevity. A 30-40% reduction in calorie intake, the typical regimen for CR, has often been brought about by alternate-day feeding – a form of IF. As such, the field must pay great attention as to whether they are assessing the impacts of DR or IF, unpublished work from our lab shows that the positive impacts of IF on hippocampal neurogenesis and cognitive performance can be derived independent of

calorie intake, suggesting that it is the period of fasting that that is acting on the NSC pool. Nutritional content, such as the amount of polyphenols and PUFAs, among other specific nutrients, has also been reported to impact on NSC function during ageing (Fernández-Fernández et al., 2012; Valente et al., 2009).

Reducing calorie intake in rodents was shown to counteract age-related cognitive decline as well as increase the number of newly generated neurons in the hippocampus (Ingram et al., 1987; Lee et al., 2000, 2002). In line with this, Hornsby et al showed that CR increased the number of mature newborn neurons in the rodent dentate gyrus and that these effects were mediated by the receptor for the orexigenic hormone, acyl-ghrelin (Hornsby et al., 2016). Furthermore, Kumar and colleagues suggest DR may aid in fighting excitotoxic injury as an increase in progenitors is seen in the SVZ, SGL, hypothalamus and cortex of adult rats (Kumar et al., 2009). In contrast, Bondolfi and colleagues found that CR did not affect the rate of proliferation but affected the survival of new–born glia in the mouse hippocampus (Bondolfi et al., 2004). Given that CR and IF (typically involving some degree of CR) have been shown to positively impact on NSC function, it follows that excessive calorie intake, as in the case of obesity and other models of metabolic disorders, will negatively affect NSC activity and may decrease adult hippocampal neurogenesis (Bondolfi et al., 2004; Kitamura et al., 2006). Furthermore, obesity was a detrimental factor in studies investigating post-stroke recovery in humans, showing that a history of increased calorie intake impairs brain repair (Kalichman et al., 2007). Interestingly, CR was also proven beneficial in elderly humans as shown by improved verbal memory scores (Witte et al., 2009). It must be considered however, that in elderly, sometimes frail individuals, restricting of calories may be too dangerous, older populations may therefore benefit from more targeted pharmacological interventions to modulate NSCs activity based on CR/IF and DR mimetics.

Though it may seem counter-intuitive that reducing calories may be beneficial to stem cells in particular, this can be explained by our historical food supply not being readily available and abundant at all times. Humans have evolved to cope with periods of reduced calorie intake, resembling the effect achieved by CR and IF experiments. A possible biological explanation for this relies on the benefits of refeeding after a fasting period, suggesting

that when an organism is “fasting” it can focus on preparing resources to act quickly and effectively when nutrients do become available (Reed et al., 1996). With respects to the NSCs of the DG in particular, their activity is possibly enhanced in the absence of nutrients owing to the necessity of “hunting behaviour” and the requirement for cognitive flexibility that must accompany it: improved cognition may be a means to ensure food is found (Mattson, 2012).

1.4 The role of nutrient-sensing pathways in neural stem cell regulation and ageing

Owing to the compelling research relating diet to longevity and to NSCs, the field is now trying to delineate the molecular pathways behind this relationship. Though many pathways are involved in NSC regulation and an equally vast amount is involved in nutrient-sensing and ageing, there is a relatively small proportion identified as relating the three. Thus far, the best characterized, and therefore most promising starting point for imminent studies, are the mTOR, Insulin and Insulin-like growth factor signalling (IIS) and Sirtuin pathways. In this section, we will focus on the available data supporting a role for these pathways in ageing, nutrient sensing and NSC regulation. See **Figure 4** for a summary of key NSC related functions affected by these pathways.

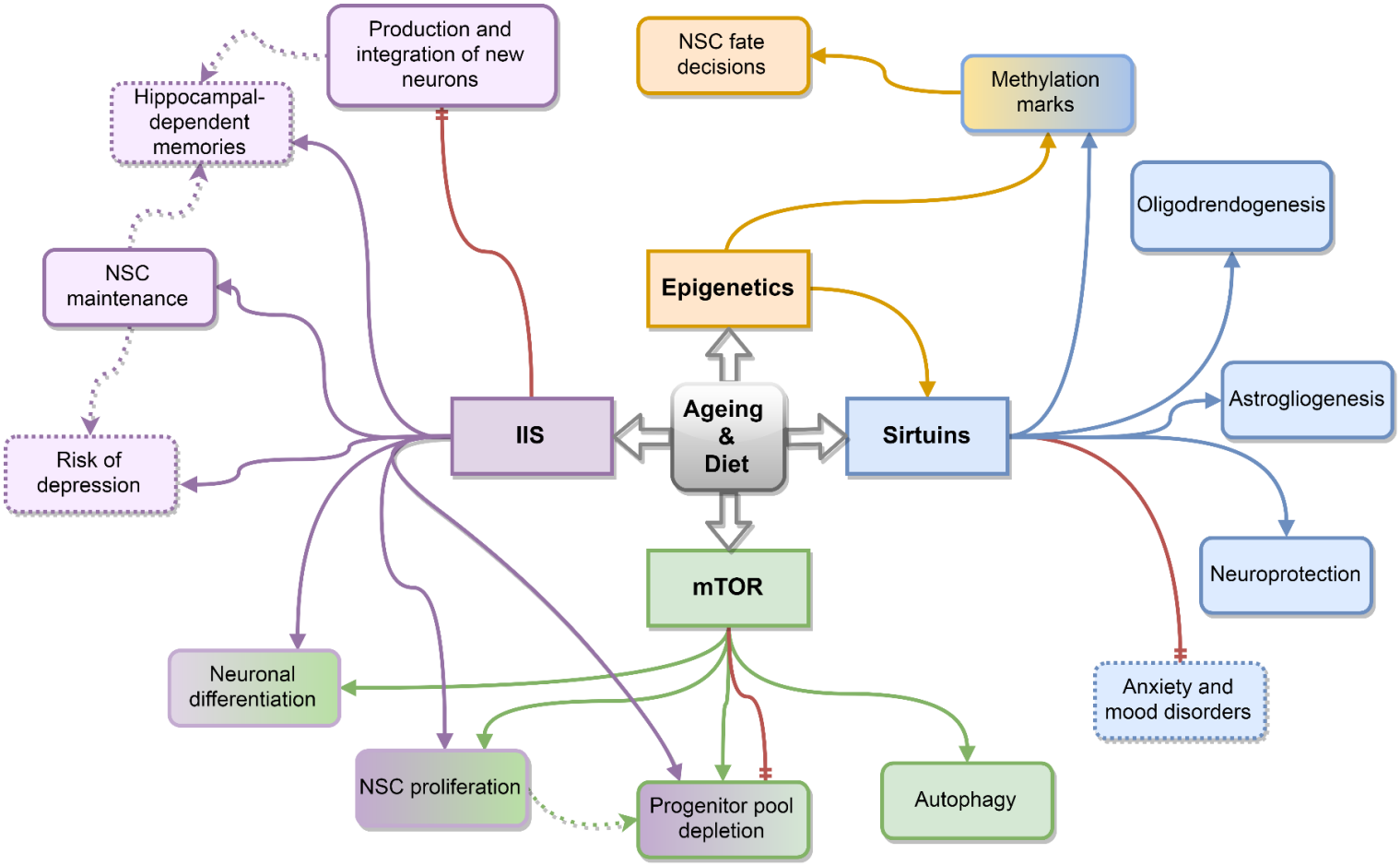

Figure 4 - Schematic summarizing the key effects of the Insulin/ Insulin-like Growth factor (IIS) (in purple), mTOR (in green), sirtuin (in blue) and epigenetic (in orange) pathways on neural stem cell (NSC) function as a result of diet and ageing. Solid arrows represent relationships between the molecular pathways (represented by the four rectangles in the center) and NSC function (represented by the outer, rounded rectangles) or related phenotypes (dotted rounded rectangles) discussed in this review. The dotted arrows connect possible molecular mechanisms behind the observed phenotypes reported in this review. Red arrows represent an effect caused by the inhibition of the pathway they stem from. Boxes with gradient colouring represent functions affected by multiple pathways

1.4.1 mTOR

The mammalian target of rapamycin (mTOR) is a classical dietary and nutrient sensing pathway. mTOR is a serine/threonine kinase. It combines with several accessory proteins including RAPTOR or RICTOR to form mTOR complex 1 (mTORC1) and mTOR complex 2 (mTORC2) respectively. The two complexes carry out different functions with mTORC1 being responsible for cell growth and metabolism while mTORC2 regulates cytoskeleton organization. Importantly, mTOR is the catalytic subunit of the complex and is inhibited by the presence of rapamycin, this inhibition however only occurs when mTOR is bound to the RAPTOR protein (Magri and Galli, 2013). mTOR activity is altered by energy and amino acid availability as well as growth factors, making it a key molecule within nutrition studies (Magri and Galli, 2013). mTOR is also involved in a feedback loop with insulin where insulin (discussed below) activates mTOR and mTOR phosphorylates the S6 kinase, which in turn inhibits insulin signalling (Blagosklonny, 2008). In the liver, branched chain amino acids (BCAA) in particular signal for mTOR activation, showing that protein intake and specific amino acids alter the total activation of mTOR (measured as phosphorylated mTOR / total mTOR) and ultimately longevity (Solon-Biet et al., 2014).

As well as functions in nutrient sensing, the mTOR pathway has also been linked to longevity (Blagosklonny, 2010). Its inhibition via ethylaxanthine and rapamycin was shown to improve longevity in yeast (Wanke et al., 2008) and mice (Fok et al., 2014; Harrison et al., 2009) respectively, leading to plans to test the compound in larger and longer-lived mammals such as companion dogs (Check Hayden, 2014). Recently, the mechanism of action behind rapamycin's role in longevity was suggested to involve a decrease in reactive oxygen species, as shown by experiments in the rodent liver (Martínez-Cisuelo et al., 2016). Notably, rapamycin treatment was shown to exert its beneficial effects even if started at advanced age, a factor, which usually greatly impairs the efficacy of life-extending interventions (Harrison et al., 2009). In addition, Tan and colleagues highlighted increased PI3K/Akt/mTOR pathway activation during ageing as the molecular mechanism responsible for replicative senescence in vascular smooth muscle cells (Tan et al., 2016). This pathway has been the focus of ageing research and is shared by both the mTOR and the insulin-like

growth factor signalling (IIS) pathways as explained in section 1.4.2. Several consequences of mTOR activation increase the risk of premature ageing and disease, these include decreased autophagy accompanied by an increase in protein production eventually causing an increase in protein agglomeration as well as an increase in inflammation(Verburgh, 2015). Furthermore, chronic mTOR activation causes increased proliferation of several types of stem cells eventually leading to progenitor pool depletion. Adequate mTOR regulation could thus be key in maintaining these populations throughout ageing (Paliouras et al., 2012; Sato et al., 2010) Though there is a limited number of studies investigating the role of mTOR within the NSC population, there have been several encouraging findings supporting key functions for this nutrient sensing pathway in NSC regulation and ageing.

Firstly, both protein deposition and inflammation are key hallmarks of neurodegenerative conditions suggesting that mTOR hyperactivity may contribute to disease progression within the CNS (O' Neill, 2013). These observations are consistent with the evidence supporting ageing as a consequence of overstimulation of signalling pathways, driven by the overabundance of nutrients. Furthermore, mTOR has also been shown to be key in dictating the proliferation rate of the adult SVZ NSC population; its inhibition in fact, caused progenitor pool depletion (Paliouras et al., 2012). In addition, Han and colleagues have also reported that, during embryonic development, mTOR carries an important role for neuronal differentiation: enhancing mTOR activity via insulin caused an increase in the number of neurons, which was counteracted by rapamycin. Intriguingly, in the presence of rapamycin the decrease in neuronal numbers was attributed to increased autophagy rather than apoptosis (Han et al., 2008). These findings also suggested the possibility of similar mechanisms taking place in adult NSCs. Indeed, Yu and colleagues showed that increased autophagic death also occurred in adult hippocampal NSC following insulin withdrawal and was accompanied by a decrease in cell density, these effects were also exacerbated by the presence of rapamycin, implicating mTOR activity (Yu et al., 2008). The authors state that in an aged environment there is decreased insulin signalling and thus increased autophagy, which may reduce the survival of stem cells. Contrary to this, the authors remark that autophagy can enhance cell survival, given its beneficial effect in clearing unwanted and malfunctioning cells, an essential mechanism in the context of ageing (Cuervo, 2008).

Elevated autophagy in response to reduced insulin signalling may thus not be a solely negative effect but further research is required to better delineate the modulatory role of mTOR activity in NSC during ageing (Gems and de la Guardia, 2013).
The limited number of studies (See **Table 1**) however, highlights the need for further investigations into the exact mechanisms of mTOR regulation in adult NSCs, with the ultimate aim of determining whether modulation of this pathway can bring preserve the NSC pool during ageing. The key effects of the mTOR pathway on NSCs elucidated this far are depicted in **Figure 4**.

1.4.2 Insulin

Insulin and Insulin-like growth factor (IGF) are two hormones closely linked to nutrition, as they respond to increased glucose. Insulin is released by the β cells of the pancreas and acts upon transmembrane tyrosine kinase receptor to activate downstream signalling pathways and cause glucose uptake by liver and muscle cells (van Heemst, 2010). Other members of the IGF family are under the control of growth hormone (GH) release by the pituitary gland. They also act upon tyrosine kinase receptors and activate downstream pathways that are often shared with insulin, coining the term insulin/ insulin-like growth factor signalling (IIS) pathway. Stimulation of the IIS pathway results in the activation of the PI3K/Akt pathway, a pathway shared with mTOR signalling, which ultimately leads to the inactivation of the FoxO transcription factors(van Heemst, 2010). While both insulin and IGF respond to carbohydrate presence, they usually carry out slightly different roles with insulin being primarily occupied with glucose metabolism and IGF with growth and survival (Rafalski and Brunet, 2011). Besides being activated by carbohydrates such as glucose, the IIS pathway is also stimulated by proteins and is involved in a feedback loop with mTOR as described in section 1.4.1 (Blagosklonny, 2008).

IIS is also extensively implicated in longevity (Bartke et al., 2013; Kimura et al., 1997); overactivation, like for mTOR, leads to decreases autophagy and ultimately to the shortening of lifespan (Verburgh, 2015). The decrease of the IIS pathway in C. elegans by Kimura and colleagues was one of the first experiments to show an increase in lifespan relating to diminished insulin signalling (Kimura et al., 1997). This was confirmed by several

other studies, with Blüher and colleagues showing that the knock-out of a fat specific insulin receptor resulted in an increase in lifespan of 18% (Blüher et al., 2003) and Taguchi et al finding that the knock-out of downstream substrates of the IIS pathway caused a 32% increase in female mice lifespan (Taguchi et al., 2007). Furthermore, serum IGF-1 levels in 31 different mouse strains negatively correlated to average lifespan (Yuan et al., 2009). Some encouraging evidence has also been found relating IIS to human longevity; IIS related polymorphisms correlate to lifespan (Bonafè et al., 2003; Kojima et al., 2004) and several centenarians were found to have loss of function mutations in the IGF-1 receptors (Suh et al., 2008). Conversely, people affected by acromegaly, characterized by increased GH release, experienced a 2-3 fold increase in death rate (Clayton, 2003; Suh et al., 2008; Verburgh, 2015). More recently, reduced growth hormone secretion, and thus indirectly IIS activity, was shown to correlate with human familial longevity (van der Spoel et al., 2016) and genome wide meta-analysis studies linked several gene loci to longevity and to levels of circulating IGF-related proteins (Teumer et al., 2016). These studies show that this pathway and its role in lifespan is conserved in more complex organisms. Several rodent studies have suggested insulin and IGF may link nutrition to organism longevity through key functions in tissue-specific stem cell maintenance. Mechanisms such as autophagy, compromised by IIS overstimulation, carry out key functions within the stem cell population. FoxO3A was proven essential for efficient clearing of age-related cellular debris which is known to prevent malfunctioning of stem cells and to lead to improved longevity (Cuervo, 2008; Warr et al., 2013). The IIS pathway also appears to have important functions on the regulation of NSCs specifically, with studies implicating it in both development and adulthood.

IGF-1 overexpression alone and IGF-1 and insulin overexpression on embryonic NSC for example, highlighted that insulin pushes towards increased differentiation while IGF-1 pushes towards a proliferative phenotype (Arsenijevic et al., 2001). Furthermore, studies have shown that overexpression of IGF-1 leads to increased brain size due to increased myelination (Carson et al., 1993). Finally, *Igf-1* null mice presented with decreased proliferation and differentiation of oligodendrocyte lineage (Ye et al., 2002).

Whether these effects persist into adulthood requires further investigation. Recently however, Chaker and colleagues showed that the inhibition of IGF-1 signalling in rodent adult olfactory bulb NSCs was able to hinder age-related stem cell decline and preserve the production and integration of new-born neurons (Chaker et al., 2015). IGF-1 was also shown to stimulate proliferation of adult hippocampal NSC both *in vivo* and *in vitro* while blocking the PI3K/Akt pathway stopped the proliferative effects of IGF-1 on NSCs (Åberg et al., 2000, 2003). This was later supported by Chigogora and colleagues finding a correlation between IGF-1 levels and an elevated risk of human depression (Chigogora et al., 2016), a disorder known to involve neurogenic and possible NSC deregulation (Hill et al., 2015). Furthermore, the deletion of the FoxO family members results in increased brain size and proliferation during development but also in a depletion of the progenitor pool and ultimately a decrease of SVZ adult neurogenesis (Paik et al., 2009; Renault et al., 2009). FoxO3 in particular seems to regulate quiescence of the adult SGL and SVZ NSC population and to have a role in oligodendrocyte regulation. FoxO transcription factors are also sensitive to oxygen changes making them ideal effectors between oxidative stress, a known aspect of ageing, and stem cell maintenance (Renault et al., 2009). Besides these studies, several others have reported pro-neurogenic effects of insulin when investigating the mTOR pathway as discussed in section 1.4.1.

Interestingly, IGF-II is produced by choroid plexus and released in the cerebrospinal fluid (CSF), allowing it to come in contact with the neurogenic niches. NSCs in the SVZ extend a process through the ventricular wall and come in contact with the CSF directly, thereby allowing its composition to directly alter their regulation. Increased presence of CSF IGF-II during development for example, promotes neurogenesis (Lehtinen et al., 2011; Ziegler et al., 2015). IGF-II is also involved in hippocampal neurogenesis in adulthood (Bracko et al., 2012). *In vitro* and vivo studies showed IGF-II involvement in promoting NSC maintenance (Ziegler et al., 2012). Studies have also linked IGF-II dependent mechanisms to hippocampal-dependent memory retention (Chen et al., 2011) and more specifically to age-related cognitive decline (Steinmetz et al., 2016) in rodents, further supporting a link between IGF-II and NSCs function and presenting a key target for further researching seeking to preserve AHN during ageing (See **Table 1**).

The overall effects of this pathway on NSC regulation however, remain inconclusive due to a limited number of concordant studies (Åberg et al., 2003; Itoh et al., 2012); some studies have reported increased IIS resulting in a beneficial increase in adult neurogenesis, for example during GH and IGF-1 mediated increases in neurogenesis as a result of exercise (Berg and Bang, 2004) or following a blueberry supplemented diet in rodents (Shukitt-Hale et al., 2015). In contrast, CR, which is known to directly target and diminish IIS, has also been proven beneficial for both cognition and longevity in rodent models of Alzheimer's disease (Parrella et al., 2013). **Figure 4** summarizes some of the NSC functions affected by the IIS pathway. As for mTOR, this highlights the need of a fine-tuned balance between IIS activation and inhibition throughout the lifespan. It is likely that several other factors such as oxidative state of the cell, biological age and brain region all play a role in this balance and can propel towards a positive or negative effect of the IIS pathway.

1.4.3 Sirtuins

Sirtuins are a group of deacetylases initially shown to extend lifespan in yeast by regulating mitochondrial function and cellular redox state (Aguilaniu et al., 2003). Deacetylases are key regulatory proteins as they can control the expression of several genes. Furthermore, sirtuin activity is NAD-dependent, making them likely candidates for the molecular link between metabolism and ageing owing to their ability to respond to the cell's energy status. Indeed, Sir2 activation in yeasts mimics CR-induced longevity, which in turn was shown to depend on the Sirtuin pathway (Lin et al., 2000). Increased lifespan as a result of sirtuin overexpression was also confirmed in other organisms such as *Drosophila* and *C. elegans* (Guarente, 2007). Similarly, the mammalian components of the sirtuin family, SIRT1 and SIRT4 have also been implicated in CR diet-regulated processes, showing that the link between metabolism and ageing could be conserved across species (Guarente, 2007). Research into Sirtuins also highlighted the importance of NAMPT, the rate limiting enzyme in mammalian NAD+ synthesis; ageing is accompanied by chronic DNA damage which leads to NAD+ depletion, Sirt1 inactivation and thus mitochondrial dysfunction (Guarente, 2014). Overexpression of NAMPT can rescue NAD+ levels and counteract these changes as shown by interesting studies investigating its effects on the accelerated ageing disorder, Cockanye

syndrome (Guarente, 2014; Scheibye-Knudsen et al., 2014; van der Veer et al., 2007). The importance of NAD+ and sirtuins in ageing was also supported by recent studies by Song and colleagues showing that NAMPT inhibition is sufficient to induce senescence in human fibroblasts(Song et al., 2015).

The above studies however did not focus on the effects of NAMPT on NSCs. Interestingly, a recent study showed that NAMPT ablation recapitulated aspects of NSC ageing such as decreased NSC proliferation in rodents (Stein and Imai, 2014), suggesting that NAMPT and the sirtuin pathway play key roles in NSC ageing as well. Studies are now beginning to integrate the role of sirtuins, ageing and diet or nutrition on the CNS specifically. For example, increased Sirt1 levels in murine brains due to CR were shown to increase anxiety and decrease exploratory drive (Libert et al., 2011). Whilst NSC function was not assessed in these studies, these conditions are known to involve deregulation of hippocampal neurogenesis (Hill et al., 2015; Libert et al., 2011) making it a plausible underlying mechanism. These studies also highlighted a possible disadvantage of increased Sirt1 activity and CR. In line with this, when the effect of SIRT1 deletion was investigated in prion disease, a condition in which neurogenic deregulation is also implicated (Gomez-Nicola et al., 2014), it was found to delay disease onset and to prolong the healthy portion of the affected animals. This was mimicked by CR (Chen et al., 2008). In contrast, others have shown that sirtuins can have neuroprotective functions in response to neuronal damage and neurodegenerative conditions; firstly, SIRT1 is upregulated in mouse models of Alzheimer's disease and amyotrophic lateral sclerosis and shown to enhance neuronal survival both *in vitro* and *in vivo* (Kim et al., 2007). Furthermore, SIRT1 was also found responsible for neuroprotective effects in murine models of axonal injury (Araki et al., 2004). SIRT1 overexpression was found to replicate the beneficial effects of CR in the context of several neurodegenerative conditions in various animal models (Gräff et al., 2013).

As many neurodegenerative conditions experience changes in neurogenesis, it is likely Sirt1 conveys some of its effects by influencing NSC function. SIRT1 activation in particular was linked to changes in neurogenesis in the perinatal SVZ; oxidizing conditions were found to

activate SIRT1 and push the progenitor pool towards astrocytic differentiation whereas a reducing environment would promote neuronal differentiation(Prozorovski et al., 2008). Similarly, blocking Sirt1 activity disengaged redox changes from SVZ NSC fate(Prozorovski et al., 2008). Rafalski et al. in contrast, showed that Sirt1 inactivation pushed NSCs towards an oligodendrocyte lineage. (Rafalski et al., 2013). Following Prozorovski's results, it is possible that the neuroprotective effect of SIRT1 activation, in part, is explained by improved CNS support from an increased number of astrocytes (See **Table 1**). An interesting avenue would be to investigate whether this finding is replicated in the DG and how this SIRT1-mediated modulation of the NSC pool changes with age.

Finally, these findings are now being investigated in human populations, Libert and colleagues for example showed that rare human SIRT1 variants are associated with anxiety and mood disorders (Libert et al., 2011). Interestingly, Sirt1 is also one of the two genes recently implicated in major depressive disorder by whole-genome sequencing findings (Cai et al., 2015). Though dietary interventions such as CR seem to be the most potent effectors of Sirtuin activation, some nutrients, like polyphenols have also been identified to directly activate components of this family (Howitz et al., 2003). Together the studies reported above, suggest the relationship between Sirt1, CR and ageing is regulated by intricate mechanisms, which become even more complex when acting upon different types of NSCs. The key NSC's functions acted upon by the sirtuin pathway are reported in **Figure 4**.

Pathway	Model	NSC	Intervention	Supporting Evidence	Study
mTOR / IIS	Rat *In Vitro*	Embryonic	Increased insulin levels	Increase in differentiated neurons, which was counteracted by rapamycin	(Han et al., 2008)
mTOR/ IIS	Rat *In Vitro*	DG	Insulin withdrawal	Increased neuronal death, exacerbated by rapamycin	(Yu et al., 2008)
IIS	Mouse *In Vitro*	SVZ and DG	*FoxO3* knockout	Decreased number of NSC and self-renewal ability	(Renault et al., 2009)
mTOR / IIS	Rat *In Vivo*	Cortex	Treated with EGCG + TBI	Reduced NSC cell death around damaged area	(Itoh et al., 2012)
IIS	Rat *In Vitro*	DG	Increased IGF-1	Decreased differentiation and increased proliferation of NSCs	(Åberg et al., 2003)
IIS	Mouse *In Vitro*	Striatal	Increased insulin	Increases NSCs differentiation	(Arsenijevic et al., 2001)
IIS	Mouse *In Vivo*	Perinatal	IGF-1 overexpression	Increase in number of neurons and of oligodendrocytes.	(Carson et al., 1993)
IIS	Mouse *In Vivo*	Perinatal	*IGF-1* KO	Decreased proliferation and differentiation of oligodendrocytes	(Ye et al., 2002)
IGF-1	Mouse *In vivo*	SVZ	IGF-1R KO	Reduced age related depletion of NSC	(Chaker et al., 2015)
IGF-II	Mouse *In Vitro*	Perinatal	IGF-II treatment	Increased NSC expansion and promoted self-renewal	(Ziegler et al., 2012)
IGF-II	Mouse *In Vitro*	DG	Sh-RNA knockdown of *IGF-II*	Impaired proliferation	(Bracko et al., 2012)
Sirtuins	Mouse *In Vitro*	Perinatal SVZ	Oxidation or Sirt1 activation	Enhanced astrocytic lineage	(Prozorovski et al., 2008)
Sirtuins	Mouse *In Vitro*	Perinatal SVZ	Reducing environment	Enhanced neuronal lineage	(Prozorovski et al., 2008)
Sirtuins	Mouse *In Vitro*	Perinatal SVZ	Sh-RNA knockdown of *Sirt1*	Disengaged neural fate from redox conditions	(Prozorovski et al., 2008)
Sirtuins	Mouse *In Vivo*	SVZ and DG	Inactivation of *Sirt1*	Increased oligodendrocyte differentiation and myelination	(Rafalski et al., 2013)
Sirtuins/ NAMPT	Mouse *In Vivo*	DG	Measuring /ablating NAMPT	NAMPT levels decrease with age, its ablation reduces NSC proliferation and oligodendrogenesis	(Stein and Imai, 2014)
Epigenetics	Mouse *In Vitro*	Embryonic	*Dnmt1* knockout	Increased astrocytic differentiation	(Fan et al., 2005)
Epigenetics	Mouse *In Vitro*	Perinatal SVZ	*Dnmt3* knockout	Impaired neuronal differentiation	(Wu et al., 2010)

Table 1 - Table summarizing studies showing supporting evidence for the role of mTOR, IIS and Sirtuin pathways in NSCs function. NSC- Neural Stem Cells, IIS -Insulin and Insulin-like Signalling, DG- Dentate Gyrus, SVZ- Sub Ventricular Zone, KO- Knockout.

1.5 Epigenetics

Epigenetics is at the forefront of ageing research, a position supported by the recent establishment of an 'epigenetic clock' by Steve Horvath, and has clear functions in adapting the organism's responses to its environment. These attributes make it a key mechanism mediating cellular and molecular responses to diet and ageing processes (Rea et al., 2015). Epigenetic modulation comprises many mechanisms and is usually identified as the driving force behind changes in gene expression, which are not due to DNA sequence mutations. Such a process clearly has very important functions in stem cell regulation of different tissues as it can confer lineage-determining decisions as well as maintain quiescence. Epigenetics also plays an important role in ageing; twin studies showed that genetic background only has a 25% influence on longevity (Herskind et al., 1996) suggesting that the remaining effects would be dictated by the environment, which usually ensues its effects through epigenetics. A role for epigenetics is also supported by the notion that the effect of genetic variations on cognition and brain structure increases with age, recently reviewed by (Papenberg et al., 2015). One of such environmental factors able to cause epigenetic changes is likely to be diet. A line of thought believes that as epigenetic changes are less permanent, it would be more efficient to target and reverse them rather than targeting any genetic mutations which may arise as a result of ageing (Beerman and Rossi, 2015; Rando and Chang, 2012). By restoring a "young" epigenetic environment one may be able to reverse age-related deficit; in a similar manner to the aforementioned heterochronic parabiosis studies (Villeda et al., 2014). Another factor supporting the notion that targeting epigenetics may be an efficient way to reverse ageing comes from studies showing that only a small number of loci are altered consistently throughout ageing, allowing for targeted interventions rather than global ones (Beerman and Rossi, 2015). Furthermore, epigenetic changes could be used as ageing biomarkers, providing important information on the ageing rate of an organism, with the potential to enable more precise preventive strategies. It is therefore important for us to understand how age and nutrition affect epigenetics and how this causes alterations in NSC regulation, disease progression and longevity. For the remainder of this section we will evaluate the evidence for such a relationship.

1.5.1 Epigenetics and nutrition

There are several studies showing perinatal or in utero nutrition can have vast effect on health later in life, mainly related to cardiovascular disease, diabetes and obesity (Choi and Friso, 2010). Interestingly, these effects were also witnessed in the offspring of the affected animals suggesting that epigenetic changes could be passed through generations. The involvement of epigenetics was also confirmed via methylome analysis, though a causal link is yet to be shown (Fontana and Partridge, 2015; Radford et al., 2014). Such mechanisms are set in place to ensure adaptation for the foetus to its environment – CR and DR prepares a foetus to food scarcity whilst over nutrition primes for a nutrient abundant environment. Studies have suggested it may be the mismatching of predicted and actual nutrient availability to cause some of the detrimental health effects later in life (Perera and Herbstman, 2011).

While epigenetic changes occurring during the malleable stages development in response to nutrition have been extensively studied, those happening during adulthood are less known. The evidence from developmental studies reported above, however shows that mechanisms are set in place for epigenetics to respond to dietary and nutritional cues through the lifespan. Indeed, diet can alter epigenetics in several ways, these include the donation of methyl groups and the regulation of several enzymes (Mathers and Ford, 2009). As well as the alterations in response to CR and DR, other dietary alterations can have effects on epigenetics, such as the intake of specific nutrients. Studies on agouti mice showed a methyl-supplemented diet was able to cause DNA hypermethylation, making it likely for diet-acquired methyl donors like choline and methionine (an essential amino acid) to have similar effects (Niculescu et al., 2006; Waterland et al., 2007; Waterland and Jirtle, 2003). Furthermore, the trace mineral zinc interacts with histone deacetylase regulation (HDAC) and causes their inhibition (Myzak et al., 2006) whilst resveratrol, a dietary phenol, activates the HDAC SIRT1 (Rafalski and Brunet, 2011). Vitamin D also appears to form an important link between nutrition, ageing and epigenetics as its varying concentrations can delay the ageing phenotype in mice and its mechanism of action is known to involve histone acetylases (HATs) and HDACs (Tuohimaa, 2009).

1.5.2 Epigenetics, ageing and neural stem cells

Several years ago it was found that cellular methyl content declines with increasing age in mammals (Wilson and Jones, 1983). This loss is likely to contribute to genomic instability, which is a hallmark of ageing cells. Recently, Horvath and colleagues showed the existence of an epigenetic clock and developed a predictor able to estimate the methylation age of most tissues or cell types, suggesting that specific epigenetic changes occur as a result of age (Horvath, 2013).

Though there are a number of possible epigenetic marks, methylation is the mark considered to be the most stable one and thus the most likely candidate for encoding ageing and nutritional changes. Methylation changes as a result of age can be divided into two main categories: those resulting from loss of fidelity when copying methylation marks and those arising from abnormal addition or removal of methylation marks. Further to this, a decrease in the activity and expression of the DNA methyltransferase DNMT1 was found with increasing age (Cooney, 1993). Interestingly, DNMT1 controls stem cell balance and lineage decisions in several tissues; its knock out in embryonic NSCs, for example, causes a preferential push towards astroglial differentiation(Fan et al., 2005). DNMT1 loss in general causes an ageing phenotype highlighting it as a key molecule governing ageing processes (Beerman and Rossi, 2015). In contrast, some housekeeping genes that are usually unmethylated seem to become methylated with age. This may be due to an increase in DNMT3 activity; DNMT3 is a methyltransferase responsible for de novo methylation, a process shown to be key in regulating stem cells as it halts self-renewal to allow differentiation. A DNMT3 knock out in mouse in fact showed impaired post-natal SVZ and SGL NSC differentiation (Wu et al., 2010) (See **Table 1**).

An important methylation mark, studied in the field of ageing and NSCs, is the methylation of lysine 27 on histone 3 (H3K27). The differing methylation of this mark in fact can regulate adult NSC differentiation; when this mark has a single methylation, transcription is enabled, when the mark has 2 or 3 methyl groups gene transcription is repressed (Zhang et al., 2014). Another epigenetic mark often involved in ageing is histone acetylation; several histone acetylases (HATs) are key in regulating the NSC pool by affecting both proliferation and

differentiation of the neural progenitors. Sirtuins as detailed above are part of this family. There is also evidence of different epigenetic marks influencing one another – i.e. DNA methylation being restricted by acetylation marks (Beerman and Rossi, 2015). See **Figure 4** for a representation of this interconnection. Mathers and Ford suggest that changes in methylation do not occur in every cell in a tissue. They explain how this leads to promoter methylation heterogeneity and thus to divergent gene expression and cellular response across different tissues with increasing age (Mathers and Ford, 2009). Together these studies show that epigenetic mechanisms are pivotal to a permissive or restricting environment for gene transcription in response to environmental cues and are therefore likely molecular effectors of nutrient intake and its ensuing effect on NSC regulation.

Finally, as well as sharing common downstream mechanisms, ageing and nutrition can also affect one another; for example, nutrient intake may change as a result of age which could then cause the age-related epigenetic changes. A reduction of fruit and vegetable intake for instance, would reduce the intake of zinc and thus affect HDAC function (Mathers and Ford, 2009). Given the prominent role played by NSCs during ageing, an exciting avenue would be to explore epigenetic changes in these cells in response to diet.

1.6 Conclusions

In conclusion, though much progress has been made in establishing the role played by nutrition in longevity, and on stem cells more broadly, its role in NSCs regulation is still to be elucidated. Whilst the positive impacts of CR and IF continue to be detailed in model systems, more targeted pharmacological approaches may be beneficial for use in frail and elderly populations. This highlights the need for a more thorough understanding of the molecular pathways involved in these dietary paradigms. Further to this, much more research into the genetic - and epigenetic - influences of diet and nutrition is required, to refine populations that potentially stand to gain the most from such interventions.

1.7 Summary of introduction

In the above review, we discussed the importance of ageing research given the changing population structure. We focussed on the impact of the hippocampus and of neurogenesis on cognitive ageing and emphasised the role played by lifestyle and genetics on the rate of cognitive decline. We outlined the current knowledge on how mTOR / IIS pathway inhibition and sirtuin activation may enhance longevity and CNS function, an effect achieved at least in part, through their impact on NSC function. We also highlight epigenetic modification as important contributors to the ageing process and as mediators for the effect of diet on longevity and NSCs.

Importantly, we emphasise the need for more human-based studies to assess whether similar mechanisms occur in both animal and human NSC regulation and suggest that a combination of diet and genetics may contribute to the surprising heterogeneity of the ageing process in humans and thereby to the discrepancies between chronological and biological age.

1.8 Thesis aims and hypotheses

We hypothesise that biological ageing is a malleable process which can be accelerated and delayed. We also hypothesise that nutrient-sensing pathway alterations are key mediators of this process and that they are especially important in the regulation on NSCs in response to ageing. Finally, we hypothesise that genetic polymorphisms in genes within these pathways, together with environmental factors such as lifestyle impact human cognition.

This thesis aims to evaluate the modulation of nutrient-sensing genes in human NSC regulation and cognition.

In particular, this thesis will address the following:

1) Test whether an aged systemic environment can alter the gene expression of candidate nutrient-sensing genes or affect the proliferation and differentiation rates of an *in vitro* model of hippocampal neurogenesis.

2) Establish a controlled cellular model of hippocampal progenitor cell ageing to assess whether it induces alterations in the proliferation and differentiation rates of human progenitor cells and whether it leads to alterations in the expression level of candidate nutrient-sensing genes.

3) Assess the role of diet, exercise and genetic polymorphisms of candidate nutrient-sensing genes on cognitive performance in an ageing human cohort.

2 Materials and Methods

This chapter reports the common materials and methods used throughout this thesis. We introduce the cell line used for all *in vitro* experiments and detail cellular and molecular analysis techniques employed throughout this thesis. The specific methods used within each chapter are outlined in chapter-specific materials and methods sections.

2.1 Human hippocampal progenitors culture - *In Vitro* model of hippocampal neurogenesis

2.1.1 Immortalisation

The human hippocampal progenitor cells (HPC) cell line HPC0A07/03A (ReNeuron Ltd., Surrey, U.K., hhtp://reneuron.com) was used for all cellular experiments in this project and was previously described in (Anacker et al., 2011) and (Johansson et al., 2008). Briefly, 12-week-old foetal female tissue was obtained in accordance with UK and USA ethical and legal guidelines following normal terminations. A small population of neural stem cells from the hippocampal region was dissected under microscopic control and grown to 50-60% passage (P) 0 confluency as a primary culture. The cells were then infected with the retroviral vector pLNCX-2 encoding the *c*-mycER^{TAM} gene construct and neomycin selection was employed to generate a conditionally immortalised cell line. This construct produces a version of the oncogene *c*-myc, which is responsible for growth, where its c-terminus is fused to a modified oestrogen receptor and its activity is therefore determined by receptor activation(Pollock et al., 2006). As this receptor is selectively activated by the synthetic drug 4-hydroxy-tamoxifen (4-OHT) at 100nM, c-Myc activity and consequently cell proliferation is dependent on the presence of 4-OHT. This attribute can be used to control proliferation and differentiation of the progenitors in an *in vitro* system by the addition and removal of 4-OHT and growth factors as illustrated in **Figure 5**. In the absence of growth factors and 4-OHT the progenitors differentiate into neurons, astrocytes and oligodendrocytes (Johansson et al., 2008).

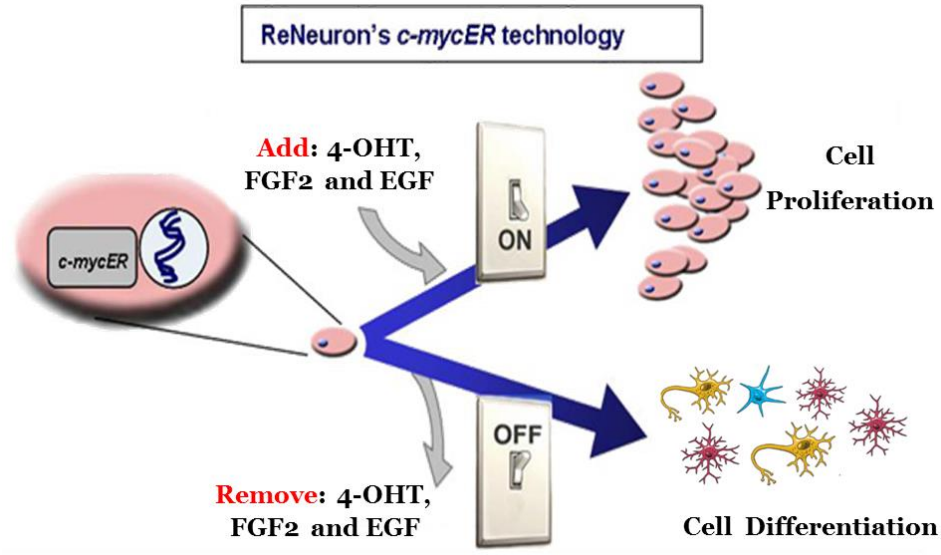

Figure 5 - Schematic of transgene function in the HPCOA07/03A cell line by ReNeuron. The cell line contains the c-Myc oncogene under the control of the estrogen receptor (ER); c-MycER. In the presence of 4-OHT (synthetic version of estrogen), c-MycER dimerizes and translocates to the nucleus, this allows promoter binding which leads to the activation of downstream pathways leading to cell proliferation, provided FGF2 and EGF are also present. In the absence of 4-OHT, the cells are unable to proliferate and begin differentiating (Pollock et al., 2006).

2.1.2 Cell bank

For most experiments, cells used in this project originated from common Thuret lab cell bank created from a passage 8 vial obtained from ReNeuron. Briefly, the passage 8 vial was thawed and passaged exponentially until passage 13. Approximately 100 passage-13 vials containing 2 million cells each were frozen in Mr Frosty™ (Thermo Fisher) and stored in liquid nitrogen. Several intermediate passages were also frozen and stored as safety measures.

2.1.3 Cell culture conditions

HPC0A07/03A cells were grown in reduced modified media (RMM) supplemented with factors outlined in **Table 2** and in the absence of any serum besides when specifically stated as part of treatments. Cells were passaged using Accutase (A1110501, Sigma) and cultured on tissue culture flasks (Nunclon, Denmark) coated with 20ug/ml mouse laminin (L2020 Sigma) at 37 ˚C, 5% CO_2 and saturated humidity. HPC03A/07 cells normally proliferate with a doubling time of 48-72 hours (Johansson et al., 2008), medium was changed fully 24 hours after passaging.

Material Names	Final Concentration	Catalogue Number / Supplier
Dulbecco's modified eagle's medium nutrient mixture f-12 ham	N/a	D6421 500ml, Sigma
Human albumin solution	0.03 %	20, Zenalb
Apo-transferrin	100 µg/ml	T1147, Sigma
Putrescine DIHCL	16.2 µg/ml	P5780, Sigma
Human recombinant insulin	5 µg/ml	I9278-5ml, Sigma
Progesterone	60 ng/ml	P8783, 1 mg Sigma
L-glutamine	2 mM	G7513, 100ml Sigma
Sodium selenite	40 ng/ml	S9133-1MG, Sigma
Additional factors for growth and proliferation media		
Epidermal growth factor (EGF)	10 ng/ml	AF 100-15-500, Peprotech
Basic fibroblast growth factor (bFGF)	20 ng/ml	EC 100-18B, 50ug Peprotech
4-hydroxytamoxifen (4OHT)	1:10 000	H7904, 5mg Sigma

Table 2 - Components of reduced modified cell culture medium (RMM) used for all cultures

2.1.4 Proliferation assay

Progenitor cells were seeded on 96-well plates (Nunclon, Denmark) at a density of $1.2x10^4$ cells per well in 3 technical replicates for cellular work or in 6-well plates (Nunclon, Denmark) at a density of $3x10^5$ for molecular work. Cells were cultured in proliferation media (RMM including EGF, bFGF and 4-OHT (See **Table 2**) for 24 hours, at which point the media was replaced by proliferation media containing the appropriate treatment for the experimental condition (See **Figure 5**) for a duration of 48 hours. In conditions where treatment consisted in the addition of human serum from young or old persons this was delivered at a concentration of 1% in proliferation media and supplemented with 1% Penicillin-Streptomycin (P/S, Life Technologies).

72 hours after seeding cells in 96-well plates were washed in Phosphate Buffered Saline (PBS), fixed with 4% paraformaldehyde (PFA) for 20 minutes at room temperature and stored at 4˚C in preparation for immunohistochemistry. Cells in 6-well plates were either harvested for RNA work by adding 1ml of TRIzol (12044977, Ambion) per well and scraping.

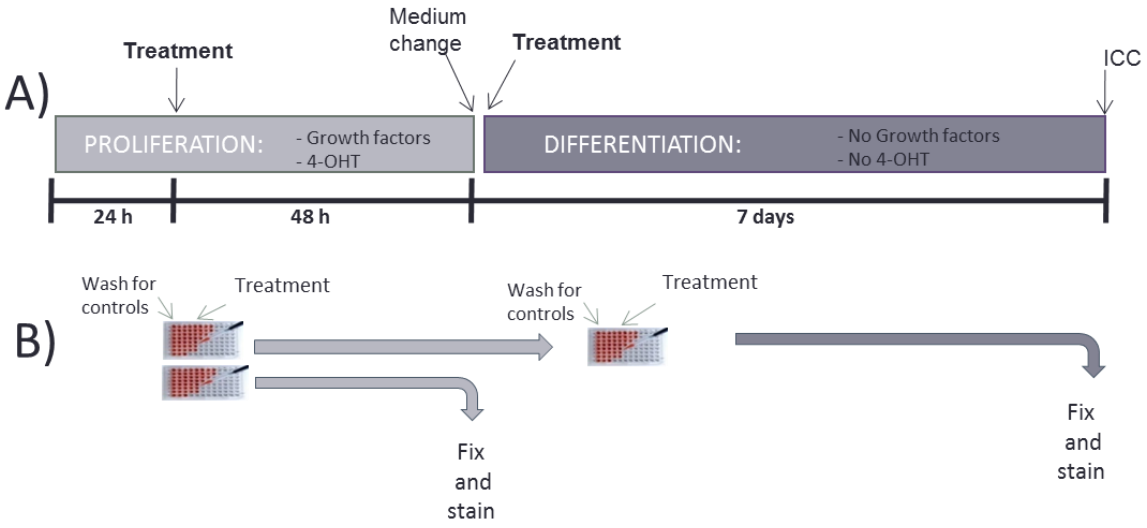

Figure 6 - Schematic of proliferation and differentiation assays. A shows the timescale of the experiments, the treatment timepoints and growth factors used. **B** displays how the above timeline can be divided to yield proliferation or differentiation assays. Cells are cultured in media containing growth factors (EGF, bFGF and 4-OHT) for the duration of the proliferation assay (first 72 hours) at which point the plates can be fixed / harvested to complete the proliferation assay. Alternatively, to begin the differentiation assay, plates undergo 2 full media changes with differentiation media (lacking EGF, bFGF and 4-OHT) and are cultured for a further 7 days in differentiation media containing treatment.

2.1.5 Differentiation assay

Progenitor cells were seeded, cultured and treated as for the proliferation assay for the first 72 hours. After the proliferation assay, instead of harvesting or fixing, cells were washed in differentiation media (RMM lacking EGF, bFGF and 4-OHT) 2 times at 30-minute intervals and finally treated with the appropriate treatment in differentiation media after a subsequent 30 minutes. Cells were then cultured for a further 7 days and harvested for RNA and DNA or fixed as described for the proliferation assay see **Figure 6** for experimental schematic.

2.1.6 Treatments

Unless specified, treatments were carried out at the 24-hour time point in proliferation and at the 72-hour timepoint at the start of differentiation at the concentrations outlined in **Table 3.** Serum treatment concentration was selected Dr. Tytus Murphy who carried out a dose-response curve testing concentrations between 0.1% and 10%. 1% serum was selected as the most efficient concentration that did not cause overconfluence, had a significant proliferative effect compared to media-only controls and made the most efficient use of a limited resource (serum from cognitively healthy older participants).

Treatment	Concentration
Serum	1%
Tert-Butyl Hydroperoxide (tBHP)	0.01µM
Hydroxyurea (HU)	1mM
Combination: tBHP And HU	0.01 µM and 1mM

Table 3 - Standard treatment concentrations

2.2 Cellular analysis

2.2.1 Immunostaining

PFA-fixed cells were blocked for 60 minutes at room temperature in blocking solution consisting of phosphate buffered saline (PBS) containing 5% normal donkey serum (D9663, Sigma), 0.3% Triton-X (93443, Sigma). Primary antibodies were diluted appropriately (**Table 4**) in blocking solution, 30µl of antibody in blocking solution was added to each well and left at 4 ˚C overnight.

Primary antibody	Dilution	Catalog # / Supplier	Usage
Rabbit anti-Ki67	1:500	Ab15580, abcam	Marker of proliferation: labels cells in G1, S, G2 and mitotic phases of cell cycle
Mouse anti-ki67	1:800	9449, CellSignalling	Marker of proliferation: labels cells in G1, S, G2 and mitotic phases of cell cycle
Rabbit anti-CC3	1:500	#9664, Cell signalling	Cleaved caspase 3, marker of apoptosis
Rabbit anti-Sox2	1:500	Ab5603, Abcam	Marker of neural stem cells (transcription factor)
Mouse anti-Nestin	1:1000	Mab5326, AMD Millipore	Marker of neural stem cells (intermediate filament)
Mouse anti-H2a.X	1:500	05-636-I, EMD Millipore	Marker of DNA repair (Histone)
Rabbit anti-DCX	1:500	Ab11267, Abcam	Marker of neuronal precursors
Mouse anti-Map2	1:500	Ab11267, Abcam	Microtubule associate protein 2, marker of immature neurons
Rabbit anti-NRF2	1:500	Ab31163, Abcam	Transcription activator involved in gene up-regulation in response to oxidative stress

Table 4 - Table showing the primary antibody used, their dilution, catalogue numbers and function.

The following day, the HPCs were washed in PBS and incubated in blocking solution for 30 minutes at room temperature, followed by 30µl/well of appropriate secondary antibody diluted in blocking solution for 2 hours at room temperature (**Table 5**). The cells were then washed 3 times and incubated with 50µl/well of 300µM DAPI (Sigma, D9542-5mg) in PBS solution for 5 minutes at room temperature. Well were washed 3 more times and stored in PBS supplemented with 0.05% sodium azide. Representative images of each marker for proliferation and differentiation assay are reported in **Figure 8** and
Figure 9 respectively.

Secondary antibody	Dilution	Catalog # / Supplier
555 Donkey Anti-rabbit IgG	1:500	A-31572, Life Technologies
488 Donkey Anti-mouse IgG	1:500	A- 21202, Life Technologies

Table 5 - Table showing the secondary antibody used, dilution and catalogue numbers.

2.2.2 Image analysis

2.2.2.1 Quantifying cellular markers

All immunostainings were quantified through the semi-automated CellInsight NXT High Content Screening (HCS) platform (ThermoScientific). The Studio software enables users to set threshold parameters to allow unbiased comparisons throughout treatments and plates. Parameters were kept constant within studies but varied throughout different experimental set ups. On rare occasions parameters were varied within studies to account for changes in the brightness of the stains (See section 08.1.1 for parameters used).

Protocols and scripts were developed using Studio's Cell Health Profiling BioApplication which relies on the nuclear stain (386 wavelength) to identify cells and set a search area for identifying other stains in the 488 and 555 wavelengths. The user first instructs the software to "autofocus" on the nuclear stain then sets an exposure time for image acquisition for each of the 3 channels and acquires several representative images. It is important the stain is visible but not oversaturated due to background noise. These images are then used to validate the selected nuclear stain, where one can discard stains too small to count as nuclei and set segmentation parameters to distinguish cell borders. The

representative images are then divided into positive images and negative control images (wells stained with DAPI and secondary antibodies alone) and average intensity thresholds are set to distinguish specific fluorescent signal from unspecific binding and background noise. The threshold must be higher than highest intensity signal seen in the negative control images (see **Figure 7**). Once positive (cells with intensity higher than the set threshold) and negative cells (cells with a lower intensity than the set threshold) are identified on sample images, the software will capture 15 fields per selected well and compute the percentage of all cells (identified via the nuclear stain) are positive for each marker. The software can also calculate other information such as nuclear area and number of cells per field. Both the calculations and the images can then be exported.

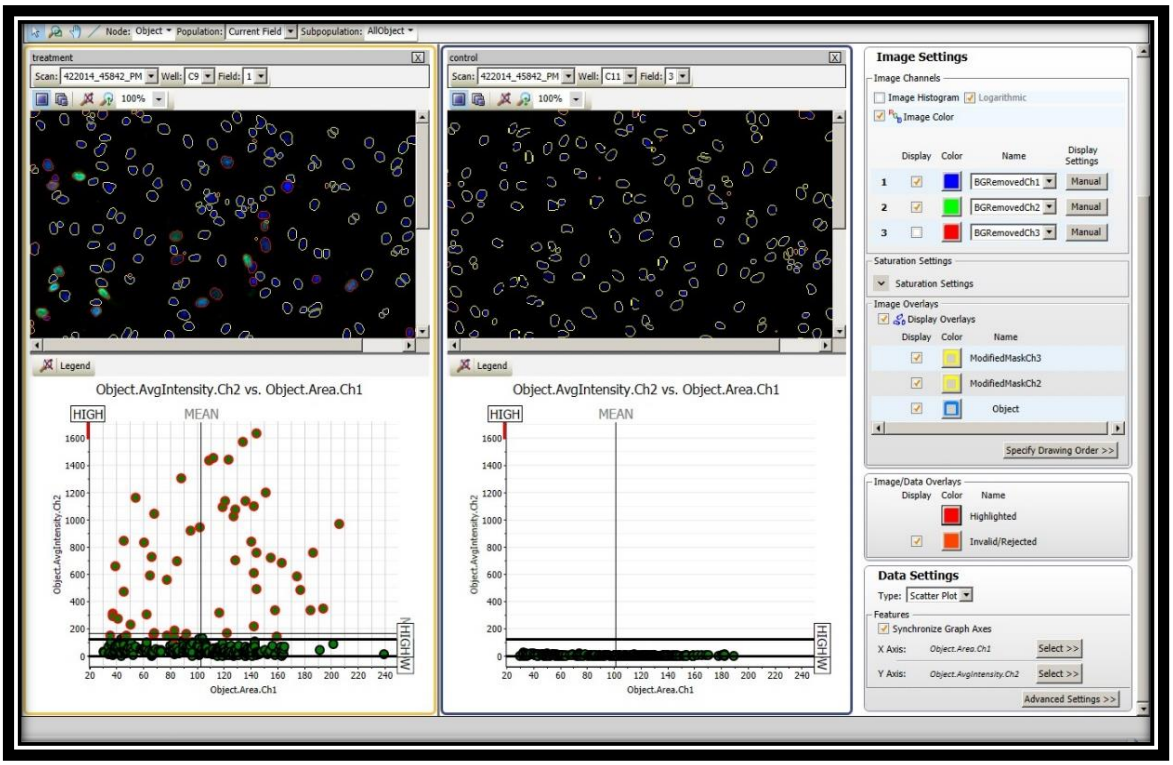

Figure 7 - Screenshot of the CellInsight Platfrom (Thermofisher) software being used to set an average intensity threshold. Positive cells are on the left and negative controls (secondary antibody alone) on the right. Below the representative images there is a scatter plot showing the average intensity for a specific channel (Ch2: channel 2) of each cell within that image. This stage of the protocol involves setting an average intensity threshold (horizontal line) above background noise and unspecific binding, we therefore set the threshold to be above the signal emitted by negative control wells. Cells surrounded by a red mask are the cells selected as having a positive stain if this threshold was to be applied

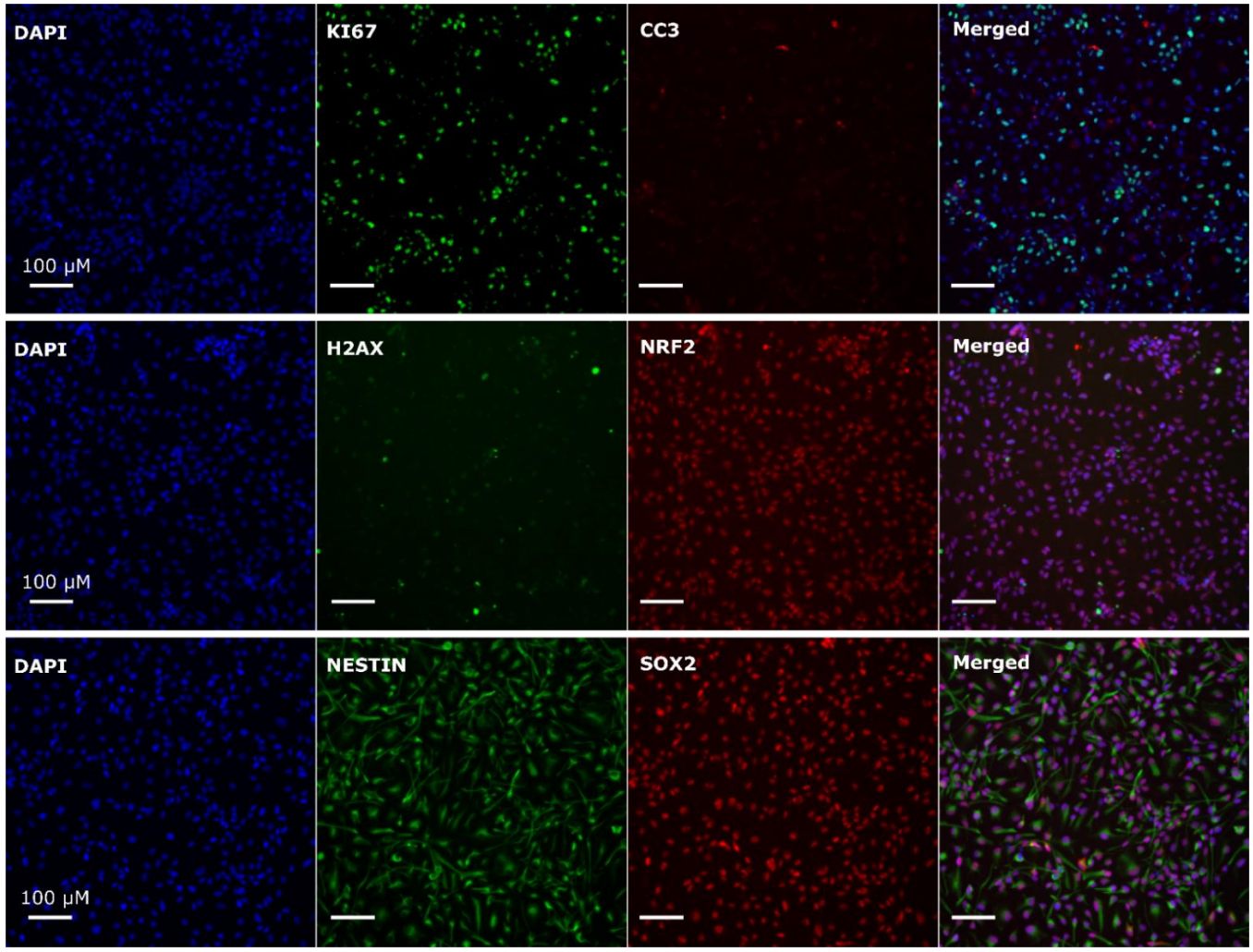

Figure 8 - Panel of representative images of immunostaining following the proliferation assay. Each square represents a field as analysed by the CellInsight software.In each row, the nuclear marker DAPI is in the image followed by Ki67 and CC3 (row 1), H2AX, NRF3 (row 2) or NESTIN and SOX2 (row 3). The final image in each row is the merged image showing all three stains combined. Scale bar representing 100µM is reported in the bottom left corner of each image.

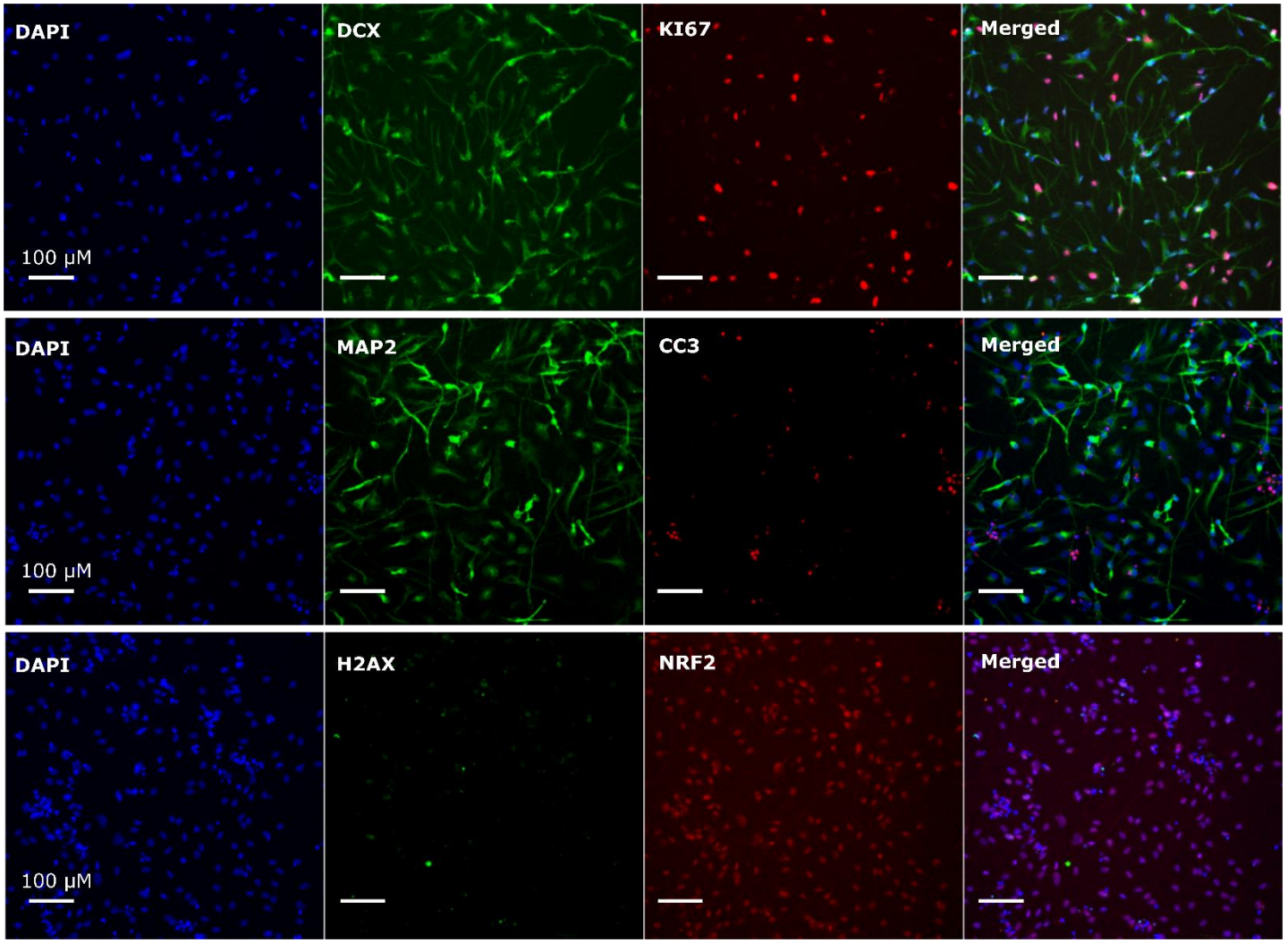

Figure 9 - Panel of representative images of immunostaining following the proliferation assay.. Each square represents a field as analysed by the CellInsight software. In each row, the nuclear marker DAPI is in the image followed by Ki67 and CC3 (row 1), H2AX, NRF3 (row 2) or NESTIN and SOX2 (row 3). The final image in each row is the merged image showing all three stains combined. Scale bar representing 100µM is reported in the bottom left corner of each image.

2.3 Molecular analysis

2.3.1 Quantitative Polymerase Chain Reaction

Quantitative Polymerase Chain Reaction (qPCR) was carried out to investigate gene expression throughout this project. Primer design methods and primer sequences are reported in section 3.2.4.

2.3.1.1 RNA extraction and DNase treatment

Cells were grown in 6-well plates underwent the proliferation or differentiation protocol explained in section 2.1.4 and 2.1.5. Each well was lysed mechanically and resuspended in 1ml TRIreagent (T9424, Sigma). Trizoled sample was transferred to phase lock tubes (Invitrogen™) and chloroform (1 chloroform : 5 trizol ratio) was added to each sample and RNA was separated by vigorous shaking and centrifuging at 10000 RPM for 5 minutes. The aqueous layer containing RNA was then transferred to a new tube, treated with 500µl of isopropanol and centrifuged. The resulting pellet containing the nucleic acids was then washed with 80% ethanol and air dried. The pellet was resuspended in 100µl H_20 and incubated on ice for 15 minutes before the addition of 10µl Sodium Acetate followed by 300µl of 100% ethanol and overnight incubation at -80˚C. Though optional, the sodium acetate was carried out on all samples to ensure the highest possible purity. The next morning samples were spun at 13000 RPM for 15 minutes, the supernatant was discarded and the wash in 80% ethanol was repeated. Samples were left to air dry and then resuspended in H_2O and assessed for purity and RNA concentration using the NanoDrop™ 1000 spectrophotometer (Thermo Scientific). If the purity indicated by the 260/280 ratio was not satisfactory, the sodium acetate step was repeated. A minimum of 1.4µg of RNA was subsequently treated with 1µl of TURBO DNA-*free* (AM1907, Life Technologies) to remove any remaining DNA, and finally with DNase Inactivation Reagent (AM1907, Life technologies), as per supplier instructions.

2.3.1.2 Reverse Transcription

0.7µg of extracted RNA was combined with 250ng of random hexamers (N8080127, nLife Technologies) and 1mM dNTP mix (RO191, Thermo Scientific) and made up to 13µl with nuclease free water (Sigma-Aldrich). The mix was heated at 65˚C for 5 minutes and then placed on ice for 1 minute before being made up to 20µl with the reagents shown in **Table 6** and nuclease free water.

Reagent	Concentration	Catalog # / supplier
First Strand buffer	1 unit	Invitrogen
Dithithretiol	5mM	18080-044, life Technologies
RNaseOUT	40 units	10777, Life Technologies
SuperScript III Reverse Transcriptase	200 units	Invitrogen

Table 6 - Table showing components for reverse transcription

Samples were then incubated at 25˚C for 5 minutes (primer annealing), 50˚C for 1 hour (optimal temperature for reverse transcriptase function), 55˚C for 30 minutes (to remove secondary structures) and 70˚C for 15 minutes (to inactivate the reverse transcriptase) before being diluted in nuclease free water. Dilutions were carried out aiming for maximal use of samples while ensuring a cycle threshold (CT) value lower than 30 to ensure efficient qPCR readouts. Dilutions varied from 1:25 to 1:35.

2.3.1.3 Thermocycler protocol

10µl of diluted cDNA was combined with 4µl 5X EvaGreen (08-24-00008, Solis BioDyne, Estonia), 2µl of 2µM primer mix and 4µl of nuclease-free water. qPCRs were carried out with the Chromo4 Real-Time PCR detector (Bio-Rad), following the protocol outlined in **Figure 10**. Following the protocol outlined in **Figure 10**, a melt curve was carried out from 60 ˚C to 90 ˚C by carrying out a plate read at each 1˚C increment. UV zapped white 96-welled qPCR plates (AB-0900/W, ThermoFisher) were used for all qPCRs. All reactions were carried out in triplicates accompanied by negative controls where cDNA was replaced by H_2O.

Figure 10 -Schematic representing the qPCR protocol. Samples were heated to 95˚C for 15 minutes to denature the cDNA and ensure all cDNA is single stranded. This is followed by 45 cycles involving 30 seconds at 95˚C for denaturation of any double strands formed by the extension step, 30 seconds at 60˚C for primer annealing and 30 seconds at 72˚C for strand extension by polymerase. Fluorescence was recorded after each cycle.

2.3.1.4 qPCR analysis

Using the Opticon Monitor™ (Bio-Rad) software, the melting curve profile for each sample was assessed and if satisfactory, the CT value and efficiency were exported. When carrying out cross-plate comparisons, the same fluorescence threshold was used across all plates to extract the corresponding CT values. The Pfaffl method was used to quantify the relative levels of the qPCR transcript. The formula is reported below:

$$\text{Ratio} = \frac{(E_{target})^{\Delta CT_{target}\,(control - sample)}}{(E_{ref})^{\Delta CT_{ref}\,(control - sample)}}$$

Where target is the target gene being analysed, ref is the average of the housekeeping genes and E = PCR efficiency. Therefore, ΔCT_{target} = difference in CT values of the target gene between sample and control conditions, ΔCT_{ref} = difference in CT values of housekeeping genes between sample and control conditions. Media only conditions and/ or low passage number cells were used as control conditions. Technical triplicates were averaged and used to generate the final CT value and efficiency used per sample. When standard deviation was above 0.3 and an outlier was present within the three replicates, the outlier was removed

3 The Systemic Milieu: A Putative Model to Induce Neural Stem Cell Ageing

3.1 Introduction

3.1.1 Cognition as an ageing biomarker

Currently, there is a lack of effective biomarkers for healthy human ageing (Lara et al., 2015). This causes difficulties in identifying healthy from pathological ageing and hinders research due to the inability to compare results across various animal models and human populations. Efforts are therefore being made to firstly define different ageing domains, and secondly to define biomarkers within these. An important domain in assessing healthy ageing is cognitive function, which can be subdivided in executive function, processing speed and episodic memory (Lara et al., 2015). Cognitive performance reliant on these three subcategories is known to decline with age. Therefore, cognitive tests assessing these functions are being proposed as useful human biomarkers of cognitive ageing (Hedden and Gabrieli, 2004). Focussing on episodic memory specifically, tests assessing pattern separation, the process responsible for distinguishing similar new patterns from known old patterns, have been widely used in both animal models (Sahay et al., 2011; Wilson et al., 2004, 2005) and human populations for this purpose (Stark et al., 2010, 2013; Yassa and Stark, 2011). In addition, tasks requiring spatial awareness such as object-location tasks are also heavily reliant on episodic memory and therefore affected by age. Object-location tasks such as paired associates learning (PAL) in fact, have also been employed in both animals and humans and show great potential for assessing age-related cognitive decline (Cès et al., 2018; Mirescu et al., 2006; Mitchell et al., 2000; Wimmer et al., 2012).

Episodic memory is defined as the recollection of events which are unique in terms of spatial and temporal context. It differs from semantic memory, which usually refers to knowledge about facts, objects or concepts (Hayes et al., 2004). Interestingly, groups have also highlighted performance on other memory tasks, such as traditional recognition reliant on semantic memory, does not decline in healthy ageing but does decline in participants with mild cognitive impairment (Stark et al., 2013). These findings suggest a battery of cognitive tasks can be employed to distinguish healthy from pathological cognitive-decline.

3.1.2 Neurogenesis and neural stem cells as ageing biomarkers

Both animal and human studies have identified the dentate gyrus of the hippocampus as having an important role in episodic memory (Berron et al., 2016; Hayes et al., 2004; Sahay et al., 2011). In particular, hippocampal neurogenesis and NSCs have repeatedly been implicated in episodic memory in animal models (Clelland et al., 2009; McAvoy et al., 2015; Sahay et al., 2011). The presence of adult neurogenesis in humans has been debated for decades and has recently been the focus of discussions as prominent journals have published opposing studies about its presence and the decline rate (Boldrini et al., 2018; Sorrells et al., 2018). Regardless, authors on both sides agree that better techniques are necessary to study neurogenesis in humans as current ones are hindered by a number of pitfalls (Boldrini et al., 2018; Kempermann et al., 2018; Lee and Thuret, 2018; Sierra et al., 2011; Sorrells et al., 2018). Currently available techniques in fact, rely mainly on post-mortem immunohistochemical analysis which prevents longitudinal studies and is impaired by marker degradation and post-mortem interval effects (Sierra et al., 2011). Rodent studies have in fact shown markers of neurogenesis such as DCX are particularly affected by post-mortem interval with as little as 8 hour-delays inducing drastic changes in the resulting DCX stain (Boekhoorn et al., 2006). Though, varying post-mortem intervals are likely to confound results, standardising these in human studies is obviously problematic.

As described in Chapter 1, the current gold standard for detecting adult hippocampal neurogenesis involves the incorporation of thymidine analogues or ^{14}C into DNA as employed by Erkisson and Spalding respectively (Eriksson et al., 1998; Spalding et al., 2013). These methods are a more direct measure of neurogenesis compared to staining methods but it has been suggested this incorporation may be the result of DNA repair rather than replication. Though this is unlikely as even extensive repair following injuries such as stroke remains undetectable by ^{14}C, it has highlighted the need for additional and differing methodologies to assess this phenomenon (Huttner et al., 2014). In line with this, the occurance of adult hippocampal neurogenesis is also supported by the ex-vivo isolation of adult human progenitor cells (Palmer et al., 2001) and extensive immunohistochemical

analysis that successfully identified cell proliferation and neuroblast markers in human post-mortem tissues (Boekhoorn et al., 2006; Curtis et al., 2003; Dennis et al., 2016b; Liu et al., 2008; Mathews et al., 2017). Despite these developments, no technique currently enables researchers to assess neurogenesis *in vivo* resulting in existing findings being confounded by aspects such as the lack of experimental control, perimortem physiological state as well as the previously discussed post-mortem interval.

Other techniques such as imaging, have been suggested but the slow rate at which neurogenesis occurs in the adult human brain suggests neurogenesis alone is unlikely to cause measurable volumetric changes (Spalding et al., 2013). Though a decline in neurogenesis may contribute to the marked decrease in human hippocampal subfield volumes seen with age. (Daugherty et al., 2016; Peters, 2006; Shing et al., 2011; Warner-Schmidt and Duman, 2006).

3.1.3 The systemic environment as an ageing biomarker

In addition to cognitive tasks, peripheral biofluids are a new promising avenue and source of ageing biomarkers. This is already being explored in age-related diseases such as Alzheimer's where blood-derived fluids such as plasma or serum are being evaluated (Geekiyanage et al., 2012; Hye et al., 2014; Song et al., 2009). The large body of evidence implicating the systemic environment in ageing and cognition discussed in the general introduction, supports the notion that blood-based analysis could provide fast, minimally invasive and cost-effective biomarkers for both healthy and pathological ageing (Maruszak et al., 2017; O'Bryant et al., 2011; Villeda et al., 2011, 2014). The effect of the systemic environment on the brain has often been ignored owing to concepts such as the blood-brain barrier suggesting the brain is a separate and isolated entity from the rest of the body. However, findings showing that especially during ageing and inflammation, the blood-brain barrier is more permeable than initially predicted, combined with parabiosis studies have proven the systemic environment is capable of affecting the brain (van der Flier and Scheltens, 2005; Villeda et al., 2014). Though there are some discrepancies between analytes identified by studies using serum or plasma, these are mainly attributed to the

differing ways of processing of the samples and the two can often be used interchangeably (Galasko and Golde, 2013). Interestingly, as discussed in section 1.3, the systemic environment has also been implicated in nutrition and neurogenesis. Understanding how the systemic environment impacts the ageing brain could thus provide a basis for useful new biomarkers in ageing research. In summary, systemic environment composition and performance on cognitive tasks are promising biomarkers for cognitive-ageing. In addition, both have strong evidence from animal models suggesting a link to adult hippocampal neurogenesis. The lack of techniques to robustly assess human adult neurogenesis however, has prevented studies from confirming this in human populations. Therefore, further research focused on developing new methodologies and translating these findings to humans is necessary.

3.1.4 Ageing research and model organisms

A variety of animal models have been employed in ageing research. As discussed in the chapter 1, studies using model organisms have identified important conserved molecular pathways and highlighted mechanisms behind ageing phenotypes. A decrease in adult neurogenesis for example, has been linked to age-related cognitive deficits thanks to rodent studies and the importance of nutrient-sensing pathways in longevity was first identified in *C. elegans* and yeast models (Conrad et al., 2014; Lees et al., 2016; Villeda et al., 2011; Walker et al., 2005). Furthermore, the importance of the systemic milieu was identified due to mouse-based parabiosis studies (Villeda et al., 2011, 2014). However, many are reporting issues in translating animal findings to humans. With meta-analyses showing that over 90% of behavioural neuroscience results fail to replicate in humans (Garner, 2014). Besides the obvious differences in lifespan across different models, this translational gap is often attributable to problems in identifying animal behaviours that resemble human cognition as well as the need to consider aspects such as emotion, social status and education which proves difficult in non-human models (Lees et al., 2016). In addition, and as discussed in the section 1.2.1 when investigating aspects such as neurogenesis, considerable differences in neuronal turnover, rate of decline and neurogenic niches have been identified (Bergmann et al., 2015; Imayoshi et al., 2008;

Spalding et al., 2013). Though some authors suggest animal models are simply in need of stricter methodology and more honest reporting of negative findings, others suggest the field ought to move towards human based studies (Garner, 2014). Nevertheless, the field is in need of projects aimed at bridging this gap (Butler, 2008; Check, 2003).

Human studies however, are accompanied by several ethical and practical restrictions which often make elucidating molecular mechanisms behind phenotypes difficult. In an attempt to bridge some of the translational gap, but preserve the advantages of easily modifiable systems, human-based *in vitro* models are often employed. Advances in laboratory techniques such as iPSCs and human immortalised cell-lines have allowed several groups to start validating animal model findings in human-based models (Anacker et al., 2011; Deng, 2017; Jiménez-Moreno et al., 2017; Zhang et al., 2013). Unpublished research by the Thuret laboratory has focused on validating the mouse-based parabiosis studies in a human-based cellular model. Murphy and colleagues showed treatment with serum from older participants caused increased cell death in human hippocampal progenitor cells when compared to treatment with serum from young participants (Murphy et al., 2018). In addition, Maruszak and colleagues showed cellular readouts from the same *in vitro* parabiosis assay were able to predict mild cognitive impairment conversion to Alzheimer's with over 90% sensitivity and specificity (Maruszak et al., 2017). Models such as these not only provide possible new biomarkers for early detection of pathology but also a new platform with which to study the molecular mechanisms behind cognitive ageing.

3.1.5 Nutrient-sensing pathways

To better understand and target cognitive health, we must identify the driving molecular mechanisms. As discussed in the general introduction, three nutrient-sensing pathways have been highlighted by existing literature as having important roles in neural stem cells and longevity. Overall dysregulation of these pathways has been identified as a key driver of ageing, but the roles of specific pathway components within this relationship are yet to be clarified. Elucidating the interaction between pathway components is a necessary first

step in understanding the role of these pathways in health and disease. Here we briefly introduce the key components of these pathways.

3.1.5.1 mTOR pathway

The mTOR pathway is a highly conserved molecular pathway responsible for cell growth, metabolism and cytoskeleton organisation (Costa-Mattioli and Monteggia, 2013). In neurons, it responds to changes in insulin, neurotransmitter, neurotrophins and cyclic AMP. These alterations signal through the phosphatidylinositol 3-kinase (PI3K)-AKT pathway to mTOR, serine/threonine kinase. The PI3K-AKT pathway is described in further detail below (see 3.1.5.2). mTOR is a central component of this pathway and forms either the mTORC1 or mTORC2 complex (see section 1.4.1). mTORC1, which has been linked to longevity in various studies (Blagosklonny, 2008; Fok et al., 2014; Harrison et al., 2009; Wanke et al., 2008), has 4 principal substrates; S6K1, 4EBP1, SREBP and GRB10. These substrates have important functions in transcriptional and translational control (Malley and Pidgeon, 2016). See **Figure 11** for a diagram of the mTOR pathway.

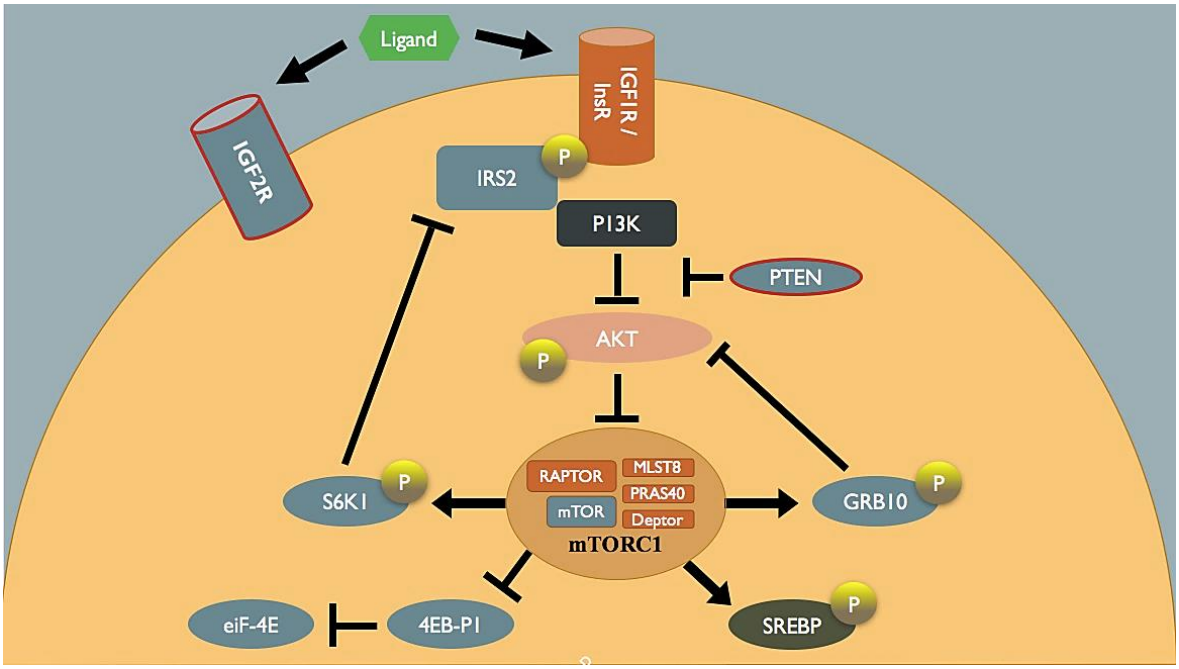

Figure 11 - mTOR pathway. Diagram showing the key players of the mTOR pathway. The extracellular space is shown in blue and the cell is shown in yellow. Ligands (in green) such as insulin bind to the insulin receptor (InsR) or the insulin-like growth factor receptor 1 (IGF1R) (in orange). This activates the insulin substrate 2 (IRS2) which initiates the phosphatidylinositol 3-kinase (PI3K) - AKT kinase cascade which culminates in the regulation of the mTORC1 complex. mTORC1 (in brown) is made up several proteins including Raptor, MLST8, PRAS40, deptor and mTOR, a serine/threonine kinase. mTOR is responsible for the phosphorylation of several downstream targets including GRB10, SREBP, 4EB-P1 and S6K. 4EB-P1 is responsible for regulating translation by interacting with eukaryotic translation initiation factor 4E (eIF4E). Finally, phosphatase and tensin homolog (PTEN) regulates this pathway by controlling the PI3K-AKT signalling cascade. Selected candidate genes in this project are shown in blue. Candidates present in multiple pathways are highlighted by a red outline.

S6K1 is a ribosomal protein kinase responsible for the phosphorylation of the S6 ribosomal protein, which induces ribosomal protein synthesis. S6K1 activation by mTOR has been linked to autophagy regulation (Chung et al., 1992; Datan et al., 2014) and negative feedback (Malley and Pidgeon, 2016). Eukaryotic translation initiation factor 4E-binding protein (4EBP1) interacts with eukaryotic translation initiation factor 4E (eIF4E). This interaction prevents the assembly of the complex responsible for recruiting 40S ribosomal subunits to the 5^{l} end of mRNAs and thereby represses translation. mTORC1 phosphorylation of 4EBP1 prevents this interaction which frees eIF4E and allows complex assembly and translation initiation (Gingras et al., 2001). Sterol responsive element binding proteins (SREBP) are basic helix-loop-helix-leucine zippers transcription factor which are responsible for regulating fatty-acid and cholesterol synthesis (Porstmann et al., 2008). Finally, growth factor receptor-bound protein 10 (GRB10) is an adaptor protein with important functions in negative feedback and mTOR pathway regulation. It has also been

suggested to have tumour suppressor functions (Liu and Liu, 2014; Malley and Pidgeon, 2016; Yu et al., 2011).

As well as the studies mentioned in the section 1.4.1, several recent publications have further implicated the mTOR pathway in neurons and NSCs. mTORC1 was found to promote neuronal differentiation in both rodents and humans and its hyperactivity was linked to increased proliferation and abnormal differentiation in human iPSCs. In addition, decreased mTORC1 activity was linked to ageing rodent NCSs and mTORC1 activation was able to restore NSC function and neurogenesis in aged mice (Lee et al., 2016; Li et al., 2017; Meng et al., 2018; Romine et al., 2015; Skalecka et al., 2016). These findings, combined with the importance of mTOR in nutrient-sensing, warrant further studies to elucidate this pathway's function in the interplay between ageing, nutrition and cognition.

3.1.5.2 Insulin and insulin-like growth factor signalling pathway

The IIS pathway is activated by carbohydrates or proteins binding to the insulin (InsR) or insulin-like growth factor (IGF1R) receptors. Upon ligand binding, intracellular Insulin-receptor substrates 1-4 (IRS 1-4) are phosphorylated. These in turn, activate either PI3K-AKT signalling or RAS-ERK signalling.

In the PI3K-AKT branch, PI3K converts phosphatidylinositol 4,5-bisphosphate (PIP2) into the second messenger phosphatidylinositol 3,4,5-trisphosphate (PIP3). Increased levels of PIP3 signal for the activation of AKT, a serine/threonine kinases that phosphorylates and inactivates FOXO transcription factors. This inactivation leads to the suppression of gene transcription. Interestingly, the conversion of PIP2 to PIP3 can be inhibited by phosphatase and tensin homolog (PTEN) a protein shared by both the mTOR and the IIS pathway (van Heemst, 2010). The RAS-ERK branch instead, relies on the kinase cascade initiated by RAF kinase which culminates in the inhibition of the translocation-Ets-leukemia virus (ETV6), a repressor of gene transcription. Genes targeted by both FOXO and ETV6 generally regulate cell growth and differentiation and have been identified as key players in longevity (Sizemore et al., 2017; White, 2015). See **Figure 12** for a diagram of the IIS pathway.

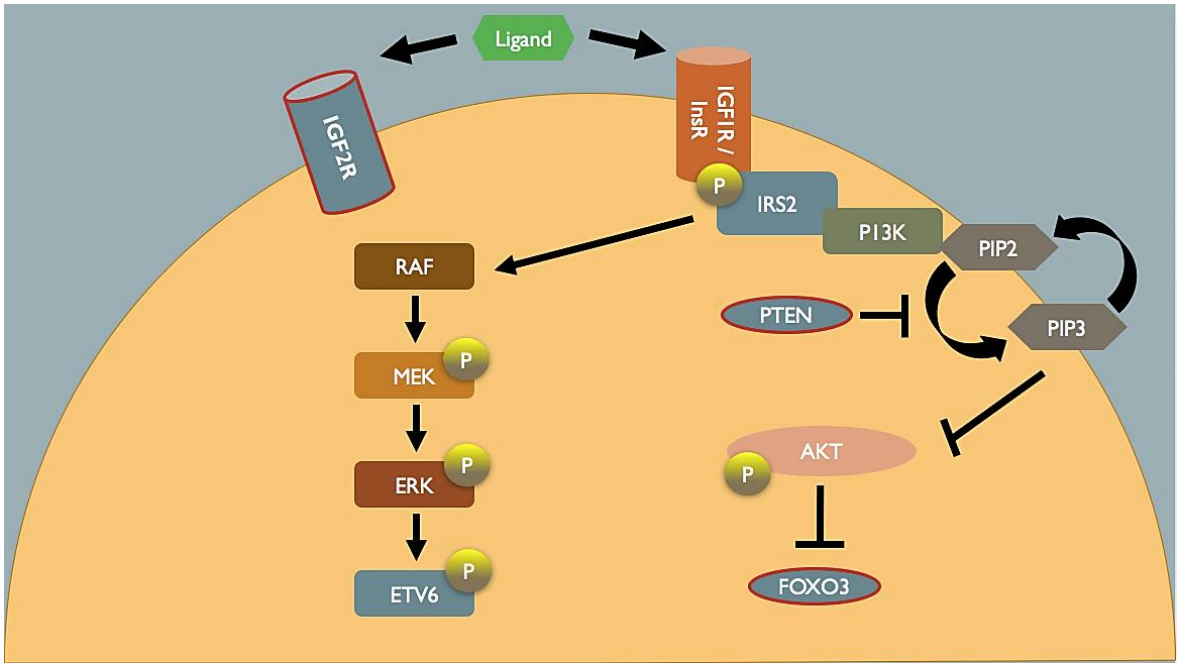

Figure 12 - Insulin and insulin-like sensing pathway. Diagram showing the key players of the insulin and insulin-like sensing pathway. The extracellular space is shown in blue and the cell is shown in yellow. Ligands (in green) such as insulin bind to the insulin receptor (InsR) and insulin-like growth factor receptor 1 (IGF1R) (in orange). Alternatively, ligands bind to the scavenger receptor insulin-like growth factor receptor 2 (IGF2R) (in blue). Upon ligand binding, InsR and IGF1R phosphorylate the insulin receptor substrate 2 (IRS2). IRS2 can activate both the phosphatidylinositol 3-kinase (PI3K) - AKT kinase cascade or RAF/ERK signalling. The RAF/ERK branch consist of a kinase cascade that culminates in the inhibition of the translocation-Ets-leukemia virus (ETV6). In the PI3K-AKT branch, PI3K (in dark green) converts phosphatidylinositol 4,5-bisphosphate (PIP2) (in grey) into the second messenger phosphatidylinositol 3,4,5-trisphosphate (PIP3) (in grey). Increased levels of PIP3 signal for the activation of AKT (in pink), a serine/threonine kinases that phosphorylates and inactivates FOXO transcription factors (in blue). Selected candidate genes in this project are shown in blue. Candidates present in multiple pathways are highlighted by a red outline.

3.1.5.3 Sirtuin pathway

Mitochondrial dysfunction and deregulated nutrient-sensing pathways are key hallmarks of an ageing organism (López-Otín et al., 2013). Hence, pathways responsible for regulating energy availability are key targets in ageing research. Sirtuin deacetylases regulate mitochondrial function and are therefore ideal mediators for the interplay between nutrition, energy balance and ageing. As discussed in section 1.4.2, several studies have already implicated sirtuins in both ageing and nutrient-sensing but the exact proteins responsible for this association remain unknown.

Sirtuins are nicotinamide adenine dinucleotide (NAD+) dependent deacetylases. Following deacetylation, nicotinamide (NAM) and 2-O-Acetyl ADP ribose are created as by-products.

In the presence of the rate-limiting enzyme Nicotinamide phosphoribosyltransferase (NAMPT), NAM is recycled back to NAD+ by the salvage pathway. Through the process of deacetylation, sirtuins control the expression of several genes involved in neuronal protection, inflammation, stress resistance, fatty acid oxidation, fatty acid mobilization, insulin secretion, glucose production and lipid homeostasis (Donmez and Outeiro; Guarente, 2014; Oellerich and Potente, 2012; Renault et al., 2009). SIRT1, the most thoroughly studied sirtuin in mammals, has also been linked to several longevity-related processes (Cantó and Auwerx, 2009; Guarente, 2014; Satoh et al., 2013). For example, SIRT1 has been associated to mitochondrial biogenesis via the inhibition of human nuclear receptor interaction protein (NRIP) and to the IIS and mTOR pathways due to inhibitory effects on FOXO3A (Cohen et al., 2004; Smith et al., 2009). Interestingly, sirt1 was also implicated in insulin secretion in pancreatic beta cells via its repression of the uncoupling protein 2 (UCP2) (Bordone et al., 2005). UCP2's important function in energy metabolism of proliferating NSCs suggests this interaction may occur in other cell types as well (Rupprecht et al., 2014). Importantly, SIRT1 has also been linked to lineage decisions owing to its inhibitory effect on MASH-1 activity; MASH-1 is a basic helix-loop-helix transcription factor that is central for neuroblast differentiation (Prozorovski et al., 2008). Despite these findings, many downstream targets and physiological functions of SIRT1 remain unknown highlighting the need for further research. See **Figure 13** for a diagram of the key molecules involved in the Sirtuin pathway.

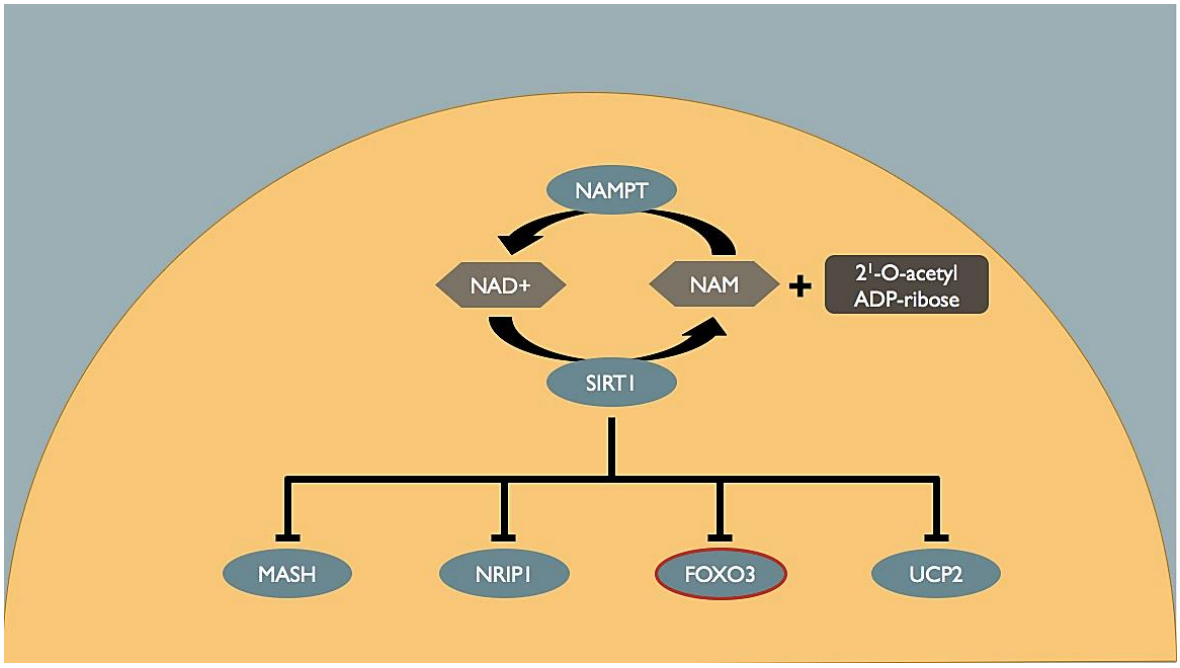

Figure 13 - Sirtuin pathway. Diagram showing some of the key molecules involved in the Sirtuin pathway. SIRT1 deacetylation causes the conversion of nicotinamide adenine dinucleotide (NAD+) to nicotinamide (NAM) and 2^{1}-O-acetyl ADP-ribose. This is recycled back to NAD+ via nicotinamide phosphoribosyltransferase (NAMPT). SIRT1-dependent deacetylation inhibits several downstream targets including nuclear receptor interaction protein 1 (NRIP1) and the transcription factors MASH and FOXO3A, linking the deacetylase to the regulation of several other pathways. In addition, SIRT1 also represses uncoupling protein 2 (UCP2) via deacetylation-independent mechanisms. Selected candidate genes in this project are shown in blue. Candidates present in multiple pathways are highlighted by a red outline.

3.1.6 ABTB1: candidate from exploratory analysis

Recent work by Murphy et al, showed expression alterations of several known and novel ageing genes following treatment of HPCs with serum from young or old donors (Murphy et al., 2018). This work highlighted the Ankyrin repeat and BTB/POZ domain-containing protein 1 (ABTB1) as one of the 10 most differentially expressed proteins in response to aged serum. In addition, this protein was also shown to undergo methylation changes in relation to age by Horvath's clock (Horvath, 2013). Though the protein's exact function remains unknown, studies have suggested a role in protein-protein interactions due to the presence of the BTB/POZ domain (Albagli et al., 1995; Geyer et al., 2003). Interestingly, a study has shown an interaction between ABTB1 and PTEN suggesting a role for ABTB1 in nutrient-sensing pathways (Unoki and Nakamura, 2001). These findings, combined with ABTB1's high expression in the dentate gyrus of the hippocampus in both mice and humans

(Allen Human Brain Atlas (2010)), warrant further research into the function of this gene in cognitive ageing.

3.1.7 Aims of this chapter

In summary, research has a highlighted the need for developing better human biomarkers of ageing in general and of cognitive-ageing specifically. In addition, there is a need to focus on translating animal models to humans and to further understand the molecular pathways responsible for the link between nutrition and longevity.

In this chapter, we focus on the effects of the systemic environment to determine its impact on human HPCs. We aim to 1) assess whether there are changes in NSC function in response to treatment with ageing serum and to relate these to human 2) imaging and 3) cognitive data belonging to the serum donors. In addition, we aim to 4) assess whether ageing serum causes gene expression alterations in candidate nutrient sensing-pathway components and 5) if these are associated to cellular changes in the NSCs. Hereby we aim to evaluate the potential use of the systemic environment as an ageing biomarker, determine the translational potential of our *in vitro* parabiosis model and assess the function of nutrient-sensing genes in human NSC maintenance.

To investigate the effects of the systemic environment, we employ an *in vitro* parabiosis model. This consists in the treatment of hippocampal progenitor cells with serum from patients of different ages to ascertain the effects of an ageing systemic environment on NSC regulation. For aims 1, 2 and 3 a cohort comprised of middle-aged to old participants is used. For aims 4 and 5 instead, we use a cohort comprised of young and old individuals to maximise the age difference between participants. See diagram below for representation of the aims and hypotheses for this chapter.

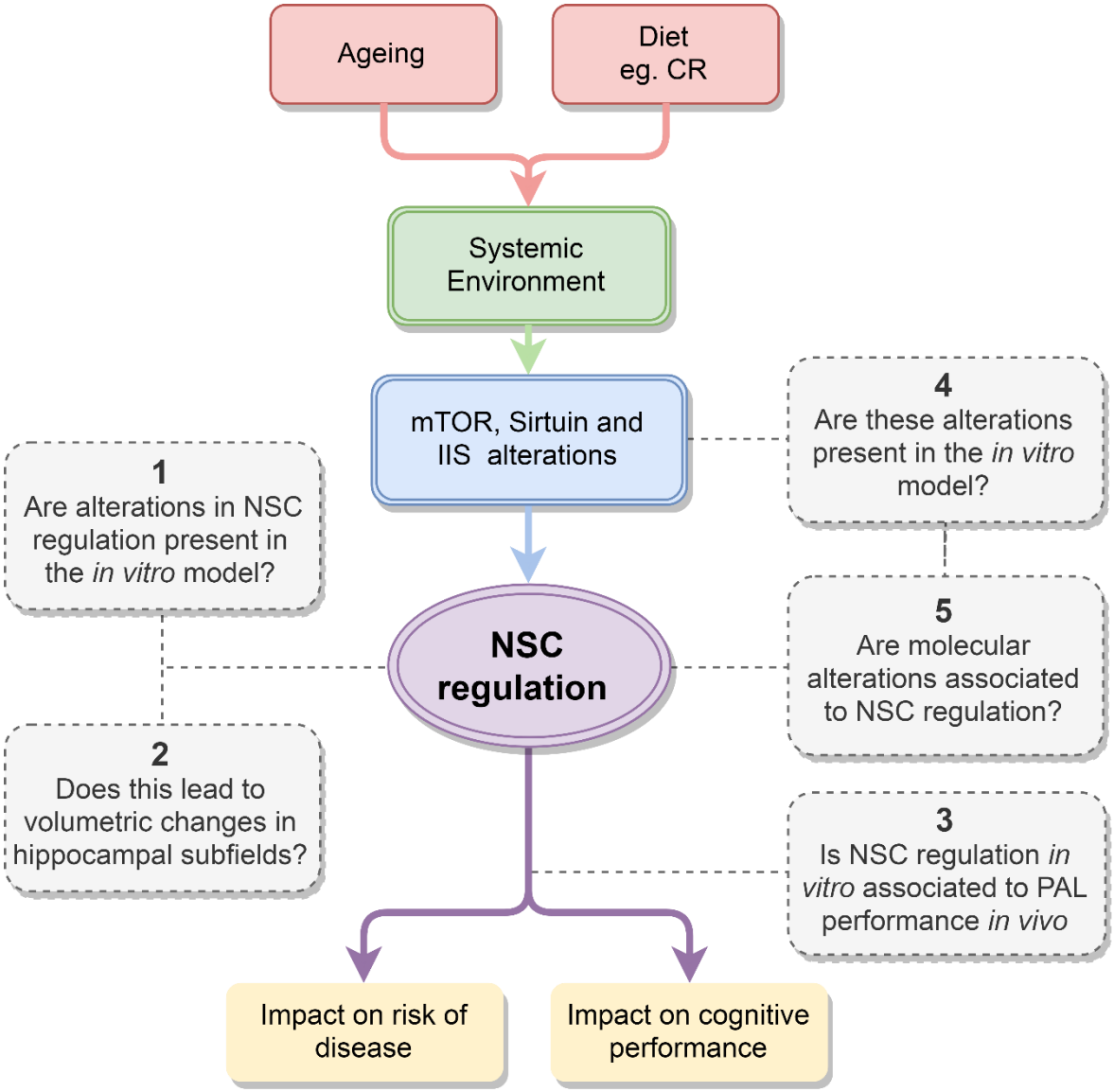

Figure 14 - Chapter 3 hypothesis. We hypothesise that ageing and diet (e.g. calorie restriction (CR)) affect the systemic environment and that in turn, this causes alterations in the mTOR, Sirtuin, and insulin and insulin-like sensing (IIS) nutrient-sensing pathways. We then hypothesise that these alterations affect the neural stem cell (NSC) regulation which leads to cognitive decline and increased risk of disease. To test these hypotheses, we aim to determine whether (1) ageing serum can cause NSC alterations in vitro and whether these alterations are associated to (2) imaging and (3) cognitive data of the serum donors. We also aim to determine (4) whether ageing serum treatment can affect the expression of nutrient-sensing pathway components and (5) whether these are associated to cellular alterations in the NSCs.

3.2 Materials and methods

3.2.1 Serum sample processing

All participants were required to fast for two hours prior to blood sample collection, which occurred in the morning. During these fasting periods, only fluids with no sugar or milk were allowed. Blood samples were collected and stored in serum separator tubes, these were inverted 5 times and allowed to rest for 30 minutes at room temperature. Tubes were then spun at 1500g for 15 minutes at 4 degrees. The serum, which was now present in the top layer of the tube was collected and stored at -80˚C. The samples were then thawed, aliquoted in working volumes into Matrix 2D storage tubes (3711, Thermo Fisher) and stored at -80˚C until use to standardise the freeze-thaw cycles. At the point of use samples were thawed at 37˚C and swirled periodically to preserve serum viability by preventing the formation of crystalline precipitates. Once thawed serum was added at a 1% concentration to cell culture media and incubated with human hippocampal progenitor cells as explained in section 2.1

3.2.2 Middle aged to old cohort (MATOC)

This cohort was used for aims 1,2 and 3 of this chapter, as outlined in section 3.1.7. Cell work using samples from middle-aged to old cohort (MATOC) was carried out in equal proportions by Dr. Tytus Murphy and myself. Recruitment, imaging and cognitive assessment were carried out by Dr. Paul Wright and other members of the O'Sullivan group. Analysis was carried out by myself and Dr. Paul Wright.

3.2.2.1 Recruitment and descriptive statistics

The middle-aged to old cohort (MATOC) from which serum samples were derived was recruited by the O'Sullivan group.

Participants used in this study were cognitively healthy control individuals recruited as part of the larger STRATEGIC study investigating memory performance in stroke patients headed by Prof. O'Sullivan and funded by the Medical Research Council. The exclusion criteria included moderate to severe head injury, diagnosis of a cognitive, neurological or major psychiatric disorders, self-referral for cognitive symptoms and a mother tongue

other than English. As Magnetic Resonance Imaging (MRI) was used, all its pertaining exclusion criteria, such as presence of pacemakers and penetrating eye injury, were applied as well. All participants gave informed, written consent and were recruited in accordance with the London-Bromley Research Ethics Committee. Serum samples of 25 individuals were available, of these 19 participants also had available cognitive score data (see table for details).

Subcohort	Number of participants	Female: male ratio	Minimum Age-Maximum Age (Mean±SD)
Imaging and Cellular	25	5:20	52.6 - 89.4 (73.2 ± 9.5)
Cognition and Cellular	19	4:15	55.6 - 89.4 (74.5 ±8.9)

Table 7 - Participants in the middle aged to old cohort. Table showing the number of participants, female to male ratio and age distribution of the middle-aged to old cohort (MATOC)

Education was scored following the coding in **Table 8**. The maximum time difference between imaging and blood sample was 2 years.

Code	Qualification
1	No qualification
2	NVQ1/SVQ1
3	O-Level/GCSE/NVQ2/SVQ2/Scottish Intermediate
4	Scottish higher, NVQ3, city and qulds, Pitman
5	A Level, Scottish Advanced Higher
6	Higher Vocational training (e.g. Diploma, NVQ4, SVQ4)
7	University degree
8	Postgraduate degree (e.g. Masters or PhD), NVQ5, SVQ5

Table 8 - Education questionnaire. Table reporting the method used to code education data within the middle aged to old cohort The first column shows the numerical value given to the participant's answer (second column).

3.2.2.2 Imaging

MRI were carried out using a 3T General Electric MR750 scanner at the Clinical Research Facility at King's College Hospital.T1-weighted images were acquired to obtain 192 sagittal slices each with a thickness of 1.2mm, a field of view of 270mm, a 1mm in-plane resolution and an acquisition matrix of 256X256. FreeSurfer(Version 6.0) (Iglesias et al., 2015; Pereira et al., 2014) was used to analyse volumetric T1-weigthed images. This software uses labels derived from an *ex-vivo* atlas of hippocampal subfields to segment the hippocampus in the acquired images. It implements an algorithm that uses a generative model and Bayesian inference. The *ex-vivo* atlas was derived from post-mortem images which were labelled manually.

In this study, the resulting hippocampal segmentations were checked visually for concordance with hippocampal boundaries by a single rater. According to these segmentations, volumes for each subfield were measured and normalised to intracranial volume extracted from FreeSurfer. This created a set of normalised subfield volumes per hemisphere per person, the volumes of each hemisphere were summed to obtain the values used in the analysis. Of the resulting subfields the CA1, CA3, CA4, dentate gyrus (DG) and the subiculum were used in the analysis as well as whole hippocampal volume.

3.2.2.3 Paired Associate Learning task

To assess associative memory, the O'Sullivan developed a version of the PAL. The task consisted in associating an object to a location. Objects were coloured and shaded line drawings known as Snodgrass and Vanderwart "like" objects (obtained from http://wiki.cnbc.cmu.edu/Objects (date accessed: 02/09/18)) and included objects like a drawing of an apple, a whistle or a coloured ball. The spatial locations were provided by a 10-box grid comprised of 4 columns with 2,3,3 and 2 boxes each. As shown in **Figure 15**.

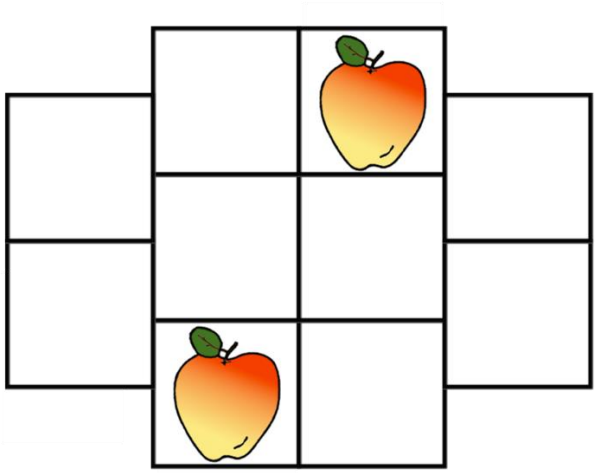

Figure 15 - Paired associate learning task - Diagram showing the recognition phase of the task designed by the o'Sullivan group. An object is show in two locations on the 10-box grid and the participant is asked to identify which on is the correct location. The objects displayed were taken from http://wiki.cnbc.cmu.edu/Objects. The task consisted of two phases. During the learning phase, participants were shown the same object in two locations on the grid (a correct and an incorrect one) they were then asked to select the correct location using a touch pad. Once one of the two locations was selected, feedback was given with a 2s delay: a green smiley face and a pleasant sound for a correct response and a red unhappy face and an unpleasant sound for an incorrect response. This was done for all 10 objects.

During the initial part of the learning phase, the choice of "correct" location on behalf of the participant was a guess. Following this however, the 10 object-location pairs were

presented another 3 times to help the participant learn the objects' locations. There was no indication of set completion and randomisation was applied within each repeat so that each 10 objects appeared in different orders but always appeared once before the next repetition. Following these 4 feedback sets, the task moved onto the recall phase. During this phase, 1 of the 10 boxes in the grid was highlighted at random and the participant was asked to recall the object belonging to that location by giving a verbal response. There was no time limit in this phase. Performance was assessed by two outcome measures: the recognition score, which consisted in the sum of all correct responses in the final 3 sets of the learning phase, and the recall score based on the number of correct recalls in the recall phase. The recognition phase has a maximum score of 30 whilst the recall phase has a maximum achievable score of 10.Statistics

Pearson correlations were carried out using SPSS and GraphPad Prism software. If a significant correlation was found linear regressions were also carried out. Age regressed values were used for regressions on cell readouts and hippocampal volumes while regressions involving PAL scores were controlled for education as well as age. When applicable Bonferroni correction was applied to correct for multiple testing.

3.2.3 Young-Old cohort

This cohort was used for aims 4 and 5 of this chapter as detailed in section 3.1.7. Dr. Tytus Murphy carried out the recruitment of young participants and tissue culture using the young-old cohort (YOC) samples. I carried out all molecular work and all analyses described here.

3.2.3.1 Recruitment and descriptive statistics

Samples from old participants were derived from cognitively healthy control subjects taking part in two ongoing disease biomarker discovery programmes: AddNeuroMed, a multicentre European study (Lovestone et al., 2009) and the Maudsley Biomedical Research Centre for Dementia Case Registry at King's Health Partners. To ensure cognitive health across participants, inclusion criteria stated participant must score more than 27/30 on the Mini Mental State Examination (MMSE) which indicates a normal cognitive level. In both programmes informed consent was obtained per the Declaration of Helsinki (1991). Furthermore, all participants with other neurological or psychiatric disease, significant

unstable illness or organ failure and alcohol or substance abuse were excluded. Samples from 22 old control subjects were obtained for this study with a mean age of 77.6 years (SD±6.43) comprised of 13 females and 9 males. Old participants' age ranged from 53-89. Young participants were recruited through internal advertising within the Institute of Psychiatry, Psychology and Neuroscience between November 2012 and June 2014. Consent and good health were confirmed via a questionnaire as part of the Alzheimer's disease biomarker programmes stated above. Serum was collected at one timepoint for each participant. 15 young control subjects were recruited with a mean age of 27.1 years (SD±5.03) comprising of 8 females and 7 males. Young participants' age ranged from 20-32. Protocols and procedures were approved by the appropriate Institutional Ethics Review Board at King's College London. Serum was extracted, as explained in section 3.2.1, and used on the cellular assay to create the *in vitro* parabiosis assay used in this chapter.

3.2.4 Primer design and gene selection

Candidate genes involved in nutrient-sensing pathways, ageing and stem cell function were selected by literature searches. The selected genes were then assessed for expression within our cell line using a microarray carried out by previous lab members. Primers for the candidate genes were designed using Primer3Plus (www.primer3plus.com). Single nucleotide polymorphisms (SNPs) were avoided and primers were designed to cross exon boundaries wherever possible. Primer sequences were also checked for single-peaked melt curves on the uMelt software (https://www.dna.utah.edu/umelt/umelt.html). Selected primer sequences (reported in **Table 9**) were sent to integrated DNA technology for oligomer synthesis. The lyophilized primers were resupsended to obtain a 100µM stock concentration and stored at -20˚C. Forward and reverse primers for each gene were also mixed and diluted in water to obtain a 2µM primer mix working solution.

Gene	Forward primer	Reverse Primer	Amplicon length
mTOR Pathway			
mTOR	TCTTCCATCAGACCCAGTGA	GCTGCCAGCGATCTGAATAA	90
GRB10	CACCTGCCTGGCTTCTATTA	TGACTGAGGAGCAGAGAAATG	102
4E-Bp1	CGGAAATTCCTGATGGAGTG	CCGCTTATCTTCTGGGCTATT	153
s6K	CATGAGGCGACGAAGGAG	GGTCCAGGTCTATGTCAAACA	101
eIF4e	GAAAAACAAACGGGGAGGAC	TCTCCAATAAGGCACAGAAGTG	105
Insulin and insulin like growth factor			
IGF2r	GAAACAGAGTGGCTGATGGA	CTGAGGGCTTTCACTGACTT	104
IRS2	CCACCATCGTGAAAGAGTGAA	CAGTGCTGAGCGTCTTCTT	91
PTEN	GGTAGCCAGTCAGACAAATTCA	CAACCAGAGTACTACCACCAAAG	105
ETV6	AGGCACCATAATCCCTCCCT	GGGGTCTGCAGCTGTTTAGT	90
FoxO3a	GGAGAGCTGAGACCAGGGTA	AGATTCTCGGCTGACCCTCT	84
Sirtuin and Nampt pathway			
Sirt1	AGAACCCATGGAGGATGAAAG	TCATCTCCATCAGTCCCAAATC	111
MASH1	GCAGCACACGCGTTATAGTA	ACTCGTTTCTAGAGGGCTAAGA	122
UCP2	CCTCTACAATGGGCTGGTTG	TCAGAGCCCTTGGTGTAGAA	105
Nrip1	GGAGACAGACGAACACTGATATT	GGTCTGTAGCAGTAAGCAGATAG	103
NAMPT	CCAGGAAGCCAAAGATGTCTAC	GAAGATGCCCATCATACTTCTCA	98
Other			
ABTB1	ACCATGAACCCGTCCTGA	AAGCAGGCATAGTACCTCCA	89
Housekeepers			
VIM	CTTTGCCGTTGAAGCTGCTA	GAAGGTGACGAGCCATTTCC	92
RPLP2	CAGAGGAGAAGAAAGATGAGAAGAA	CTTTATTTGCAGGGGAGCAG	101
ACTG1L	GGCTGAGTGTTCTGGGATTT	GGCCAAAGACATCAGCTAAGA	125

Table 9 - **Primer sequences for target and housekeeping genes**. Primer pairs and respective amplicon lengths for each gene used in quantitative polymerase chain reaction experiments. Genes are subdivided according to pathway.

Based on the microarray previously carried out by our group, the following housekeepers were selected; Vimentin, Ribosomal Protein Large P2 (RPLP2) and Gamma Actin1 (ACTG1). These genes were selected as the genes undergoing the least variability following both media-only and treatment conditions across 5 different time-points in the genome-wide array. Variability was assessed by measuring the coefficient of variation - dividing the standard deviation of expression by the mean expression. A low coefficient of variation is regarded as the gold-standard in housekeeper selection (Hill et al., 2014). Negligible variability between conditions was also seen across qPCR results in the present study. Primers for these are reported in **Table 9.** The primers were also checked for specificity by

agarose gel electrophoresis. Briefly, agarose gels were made with 1x tris-acetate-EDTA (TAE) buffer and agarose (A9539, Sigma-Aldrich) at a concentration of 1.5%. After melting the agarose in TAE, ethidium bromide (1% solution in water, 111615, MerckMillipore) was added at 1µl/100ml TAE and the solution was poured into moulds containing well combs. Samples were mixed with 1x DNA Loading Dye (R0611, Thermo Fisher Scientific) and loaded into the wells of the solidified gel alongside a 100 base-pair DNA ladder (07-11-00050, Solis Biodyne). The gel was run with 1% TAE at 4V/cm for approximately 30 minutes and analysed using the BioSpectrumAC Imaging System (UVP) and the Vision Works LS software (UVP).Statistics

Statistical analysis for qPCR data was carried out using the GraphPad Prism software. The Shapiro-Wilkin test was used to test for normality. Accordingly, parametric t-tests or the non-parametric Mann-Whitney tests were carried out to compare the relative expression between the young and old subgroups for each gene. Relative expression and cellular readouts were tested for associations with correlations. If a significant correlation was found, linear regressions were carried out to investigate this association. The significance threshold was then adjusted according to the number of multiple comparisons as per the Bonferroni method.

3.3 Results

In this chapter, the MATOC cohort was used to test whether serum can alter cellular readouts according to age of the donor in an *in vitro* NSC parabiosis model. We also aimed to correlate the cellular readouts to hippocampal volumes and cognition. Finally, using the Young-Old cohort we aimed to identify molecular effectors behind these associations by testing the expression levels of candidate nutrient-sensing genes within this *in vitro* assay.

3.3.1 Cellular readouts following *in vitro* parabiosis assay are not associated with age but to hippocampal subfield volumes in MATOC cohort.

To test whether serum donor's age impacted the cellular readouts following the differentiation assay of the parabiosis model were first tested for correlation to serum donor's age. Immunocytochemical analysis followed by Pearson's correlations revealed no association between the expression of CC3 (apoptosis marker), H2AX (DNA damage marker), MAP2 (immature neuron marker), DCX (neuroblast marker), Ki67 (proliferation marker) or the number of cells following the assay and participant's age (see Figure 16). The p and R values of each correlation are reported in **Table 10.**

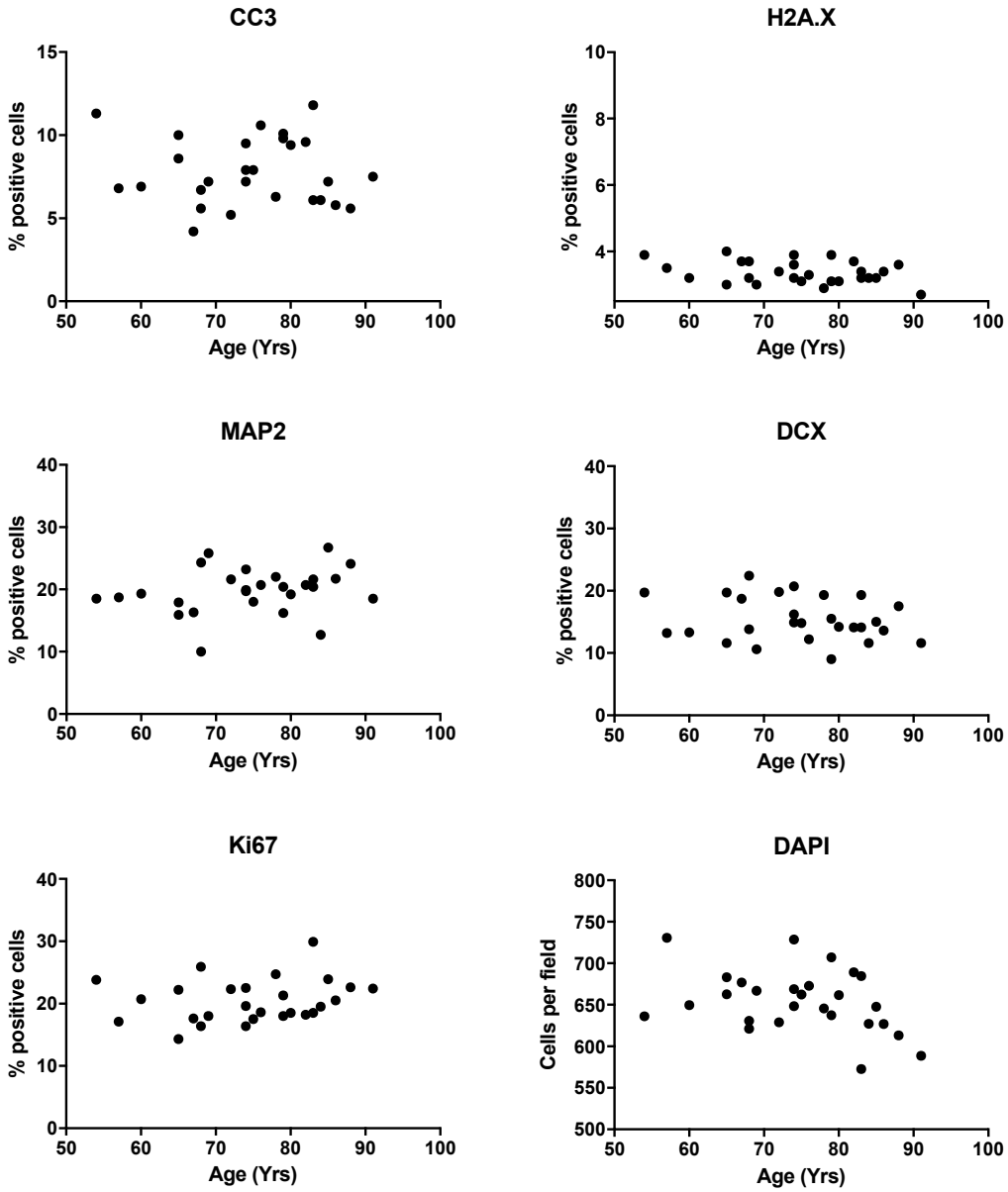

Figure 16 - Effect of serum donor's age on cellular markers. Scatterplots showing the percentage of positive HPC0A07/03A cells for each cellular marker following serum treatment and the corresponding participant's age. Markers for apoptosis (CC3), DNA damage (H2AX), immature neurons (MAP2), neuroblasts (DCX) and proliferation (Ki67) are reported. Also reported is the number of cells per field as a measure of cell density based on the nuclear marker DAPI. Each dot represents a participant.

Cellular readouts	r	p value
Age and CC3%	-0.05	0.82
Age and H2AX%	-0.26	0.20
Age and MAP2%	0.31	0.12
Age and DCX%	-0.18	0.36
Age and KI67%	0.28	0.16
Age and Cells per Field	-0.36	0.06

Table 10 - Correlation results of the effect of serum donor's age on cellular markers. Table showing the r value and p value of each Pearson's correlation assessing the association between each cellular marker and serum donor's age.

To assess if the cellular readouts of the *in vitro* parabiosis assay were related to hippocampal volumes, subfield volumes were investigated. First, each relevant subfield was tested for association to participant's age. This revealed strong associations between each subfield and participant's age. Following linear regressions, increased age was found to be predictive of decreased subiculum, dentate gyrus, CA1, CA3, CA4 and whole hippocampus volumes. Graphs for these associations are in **Figure 17**. p values and r and r^2 for each correlation and linear regression are reported in **Table 11**.

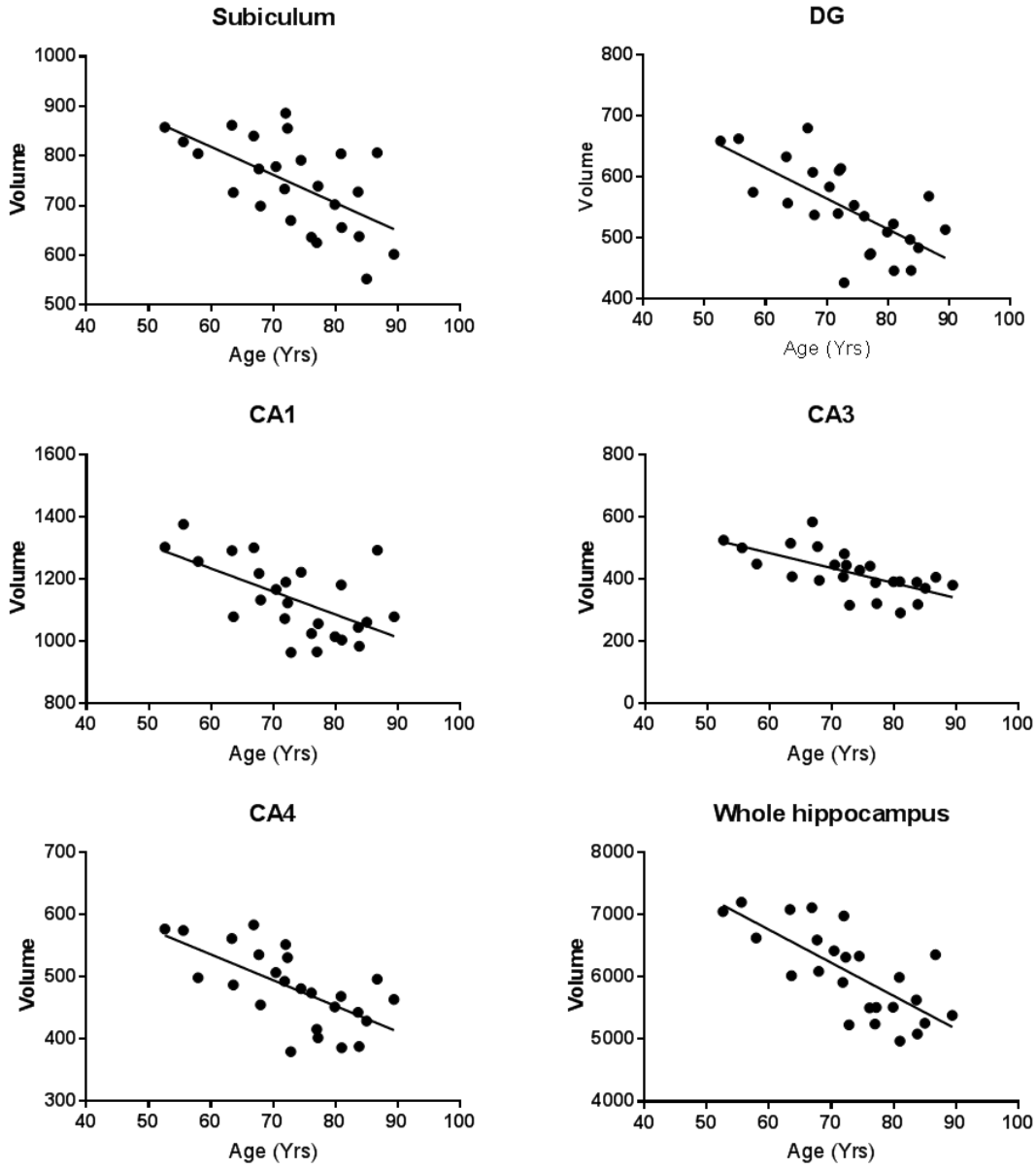

Figure 17 - Effect of age on hippocampal subfield volume - Scatterplots showing linear regressions assessing the relationship between hippocampal volumes and participant's age in years. Liner regression line is shown on each graph. **DG** - Dentate Gyrus

Age and Subfields Volumes	r	r^2	p value
Age and Subiculum	**-0.59**	**0.36**	**0.002***
Age and Dentate Gyrus (DG)	**-0.57**	**0.35**	**0.003***
Age and CA1	**-0.78**	**0.43**	**<0.0001***
Age and CA3	**-0.70**	**0.43**	**<0.0001***
Age and CA4	**-0.72**	**0.47**	**<0.0001***
Age and Whole Hippocampus	**-0.74**	**0.54**	**<0.0001***

Table 11 - Correlation and linear regression results of the effect of age on hippocampal subfield volumes - Table showing the results of correlations and linear regressions testing the association between age and hippocampal volumes. r value following Pearson's correlation and the r^2 and p values following linear regressions are reported. Following Bonferroni correction to account for the 6 multiple comparisons, the significance threshold for this analysis was set to 0.0083. Significant results before correction are in bold. * denotes results surviving multiple testing correction.

Once the association of subfields and hippocampus volume with age was confirmed, cellular markers were tested for association to each subfield's volume and to whole hippocampus volume. To do this, the percentage positive cells for each marker following incubation with serum was tested for association to the serum donor's subfield and whole hippocampus volumes. Values were age-regressed to account for the strong effect of age on hippocampal volumes. No association was found between volumes and CC3, MAP2, Ki67 expression or cell density (See section 8.2.1 in appendix for correlation matrix). However, the level of DNA damage, shown by H2AX expression in the HPCs, correlated with Subiculum, CA3, CA4 and Whole hippocampus volumes. In addition, the number of neuroblasts, as shown by DCX expression in the HPCs, correlated with dentate gyrus, CA3, CA4 and whole hippocampus volume. Due to the large number of multiple comparisons (36) needed to test each marker against each subfield, these associations did not survive multiple testing. Correlation and linear regression results for H2AX and DCX are reported in **Table 12** and **Table 13** respectively. **Figure 18** and **Figure 19** shows the scatterplots illustrating these associations.

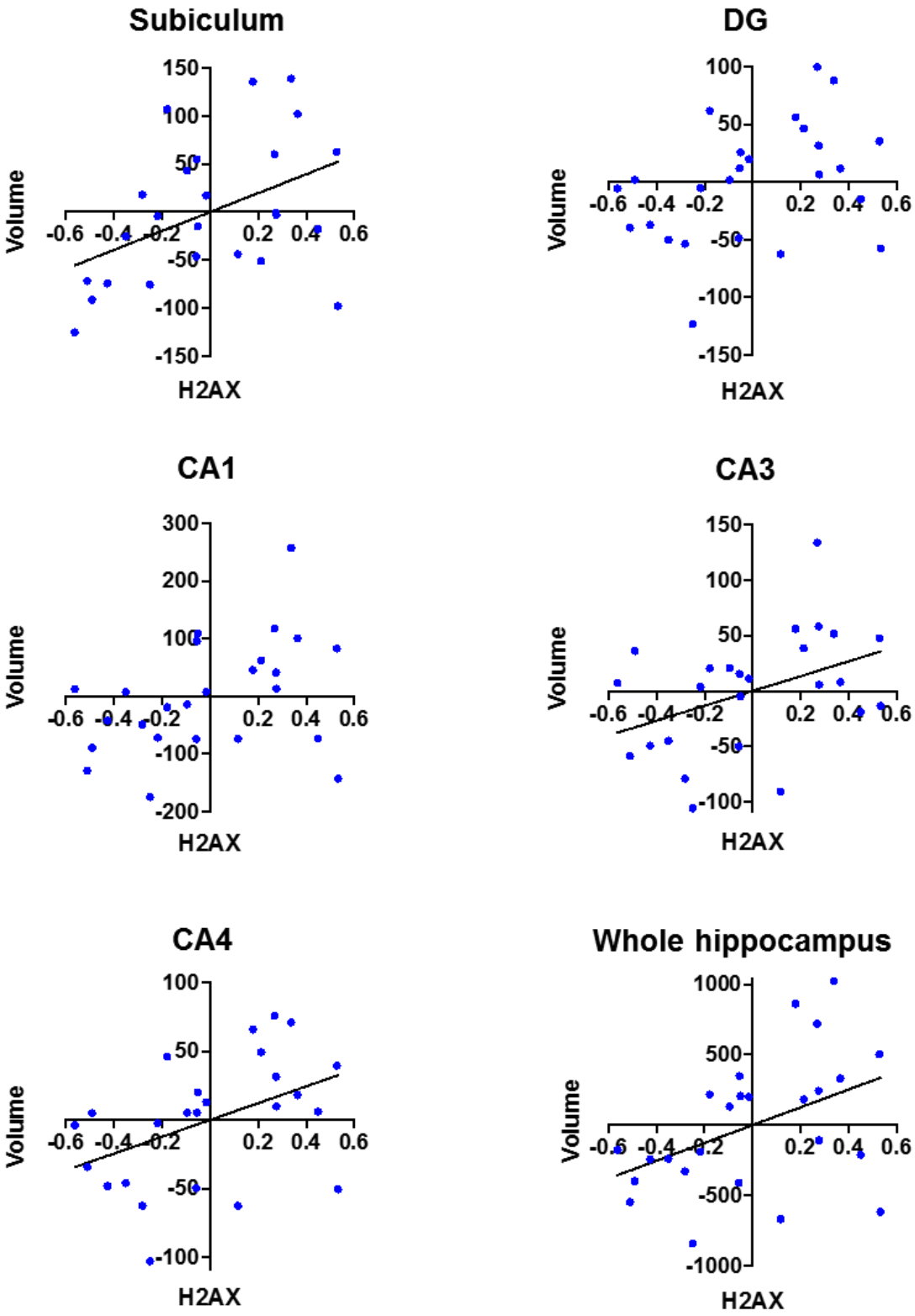

Figure 18 - **Associations of DNA damage marker to hippocampal subfield volumes** Scatterplots showing the association between DNA damage (H2AX expression) following serum incubation and serum donor's hippocampal volumes. In each graph, the x-axis shows the age-regressed percentage of HPC0A07/03A cells positive for H2AX expression and the y-axis shows the age-regressed volume of the specific hippocampal subfield. Linear regression line shown in black, graphs with no line indicate non-significant correlation results. Values are age-regressed. **DG-** Dentate gyrus.

H2AX and Subfield Volumes	r	r^2	p value
H2AX and Subiculum	**0.43**	**0.20**	**0.025**
H2AX and Dentate Gyrus (DG)	0.38	0.14	0.061
H2AX and CA1	0.41	0.15	0.053
H2AX and CA3	**0.39**	**0.17**	**0.039**
H2AX and CA4	**0.49**	**0.19**	**0.029**
H2AX and Whole Hippocampus	**0.45**	**0.19**	**0.028**

Table 12 - Correlation and linear regression results for the association of DNA damage marker to hippocampal subfield volumes Table showing the results of correlations and linear regressions testing the association between H2Ax expression following the parabiosis assay and serum donor's hippocampal volumes. r value following Pearson's correlation and the r^2 and p values following linear regressions are reported. Bonferroni correction was used to account for 36 multiple comparisons (6 subfields and 6 markers), the significance threshold for this analysis was set to 0.0014. Significant results before correction are in bold. No association survived multiple testing correction.

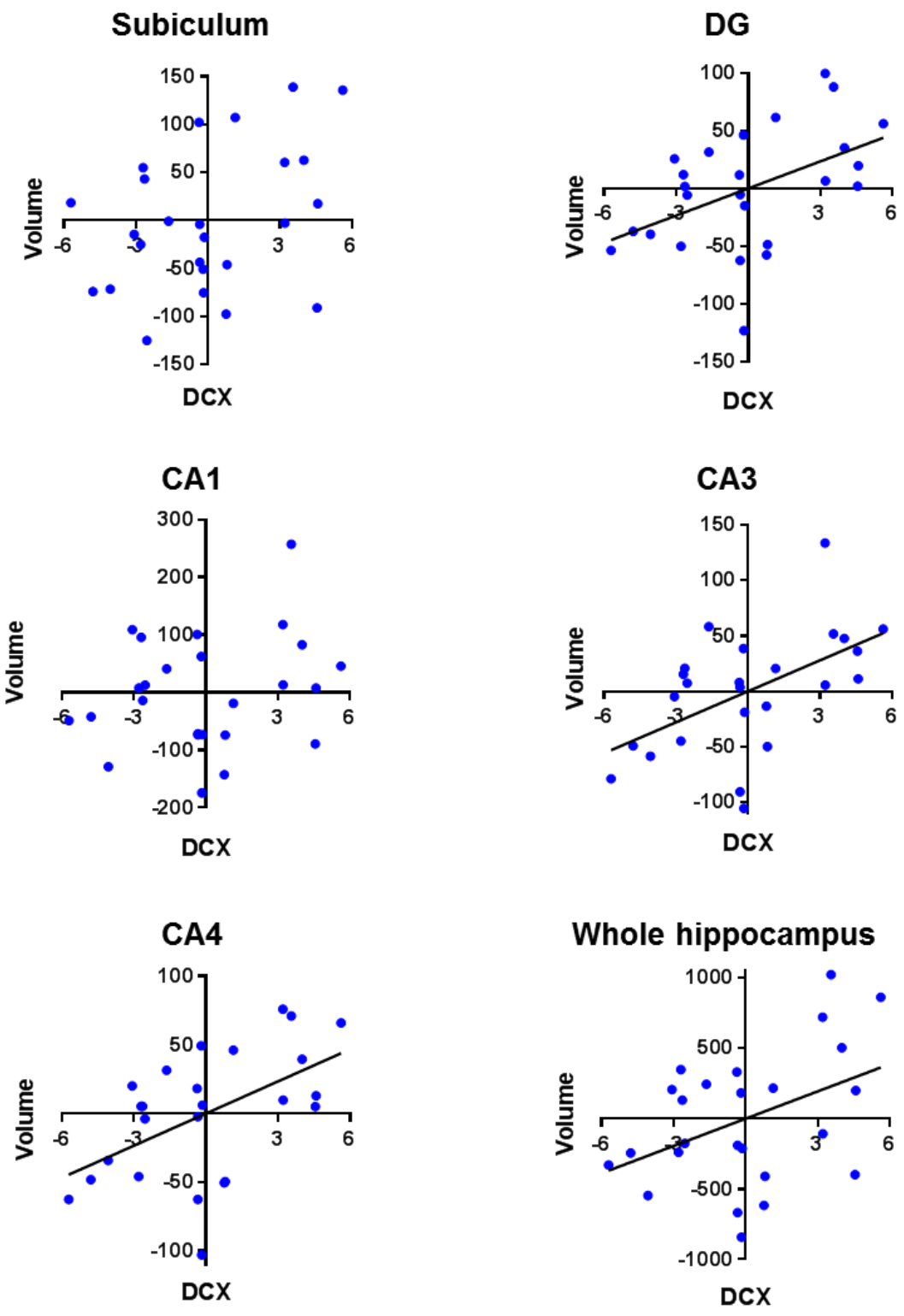

Figure 19 - Associations of neuroblast marker to hippocampal subfield volumes - Scatterplots showing the association between number of neuroblasts (DCX expression) following serum incubation and hippocampal volumes. In each graph, the x-axis shows the age-regressed percentage of HPC0A07/03A cells positive for H2AX expression and the y-axis shows the age-regressed volume of the specific hippocampal subfield. Linear regression line shown in black, graphs with no line indicate non-significant correlation results. Values are age-regressed. **DG**- Dentate gyrus.

DCX and Subfield Volumes	r	r^2	p value
DCX and Subiculum	0.28	0.14	0.065
DCX and Dentate Gyrus (DG)	**0.45**	**0.23**	**0.016**
DCX and CA1	0.10	0.06	0.258
DCX and CA3	**0.50**	**0.30**	**0.005**
DCX and CA4	**0.47**	**0.28**	**0.007**
DCX and Whole Hippocampus	**0.32**	**0.18**	**0.035**

Table 13 - Correlation and linear regression results for the association of neuroblast marker to hippocampal subfield volumes - Table showing the results of correlations and linear regressions testing the association between DCX expression following the parabiosis assay and serum donor's hippocampal volumes. r value following Pearson's correlation and the r^2 and p values following linear regressions are reported. Bonferroni correction was used to account for 36 multiple comparisons (6 subfields and 6 markers), the significance threshold for this analysis was set to 0.0014. Significant results before correction are in bold. No association survived multiple testing correction.

3.3.2 Cellular readouts following *in vitro* parabiosis assay are associated to performance on PAL task in MATOC.

Next, to assess the relationship between cellular readouts resulting from the parabiosis assay and cognition, we investigated PAL performance. Firstly, PAL was tested for correlation with age and education to assess whether these affected PAL score. Performance on the recall phase, but not the recognition phase, of the PAL task showed a negative association with participant's age. In contrast scores from the recognition phase, but not the recall phase, of the PAL task were positively correlated with the participant's level of education. These results suggest participants with lower education levels and increased age are more likely to perform badly on the PAL task. Results from the Pearson's correlations and subsequent linear regressions are reported in **Table 14**. These associations however, did not survive Bonferroni correction. Scatterplots of the 4 correlations are reported in **Figure 20.**

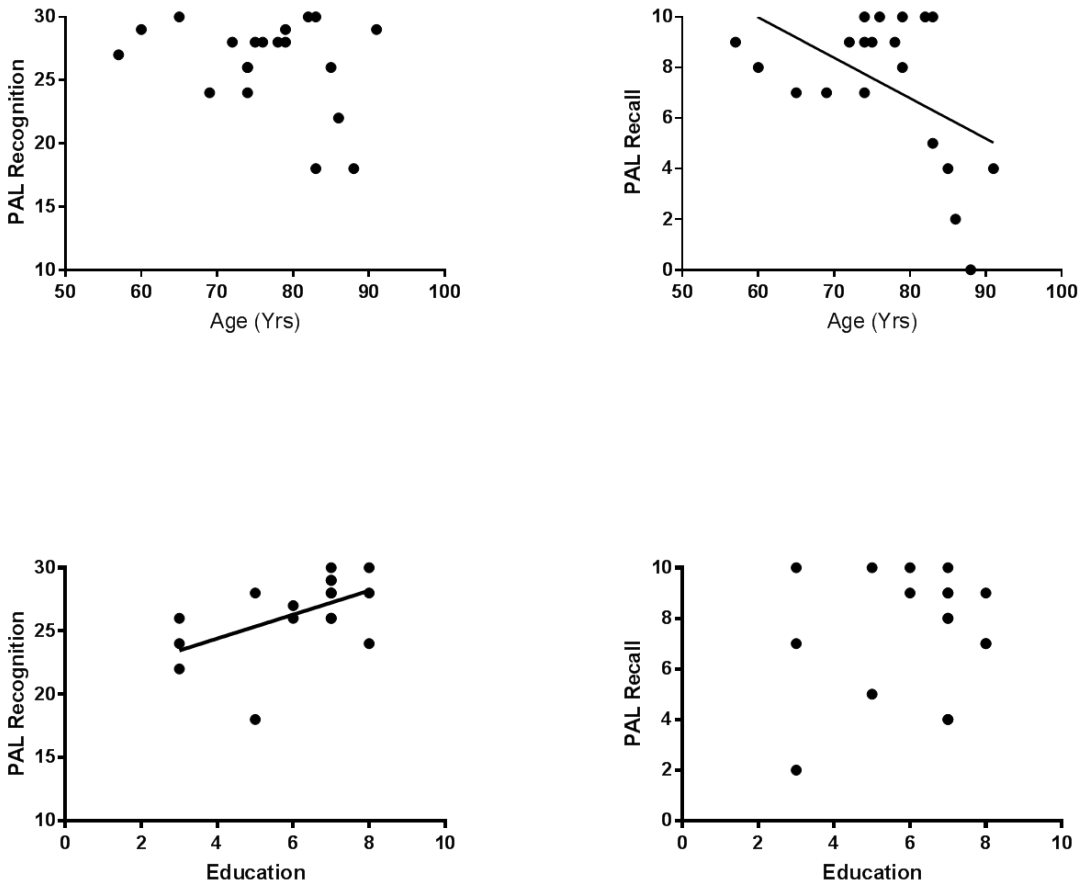

Figure 20 - Effect of age and education on paired associates learning task - Scatterplots showing the association of recall and recognition on paired associates learning (PAL) scores to age and education. In each graph, age is reported on the x-axis and PAL recall or PAL recognition is on the y-axis. Linear regression line shown in black, graphs with no line indicate non-significant correlation results.

PAL and Covariates	r	r^2	p value
PAL Recognition and Age	-0.30	0.09	0.198
PAL Recall and Age	**-0.49**	**0.24**	**0.028**
PAL Recognition and Education	**0.53**	**0.28**	**0.029**
PAL Recall and Education	-0.07	0.03	0.536

Table 14 - Correlation and linear regression results for the effect of age and education on paired associated learning task - Table showing the results of correlations and linear regressions testing the association between paired associated learning (PAL) score and age or education level. r value following Pearson's correlation and the r^2 and p values following linear regressions are reported. Following Bonferroni correction to account for 4 multiple comparisons, the significance threshold for this analysis was set to 0.0125. Significant results before correction are in bold. No association survived multiple testing correction.

Next, to address the 3rd aim of this chapter (outlined in section 3.1.7), we assessed the relationship between cellular readouts resulting from the parabiosis assay and PAL

performance. Given the above results showing a possible association of PAL performance to age and education, age and education regressed PAL values were used. in Pearson's correlations showed no association to PAL performance for cell death (CC3), DNA damage (H2AX), neuroblast number (DCX) or proliferation (KI67). The number of immature neurons, as evidenced by the percentage of cells positive for MAP2, showed significant association to PAL recognition scores. This result indicates serum from participants with worse PAL recognition scores induced an increase in immature neurons. Furthermore, cell density, as evidence by cells per field, showed significant association to PAL recall scores. This indicates serum from participants who performed better on the recall phase of the cognitive task induced an increase in cell number. Importantly, these associations did not survive multiple testing correction. **Table 15** and **Table 16** show the Pearson's correlation and linear regression results assessing the association between cellular readouts and PAL performance. **Figure 21** shows scatterplots of the association between MAP2 and cells per field to PAL performance.

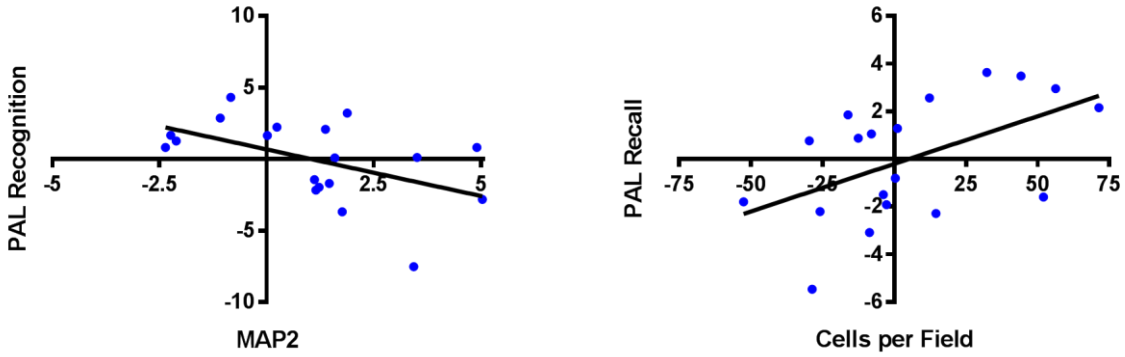

Figure 21 - Association between cellular markers and paired associates learning task - Scatterplots showing **RIGHT** the association of performance on the recognition phase of the paired associates learning (PAL recognition) (y-axis) to MAP2 expression in the *in vitro* model following treatment with corresponding serum (x-axis) and **LEFT** the association of performance on the recall phase of the paired associates learning (PAL recall) (y-axis) to cell density (cells per field) in the *in vitro* model following treatment with corresponding serum (x-axis). Linear regression line shown in black.

PAL Recognition and Cellular	r	r^2	p value
PAL and CC3%	0.39	-	NS (>0.05)
PAL and H2AX%	-0.34	-	NS (>0.05)
PAL and MAP2%	**-0.51**	**0.25**	**0.029**
PAL and DCX%	-0.26	-	NS (>0.05)
PAL and KI67%	-0.15	-	NS (>0.05)
PAL and Cells per Field	0.18	-	NS (>0.05)

Table 15 - Correlation and linear regression results for the association of performance on paired associates learning recognition and cellular markers - Table showing the results of correlations and linear regressions testing the association between paired associates learning (PAL) recognition score and cellular marker expression following the parabiosis assay. r value following Pearson's correlation and the r^2 and p values following linear regressions are reported. Following Bonferroni correction to account for 4 multiple comparisons, the significance threshold for this analysis was set to 0.0125. Significant results before correction are in bold. No association survived multiple testing correction.

PAL Recall and Cellular	r	r^2	p value
PAL and CC3%	0.38	-	NS (>0.05)
PAL and H2AX%	0.08	-	NS (>0.05)
PAL and MAP2%	-0.31	-	NS (>0.05)
PAL and DCX%	-0.03	-	NS (>0.05)
PAL and KI67%	-0.29	-	NS (>0.05)
PAL and Cells per Field	**0.54**	**0.27**	**0.022**

Table 16 - Correlation and linear regression results for the association of performance on paired associates learning recall and cellular markers Table showing the results of correlations and linear regressions testing the association between paired associates learning (PAL) recall score and cellular marker expression following the parabiosis assay. r value following Pearson's correlation and the r^2 and p values following linear regressions are reported. Following Bonferroni correction to account for 4 multiple comparisons, the significance threshold for this analysis was set to 0.0125. Significant results before correction are in bold. No association survived multiple testing correction.

3.3.3 Molecular pathways mediating the impact of the systemic milieu on hippocampal NSCs

To address the final two aims of this chapter, we performed a literature-based candidate gene selection. Following this, the expression levels of the selected genes were tested using serum from the YOC cohort. As opposed to the MATOC cohort used thus far, this cohort allowed for the direct comparison of the effects of young donor serum to those of old donor serum. Given the heterogeneity seen following the work with the MATOC cohort, we believed this experimental setup was better suited to identify molecular alterations.

3.3.3.1 Candidate gene selection

After encouraging results suggesting a relationship between the assay's cellular readouts and human cognitive and imaging data, we aimed to investigate the molecular pathways driving these associations.

As detailed in the chapter 1, literature search revealed the mTOR, IIS and Sirtuin pathways to be key mediators in the interplay between nutrition, ageing and stem cell function. Furthermore, ABTB1 was highlighted as differentially expressed (14% decrease, p value 0.001, Murphy *et al*. in prep.) in a microarray carried out by previous lab members. As well as ABTB1, 5 genes in each pathway were selected as candidate genes within this chapter. The 5 genes were selected to span various levels of the signalling cascade, therefore key receptors, second messengers and effector molecules were selected.

3.3.3.2 Expression of candidate genes is unaltered in Young to Old cohort

To assess the role of the candidate genes in the parabiosis assay, a case-control cohort was used. The YOC cohort was comprised of young or old participants allowing the comparison of gene expression between the two groups following the differentiation assay. Shapiro-Wilk normality test was used to determine which comparison test to use. For normally-distributed data the Welch's t-tests were used to compare the expression levels of each gene in the young and old groups. Due to different sample sizes (15 young and 22 old) and different variances between subgroups, Welch's t-test was selected over Student t-test. Degrees of freedom and p values for each test are reported in **Table 17** For data without normal distribution, Mann-Whitney *U* tests were used to compare the two groups. U statistic and p values are reported in **Table 18**. Following Bonferroni correction, no gene showed significant differences in expression levels between cells treated with serum from young and old participants. Graphs for the 16 tests are shown in **Figure 22.**

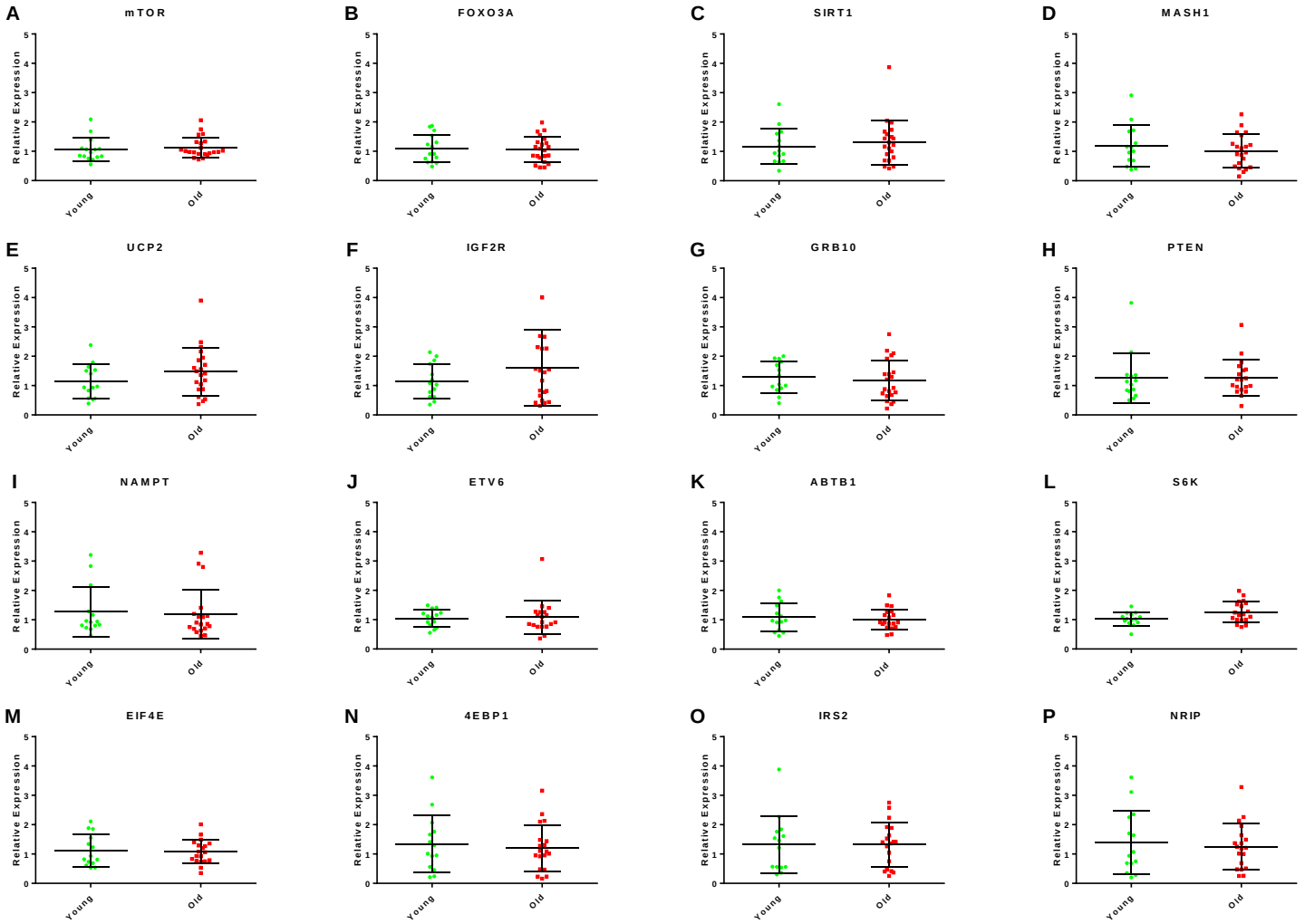

Figure 22 - Candidate gene expression following in vitro parabiosis - Gene expression levels of the 16 candidate genes by the HPC0A07/03A cells following treatment with serum from the young (green) and old (red) subgroups of the young to old cohort. In all graphs, relative expression is on the y-axis . Error bars represent standard deviation.

Gene	Test	df	p value
FOXO3A	Welch's t-test	0.190	0.851
MASH1	Welch's t-test	0.780	0.443
UCP2	Welch's t-test	1.396	0.172
GRB10	Welch's t-test	0.540	0.593
ABTB1	Welch's t-test	0.498	0.623
S6K	**Welch's t-test**	**2.319**	**0.027**
EIF4E	Welch's t-test	0.234	0.817
4EBP1	Welch's t-test	0.454	0.654
NRIP	Welch's t-test	0.437	0.666

Table 17 - Welch's t-test results comparing gene expression following treatment with young or old serum - Table showing the results of the t-tests carried out to compare the expression levels of candidate genes in the HPC0A07/03A following treatment with serum from either the young or old subgroups. Gene expression was measured as relative expression following the serum assay. df - Degrees of freedom. Following Bonferroni correction to account for 16 multiple comparisons, the significance threshold for this analysis was set to 0.0031. Significant results before correction are in bold. No result survived multiple testing correction

Gene	Test	df	p value
MTOR	Mann-Whitney U test	136.5	0.387
SIRT1	Mann-Whitney U test	129.5	0.566
IGF2R	Mann-Whitney U test	124.5	0.459
PTEN	Mann-Whitney U test	117	0.571
NAMPT	Mann-Whitney U test	118.5	0.609
ETV6	Mann-Whitney U test	124.5	0.767
IRS2	Mann-Whitney U test	131	0.950

Table 18 - Mann-Whitney U tests results comparing gene expression following treatment with young or old serum - Table showing the results of the Mann-Whitney U tests carried out to compare the expression levels of candidate genes in the HPC0A07/03A cells following treatment with serum from either the young or old subgroups. Gene expression was measured as relative expression following the serum assay. df – Degrees of freedom. Following Bonferroni correction to account for 16 multiple comparisons, the significance threshold for this analysis was set to 0.0031..

3.3.3.3 Associations between candidate gene expression levels and cellular readouts

Due to the lack of significant differences in gene expression between young and old subgroups, we investigated whether gene expression related to cellular readouts (i.e. KI67, CC3, MAP2 and DCX expression or cell density) irrespective of participant age.

Following Shapiro-Wilk normality test, all variables showed a normal distribution except for Ki67 values. Ki67 data was therefore log-transformed and retested for normality. Log(%Ki67) showed a normal distribution and was therefore used in this section. Pearson's correlations were used to assess potential associations between molecular and cellular

readouts following the *in vitro* parabiosis assay. Expression levels of MASH, ETV6, S6K, EIF4E, 4EBP1, IRS2, NRIP showed no correlation to cellular readouts. See appendix section 8.2.2 for p and r values of these correlations. The remaining genes showed interesting correlations to cellular readouts and are reported below.

3.3.3.3.1 Significant correlations with genes in the mTOR pathway

mTOR expression showed a positive correlation with cell number. There was no correlation with other cellular markers. **Figure 23** shows the graph representing the association between cell number and mTOR expression. Correlation results for both significant and non-significant associations between mTOR expression and cellular markers are reported in **Table 19** GRB10, another molecule involved in mTOR signalling showed a similar association to cell density: increase GRB10 expression was correlated to increased cell number. Again, this was not reflected in correlations with other cellular markers. See **Table 20** for r and p values of the correlations testing GRB10 expression and cellular markers for association. See **Figure 23** for the graph showing this association.

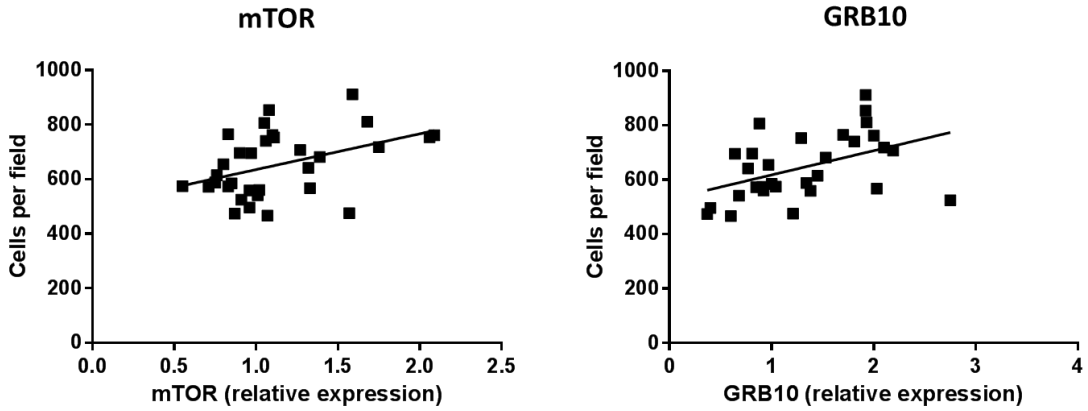

Figure 23 - Association between genes in the mTOR pathway and cellular markers - Scatterplots showing the significant correlation between (**Left**) mTOR and cell density (cells per field) and (**Right**) GRB10 and cell density (cells per field) following the *in vitro* parabiosis assay. Each dot represents a participant. Line of best fit is shown on each graph.

mTOR	r	p value
mTOR and Ki67	0.02	NS (0.917)
mTOR and CC3%	-0.20	NS (0.292)
mTOR and MAP2%	0.18	NS (0.479)
mTOR and DCX%	-0.22	NS (0.251)
mTOR and cells/field	**0.42**	**0.016**

Table 19 - Correlations results for the association of cellular markers and mTOR gene expression - Table reporting the Pearson's correlation results of mTOR expression and cellular markers. Cellular markers include proliferation (KI67), apoptosis (CC3), immature neurons (MAP2), neuroblasts (DCX) and cell density (cells /field). All markers except for cell density are defined as the percentage of cells positive for that marker relative to the total number of cells following the serum assay. Expression levels are the resulting gene expression levels following the *in vitro* parabiosis assay. Significant results in bold

GRB10	r	p value
GRB10 and Ki67	-0.32	NS (0.088)
GRB10 and CC3%	-0.19	NS (0.335)
GRB10 and MAP2%	0.26	NS (0.192)
GRB10 and DCX%	0.11	NS (0.586)
GRB10 and cells/field	**0.45**	**0.012**

Table 20 - Correlations results for the association of cellular markers and GRB10 gene expression Table reporting the Pearson's correlation results of GRB10 expression and cellular markers. Cellular markers include proliferation (KI67), apoptosis (CC3), immature neurons (MAP2), neuroblasts (DCX) and cell density (cells /field). All markers except for cell density are defined as the percentage of cells positive for that marker relative to the total number of cells following the serum assay. Expression levels are the resulting gene expression levels following the *in vitro* parabiosis. Significant results in bold.

3.3.3.3.2 Significant correlations with Insulin and insulin-like pathway genes

Expression levels of FOXO3A, a key molecule in the IIS pathway, correlated with the apoptosis marker (CC3), the number of immature neurons (MAP2) and cell density. These results show increased FOXO3A expression was associated to increased numbers of cells in general and immature neurons in particular. In addition, FOXO3A expression levels were associated with decreasing apoptosis. See **Figure 24** and **Table 21** for graphs and results of these correlations respectively. Expression of PTEN, a negative regulator of the IIS pathway, was negatively correlated with cell density but not to other markers. **Figure 24** shows the graphical representation of this association and **Table 22** reports the correlation results of all correlations testing PTEN expression level for association. Expression of IGF2R, the scavenger receptor of the IIS pathway, showed a significant and negative association to cell density and no association to any of the other markers. See **Figure 24** and **Table 23** for graphs and results of the correlation pertaining to IGF2R expression levels and cellular markers.

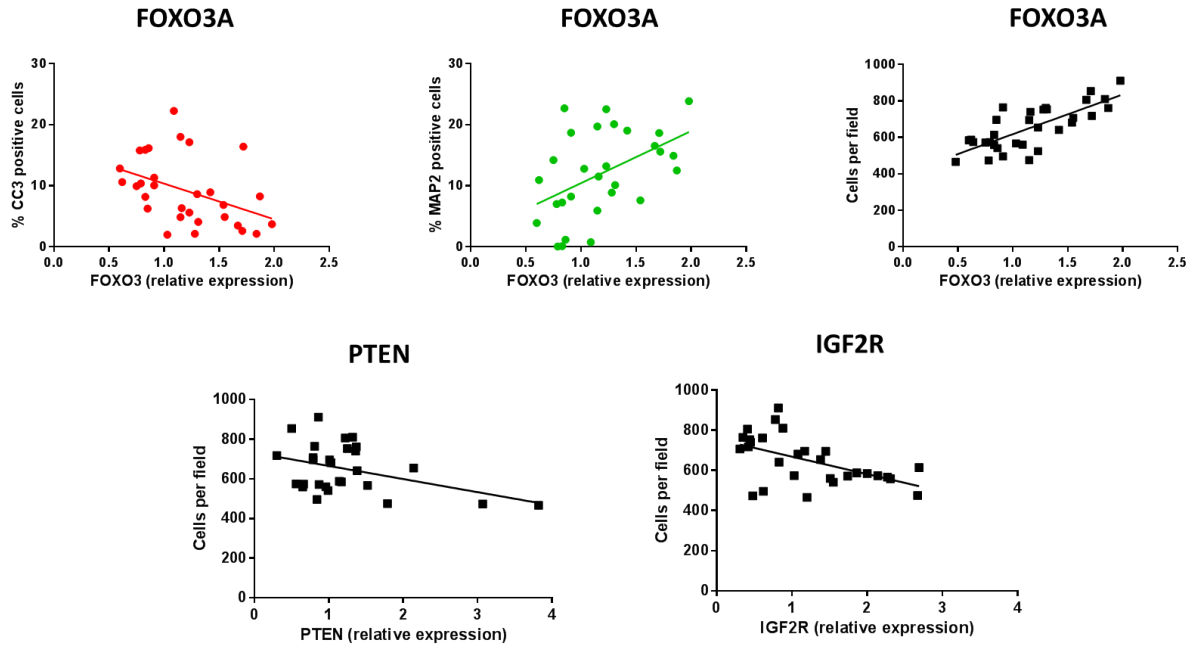

Figure 24 - Association between genes in the Insulin and Insulin-like pathway and cellular markers (**FOXO3A**) Scatterplots showing the significant correlation between FOXO3A expression, apoptosis (CC3), immature neurons (MAP2%) and cell density (cells per field) following the parabiosis assay. (**PTEN**) Scatterplot showing the significant correlation between PTEN and cell density (cells per field) following the parabiosis assay. (**IGF2R**) Scatterplots showing the significant correlation between IGF2R expression and cell density (cells per field) following the in vitro parabiosis assay. Each dot represents a participant. Line of best fit is shown on each graph.

FOXO3	r	p value
FOxO3a and Ki67%	-0.18	NS (0.335)
FOXO3A and CC3%	**-0.42**	**0.022**
FOXO3A and MAP2%	**0.48**	**0.009**
FOXO3A and DCX%	-0.13	NS (0.503)
FOXO3a and cells/field	**0.76**	**<0.0001***

Table 21 - Correlations results for the association of cellular markers and FOXO3A gene expression Table reporting the Pearson's correlation results of FOXO3A expression and cellular markers. Cellular markers include proliferation (KI67), apoptosis (CC3), immature neurons (MAP2), neuroblasts (DCX) and cell density (cells /field). All markers except for cell density are defined as the percentage of cells positive for that marker relative to the total number of cells following the serum assay. Expression levels are the resulting gene expression levels following the *in vitro* parabiosis assay. Significant results in bold.

PTEN	r	p value
PTEN and Ki67	-0.04	NS (0.843)
PTEN and CC3%	0.05	NS (0.824)
PTEN and MAP2%	-0.04	NS (0.843)
PTEN and DCX%	0.02	NS (0.918)
PTEN and cells/field	**-0.41**	**0.031**

Table 22 - Correlations results for the association of cellular markers and PTEN gene expression Table reporting the Pearson's correlation results of PTEN expression and cellular markers. Cellular markers include proliferation (KI67), apoptosis (CC3), immature neurons (MAP2), neuroblasts (DCX) and cell density (cells /field). All markers except for cell density are defined as the percentage of cells positive for that marker relative to the total number of cells following the serum assay. Expression levels are the resulting gene expression levels following the *in vitro* parabiosis assay. Significant results in bold.

IGF2R	r	p value
IGF2r and Ki67	0.26	NS (0.166)
IGF2r and CC3%	0.40	NS (0.037)
IGF2r and MAP2%	-0.32	NS (0.101)
IGF2r and DCX%	0.38	NS (0.046)
IGF2r and cells/field	**-0.53**	**0.003**

Table 23 - Correlations results for the association of cellular markers and IGF2R gene expression Table reporting the Pearson's correlation results of IGF2R expression and cellular markers. Cellular markers include proliferation (KI67), apoptosis (CC3), immature neurons (MAP2), neuroblasts (DCX) and cell density (cells /field). All markers except for cell density are defined as the percentage of cells positive for that marker relative to the total number of cells following the serum assay. Expression levels are the resulting gene expression levels following the *in vitro* parabiosis assay. Significant results in bold.

3.3.3.3.3 Significant correlations with genes in the Sirtuin pathway

Expression levels of NAMPT, the rate limiting enzyme in NAD+ biosynthesis, showed a significant association with increased proliferating cells (KI67). As shown by the results in **Table 24**, this increase was not accompanied by changes in other cellular markers. **Figure 25** shows the association between increasing number of KI67 positive cells and increasing NAMPT expression. UCP2, another protein in the sirtuin pathway, showed a similar association to proliferating cells. As for NAMPT, this was accompanied by a lack of further association to cellular markers changes **Figure 25** displays this association.

As shown in **Table 26**, there were no significant associations between cellular readouts and SIRT1 expression.

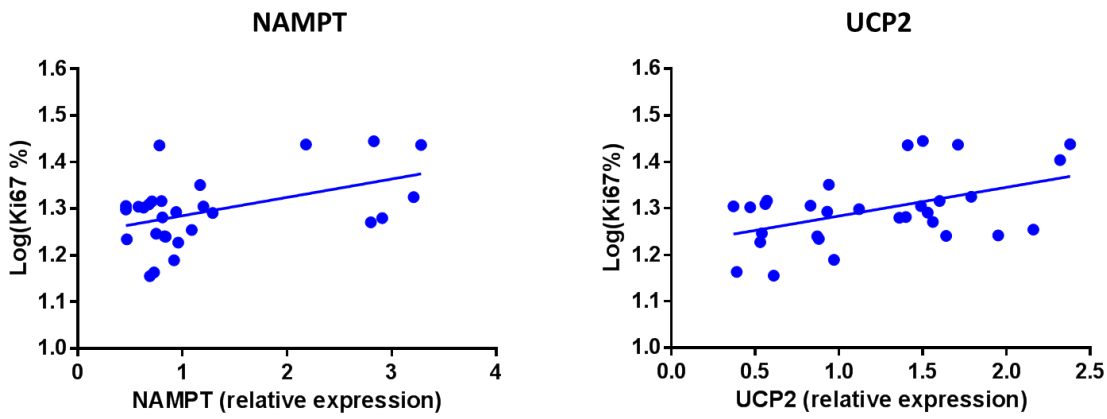

Figure 25 - Association between genes in the sirtuin pathway and cellular markers - Scatterplot showing the significant correlation between NAMPT expression and proliferation in the HPC0A07/03A cells following the parabiosis assay. Each dot represents a participant. Line of best fit is shown. Y axis shows the Log transformed percentage of cells positive for KI67, y axis reports the relative expression of NAMPT

NAMPT	r	p value
NAMPT and Ki67%	**0.47**	**0.012**
NAMPT and CC3%	0.08	NS (0.700)
NAMPT and MAP2%	-0.20	NS (0.340)
NAMPT and DCX%	-0.13	NS (0.530)
NAMPT and cells/ field	0.08	NS (0.700)

Table 24 - Correlations results for the association of cellular markers and NAMPT gene expression Table reporting the Pearson's correlation results of NAMPT expression and cellular markers. Cellular markers include proliferation (KI67), apoptosis (CC3), immature neurons (MAP2), neuroblasts (DCX) and cell density (cells /field). All markers except for cell density are defined as the percentage of cells positive for that marker relative to the total number of cells following the serum assay. Expression levels are the resulting gene expression levels following the *in vitro* parabiosis assay. Significant results in bold.

UCP2	r	p value
UCP2 and Ki67%	**0.48**	**0.008**
UCP2 and CC3%	0.07	NS (0.720)
UCP2 and MAP2%	-0.34	NS (0.086)
UCP2 and DCX%	-0.03	NS (0.894)
UCP2 and cells/ field	-0.24	NS (0.212)

Table 25 - Correlations results for the association of cellular markers and UCP2 gene expression Table reporting the Pearson's correlation results of UCP2 expression and cellular markers. Cellular markers include proliferation (KI67), apoptosis (CC3), immature neurons (MAP2), neuroblasts (DCX) and cell density (cells /field). All markers except for cell density are defined as the percentage of cells positive for that marker relative to the total number of cells following the serum assay. Expression levels are the resulting gene expression levels following the *in vitro* parabiosis assay. Significant results in bold.

SIRT	r	p value
SIRT and Ki67	0.31	NS (0.092)
SIRT and CC3%	0.20	NS (0.319)
SIRT and MAP2%	0.01	NS (0.951)
SIRT and DCX%	0.20	NS (0.314)
SIRT and cells/field	-0.19	NS (0.316)

Table 26 - Correlations results for the association of cellular markers and SIRT1 gene expression Table reporting the Pearson's correlation results of ABTB1 expression and cellular markers. Cellular markers include proliferation (KI67), apoptosis (CC3), immature neurons (MAP2), neuroblasts (DCX) and cell density (cells /field). All markers except for cell density are defined as the percentage of HPC0A07/03A cells positive for that marker relative to the total number of cells following the serum assay. Expression levels are the resulting gene expression levels following the *in vitro* parabiosis assay.

3.3.3.3.4 Significant correlations with ABTB1

Finally, correlations testing the association of ABTB1 to cellular markers results showed a number of interesting associations. As shown in **Table 27**, increased expression of ABTB1 correlated with an increase in cell number (cells per field), as well as an increase in immature neurons (MAP2) and a decrease in apoptotic cell death (CC3). Increased ABTB1 also correlated with decreased proliferation. **Figure 26** depicts the significant correlations between ABTB1 expression and KI67, CC3, MAP2 and cell density.

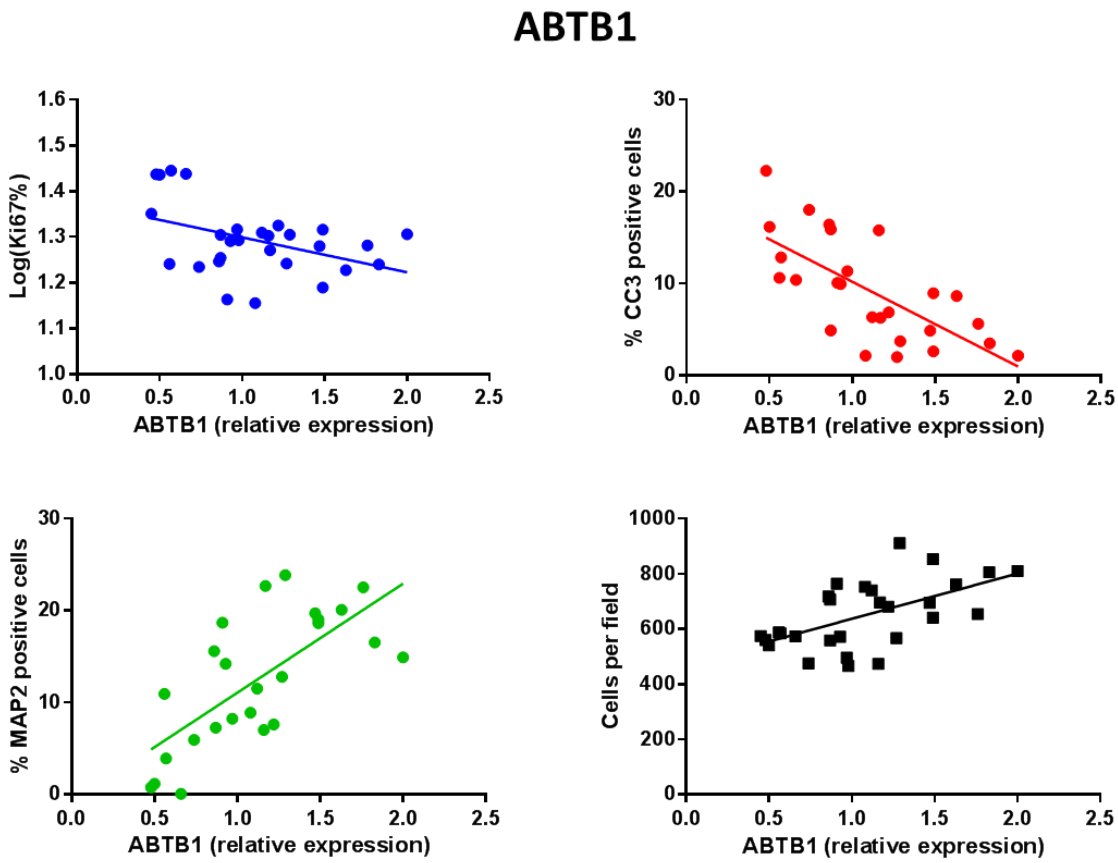

Figure 26 - Association of ABTB1 to cellular markers - Scatterplots showing the significant correlations between ABTB1 expression (x-axis) and proliferation (KI67), apoptosis (CC3), immature neurons (MAP2) and cell density (cells per field) (y-axis) in the HPC0A07/03A cells following the *in vitro* parabiosis assay. Each dot represents a participant. Line of best fit is shown. Log transformed percentage of cells positive for KI67 is reported in the first graph.

ABTB1	r	p value
ABTB1 and Ki67%	**-0.43**	**0.024**
ABTB1 and CC3%	**-0.69**	**<0.0001**
ABTB1 and MAP2%	**0.70**	**<0.0001**
ABTB1 and DCX%	-0.01	NS (0.959)
ABTB1 and cells/ field	**0.58**	**0.001**

Table 27 - Correlations results for the association of cellular markers and ABTB1 gene expression Table reporting the Pearson's correlation results of ABTB1 expression and cellular markers. Cellular markers include proliferation (KI67), apoptosis (CC3), immature neurons (MAP2), neuroblasts (DCX) and cell density (cells /field). All markers except for cell density are defined as the percentage of cells positive for that marker relative to the total number of cells following the serum assay. Expression levels are the resulting gene expression levels following the serum assay. Significant results in bold

3.4 Discussion

In this chapter, we aimed to assess whether serum affected cellular readouts of NSC function, whether this was related to human cognitive and imaging data and finally, whether alterations in nutrient-sensing pathways accompanied these changes. We report no effects of serum age on cellular readouts but show interesting associations between cellular readouts and both PAL performance and hippocampal subfield volumes. Finally, we report correlations between cellular readout and the expression levels of several nutrient-sensing genes following the serum assay that are irrespective of serum donor's age.

3.4.1 Translational potential of the *in vitro* parabiosis assay

To address the first aim of this chapter, we tested cellular readouts for association with serum donor's age. We tested cellular markers for apoptotic cell death, DNA damage, immature neurons, neuroblasts, proliferation and cell density. No marker showed association to donor age in the middle to old-age MATO cohort. This was surprising given the rodent literature suggesting an ageing systemic environment causes alterations in hippocampal NSCs (Katsimpardi et al., 2014; Villeda et al., 2011, 2014). Given previous research in this *in vitro* model showing increased apoptosis following treatment with aged serum when compared to treatment with young serum, the lack of association may be explained by the age-range of the serum donors. In this study, the participants ranged from 52 to 89 which is nearly identical to the age range of the old subgroup used by Murphy et al. (53-89) (Murphy et al., 2018). This suggests that either the effects of an ageing systemic environment plateaus off past middle-age and therefore the effects of a middle-aged serum are not significantly different to those of older serum, or that a wider age gap is necessary to detect these effects. Besides the difference in age, the experimental design used by Murphy, consisted in distinct young and old subgroups with a 20-year age difference between the two groups. These differences may have allowed for more easily detectible differences than the design used here. The wider experimental age-range used by Murphy et al for example, may have made the results less susceptible to interindividual differences, a known issue in human research (Mori et al., 2009; Van Rooij et al., 1994).

Next, to gain insight into the translatability of this *in vitro* model, we assessed whether cellular readouts following the exposure of our hippocampal progenitors to donor serum related to the donor's own hippocampal volume. To do this, we first we assessed the effect of age on hippocampal volumes corrected for whole-brain volume. We report a predictive effect of age on volume for all hippocampal subfields as well as whole hippocampus. Our results are in line with several studies reporting a reduction in hippocampal subfield volumes (Peters, 2006; Shing et al., 2011; Warner-Schmidt and Duman, 2006). This reduction is often attributed to neuronal and dendritic loss but the exact mechanisms behind this phenomenon remain unclear (Daugherty et al., 2016). Authors have however highlighted contradicting results when investigating age-related changes in hippocampal subfield volumes, with some reporting no associations and others reporting associations of certain subfields alone. (Daugherty et al., 2016; Mueller et al., 2011; Raz and Rodrigue, 2006; Van Petten, 2004). Mueller and colleagues for example, initially reported a correlation between age and CA1 volume but a lack of association between age and subiculum, CA2 or CA3/4 (Mueller et al., 2007) and only later found an association with CA3/DG as well (Mueller and Weiner, 2009). Shing and colleagues suggest these contradictions may depend on other age associated-factors such as vascular risk confounding the results (Shing et al., 2011). Others suggest the ambiguous findings are a result of the cytoarchitectonic heterogeneity of the hippocampal formation which presents with distinct subfields and requires high spatial resolution to be analysed. Until recently, inadequacies in imaging resolution and available techniques have prevented accurate segmentation of the subfields and have contributed to discrepancies between studies (Iglesias et al., 2015). Results in the present study were obtained using the latest FreeSurfer algorithm which ensures accurate segmentation and allows for the novel separation of the CA3, CA4 and DG subfields providing stronger support for the existing evidence of an age-related decline in hippocampal volume (Iglesias et al., 2015, 2016).

Upon assessing the substantial effect of age on hippocampal volumes, subfield volumes were age-regressed for subsequent analysis. Partial correlations evaluating the association between participant hippocampal subfield volumes and cellular readouts showed interesting results. Increased DNA damage in the HPCs following incubation with serum,

was predictive of larger subiculum, CA3, CA4 and whole hippocampus volumes. Similarly, increased number of neuroblasts following the *in vitro* assay was predictive of increased DG, CA3, CA4 and whole hippocampus volumes. These associations however, did not survive correction for multiple testing, further research and larger samples are needed to confirm these associations. Nevertheless, the high proportion of subfields correlating to both cellular markers suggests these associations are not by chance. Were these associations to be confirmed, they would support the translatability of this cellular assay demonstrating how the systemic milieu is biologically relevant and a reflection of hippocampal volumes. The associations between neuroblast number and hippocampal volumes are of particular interest given recent results by Powell et and colleagues. Using the same hippocampal progenitor line used here, Powell and colleagues showed that differentiation caused the upregulation of a gene set that was significantly enriched for genes predictive of hippocampal volume (Powell et al., 2017). These results suggest similar mechanisms are involved in both the regulation of the differentiation process and in the determination of hippocampal volumes. This is in line with our data showing a positive association between neuroblast number and DG, CA3, CA4 and whole hippocampal volume. It is also interesting to note that an increase in neuroblasts being associated to larger subfield volumes is supportive of the possible effect of neurogenesis on brain volume (Daugherty et al., 2016). Further studies assessing the maturation and integration potential of the neuroblasts and resulting neurons however, would be needed to support this claim.

In addition to these findings, we also report the resulting number of cells and immature neurons following the *in vitro* assay are predictive of performance on PAL, validating further the translatability of the assay. Incubation with serum from individuals with better performance on PAL, led to fewer immature neurons in culture but higher overall cell density. While the higher cell density is also supportive of a role of neurogenesis in PAL performance, the lower number of immature neurons is surprising especially given the lack of association with apoptosis or cell proliferation. The higher number of immature neurons upon treatment with serum from participants with poorer PAL performances, suggests either a negative role for new neurons in the formation of new memories or a compensatory mechanism attempting to create new neurons to counteract cognitive

decline. There is indeed evidence from existing literature for both a role for neurogenesis as a destabilizing mechanism that may lead to memory loss and as a compensatory mechanism for neuronal damage (Epp et al., 2016; Kuhn et al., 2001). Interesting research by the Frankland group has in fact highlighted that an increase in neurogenesis can weaken existing memories while facilitating the encoding of new conflicting information. Importantly, the group has also shown that the timing of training in relation to the increase neurogenesis plays a key role in neurogenesis-mediated forgetting (Epp et al., 2016; Gao et al., 2018). As the temporal dynamics of neurogenesis are key for both a destabilising and a compensatory function, further research is needed to discern which is occurring here.

It is important to note that the number of immature neurons was associated to the score obtained in the recognition phase of the cognitive task while the association to cell density was linked to performance in the recall phase. Different cognitive processes are responsible for performance in each phase of the task; the recognition phase has been associated to memory encoding while the recall phase has been associated to both encoding and retrieving (Lowndes et al., 2008). The finding that immature neuron number decreases with improved performance in the PAL recognition phase, may thus be in line with findings from the Frankland group suggesting increased neurogenesis selectively destabilises recently encoded memories (Gao et al., 2018). It is therefore possible that performance in each phase is differentially affected by the composition of systemic environment and that this is reflected in our cellular model readouts. However, it is also possible that differences seen here between the two PAL phases are due to the limited number of participants available. The direction of the association between immature neurons and PAL was the same for both PAL phases but the correlation between PAL recall and immature neurons did not achieve significance. The same goes for cell density: the association between cell density and PAL recognition was similar to that between cell density and recall but escaped significance, possibly due to low power. This suggests similar cellular readouts are associated to performance in both phases but by chance only satisfy the significance threshold in one of the phases. Similarly, we report a negative association between age and PAL recall but not age and PAL recognition and between level of education and PAL recognition but not PAL recall. These results are in line with existing literature showing a strong and detrimental

effect of age on PAL performance and support the notion that education is an important factor to consider when assessing cognitive performance (Barnett et al., 2015; Bento-Torres et al., 2017; Blackwell et al., 2010; Lee et al., 2013). As was the case for the cellular readouts, age showed a similar trend in terms of direction of association to both PAL recall and PAL recognition suggesting that the low number of participants is a limiting factor within this study. In line with this, no association survived multiple testing suggesting further research, with larger cohort sizes,is needed to confirm these findings and assess the translational potential of this assay. Interestingly, unpublished research by the O'Sullivan group explored the association between PAL performance and hippocampal subfields in the MATO cohort used in the present study and found a positive association between CA1 and PAL recall (Hartopp et al., 2018). This association is supportive of a role for the hippocampus in object-location tasks such as PAL. Furthermore, the possible association between our cellular readouts and PAL performance is suggestive of the involvement of adult hippocampal neurogenesis. Though a direct association between object-location tasks and neurogenesis has not been shown, the spatial element and the, only subtle, differences between correct and incorrect answers in PAL suggests such tasks may entail aspects of pattern separation and therefore be reliant on neurogenesis.

3.4.2 Nutrient-sensing pathway alterations are associated to cellular readouts

We aimed to identify whether treatment with young or aged serum triggered gene expression alterations in nutrient-sensing pathways and whether these were related to cellular readout variations. We report no significant alterations according to age group in any of the 16 genes examined following serum treatment. As previous research in this cohort by Murphy et al showed expression alterations in other genes such as MAP3K7, ENDOG and RFN126, this data suggests nutrient-sensing genes are more susceptible to interindividual variation than those tested by Murphy and colleagues (Murphy et al., 2018). Nutrient-sensing pathways are closely linked to lifestyle factors such as diet and exercise (Kapahi et al., 2010; Walker et al., 2005). Therefore, while these pathways are also likely to be affected by age, not accounting for aspects such as diet may mask this association. This is particularly important in our assay owing to the use of the systemic environment whose

composition is known to be greatly affected by nutritional intake. To assess the effect of serum on these molecular pathways, we adopted an endophenotype approach based on stem cell maintenance; we evaluated the association between gene expression and cellular readout irrespective of age. Hereby, 8 genes were highlighted as being associated to cellular markers following serum treatment. Notably, this approach highlighted interesting genes across all 3 nutrient-sensing pathways: mTOR, IIS and sirtuin as well as ABTB1. **Table 28** summarises these associations.

Gene	Ki67	CC3	MAP2	DCX	Cell density
mTOR	-	-	-	-	
GRB10	-	-	-	-	
FOXO3A	-			-	
PTEN	-	-	-	-	
IGF2R	-	-	-	-	
NAMPT		-	-	-	-
UCP2		-	-	-	-
ABTB1				-	

Table 28 - Summary of the significant associations between cellular and molecular readouts following the *in vitro* parabiosis assay. Table showing positive (in green) and negative (in red) correlations between gene expression and cellular readout. "-" denotes results with no significant association. All genes that showed significant associations to at least one cellular readout are reported in the first column. Gene expression was compared to cellular readouts of proliferation (Ki67), apoptosis (CC3), immature neurons (MAP2), neuroblasts (DCX) and cell density.

Firstly, our data supports a role for the mTOR pathway in stem cell maintenance. We report positive associations to cell density for both mTOR and GRB10 expression levels. This relationship is supported by studies showing mTOR positively regulates cell proliferation (Sarbassov et al., 2005). The inhibition of mTOR has been associated to decreased proliferation and selective induction of apoptosis in several cell lines, but to our knowledge this has not yet been explored in human NSCs. Interestingly, GRB10 which is positively regulated by mTOR showed a similar association (Laplante and Sabatini, 2012; Thoreen et al., 2009; Yu et al., 2009). Surprisingly, both GRB10 and mTOR expression levels showed no correlation with apoptosis or proliferation. Suggesting other mechanisms are responsible for the higher cell number or that a combination of both is involved making the changes in each undetectable. The positive association between mTOR and GRB10 expression was also

confirmed by our own experiments as was a negative association between PTEN and GRB10 (see appendix section 8.2.3).

In addition, our data supports a role for the IIS, and particularly for FOXO3A, in NSC function. Increased levels of FOXO3A were accompanied by an increase in cell number, our data suggests this increase can be explained by a decrease in apoptotic cell death as evidenced by the negative association between FOXO3A levels and CC3 positive cells. The higher number of immature neurons (MAP2 positive cells) associated with increasing FOXO3A expression is suggestive of a push towards neuronal differentiation. Surprisingly however, there was no association to neuroblast number (DCX positive cells) suggesting the higher proportion of immature neurons may be due to the selective apoptosis of other cell types. PTEN and IGF2R, two other components of the IIS pathway, also showed associations to cell number; both showed opposite associations to that seen between FOXO3A and cell number. Interestingly, both PTEN and IGF2R are responsible for the negative regulation of the IIS pathway by inhibiting the conversion of PIP2 to PIP3 and acting as a scavenger receptor respectively. Surprisingly, given the important function for IIS in regulating proliferation and cell growth, FOXO3a, PTEN and IGF2R all showed no association to the expression of the proliferation marker KI67. This may be attributable to a slowing of the cell cycle which would ultimately result in lower proliferation levels but would not be reflected in a decrease in KI67 positive cells. Despite this, our results are in line with those from rodent studies showing the involvement of the IIS in NSC maintenance and differentiation regulation (Åberg et al., 2000, 2003; Chaker et al., 2016).

Genes involved in the sirtuin pathway, a pathway responsible for regulating mitochondrial function and energy availability, also showed interesting associations to *in vitro* cellular markers. This is of particular interest given the mounting evidence linking energy metabolism alterations to ageing (López-Otín et al., 2013). NAMPT, the enzyme responsible for the conversion of NAM back to NAD+ and therefore the rate limiting enzyme for SIRT1-dependent deacetylation, showed a positive correlation with the proportion of proliferating cells (Guarente, 2007). As did UCP2, a protein downstream of SIRT1 but unrelated to its deacetylation activity. Our results aligned with rodent studies showing

NAMPT ablation led to decreased NSC proliferation and UCP2 deficiency led to decreased proliferation of liver cells (Elorza et al., 2008; Stein and Imai, 2014). Surprisingly however, we saw no significant associations between cellular readouts and SIRT1 expression despite the key function of SIRT1 in the sirtuin pathway. Further studies assessing pathway regulation at other levels, such as through post-translation modifications, are necessary to elucidate the exact mechanism through which ageing impacts this pathway.

Finally, we report higher ABTB1 levels being associated to higher cell density, higher proportion of immature neurons, lower cell death and lower proportion of proliferating cells. Besides a role in basic cellular functions involving protein-protein interactions, the exact role of ABTB1 remains unknown. Its importance in ageing however, was highlighted by both Horvath's clock and by previous work by Murphy et al (Horvath, 2013; Murphy et al., 2018). The results presented here suggest for the first time that ABTB1 expression is involved in NSC regulation and in particular, is associated to a shift towards neuronal differentiation and away from proliferation. To our knowledge, this is the first study linking ABTB1 to NSCs yet this association is supported by studies showing an interaction between ABTB1 and PTEN a key regulatory molecule of the mTOR and IIS pathway (Unoki and Nakamura, 2001). These findings therefore, provide insight into a potential new role for ABTB1. Additionally, given the interaction of ABTB1 with PTEN, a known regulator of nutrient-sensing pathways, these findings highlight ABTB1 as a novel candidate in the search of mediators responsible for the interplay between ageing, nutrition and NSC regulation.

3.4.3 Summary and future directions

In summary, we report associations between cellular readouts of the human *in vitro* NSC model and hippocampal subfield volumes, between cellular readouts and cognitive performance and between cellular readouts and gene expression levels of nutrient-sensing pathway components. Despite the lack of association between cellular readouts and chronological age itself, the links established in this study with these three age-related phenotypes, are suggestive of an important role of NSCs in ageing and for the neuro-translatability of the systemic environment, and of this *in vitro* model specifically, in ageing

research. Our findings support the notion of a discrepancy between chronological and biological ageing, and the use of endophenotype approaches to study human ageing. Finally, our data also supports an important role for ABTB1 and the mTOR, IIS and sirtuin pathways in human NSC maintenance and finds several rodent findings relevant to human cellular biology. It also shows potential differences and highlights the need for further studies, with more controlled human interventions, to fully elucidate whether the NSC changes precede the expression level alterations or vice versa. Finally, given the importance of post-translational modifications in nutrient-sensing pathways other techniques such as western-blots to gain information on protein expression and protein modifications such as phosphorylation, may provide additional information on the involvement of these candidate genes in NSC maintenance.

3.4.4 Limitations

Despite exciting results, this study was subject to a number of limitations. Firstly, though the *in vitro* model used here enabled the study of molecular mechanisms associated to specific *in vivo* phenotypes in a human context, it was not free of limitations. Firstly, cell-models are somewhat removed from an *in vivo* system making it challenging to account for any organism-wide compensatory mechanisms that maybe occurring. Further to this, our model specifically, is hindered by the lack of microglia which are known to have key effects in both ageing and NSC regulation (De Lucia et al., 2016; Norden and Godbout, 2013; Perry et al., 2002) and by the use of 'young' foetal neural stem cells to study ageing. Were a cell line derived from adult hippocampi available, it would be interesting to repeat this study using adult NSCs to test whether intrinsic changes as well as extrinsic ones drive NSC alterations in ageing. In addition, as studying the effects of an ageing systemic environment is a key area in biogerontology, future studies must take into account lifestyle factors such as nutrition when employing this as an experimental variable. Finally, larger participant numbers would benefit studies such as the present one by providing stronger statistical power to detect associations

4 Oxidative stress, DNA damage and passaging: An Alternative Multimodal Model to Induce Neural Stem Cell Ageing

In chapter 3, we investigated the use of serum from participants of varying ages to create an *in vitro* parabiosis assay to model ageing. Whilst this proved a useful model to study human variability, a more controlled ageing model is required to assess gene expression in response to ageing. To this end, we set up an alternative ageing model that replicates several aspects of ageing to test the expression levels of the candidate genes highlighted in the previous chapter.

4.1 Introduction

4.1.1 Oxidative stress in ageing and neural stem cells.

Oxidative stress (OS) is a known hallmark of ageing (López-Otín et al., 2013). To understand how this contributes to the ageing phenotype, it is important to first describe the different agents involved in this biological response.

Oxidants and oxidative agents are key players in oxidative stress, they are chemical species that either remove electrons from other species or transfer electronegative atoms. Accordingly, reducing agents donate electrons to other chemical species, as part of a reduction-oxidation (redox) reaction, thereby becoming oxidised. Importantly, free radicals are oxidants that have unpaired electrons in their outer orbital which allows them to interact with non-radical species and start free radical chain reactions. In biological species, an important type of free radicals are reactive oxygen species (ROS). ROS are highly unstable ions that react with other molecules to gain stability, these can be either oxygen radicals or non-radicals that are oxidising agents. To compensate for the damage caused by ROS, biological systems employ antioxidants as part of oxidative defence (Halliwell, 2006). Antioxidants are able to either delay or prevent substrate oxidation and are usually controlled by master regulators. One such regulator is nuclear factor erythroid 2–related factor 2 (Nrf2) a major antioxidant transcription factor and master regulator of the cellular defence pathway (Vomund et al., 2017). It is responsible for controlling genes involved in

DNA damage recognition as well as the repair removal and degradation of damaged proteins (Bakunina et al., 2015).

OS occurs when there is an imbalance between oxidants and antioxidants in favour of oxidants. This imbalance can be caused either by excessive ROS or by a decrease in antioxidative response and can lead to redox disruption, signalling-pathway alterations, lipid peroxidation and DNA and protein damage (Bakunina et al., 2015). Low levels of OS however, are also a side product of several routine processes such as cell differentiation, making OS consequences largely dependent on tissue and cell types. ROS levels are even thought to be responsible for regulating the proliferation-differentiation balance in stem cells (Bigarella et al., 2014; Chiu and Dawes, 2012; Hochmuth et al., 2011; Myant et al., 2013). Adequate regulation of ROS and prevention of oxidative damage in stem cells is therefore essential to maintain functional stem cells (Wallace, 2005).

Due to its high metabolic rate and only modest antioxidant levels, the brain is particularly susceptible to OS and oxidative damage. It follows that OS plays an important role in NSC maintenance (Bakunina et al., 2015). Supporting this, studies investigating the production of H_20_2 showed it is generated by hippocampal stem and progenitor cells to regulate intracellular pathway and thereby regulate their proliferation (Dickinson et al., 2011). In addition, experiments showing H_20_2 supplementation causing an overall increase in NSC proliferation and lower endogenous ROS levels being associated to a decline in NSC self-renewal showed the importance of endogenous and exogenous ROS in NSCs (Le Belle et al., 2011). In line with this, adult neurogenesis was shown to transiently generate OS both *in vivo* and *in vitro*; Walton and colleagues showed the highest concentrations of oxidised DNA and lipid markers, two OS hallmarks, were found in the dentate gyrus of the hippocampus and that isolated mouse NSCs undergoing the highest levels of proliferation also showed the highest levels of OS load (Walton et al., 2012).

In addition to its role in stem cell maintenance, OS also plays a key role in ageing. Ageing is in fact sometimes regarded as the accumulation of damage caused by ROS over an extended period of time. This notion was initially proposed by Harman's "free radical

theory of ageing" which suggested lifespan could be extended by augmenting antioxidant defences (Harman, 1956). In line with this, there is overwhelming evidence showing increased oxidative damage with age in general and in the brain specifically (Dröge and Schipper, 2007; López-Otín et al., 2013; Wallace, 2005). Notably, human studies by Rinaldi and colleagues also showed a correlation between age-related memory impairments and both brain and plasma antioxidant levels (Rinaldi et al., 2003).

Initially Harman's theory appears to diverge from the one tested throughout this thesis suggesting specific genes within nutrient-sensing pathways are responsible in part for animal and human longevity. However, advances in our understanding of the causes and consequences of ROS, OS and oxidative damage have highlighted the two theories may complement one another (Dröge and Schipper, 2007). Several components of nutrient-sensing pathways have in fact been highlighted as key players in oxidative responses. The FOXO transcription factors for example, regulate cell metabolism and oxidative response, in part, by promoting the expression of antioxidants (Signer and Morrison, 2013). In addition, the insulin and mTOR signalling pathways were shown to be involved in the cellular response to OS following H_20_2 treatment of chinese hamster ovary cells (Schmitt et al., 2005). Finally, sirtuins have been repeatedly shown to have important functions in regulating ROS levels owing to both their deacetylation activity and their role in mitochondrial regulation, this, combined with their susceptibility to food-derived polyphenols such as resveratrol, makes them exciting candidates to mediate the link between nutrition, ageing and OS (Howitz et al., 2003; Lombard et al., 2011; Merksamer et al., 2013). Given these links, studies elucidating the relationship between ageing, nutrient-sensing pathways and OS in human models are an important next step in ageing research.

4.1.2 Senescence in ageing neural stem cells.

Cellular senescence is another known hallmark of ageing. It is defined as an irreversible cellular response to exogenous or endogenous sources that causes otherwise proliferative cells to cease proliferating in response to growth factors (Campisi and d'Adda di Fagagna, 2007). However, along with cell-cycle arrest, senescent cells also undergo morphological epigenetic, mitochondrial, metabolic and protein expression changes (Tan et al., 2014).

Senescence was initially thought to be a direct consequence of telomere shortening; a phenomenon that occurs with each replication due to the inability of DNA polymerase to elongate single stranded 3' ends. Telomere-shortening gave rise to the concept that a mammalian cell population may only replicate a finite number of times before cell division stops, which is usually referred to as the Hayflick limit (Watts, 2011).

The Hayflick limit has long been considered the number one driver of senescence, however, studies have now begun identifying other inducers of senescence. These are usually classified in two main groups: replicative senescence and stress-induced senescence. Replicative senescence encompasses telomere-shortening as suggested by Hayflick, it activates DNA damage responses that trigger cell-cycle arrest by regulating tumour suppressor genes and cell-cycle kinases (Di Micco et al., 2008). Stress-induced senescence instead, is independent of telomere shortening and can be induced by DNA damage, sub-cytotoxic doses of oxidative stress, calcium dysregulation and protein misfolding. Like replicative senescence, this type of senescence also typically up-regulates tumour suppressor genes like p53, p21 and p16 but importantly, it is not dependent on continuous proliferation. A third classification, oncogene induced senescence, is also proposed which is a specific type of stress-induced senescence caused by the activation of an oncogene (Larsson, 2011). While some downstream targets and consequences of senescence are specific the type of senescence, others are shared regardless of the inducer. Most types of senescence for example, will cause p16 upregulation (Tan et al., 2014).

In mammalian organisms, cells expressing senescence markers accumulate with age specifically at sites of age-related pathology; this suggests senescence may play a contributing role to organismal ageing (Campisi and d'Adda di Fagagna, 2007). Given the strong association between proliferation and senescence, research aimed at elucidating senescence's contribution to ageing has focused on stem and progenitor cells and resulted in studies showing age-dependent rises in senescence markers such as p16-expressing stem and progenitor cells (Campisi and d'Adda di Fagagna, 2007; Janzen et al., 2006; Molofsky et al., 2006). p16 expressing progenitor cells were also associated to brain-ageing

related phenotypes such as a decline in neurogenesis and forebrain progenitors in mice (Molofsky et al., 2006). In addition, NSC senescence was implicated in neurogenesis by studies showing telomere shortening in aged mouse hippocampal NSC related to decreased neuritogenesis and neuronal differentiation (Ferrón et al., 2009). In line with this, a recent study showed short treatments with hydroxyurea (HU), an anti-neoplastic drug that represses ribonucleotide reductase and thereby incurs double strand breaks in DNA, caused senescence-like changes in human NSC proliferation and DNA damage (Daniele et al., 2016).

Senescence in neuronal cells remains a relatively unexplored field possibly due to their low proliferation rates and the, only recently disproven, notion that senescence only occurs in highly proliferative cells. The discovery that senescence occurs through mechanisms other than Hayflick's limit in fact, has expanded senescence research into post-mitotic cells such as neurons. Indeed, Panossian and colleagues showed senescence phenotypes in wake neurons and notably linked them to SIRT1 levels (Panossian et al., 2011) while Jurk and colleagues showed increased senescence-associated β-galactosidase (SA βgal) following DNA damage in mouse post-mitotic purkinje cells *in vivo* (Jurk et al., 2012). SA βgal is a lysosomal enzyme that catalyses the hydrolysis of galactosides at pH6 in senescent but not in young cells and is therefore widely employed in ageing research (Hall et al., 2016). SA βgal was also used to show prolonged culture of rat hippocampal neurons caused senescence-like phenotypes as did rat cerebral granule neuron culture (Dong et al., 2011; Uday Bhanu et al., 2010).

These studies prove the presence of senescence in NSCs as well as in post-mitotic cells like neurons and highlight the importance of DNA damage as well as that of increased proliferation in causing senescent phenotypes. They also support the need for future studies to study the contribution of senescent neuronal cells in ageing. Identifying senescence however, remains challenging as there is no single gold-standard marker of a senescent state. Studies have instead focused on identifying several phenotypes which, in aggregate, can mark as cell as senescent. The two most obvious senescence phenotypes are the permanent cell cycle arrest and the acquisition of a senescent morphology. Besides

the decrease in proliferation, senescent cells in fact, show considerable morphological alterations usually consisting in flattened enlarged and irregular cell bodies. These alterations are usually accompanied by DNA damage, increased expression of SA-βgal and the upregulation of cell cycle regulators such as p16. When several of these alterations are detected a cell is said to be senescent (Hernandez-Segura et al., 2018; Rodier and Campisi, 2011).

4.1.3 Aims of this chapter

Research has shown stem cell ageing and NSC ageing in particular, are accompanied by a number of exogenous and endogenous alterations such as increases in ROS resulting OS, DNA damage accumulation and signalling pathway alterations. Though studies have focused on identifying the contribution for each of these aspects to the overall ageing phenotype of NSCs, they have also highlighted the multifaceted nature of ageing. A more holistic approach to modelling ageing may therefore be more realistic than only modelling some of its characteristics. In addition, there is only a limited number of studies assessing these in human models of NSCs. Therefore, in this chapter we set the following aims. 1) Set up a human NSC ageing model that encompasses OS, DNA damage and prolonged proliferation to model several aspects of ageing and to elucidate their individual and combined effects. To this end, tert-Butyl hydroperoxide (tBHP) is employed as a H_20_2 analogue, to mimic oxidative stress within the neurogenic niches, hydroxyurea is employed to induce DNA damage and stress-induced senescence and prolonged passaging is employed to mimic aged NSCs which would accrue damage as would happen *in vivo* over time. 2) Assess whether this multimodal NSC ageing model can induce cellular changes indicative of neurogenic or NSC maintenance alterations. 3) Assess whether this novel multimodal NSC ageing model induces molecular alterations in the candidate nutrient-sensing genes selected in the previous chapter.

Figure 27 shows the rationale behind the aims and hypotheses of this project.

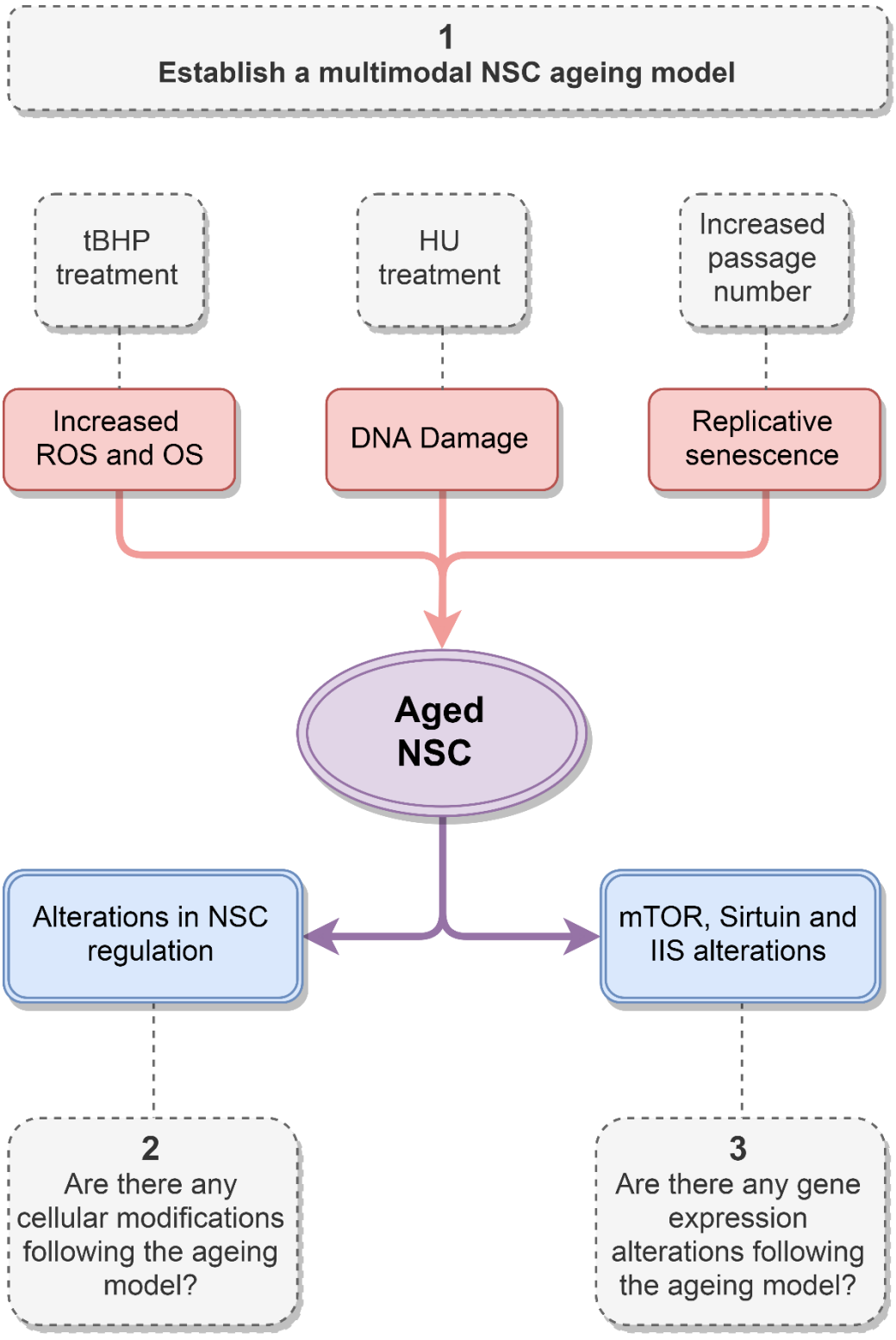

Figure 27 - Chapter 4 hypothesis. We hypothesise that increased levels of reactive oxygen species (ROS) and oxidative stress (OS), DNA damage and replicative senescence contribute to neural stem cell (NSC) ageing. Therefore, we aim to set up an i*n vitro* ageing model which encompasses these three aspects by establishing viable doses of tert-Butyl hydroperoxide (tBHP) and hydroxyurea (HU) as well as determining passage numbers that might replicate ageing phenotypes (**1**). Next, we aim to establish whether this ageing model leads to cellular modifications by quantifying cellular markers of neurogenesis and NSC maintenance (**2**). Finally, we aim to assess whether the ageing model causes alterations in the TOR, sirtuin or insulin and insulin-like signalling (**IIS**) pathways (**3**).

4.2 Materials and methods

4.2.1 Ageing cell bank

To mimic aged NSCs and to replicate the accumulation of damage increased, high passage cells were compared to low passage cells. To do this, a cell bank of high and low passages was created. This enabled us to have a stock of low passage number vials (p16) and of high passage number vials (p22) all with the same number of freeze-thaw cycles to minimise any interexperimental variability. This was achieved by using 2 vials with an intermediate passage (p11) from the original cell bank and passaging them exponentially until passage 14. 14 passage 14 vials (each containing 2 million cells) were frozen and stored while remaining cells were passaged further and exponentially until passage 22 when another 14 vials were frozen and stored (see **Figure 28**). These cells were used in all experiments comparing young and old passage numbers.

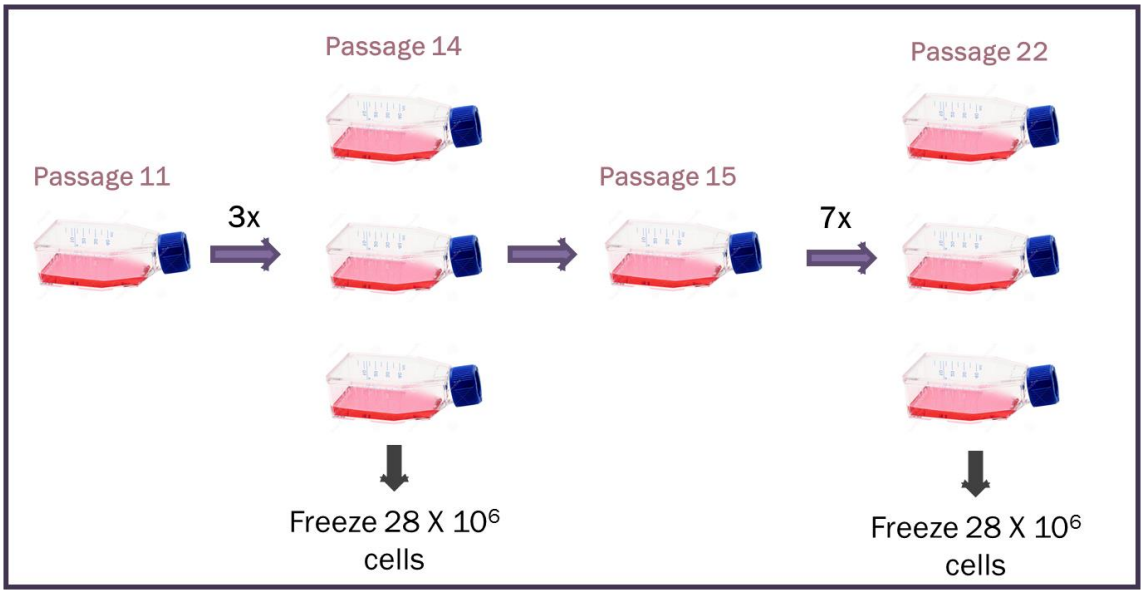

Figure 28 - Schematic of ageing cell bank methods - Passage 11 HPC0A07/03A cells were passaged exponentially for 3 passages; 28 million passage-14 cells were frozen in whilst a subset was carried on for an additional 7 passages obtaining a further 28 million cells at passage 22. Both sets of cells (passage 14 and passage 22) underwent two freeze-thaw cycles prior to use and were cultured in identical conditions.

Throughout the experiments outlined in this chapter, HPCs were treated with varying concentrations of tBHP (Fisher Scientific,10703571) and HU (Sigma, H8627) to establish a new senescence model. t-BHP was stored at 4˚C for a maximum of 2 weeks since opening, HU was dissolved in ddH_2O aliquoted and stored at -20˚C until use. Both t-BHP and HU were

diluted to target concentrations in culture media prior to incubation with HPCs. Concentration and assay durations match those explained in section 2.1.6 unless otherwise stated. When setting up the model, 3 different incubation times were tested for HU; the standard incubation of 48 hours, an 8-hour incubation and a 3-hour incubation. Cells undergoing the shorter incubation times of 8 and 3 hours underwent media changes at the usual 'treatment' timepoints. As shown in **Figure 29**, all other assay parameters and timings were kept the same. Importantly, as the aim was to analyse short term effects, cells undergoing the differentiation assay that were destined for 8- and 3-hour incubations were not treated during the proliferation portion of the assay. Control wells for each incubation period received a media-only wash at the treatment timepoint.

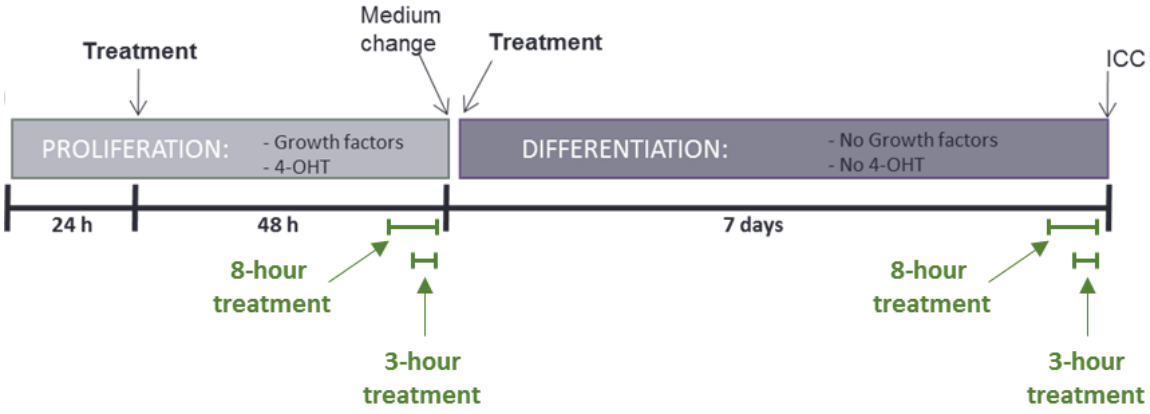

Figure 29 - Schematic of proliferation and differentiation assays including shorter incubations for hydroxyurea (HU). Timescale of the experiments showing the treatment timepoints and growth factors used. Cells are cultured in media containing growth factors (EGF, bFGF and 4-OHT) for the duration of the proliferation assay (first 72 hours) at which point the plates can be fixed to complete the proliferation assay. Alternatively, to begin the differentiation assay, plates undergo 2 full media changes with differentiation media (lacking EGF, bFGF and 4-OHT) and are cultured for a further 7 days in differentiation media containing treatment. Standard treatment timepoints shown in black and used in previous chapters were at the 24-hour and 48-hour timepoint. Shorter incubations periods tested in this chapter are shown in green. For both the 8-hour and 3-hour treatment, overall assay parameters are kept the same. Cells are washed with control media at the 24-hour and 48-hour timepoints and then treated later in the assay, 8 or 3 hours prior to fixing. Cells undergoing the differentiation assay and destined for 8- or 3-hour incubation were not treated during the proliferation portion of the assay.

4.2.2 Morphological analysis

In a subset of experiments involving DCX and Map2 staining (see section 2.2) for staining methods), morphological analysis was carried out using the Columbus ™ Image Data

Storage and Analysis System version 2.5.0 (Perkin Elmer). Images were acquired on the CellInsight as described in see section 2.2) and exported onto the Columbus platform. Similarly to the CellInsight analysis, the DAPI stain was used to identify the nuclei. Map2 or DCX stain was then used to identify the cytoplasm and again positive stains were distinguished from non-specific signal using thresholding methods. Once the population of either Map2 or DCX positive cells was selected, machine learning was carried out to class the cells into either a 'stunted' or an 'elongated' morphology in an unbiased manner. The machine learning protocol involves a training phase in which a subset of images is used to train the machine to recognise the different morphological properties characterising each subclass. The software was always trained on a minimum of 5 fields. This is followed by a checking phase in which the user can see whether the correct cells are being selected for each class (See **Figure 30**). Once the parameters are set, the software can calculate the percentage of cells belonging to each class across the entire plate as well as identify which morphological properties were used to create the classes and specifically how these properties differ. Details on the parameters used for the machine learning protocol and the pertinent scripts can be found in appendix section 8.3.1.1 .

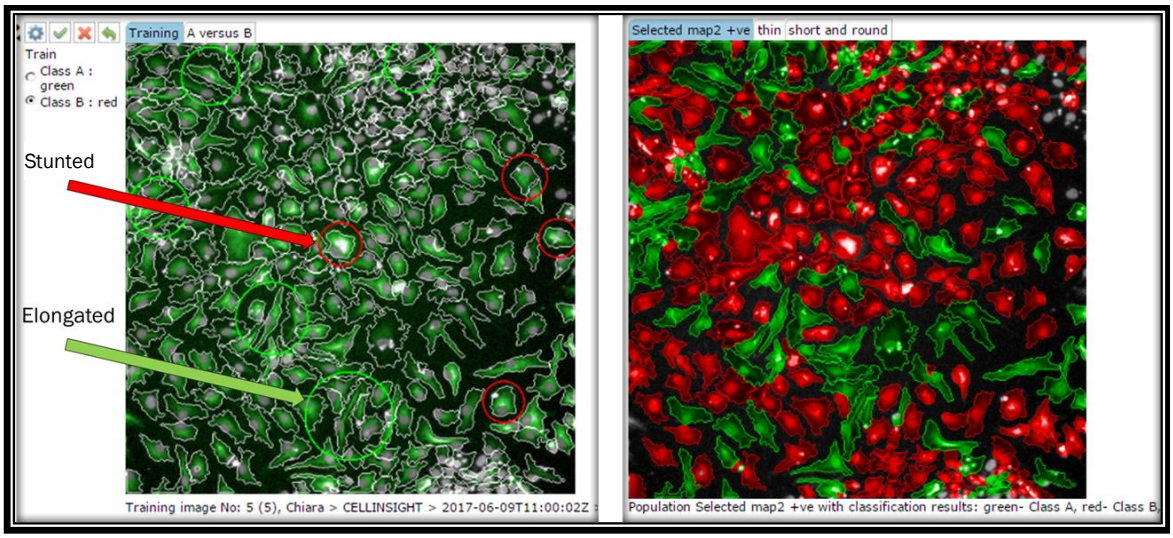

Figure 30 - Morphological analysis on Columbus software. On the left is a representative image of the training phase of the Machine Learning protocol showing how the user selects sample cells for each of the classes (here identified as "stunted" in red and "elongated" in green. On the right is a representative image of the "checking phase" in which the software assigned a class to the remaining cells and highlighted them in either red or green if identified as belonging to the "stunted" or "elongated" class respectively.

4.2.3 Statistical analyses

GraphPad Prism was used for all analysis in this chapter. For all analyses Bonferroni correction was applied to correct for multiple testing.

4.2.3.1 Immunocytochemistry

Cells were stained and analysed as explained see section 2.2 . The percentage of positive cells for three biological replicates was averaged per condition. Conditions were then compared with one-way ANOVAs or two-way ANOVAs. One-way ANOVAs were used when comparing the different treatments or passage numbers and two-way ANOVAs were used to compare conditions in which both treatment and passage number varied. Following significant one-way ANOVAs the Bonferroni post-hoc test was carried out in GraphPad Prism. When two-way ANOVAs identified significant variance between groups, Fisher least significant difference (LSD) was carried out on GraphPad Prism to calculate degrees of freedom, t and p values. To apply multiple testing corrections, the Bonferroni method was applied and the significance threshold was lowered, according to the number of multiple comparisons, to adjust for the increased probability of false discovery. The relevant significance threshold for each set of results is reported in the results section. This was done to ensure the correct number of multiple comparisons was corrected for rather than the default number set by GraphPad Prism.

4.2.3.2 Morphological analysis

The percentage of cells with stunted morphology for three biological replicates was averaged per condition. Conditions were then compared with either one-way or two-way ANOVAs as explained above.

4.2.3.3 qPCR analysis

qPCR analysis was carried out as explained in section 2.3 and section 3.2.4 The relative expression was calculated using the Pfaffl method within each biological replicate. The three biological replicates were then averaged per condition and the conditions compared with one-way or two-way ANOVAs as explained above.

4.3 Results

In this chapter, we set up an *in vitro* ageing model that encompasses several aspects of ageing NSCs. We aimed to establish whether this novel multimodal model induced changes in the HPCs and to investigate the expression levels of the 9 candidate genes selected in Chapter 3.

4.3.1 Establishing a multimodal ageing model

4.3.1.1 Selecting treatment concentrations and timings

Firstly, we aimed to select viable concentrations for the two treatments involved in the ageing model. Three different tBHP concentrations were tested as well as six HU concentrations across three different timepoints. For this preliminary work cells were treated either during proliferation or during differentiation. In addition to the standard incubation times of 48 hours for the proliferation assay and 7 days for the differentiation assay, experiments assessing HU also tested two new incubation periods of 8 and 3 hours prior to fixing. Both tBHP and HU caused considerable reductions in cell number at higher concentrations following the standard proliferation (**Figure 31**) and differentiation (**Figure 32**) assays. Shorter incubation periods with higher concentrations of HU however, did not show this toxicity see **Figure 31** and **Figure 32**. Representative images for these results are shown in **Figure 33**.

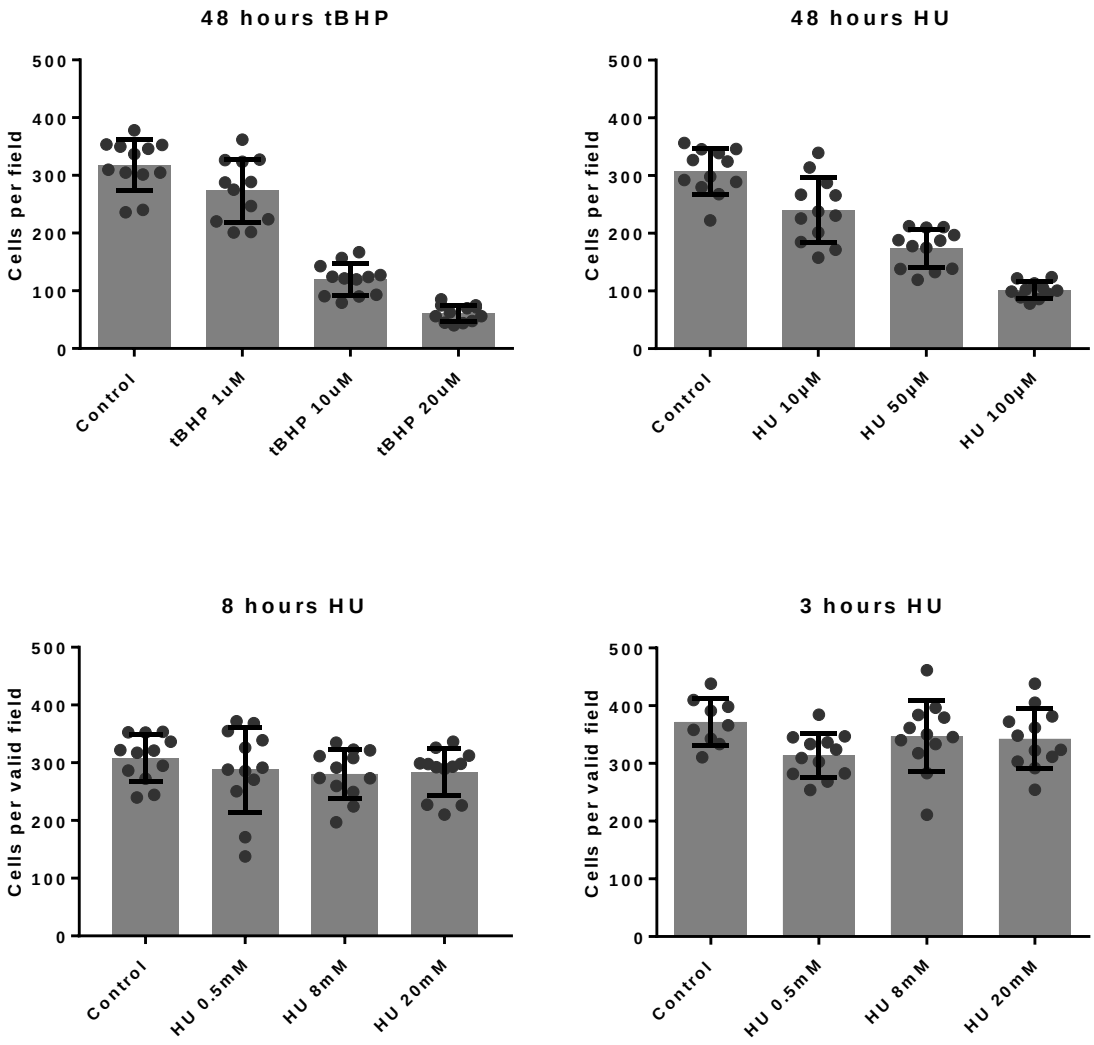

Figure 31 - Proliferation assay: Selecting tert-Butyl hydroperoxide (tBHP) and hydroxyurea (HU) concentrations. Graphs showing the resulting HPC0A07/03A cell density (cells per field) following treatments during the human progenitor cell proliferation assay. HPC0A07/03A passage 17 cells were used for all conditions. The top row shows standard incubation periods of 48 hours. The left graph shows cell density decreasing with increasing tBHP concentrations (1µM, 10µM and 20 µM) compared to controls treated with media only. The graph on the right shows decreasing cell density with increasing HU concentrations (10µM, 50 µM, 100µM). The bottom row shows the resulting cells per field following shorter incubation periods with HU; 8-hour incubation on the left and 3-hour incubation on the right. In all cases, cells were fixed 72 hours after seeding. Standard deviation is reported as error bars. Each dot represents a technical replicate. 12 technical replicates are shown.

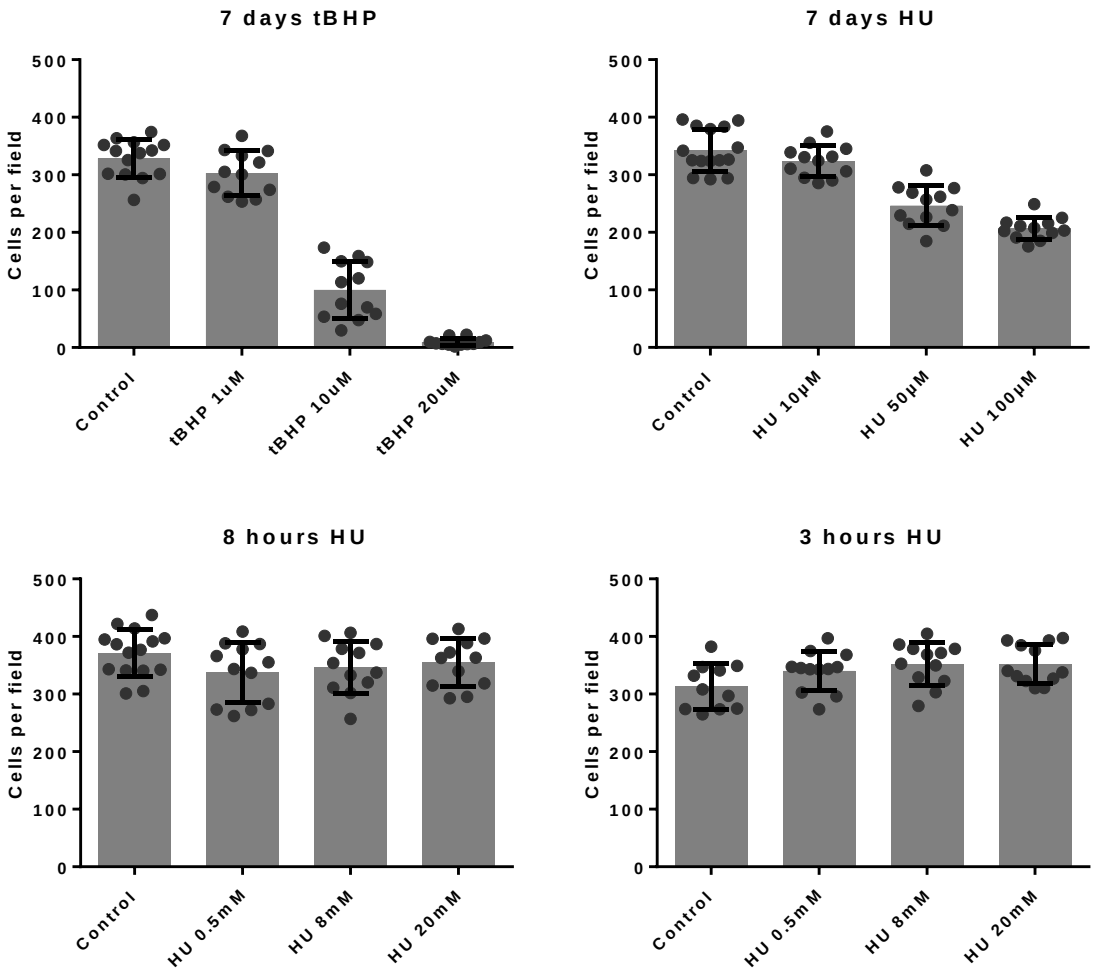

Figure 32 - Differentiation assay: Selecting tert-Butyl hydroperoxide (tBHP) and hydroxyurea (HU) concentrations. Graphs showing the resulting cell density (cells per field) following various treatments during the human progenitor cell differentiation assay. HPC0A07/03A passage 17 cells were used for all conditions. The top row shows standard incubation periods of 48 hours. The left graph shows cell density decreasing with increasing tBHP concentrations (1µM, 10µM and 20 µM) compared to controls treated with media only. The graph on the right shows decreasing cell density with increasing HU concentrations (10µM, 50 µM, 100µM). The bottom row shows the resulting cells per field following shorter incubation periods with HU; 8-hour incubation on the left and 3-hour incubation on the right. In all cases, cells were not treated during the proliferation assay (72 hours). They were then either washed and treated at the 72 hour timepoint and left to differentiate for a further 7 days or washed at the 72 hour timepoint and allowed to differentiate in media only conditions until treatment 8 or 3 hours prior to fixing. Cells were always fixed 9 days after seeding. Standard deviation is reported as error bars. Each dot represents a technical replicate. 12 technical replicates are shown.

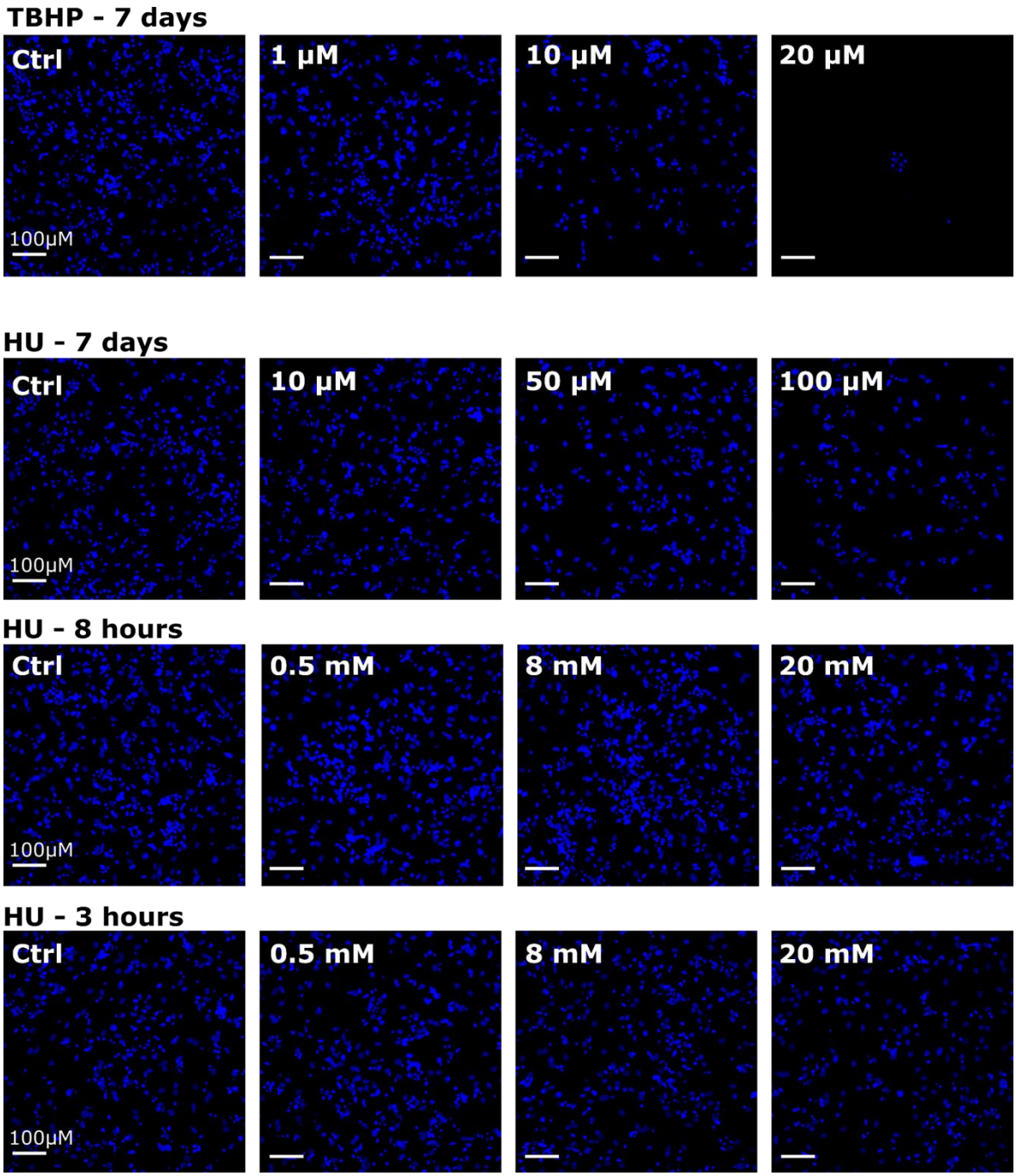

Figure 33 - Representative images of DAPI stain following the differentiation assay with tert-Butyl hydroperoxide (tBHP) or hydroxyurea (HU) treatments. Each square represents a field as analysed by the CellInsight software. HPC0A07/03A passage 17 cells were used for all conditions. DAPI (in blue) stains the cell nucleus by binding to DNA. DAPI stain was quantified using the CellInsight software to quantify cell density. Treatment concentration is reported in the top left corner of each image. Treatment duration is reported in the top left corner of each row. First row shows the DAPI stain of cells following tBHP treatment of 7 days at each concentration tested: 10µM and 20µM show a considerable reduction in cell number. The second row shows DAPI stain of following HU treatment of 7 days, as for tBHP higher concentrations appear to cause reductions in cell number. The third row shows the resulting DAPI following an 8-hour incubation with HU and the bottom row shows the DAPI stain of cells following a 3-hour incubation with HU. Both shorter incubations do not show an obvious change in cell number.

These changes were accompanied by promising alterations in cellular markers suggesting tBHP treatment during the proliferation assay caused dose-dependent changes in stemness (SOX2), apoptosis (CC3), proliferation (Ki67) while tBHP treatment during the differentiation assay caused changes in apoptosis rate, proliferation rate, neuroblasts numbers (DCX) and immature neurons numbers (MAP2). Preliminary results also suggested treatment with HU during the proliferation assay caused changes in apoptosis and DNA damage (H2AX) while HU treatment during the differentiation assay caused possible increases in apoptosis, proliferation, DNA damage and immature neurons (see appendix section 8.3.2.1 for graphs). As these experiments were carried out as a single biological replicate and 3 technical replicates to assess treatment viability, statistical analysis of these results was not possible. Rather, these results were used to confirm treatment did cause unexpected changes in cell markers and to inform concentration choice. Given most cellular marker alterations seemed to already be present at the lower concentrations, which were not accompanied by extensive cell loss, these were selected for further experiments. A tBHP concentration of 1µM and HU concentrations of 10µM and 50µM at standard treatment timepoints were selected.

Cell density was assessed at these concentrations following individual and combination (tBHP + HU) treatment at both proliferation and differentiation timepoints. One-way ANOVAs on 3 biological replicates showed a statistically significant change in cell density between treatment groups following the proliferation assay ($F(5,12) = 7.12$, $p = 0.0026$). Post-hoc analysis using the Bonferroni method revealed a significant reduction in cells per field in the 50µM HU group relative to control ($t(12)=3.52$, $p = 0.02$) and in the 1µM tBHP + 50µM HU treatment group relative to control ($t(12)=4.69$, $p = 0.003$). Other treatment groups did not show cell density differences relative to controls.

In addition, one-way ANOVAs on 3 biological replicates also showed a statistically significant change in cell density between treatment groups following the differentiation assay $F(5,12) = 9.64$, $p = 0.0007$. Bonferroni post-hoc analysis revealed, similarly to the proliferation assay results, that there was a significant decrease in cell number in both the 50µM HU treatment group ($t(12)=4.37$, $p = 0.0046$) and the 1µM tBHP + 50µM HU

treatment group (t(12)=3.52, p = 0.02) relative to control. No other treatment groups showed changes in cell density. See **Figure 34** for graphs of the proliferation and differentiation assay results and **Figure 35** for representative images of these results.

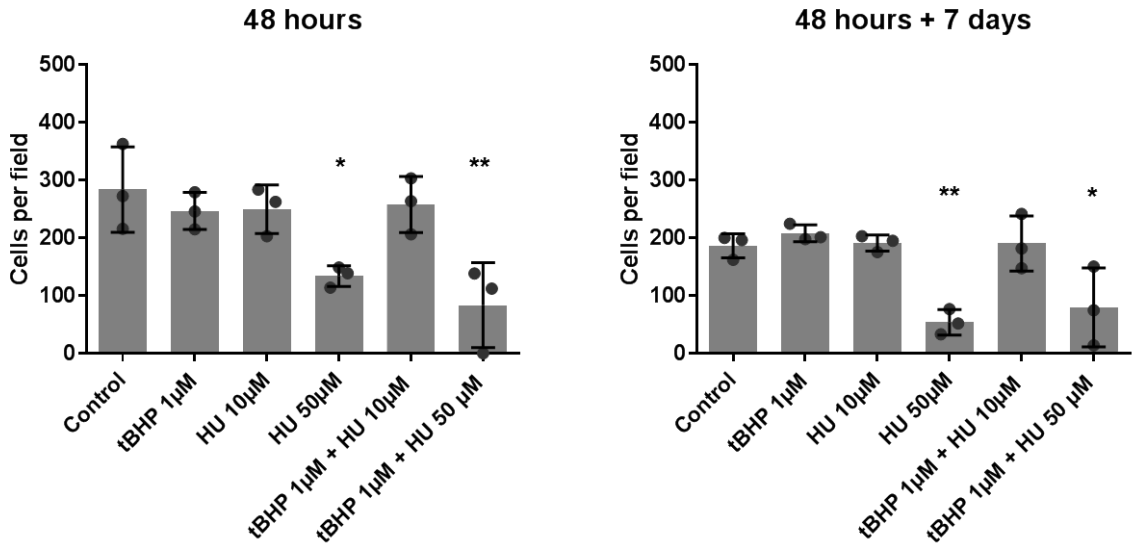

Figure 34 - Cell number (cells per field) following individual and combination treatments with tert-Butyl hydroperoxide (tBHP) and hydroxyurea (HU). Left graph: Proliferation assay results, HPC0A07/03A passage 17 cells were seeded and treated after 24 hours with either 1µM tBHP, 10µM HU, 50µM HU, 1µM tBHP + 10µM HU or 1µM tBHP + 50µM HU. Cells were incubated with the corresponding treatment for 48 hours and then stained with DAPI and analysed with the CellInsight software. The 50µM HU treatment group showed a 52.9% reduction in cell number relative to the media-only control while the 1µM tBHP + 50µM HU showed a 70.6% reduction in cell number relative to media-only control. Other treatments showed no significant effects on cell number. **Right graph**: Differentiation assay results, cells were seeded and treated after 24 hours with either 1µM tBHP, 10µM HU, 50µM HU, 1µM tBHP + 10µM HU or 1µM tBHP + 50µM HU. Cells were incubated with the corresponding treatment for 48 hours, cells were then allowed to differentiate and were incubated with the corresponding treatment for 7 further days before being stained with DAPI and analysed with the CellInsight software. The 50µM HU treatment group showed a 71.1% reduction in cell number relative to the media-only control while the 1µM tBHP + 50µM HU showed a 57.3% reduction in cell number relative to media-only control. Other treatments showed no significant effects on cell number. Error bars represent standard deviation. One-way ANOVAs followed by Bonferroni post-hoc analysis. 3 biological replicates and 3 technical replicates. Significance displayed as * $p < 0.05$, ** $p < 0.01$.

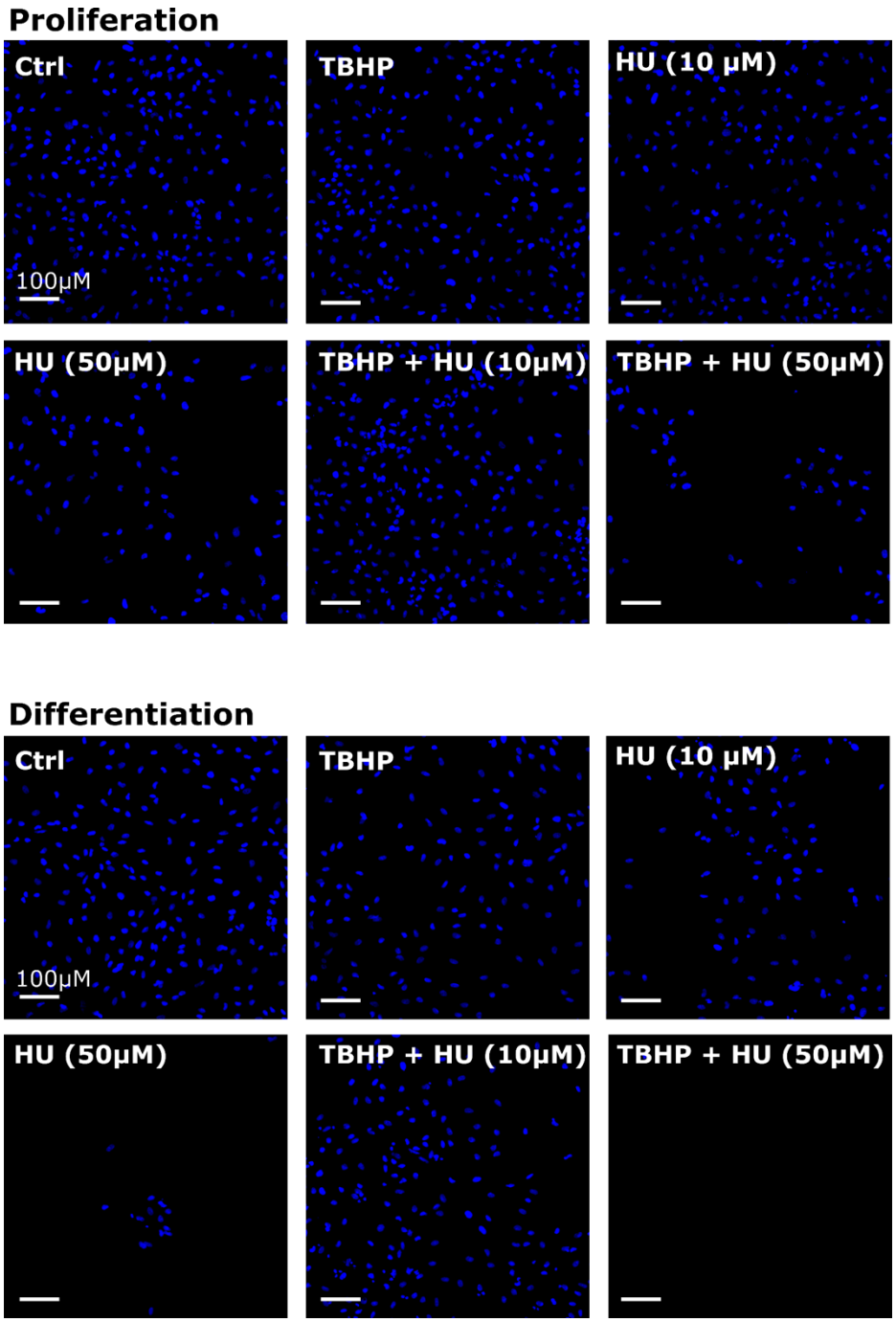

Figure 35 - Representative images of DAPI stain following the proliferation and differentiation assay with tert-Butyl hydroperoxide (tBHP) or hydroxyurea (HU) treatments. Each square represents a field as analysed by the CellInsight software. DAPI (in blue) stains the cell nucleus by binding to DNA. DAPI stain was quantified using the CellInsight software to quantify HPC0A07/03A cell density. Treatment concentration is reported in the top left corner of each image. **Top Panel:** DAPI stain following the proliferation assay; 48-hour incubation with treatment. **Bottom Panel:** DAPI stain following the differentiation assay; this included a 48-hour incubation during proliferation and a 7-day incubation during differentiation

4.3.1.2 Selecting passage number

Next, we aimed to assess the effects of increasing passage number. Preliminary work was therefore carried out to determine whether cells were able to grow until high passages and whether they retained their stemness and proliferative abilities during the proliferation assay and their differentiation abilities during the differentiation assay. Therefore, cells per field and percentage positive cells for Ki67 (proliferation), nestin (stemness) and SOX2 (stemness) were quantified following the proliferation assay. Similarly, following the differentiation assay, cells per field and the percentage positive cells for Ki67 (differentiation), DCX (neuroblasts) and MAP2 (immature neurons) were quantified. The effect of combination treatment (1µM tBHP + 10µM HU) at different passage numbers was also assessed. As this work was carried out as pilot work (2 biological replicates, 3 technical replicates), no statistical analysis was carried out. Following both the proliferation and the differentiation assay, cell number appeared stable throughout passages and only slightly affected by treatment. In addition, all stemness, proliferation and differentiation markers continued to be expressed regardless of passage number. These results showed that higher passage numbers are indeed a viable experimental condition. Though there were some fluctuations in cell marker expression, most higher passages showed comparable expression across markers, therefore passage 26 was selected for future experiments as a high, yet easily obtainable, passage given the passage 22 cell bank. These preliminary results are reported in **Figure 36** and **Figure 37**.

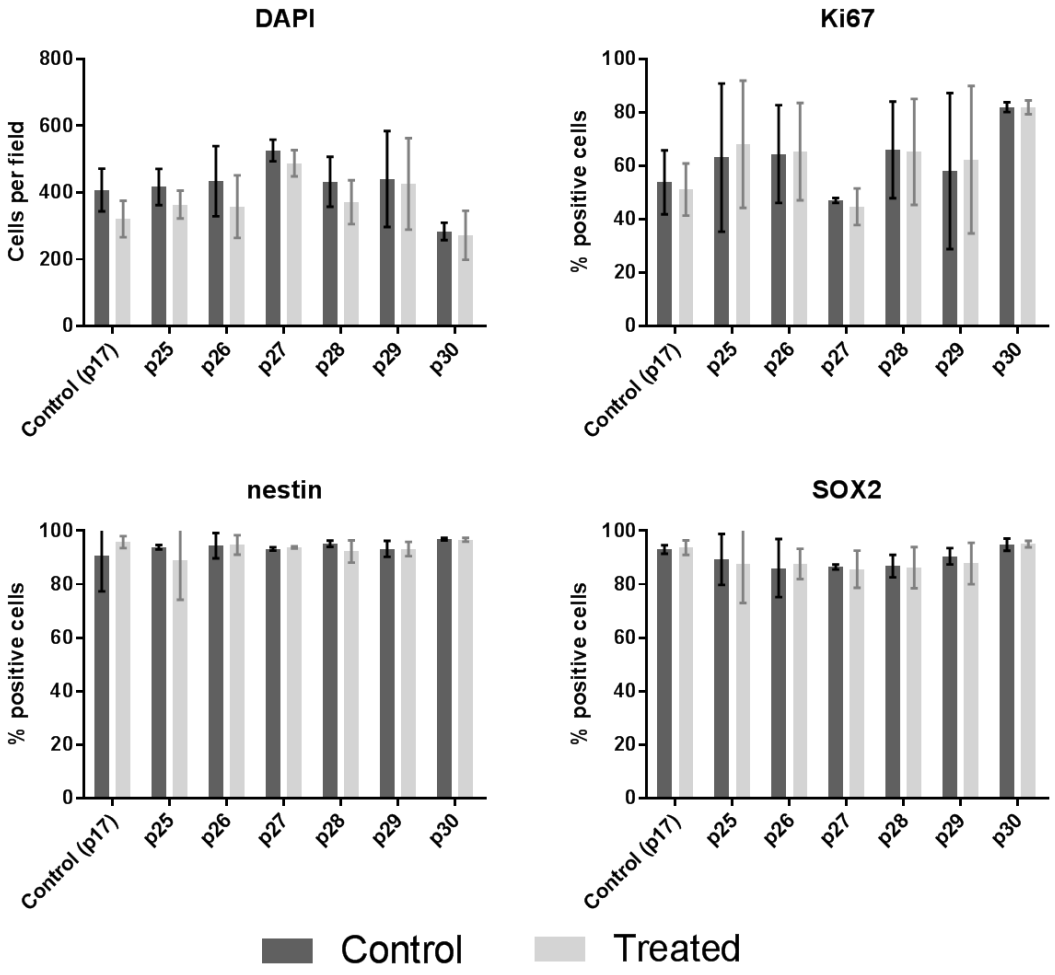

Figure 36 - Proliferation markers are expressed at different passage number. Proliferation assay results, HPC0A07/03A cells at different passage numbers were seeded and incubated with media-only or treated after 24 hours and incubated with 1µM tert-Butyl hydroperoxide (tBHP) + 10µM hydroxyurea (HU) for 48 hours. Passage numbers included 17 (p17) as a control and several higher passages ranging from passage 25 (p25) to passage 30 (p30). **DAPI**: DAPI was used to quantify the number of cells per field (y-axis); treatment (light grey) appeared to cause slight reductions in cell number at most passage numbers. Besides some fluctuations passage number did not seem to affect cell number. **Ki67**: Ki67 was used to assess proliferation, the percentage of cells positive for this marker is displayed on the y-axis. Ki67 was expressed at all passage numbers and did not seem affected by treatment (light grey). **Nestin** and **SOX2** graphs show the percentage positive cells (y-axis) for these stemness markers. Cells at all passage numbers retained their stemness as evidenced by largely unchanged SOX2 and nestin expression. Dark grey: media-only controls. Light grey: with 1µM tBHP + 10µM HU. Two biological replicates, 3 technical replicates. Error bars display standard deviation.

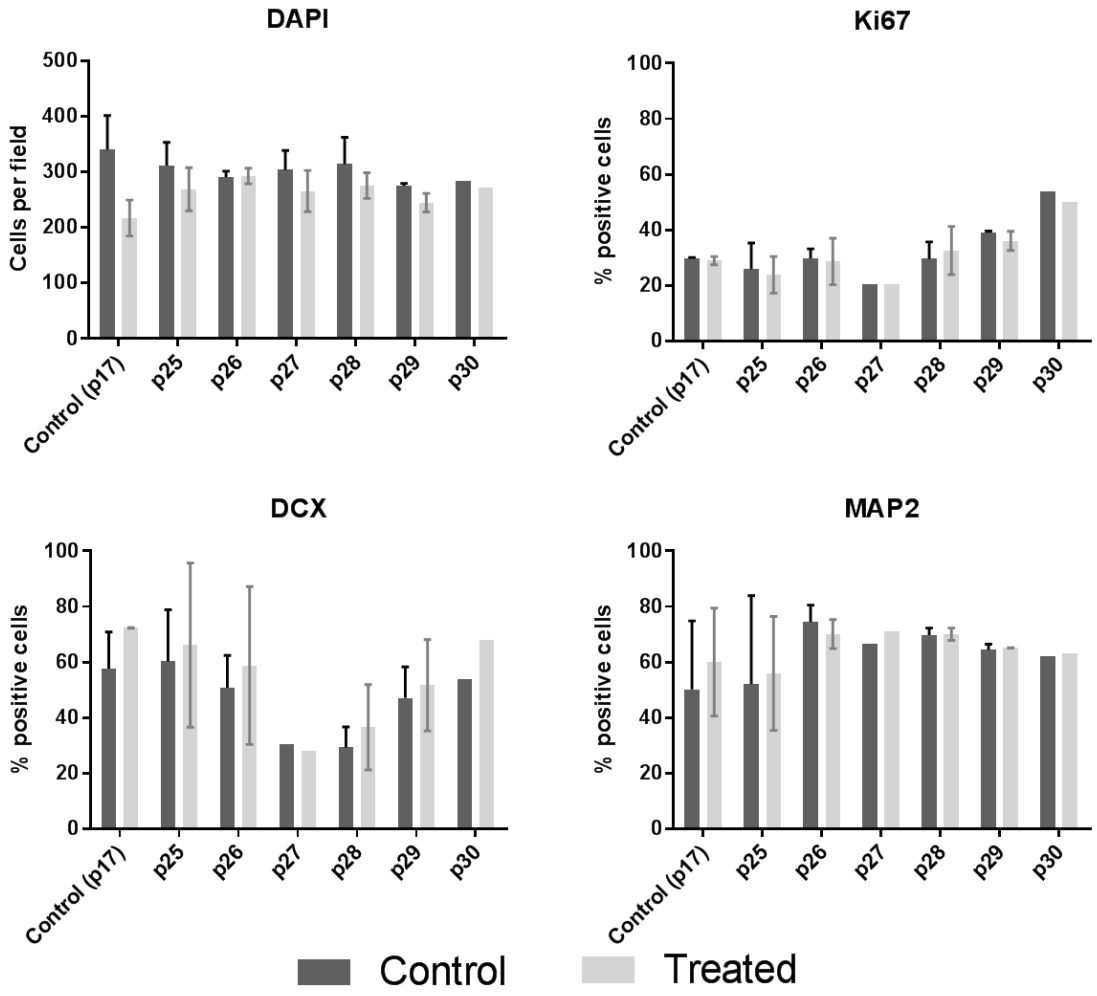

Figure 37 - Differentiation markers are expressed at different passage number. Differentiation assay results, HPC0A07/03A cells at different passage numbers were incubated in either media only conditions or with 1µM tert-Butyl hydroperoxide (tBHP) + 10µM hydroxyurea (HU) for 48 hours during the proliferation stage and for 7 days during the differentiation stage. Passage numbers included 17 (p17) as a control and several higher passages ranging from passage 25 (p25) to passage 30 (p30). **DAPI**: DAPI was used to quantify the number of cells per field (y-axis); treatment (light grey) appeared to cause slight reductions in cell number at most passage numbers. Besides some fluctuations passage number did not seem to affect cell number. **Ki67**: Ki67 was used to assess any remaining proliferation during the differentiation assay, the percentage of cells positive for this marker is displayed on the y-axis. Low levels of Ki67 was expressed at all passage numbers with a possible increase at higher passages. It did not seem affected by treatment (light grey). **DCX** and **MAP2** graphs show the percentage positive cells (y-axis) for the neuroblast maker (DCX) and immature neuron (MAP2). Cells retained their ability to differentiate towards a neuronal lineage at high passage numbers and did not appear affected by treatment (light grey). Two biological replicates (p27 and p30 only have 1 biological replicate), 3 technical replicates. Error bars display standard deviation.

4.3.2 Validation of the ageing model

4.3.2.1 Cellular readouts remain unaltered following ageing model

The preliminary work described in section 4.3.1 highlighted tBHP concentration of 1µM and HU concentrations of 10µM and 50µM as possible treatment concentrations and passage 26 as a practical passage number to use as part of the ageing model.

To validate the ageing model, we investigated its effect on cellular readouts for NSC maintenance. Firstly, we focused on the effects of individual and combination treatments and assessed proliferation, differentiation, apoptosis, stemness, oxidative-stress response (NRF2) and DNA damage (H2AX) in proliferating and in differentiating cells. Following the proliferation assay, one-way ANOVAs showed no significant variation between treatment groups for the percentage of CC3 positive cells ($F(5,11) = 0.86$ $p = 0.53$), SOX2 positive cells ($F(5,11) = 1.17$ $p = 0.38$), nestin positive cells ($F(5,11) = 0.50$ $p = 0.77$), NRF2 positive cells ($F(5,11) = 0.26$ $p = 0.92$) or H2AX positive cells ($F(5,11) = 0.88$ $p = 0.52$). Significant variation between treatment groups however, was identified in the percentage of Ki67 positive cells ($F(5,11) = 4.49$ $p = 0.02$). Bonferroni post-hoc analysis revealed this was due to a decrease in the percentage of Ki67 positive cells in the 50µM HU treatment group relative to control ($t(11)=3.43$, $p = 0.03$). There was no difference in Ki67% in any other treatment groups including the combination treatment of 1µM tBHP + 50µM HU. See **Figure 38** for graphs reporting the effect of treatments on cellular markers following the proliferation assay.

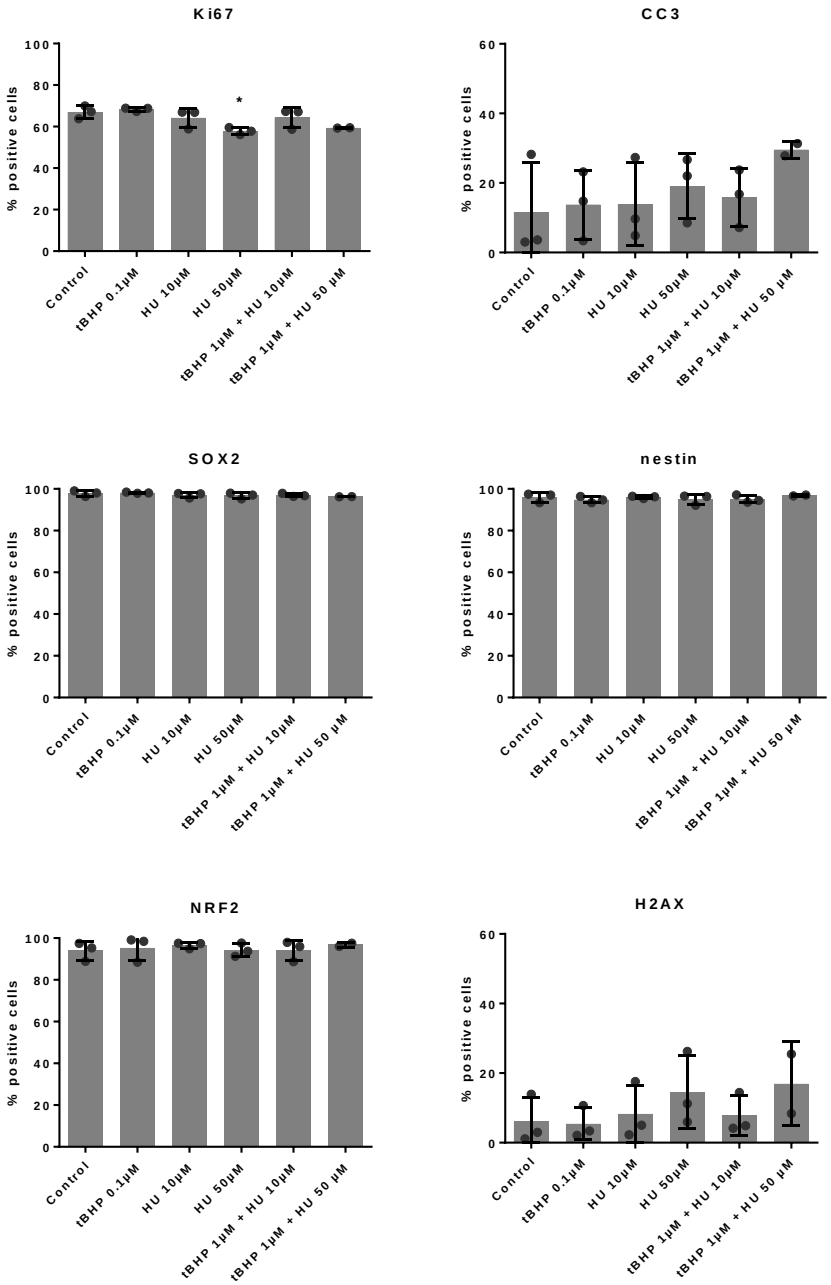

Figure 38- Proliferation markers following individual or combination treatment of tert-Butyl hydroperoxide (tBHP) and hydroxyurea (HU). Proliferation assay results; passage 17 HPC0A07/03A cells were seeded and after 24hrs incubated with either 1µM tBHP, 10µM HU, 50µM HU, 1µM tBHP + 10µM HU or 1µM tBHP + 50µM HU for 48 hours. Cells were then fixed and stained for cellular markers. In each graph the percentage of positive cells for each marker is displayed on the y-axis. **Ki67**: Ki67 was used to assess proliferation. There was a significant reduction in Ki67% positive cells in the 50µM HU treatment group. **CC3** Graph showing the percentage positive cells for CC3, an apoptosis marker, remained unchanged between treatment groups. **SOX2 and nestin** Graphs showing the percentage positive cells for SOX2 and nestin, stemness markers, remained unchanged between treatment groups. **NRF2** Graph showing the percentage of cells positive for NRF2, an oxidative stress response marker, remained unchanged between treatment groups. **H2AX** Graph showing the percentage of cells positive for H2AX, a marker for DNA damage, remained unchanged between treatment groups. One-way ANOVAs followed by Bonferroni post-hoc. 3 biological replicates, 3 technical replicates. Error bars display standard deviation. * symbolises p value < 0.05.

Following the differentiation assay, one-way ANOVAs showed no significant variation between treatment groups for the percentage of Ki67 positive cells ($F(5,12) = 0.23$ $p = 0.94$), CC3 positive cells ($F(5,12) = 1.98$ $p = 0.15$), DCX positive cells ($F(5,12) = 0.02$ $p = 0.99$), MAP2 positive cells ($F(5,12) = 1.60$ $p = 0.23$) or NRF2 positive cells ($F(5,11) = 0.49$ $p = 0.78$). Significant variation between treatment groups however, was found in the percentage of H2AX positive cells ($F(5,11) = 3.49$ $p = 0.039$). Bonferroni post-hoc analysis revealed this was due to an increase in the percentage of H2AX positive cells in the 50µM HU treatment group relative to control ($t(11)=3.51$, $p = 0.03$). There was no difference in H2AX% in any other treatment groups including the combination treatment of 1µM tBHP + 50µM HU.

Importantly however, during both assays, the cell number was greatly affected by the higher concentration of HU (see section 4.3.1.1) explaining the large standard deviation in the cellular marker results for the treatment groups involving 50µM HU and suggesting the changes in Ki67 and H2AX may be artefacts. See **Figure 39** for graphs reporting the effect of treatments on cellular markers following the differentiation assay.

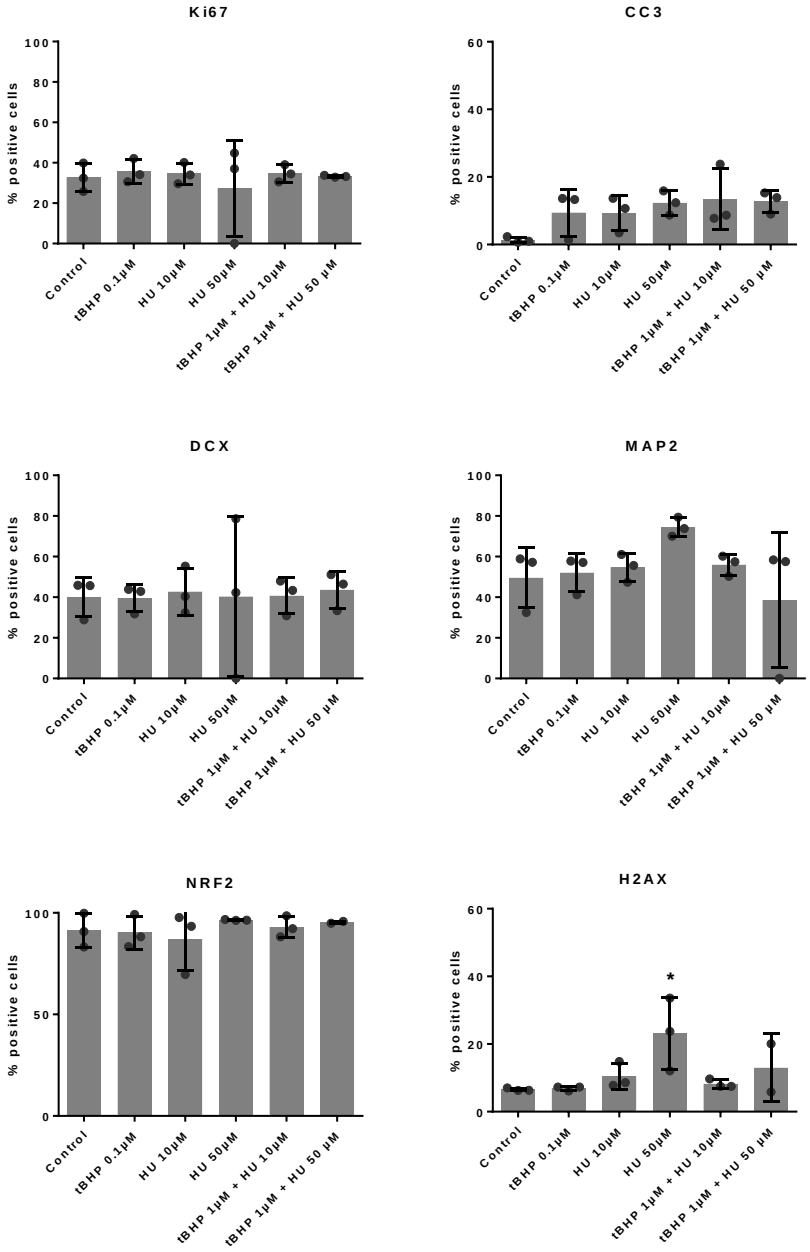

Figure 39 - Differentiation markers following individual or combination treatment of tert-Butyl hydroperoxide (tBHP) and hydroxyurea (HU). Differentiation assay results; passage 17 HPC0A07/03A cells were incubated in either media only conditions or with either 1µM tert-Butyl hydroperoxide (tBHP), 10µM hydroxyurea (HU), 50µM HU, 1µM tBHP + 10µM HU or 1µM tBHP + 50µM HU during the proliferation stage and for 7 days during the differentiation stage. In each graph the percentage of positive cells for each marker is displayed on the y-axis. **Ki67**: Ki67 was used to assess proliferation. There was no significant change in the percentage of Ki67 positive cells between treatment groups. **CC3** Graph showing the percentage positive cells for CC3, an apoptosis marker, remained unchanged between treatment groups. **DCX** Graph showing the percentage of cells positive for DCX, a neuroblast marker, remained unchanged between treatment groups. **MAP2** Graph showing the percentage of cells positive for MAP2, a marker for immature neurons, remained unchanged between treatment groups. **NRF2** Graph showing the percentage of cells positive for NRF2, an oxidative stress response marker, remained unchanged between treatment groups. **H2AX** Graph showing the percentage of cells positive for H2AX, a marker for DNA damage, throughout treatment groups. H2AX% positive cells remained largely unchanged besides a significant increase in the 50µM HU treatment group. One-way ANOVAs followed by Bonferroni post-hoc. 3 biological replicates, 3 technical replicates. Error bars display standard deviation. * symbolises p value < 0.05.

Next, we assessed the variation in these 6 cellular markers in treated and untreated passage 17 and passage 26 cells with the aim to validate the tri-modal *in vitro* model. For these experiments, the most promising treatment was selected, i.e.1µM tBHP + 10µM HU. The percentage of positive cells was assessed following both the proliferation and the differentiation assays. Following the proliferation assay, two-way ANOVAs revealed there was no significant variation between groups in any of the cellular markers. Effect of passage: **Ki67** $F(1, 8) = 1.19$ $p=0.31$, **CC3** $F(1, 8) = 1.30$ $p=0.29$, **SOX2** $F(1, 8) = 0.89$ $p=0.37$, **nestin** $F(1, 8) = 0.06$ $p=0.81$, **NRF2** $F(1, 8) = 3.28$ $p=0.11$, **H2AX** $F(1, 8) = 0.010$ $p=0.92$. Effect of treatment: **Ki67** $F(1, 8) = 0.02$ $p=0.90$, **CC3** $F(1, 8) = 0.10$ $p=0.76$, **SOX2** $F(1, 8) = 0.02$ $p=0.88$, **Nestin** $F(1, 8) = 0.36$ $p=0.56$, **NRF2** $F(1, 8) = 0.19$ $p=0.68$, **H2AX** $F(1, 8) = 0.032$ $p=0.86$. Interaction: **Ki67** $F(1, 8) = 0.004$ $p=0.95$, **CC3** $F(1, 8) = 0.70$ $p =0.43$, **SOX2** $F(1, 8) = 0.008$ $p=0.93$, **nestin** $F(1, 8) = 0.28$ $p =0.61$, **NRF2** $F(1, 8) = 0.22$ $p =0.65$, **H2AX** $F(1, 8) = 0.006$ $p=0.94$. See **Figure 40** for graphs reporting the effect of treatments and passage number on cellular markers following the proliferation assay.

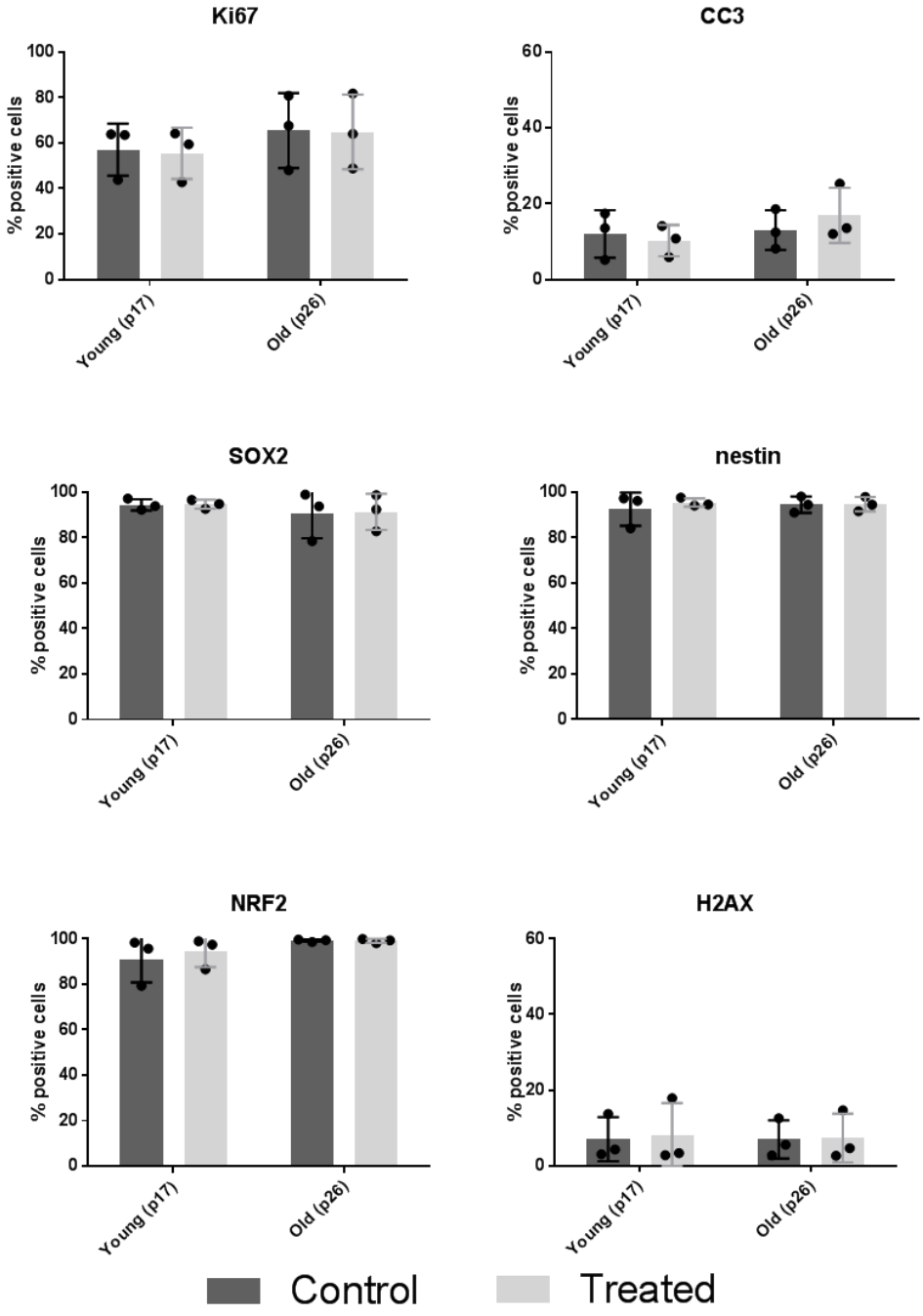

Figure 40 - Proliferation markers following increase passage and treatment. Proliferation assay results; HPC0A07/03A cells were incubated in either media only conditions or with 1µM tBHP + 10µM HU during the proliferation assay. In each graph, the percentage of positive cells for each marker is displayed on the y-axis. **Ki67**: Ki67 was used to assess proliferation. There was no significant change in the percentage of Ki67 positive cells between experimental conditions. **CC3** Graph showing the percentage positive cells for CC3, an apoptosis marker, remained unchanged between experimental conditions. **DCX** Graph showing the percentage of cells positive for DCX, a neuroblast marker, remained unchanged between experimental conditions. **MAP2** Graph showing the percentage of cells positive for MAP2, a marker for immature neurons, remained unchanged between experimental conditions. **NRF2** Graph showing the percentage of cells positive for NRF2, an oxidative stress response marker, remained unchanged between experimental conditions. **H2AX** Graph showing the percentage of cells positive for H2AX, a marker for DNA damage, between experimental conditions. H2AX% positive cells remained unchanged. One-way ANOVAs followed by Bonferroni post-hoc. 3 biological replicates, 3 technical replicates. Error bars display standard deviation.

Similarly, following the differentiation assay, two-way ANOVAs revealed there was no significant variation between groups in any of the markers. Effect of passage: **Ki67** F (1, 8) = 0.09 p=0.77, **CC3** F (1, 8) = 0.02 p=0.89, **DCX** F (1, 8) = 0.95 p=0.36, **MAP2** F (1, 8) = 0.18 p=0.68, **NRF2** F (1, 8) = 0.36 p=0.57, **H2AX** F (1, 8) = 0.11 p=0.75 Effect of treatment: **Ki67** F (1, 8) = 0.87 p=0.38, **CC3** F (1, 8) = 1.16p=0.31, **DCX** F (1, 8) = 0.67 p=0.44, **MAP2** F (1, 8) = 0.002 p=0.96, **NRF2** F (1, 8) = 0.11p=0.74, **H2AX** F (1, 8) = 0.05 p=0.83 Interaction: **Ki67** F (1, 8) = 0.30p=0.60, **CC3** F (1, 8) = 0.78p=0.40, **DCX** F (1, 8) = 0.07 p=0.80, **MAP2** F (1, 8) = 0.08 p=0.78, **NRF2** F (1, 8) = 0.29 p=0.60, **H2AX** F (1, 8) = 0.03 p=0.87. See **Figure 41** for graphs reporting the effect of treatments and passage number on cellular markers following the differentiation assay.

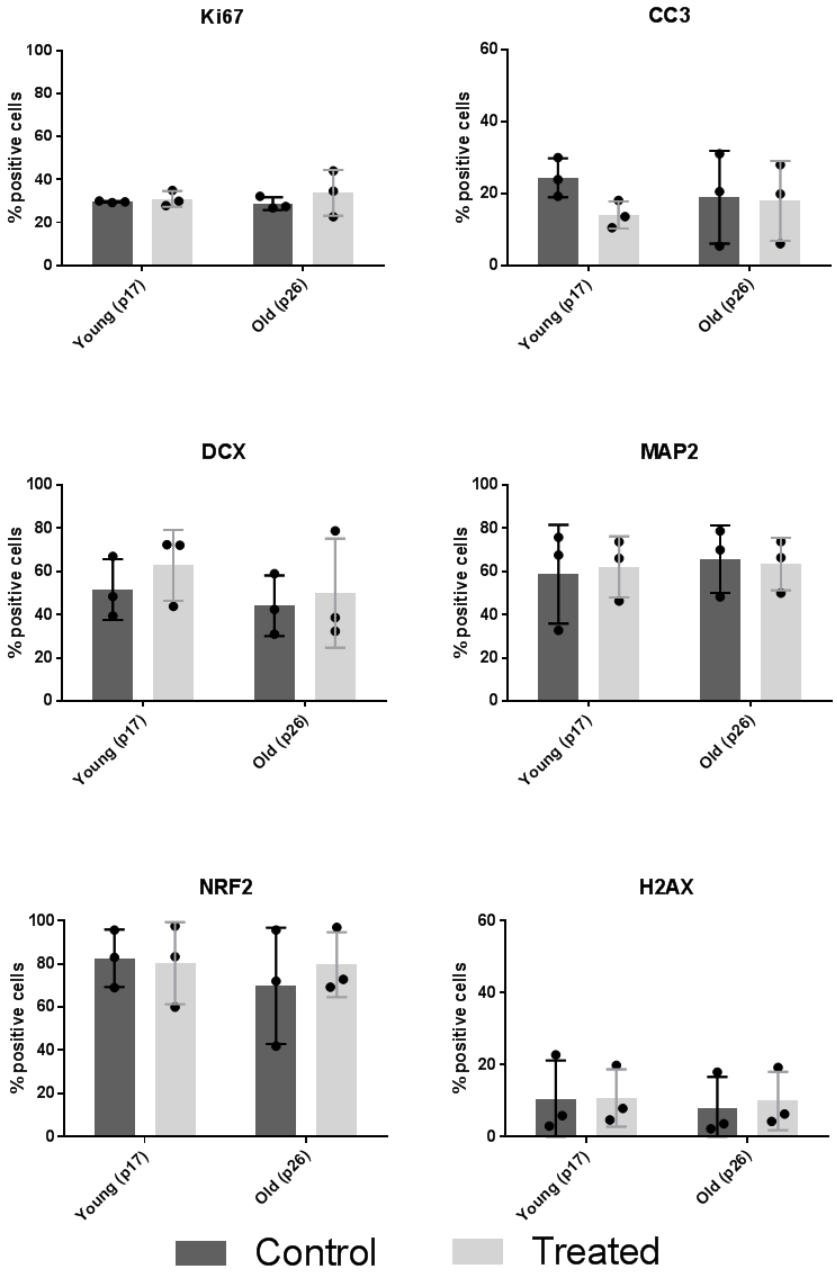

Figure 41 - Differentiation markers following increase passage and treatment. Differentiation assay results; HPC0A07/03A cells were incubated in either media only conditions or with, 1µM tBHP + 10µM HU during the proliferation stage and for 7 days during the differentiation stage. In each graph, the percentage of positive cells for each marker is displayed on the y-axis. **Ki67**: Ki67 was used to assess proliferation. There was no significant change in the percentage of Ki67 positive cells between experimental conditions. **CC3** Graph showing the percentage positive cells for CC3, an apoptosis marker, remained unchanged between experimental conditions. **DCX** Graph showing the percentage of cells positive for DCX, a neuroblast marker, remained unchanged between experimental conditions. **MAP2** Graph showing the percentage of cells positive for MAP2, a marker for immature neurons, remained unchanged between experimental conditions. **NRF2** Graph showing the percentage of cells positive for NRF2, an oxidative stress response marker, remained unchanged between experimental conditions. **H2AX** Graph showing the percentage of cells positive for H2AX, a marker for DNA damage, between experimental conditions. H2AX% positive cells remained unchanged. One-way ANOVAs followed by Bonferroni post-hoc. 3 biological replicates, 3 technical replicates. Error bars display standard deviation.

4.3.2.2 Morphological alterations as a result of passaging

Despite there being no change in the number of neuroblasts or immature neurons, there were noticeable morphological differences in these cell types with passage number. In cultures with higher passage numbers, both DCX and MAP stained cells appeared more round in than in their lower passage counter parts. To investigate this phenotype, machine learning was carried out to quantify the proportion of cells with this stunted morphology as compared to those with the usual more elongated morphology typically seen in lower passage numbers. Two-way ANOVAs on the results of machine learning carried out on MAP2 stains, showed there was significant variation in between groups and that 83% of the variation was due to passage number ($F(1, 8) = 41.39$ $p=0.0002$). There was no effect of treatment ($F(1, 8) = 3e\text{-}007$ $p=0.99$) or interaction effect ($F(1, 8) = 0.60$ $p=0.46$). Fisher's LSD post-hoc analysis revealed this variation was due to an increase in the proportion of MAP2 positive cells with stunted morphology in the untreated passage 26 group when compared to their proportion in the untreated passage 17 group ($t(8) = 5.096$ $p=0.0009$). Similarly, treated passage 26 cells showed a significantly different proportion of stunted MAP2 positive cells when compared to treated passage 17 cells ($t(8) = 4.55$ $p=0.004$).

Bonferroni correction was applied manually, and the significance threshold was set to 0.017 to correct for 3 multiple comparisons. Similarly, two-way ANOVAs on the machine learning results carried out on DCX stains, showed there was significant variation in between groups and that 81% of the variation was due to passage number ($F(1, 8) = 35.28$ $p=0.0003$). There was no effect of treatment ($F(1, 8) = 0.3273$ $p=0.5830$) or interaction effect $F(1, 8) = 0.1832$ $p=0.6799$). Fisher's LSD post-hoc analysis revealed this variation was due to an increase in the proportion of DCX positive cells with stunted morphology in the untreated passage 26 group when compared to their proportion in the untreated passage 17 group ($t(8) = 4.503$ $p=0.002$). Similarly, treated passage 26 cells showed a significantly different proportion of stunted DCX positive cells when compared to treated passage 17 cells ($t(8) = 3.90$ $p=0.005$). Bonferroni correction was applied manually, and the significance threshold was set to 0.017 to correct for 3 multiple comparisons (passage 17 control vs passage 26 control, passage 17 control vs passage 17 control and passage 26 treated vs passage 26 treated).

Furthermore, machine learning results showed that similar factors were used to determine whether each cell belonged to the stunted or the elongated morphology subgroup for both MAP2 and DCX positive cells. For MAP2 positive cells, cytoplasm width to length ratio, cytoplasm width, nucleus area and nucleus roundness were used, and all were higher in stunted cells compared to elongated ones. Similarly, for DCX positive cells, cytoplasm width to length ratio, cytoplasm roundness, nucleus area and nucleus roundness were used to determine the subgroup each cell belonged to (see annex section 8.3.2.3). See **Figure 42** for graphical representations of the morphological change in DCX and MAP2 positive cells and for representative images of this change.

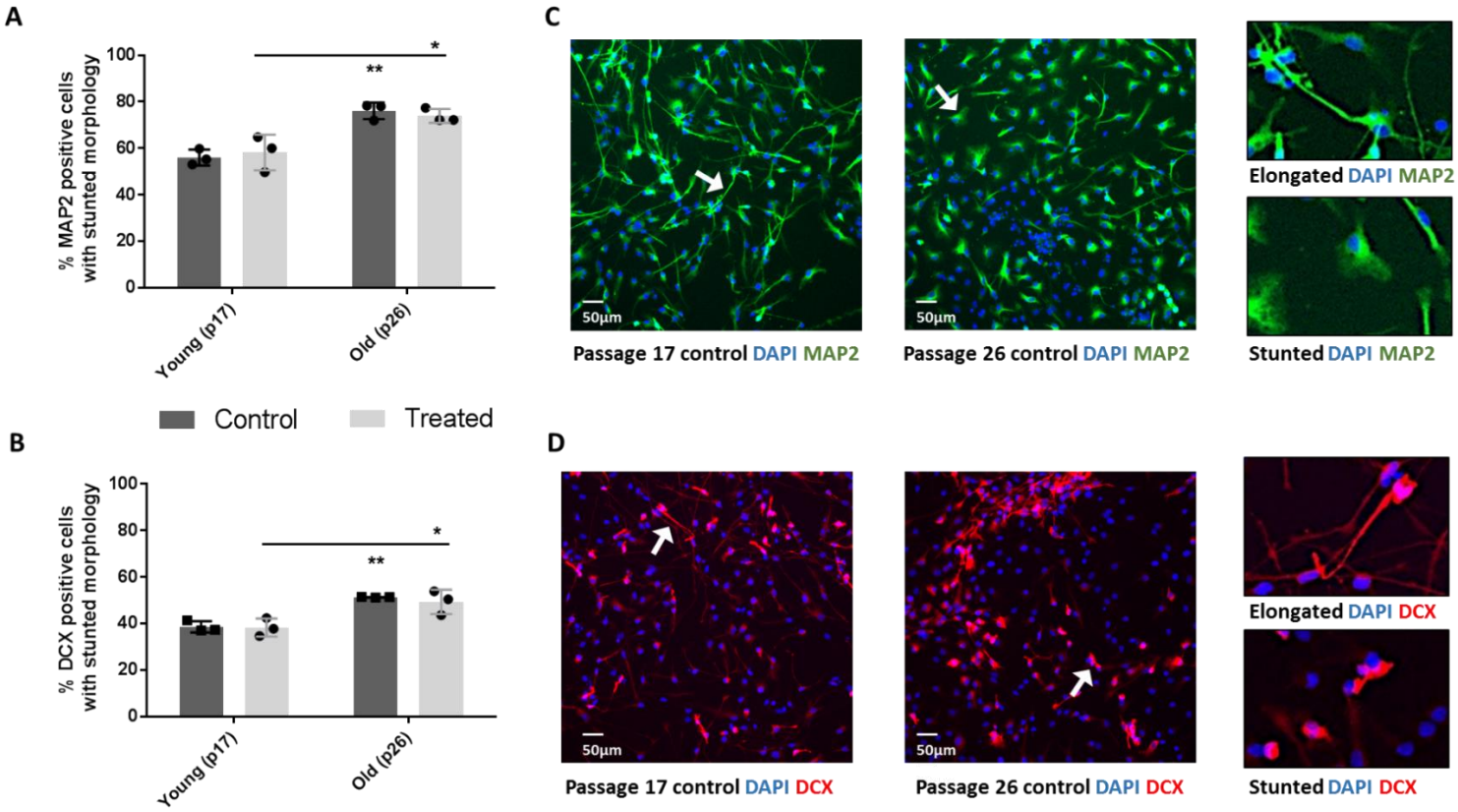

Figure 42 - Map2 and DCX positive cell morphology following increased passage number and treatment. Differentiation assay results; passage 17 (p17) and passage 26 (p26) HPC0A07/03A cells were incubated in either media only conditions (control) or with 1µM tert-Butyl hydroperoxide (tBHP) + 10µM hydroxyurea (HU) (treated) during the proliferation stage and again for 7 days during the differentiation stage. Machine learning was used to quantify the proportion of rounded (stunted morphology) and the proportion of elongated cells in MAP2 positive cells **(A**) and DCX positive cells (**B**). According to results from both markers, there was a significantly higher proportion of cells with stunted morphology in p26 cells compared to p17 cells in both treated and untreated groups. **(C)** and **(D)** show representative images of MAP2 and DCX positive untreated cells at passage 17 and at passage 26. Cells with typical elongated or stunted morphology are indicated by white arrows and reported at a higher magnification on the right with the pertinent label. Two-way ANOVAs. 3 biological replicates, 3 technical replicates. Error bars display standard deviation. Manual Bonferroni correction set the significance threshold to $p < 0.017$ therefore * symbolises p value <0.0017, ** $p < 0.003$.

Importantly, this morphological change was also reflected in the preliminary data looking at passage number 25-30 (see appendix 8.3.2.2) suggesting this phenotype may become increasingly apparent as passage number increases. Furthermore, as suggested by the combination-treatment data shown above, treatment had no effect on morphology (see **Figure 43**). One-way ANOVAs showed this was the case for all combinations tested as well as for individual treatments in both DCX positive cells (F (5, 12) = 0.33 p=0.88) and MAP2 positive cells (F (5, 11) = 0.33 p=0.89).

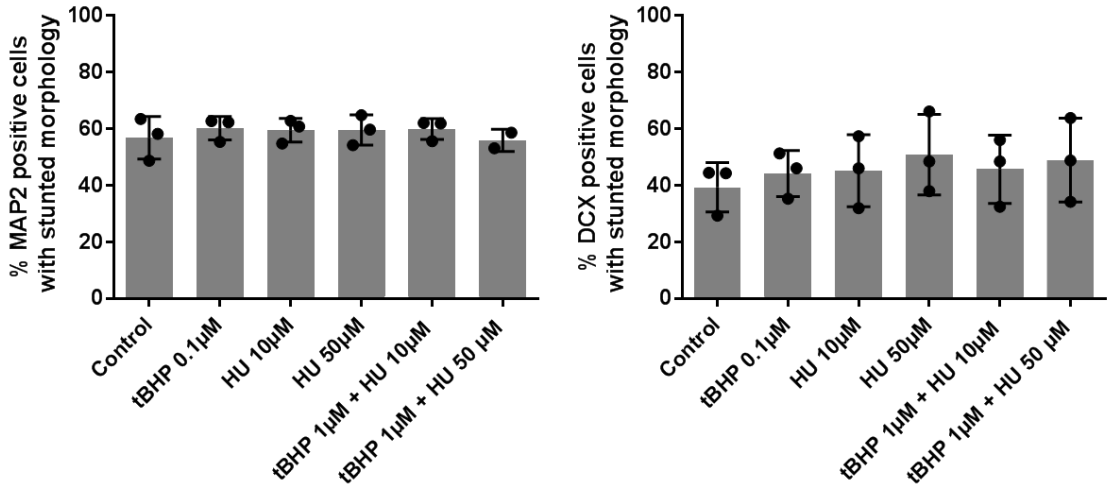

Figure 43 - Map2 and DCX positive cell morphology following treatment. Differentiation assay results; HPC0A07/03A cells were incubated in either media only conditions (control) or with either 1µM tert-Butyl hydroperoxide (tBHP), 10µM hydroxyurea (HU), 50µM HU, 1µM tBHP + 10µM HU or 1µM tBHP + 50µM HU during the proliferation stage and for 7 days during the differentiation stage. Machine learning was used to quantify the proportion of rounded (stunted morphology) and the proportion of elongated cells in MAP2 positive cells **(left**) and DCX positive cells (**right**). According to results from both markers, there was no significant variation across groups. One-way ANOVAs. 3 biological replicates, 3 technical replicates. Error bars display standard deviation.

4.3.3 Ageing model alters expression of genes of interest

After assessing interesting morphological alterations in higher passages which were presumably related to ageing phenotypes, we aimed to evaluate whether treatment and passage number affected the expression levels of the 9 candidate genes highlighted in the previous chapter. Therefore, we quantified expression of FOXO3A, SIRT1, IGF2R, ABTB1, NAMPT, PTEN, UCP2, GRB10 and mTOR in passage 17 and passage 26 cells in treated and untreated conditions via qPCR. mRNA levels were assessed after both the proliferation and the differentiation assays.

Firstly, the candidate genes' expression levels were compared between control, tBHP only, HU only and combination treatment (tBHP + HU). The previously selected concentrations of 1μM tBHP and 10μM HU were used in this experiment. One-way ANOVAs showed there was no variation between the 4 treatment groups for any of the genes that were tested. See **Figure 44** for the graphs relating to the proliferation assay and **Figure 45** for the graphs relating to the differentiation assay. Proliferation assay results: **FOXO3A** F (3, 8) =0.81, p=0.52, **SIRT1** F (3, 8) = 0.61 p=0.62, **IGF2R** F (3, 8) = 1.42 p=0.31, **ABTB1** F (3, 8) = 1.61 p=0.26, **NAMPT** F (3, 8) = 0.13 p=0.94, **PTEN** F (3, 8) = 0.23 p=0.87, **UCP2** F (3, 8) = 0.24 p=0.87, **GRB10** F (3, 8) = 0.07 p=0.97, **mTOR** F (3, 8) = 0.14 p=0.93. Differentiation assay results: **FOXO3A** F (3, 8) = 0.03 p=0.99, **SIRT1** F (3, 8) = 0.21 p=0.89, **IGF2R** F (3, 8) = 0.81 p=0.52, **ABTB1** F (3, 8) = 0.68 p=0.59, **NAMPT** F (3, 8) = 0.17 p=0.91, **PTEN** F (3, 8) = 0.04 p=0.99, **UCP2** F (3, 8) = 0.08 p=0.97, **GRB10** F (3, 8) = 0.04 p=0.99, **mTOR** F (3, 8) = 0.17 p=0.92.

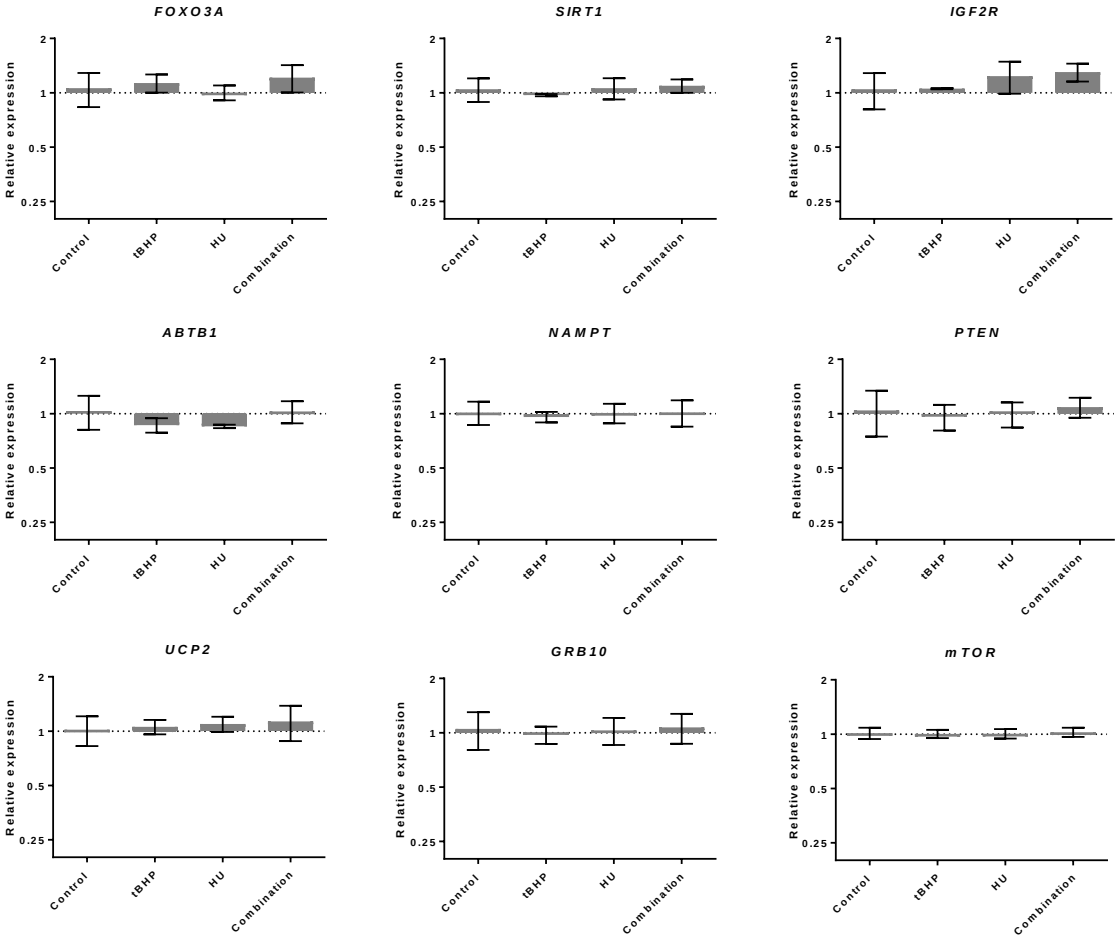

Figure 44 - Candidate gene expression levels following individual and combination treatment: Proliferation assay. HPC0A07/03A cells were incubated in either media only conditions (control) or with 1µM tert-Butyl hydroperoxide (tBHP), 10µM hydroxyurea (HU) or 1µM tBHP + 10µM HU (Combination) during the proliferation assay. Quantitative polymerase chain reaction (qPCR) was used to measure gene expression. Y-axis show the expression of each gene relative to control as calculated by the Pfaffl method. FOXO3A, SIRT1, IGF2R, ABTB1, NAMPT, PTEN, UCP2, GRB10 and mTOR expression were not found to be altered following treatment. One-way ANOVAs 3 biological replicates, 3 technical replicates. Error bars represent standard deviation. Y-axis is a log scale.

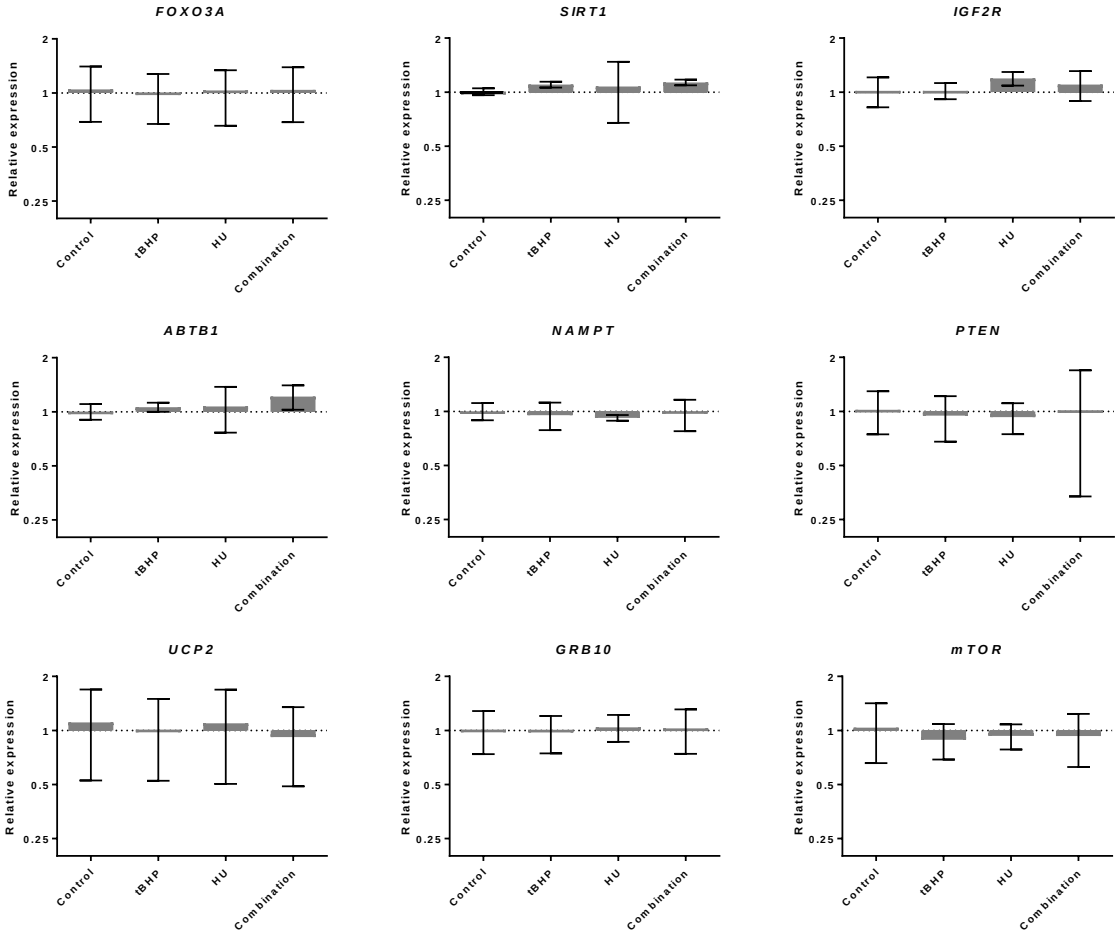

Figure 45 - Candidate gene expression levels following individual and combination treatment: Differentiation assay. HPC0A07/03A cells were incubated in either media only conditions (control) or with 1µM tert-Butyl hydroperoxide (tBHP), 10µM hydroxyurea (HU) or 1µM tBHP + 10µM HU (Combination) during the proliferation stage and for 7 days during the differentiation stage. Quantitative polymerase chain reaction (qPCR) was used to measure gene expression. Y-axis show the expression of each gene relative to control as calculated by the Pfaffl method. FOXO3A, SIRT1, IGF2R, ABTB1, NAMPT, PTEN, UCP2, GRB10 and mTOR expression were not found to be altered following treatment. One-way ANOVAs 3 biological replicates, 3 technical replicates. Error bars represent standard deviation. Y-axis is a log scale.

Next, the effect of passage number on expression levels was investigated as well as the effect of combining treatment and passage number. For this, we compared treated and untreated passage 17 cells, untreated passage 17 cells and untreated passage 26 cells and treated passage 17 and treated passage 26 cells. Graphs for these experiments are reported in **Figure 46**. Following the proliferation assay, two-way ANOVAs highlighted significant variation in FOXO3A, NAMPT and GRB10 expression levels.

FOXO3A analysis showed 70% of the variation was due to passage number (F (1, 8) = 20.15 p=0.002) whilst there was no effect of treatment (F (1, 8) = 0.45 p=0.52) or interaction (F (1, 8) = 0.006 p=0.94). Accordingly, Fisher's LSD post-hoc analysis revealed FOXO3A messenger RNA (mRNA) levels in the passage 17 untreated and passage 26 untreated groups was significantly different (t(8) 3.23 p= 0.012) as well as the difference in expression between passage 17 treated and passage 26 treated subgroups (t(8)= 3.12 p= 0.014). These results show that in both treated and untreated cells, higher passage number causes decreased FOXO3A expression.

NAMPT mRNA levels showed 82% of the variation between groups was due to passage (F (1, 8) = 120.2 p<0.0001), 6% treatment (F (1, 8) = 8.73 p=0.018) and 7% due to interaction effects (F (1, 8) = 10.1 p=0.013). Post-hoc analysis showed untreated passage 17 and passage 26 were significantly different (t(8) 5.50 p= 0.0006) as well as treated passage 17 and passage 26 cells (t(8) 9.998 p= <0.0001) and treated and untreated passage 26 cells (t(8) 4.34 p=0.0025). These results show that passage number alone causes increased NAMPT levels in culture and that there is a summative effect of passage number and treatment but that treatment alone is not able to elicit expression changes.

GRB10 also showed 85% of variation was due to passage (F (1, 8) = 63.25 p<0.0001). number following the proliferation assay. Treatment (F (1, 8) = 1.80 p=0.22) and interaction between treatment and passage number had no effect (F (1, 8) = 0.99 p=0.35). Post-hoc analysis showed untreated passage 17 and untreated passage 26 cells displayed significantly different expression levels of GRB10 (t(8) 6.33 p= 0.0002) as did treated passage 17 and passage 26 cells t(8)= 4.92 p= 0.0012.

All other genes showed no mRNA level changes between groups following the proliferation assay. Passage number effect: **SIRT1** F (1, 8) = 4.13 p=0.08, **IGF2R** F (1, 8) = 0.07 p=0.80, **ABTB1** F (1, 8) = 2.87 p=0.13, **PTEN** F (1, 8) = 0.50 p=0.50, **UCP2** F (1, 8) = 2.63 p=0.14, **mTOR** F (1, 8) = 1.06 p=0.33. Treatment effect: **SIRT1** F (1, 8) = 1.14 p=0.32, **IGF2R** F (1, 8) = 1.2 p=0.30, **ABTB1** F (1, 8) = 1.00 p=0.35, **PTEN** F (1, 8) = 0.27 p=0.62, **UCP2** F (1, 8) = 0.10 p=0.76, **mTOR** F (1, 8) = 0.23 p=0.65. Interaction effect: **SIRT1** F (1, 8) = 0.24 p=0.64, **IGF2R**

F (1, 8) = 0.96 p=0.36, **ABTB1** F (1, 8) = 0.02 p=0.89, **PTEN** F (1, 8) = 0.03 p=0.87, **UCP2** F (1, 8) = 0.01 p=0.92, **mTOR** F (1, 8) = 0.31 p=0.59.

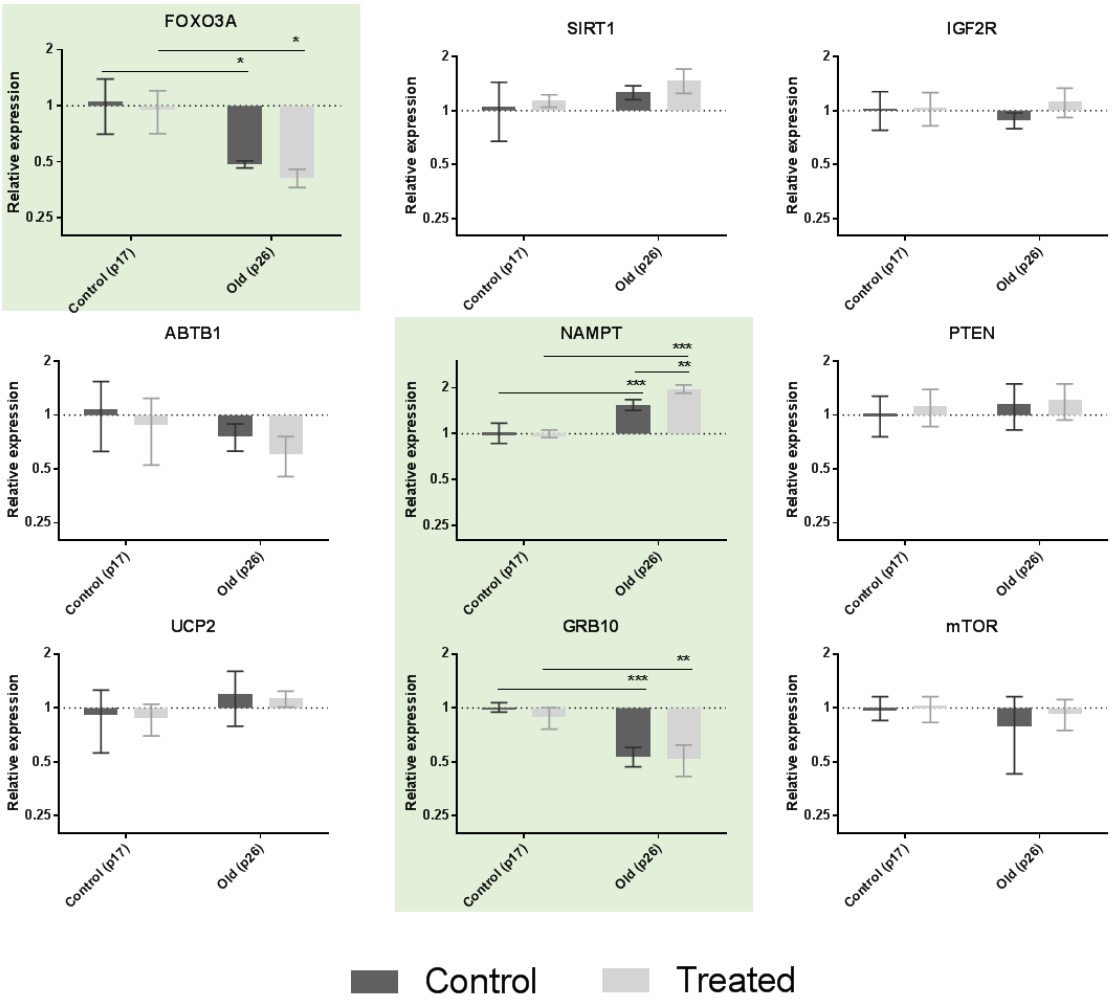

Figure 46 - Candidate gene expression levels in passage 17 (p17) and passage 26 (p26) cells following combination treatment: Proliferation assay. HPC0A07/03A cells were incubated in either media only conditions (control) or with 1µM tBHP + 10µM HU (Treated) during the proliferation assay. Quantitative polymerase chain reaction (qPCR) was used to measure gene expression. Y-axis show the expression of each gene relative to control as calculated by the Pfaffl method. **FOXO3A** expression levels decreased as a result of passage number. While **NAMPT** expression levels showed an increase due to passage number and a significant interaction between passage number and treatment caused a further increase in NAMPT expression as a result of treatment on higher passage cells. **GRB10** expression levels also decreased as a result of passage number both in control and treated conditions. Significant results highlighted by green squares, all other genes (**SIRT1**, **IGF2R**, **ABTB1**, **PTEN**, **UCP2** and **mTOR**) showed no significant alterations in gene expression following treatment or passage number increase. Two-way ANOVAs, 3 biological replicates, 3 technical replicates. Error bars represent standard deviation. Y-axis is a log scale. Bonferroni correction to control for 3 multiple comparisons set significance threshold to p<0.017. Therefore, * symbolises p<0.017 and ** symbolises p<0.003.

mRNA levels of the 9 candidate genes were also assessed following the differentiation assay (see **Figure 47**). Two-way ANOVAs showed significant variation across groups in the gene expression of FOXO3A, PTEN, GRB10 and mTOR. The source of variation for FOXO3A was due to passage number 75% ($F(1, 8) = 26.3$ $p=0.0009$). Treatment ($F(1, 8) = 0.59$ $p=0.46$) and interaction ($F(1, 8) = 0.10$ $p=0.75$) showed no significant effects. Fisher's LSD post-hoc analysis revealed untreated passage 17 and passage 26 groups displayed significant variation ($t(8) = 3.35$ $p= 0.0095$) as did treated passage 17 and passage 26 groups ($t(8) = 3.84$ $p= 0.005$). As for proliferation, increased passage number appeared to cause a decrease in FOXO3A expression.

Similarly, PTEN mRNA levels showed 50% of the variation due to passage number ($F(1, 8) = 11.37$ $p=0.0098$) while treatment ($F(1, 8) = 1.11$ $p=0.32$) and interaction ($F(1, 8) = 2.12$ $p=0.18$) showed no effect on variance. Fisher's LSD showed treated passage 17 and passage 26 displayed significantly different PTEN levels ($t(8) = 3.415$ $p= 0.0092$). This was not the case for untreated cells which showed no difference in PTEN expression at passage 17 compared to passage 26 ($t(8)=1.354$ $p=0.21$). These results suggest that treatment of higher passage number cells, but not of cells with lower passage numbers, causes a decrease in PTEN levels.

GRB10 analysis showed 84% of the variance between groups was caused by passage number ($F(1, 8) = 47.84$ $p=0.0001$). Again, treatment ($F(1, 8) = 0.009$ $p=0.93$) and interaction ($F(1, 8) = 0.14$ $p=0.72$) showed no significant effects. Unlike for PTEN, GRB10 expression was significantly different between both untreated passage 17 and passage 26 cells ($t(8) = 4.63$ $p=0.0017$) and between treated passage 17 and passage 26 cells ($t(8) = 5.152$ $p= 0.0009$). These results are similar to those of the proliferation assay suggesting GRB10 levels are consistently lowered during both proliferation and differentiation as a result of increased passage numbers.

Finally, analysis of mTOR levels following the differentiation assay showed significant variation between groups with 48% of the total variation attributable to passage number ($F(1, 8) = 8.30$ $p=0.02$) and no significant effect on variation of treatment ($F(1, 8) = 0.77$

p=0.40) and interaction effects (F (1, 8) = 0.50 p=0.50). Similarly to PTEN, there was significant variance in mTOR expression levels between treated passage 17 and passage 26 cells (t (8) = 2.54 p= 0.035) but not between untreated passage 17 and passage 26 cells (t (8) = 1.539 p= 0.16). This suggests mTOR levels are lowered in cells with higher passage numbers.

All other genes showed no significant variance between groups following the differentiation assay. Passage number effect: **SIRT1** F (1, 8) = 2.35 p=0.16, **IGF2R** F (1, 8) = 0.32 p=0.59, **ABTB1** F (1, 8) = 0.98 p=0.35, **NAMPT** F (1, 8) = 0.14 p=0.71, **UCP2** F (1, 8) = 0.72 p=0.42. Treatment effect: **SIRT1** F (1, 8) = 0.27 p=0.62, **IGF2R** F (1, 8) = 0.31 p=0.59, **ABTB1** F (1, 8) = 0.49 p=0.50, **NAMPT** F (1, 8) = 0.08 p=0.78, **UCP2** F (1, 8) = 0.04 p=0.84. Interaction effect: **SIRT1** F (1, 8) = 0.08 p=0.79, **IGF2R** F (1, 8) = 0.0006 p=0.98, **ABTB1** F (1, 8) = 0.03 p=0.88, **NAMPT** F (1, 8) = 0.77 p=0.40, **UCP2** F (1, 8) = 0.02 p=0.89

For all analyses involving two-way ANOVAs comparing passage number and treatment effects, manual Bonferroni correction was applied to account for 3 comparisons. The significance threshold was therefore set to 0.017. All results reported as significant, except the difference in mTOR mRNA levels between treated passage 17 and passage 26 cells, survived this threshold.

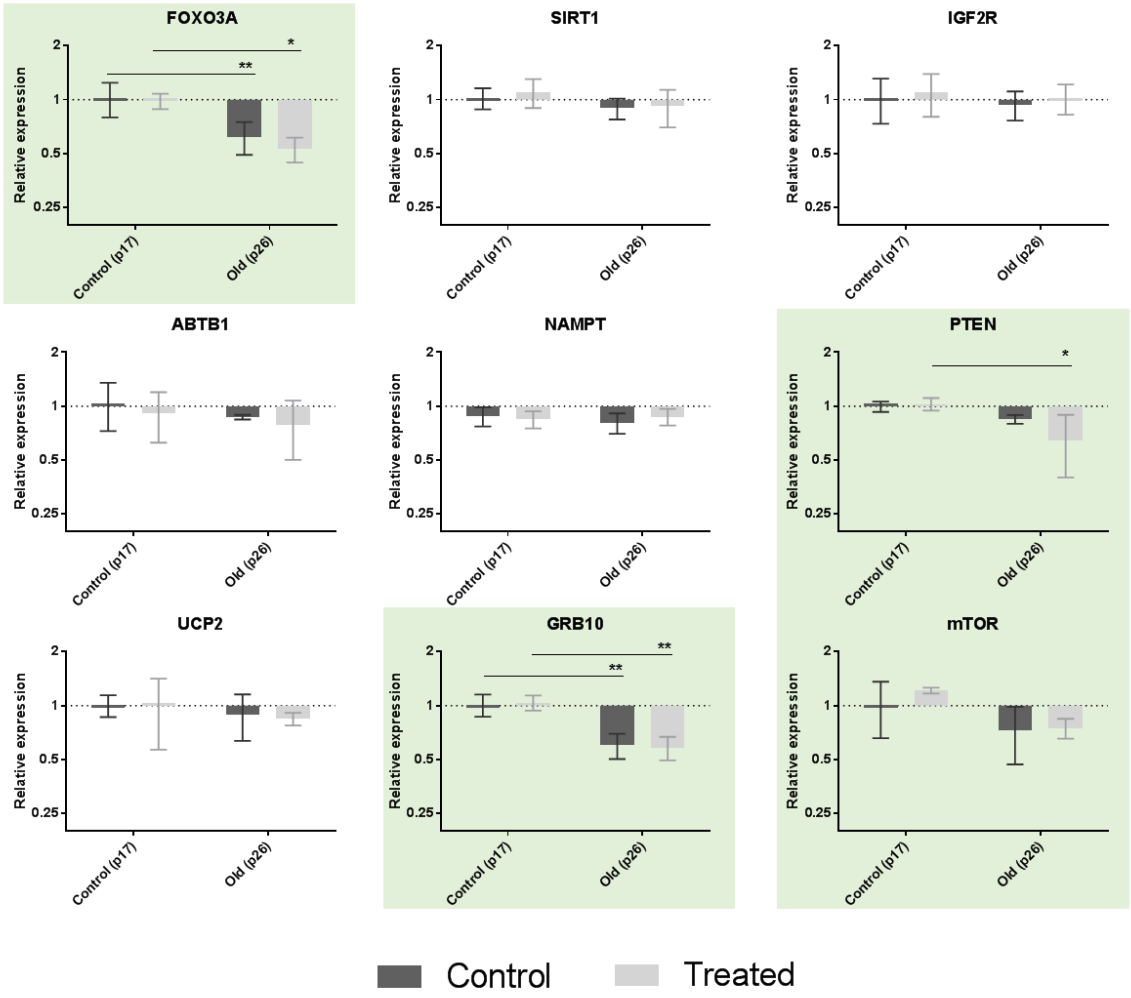

Figure 47 - Candidate gene expression levels in passage 17 (p17) and passage 26 (p26) cells following combination treatment: Differentiation assay. HPC0A07/03A cells were incubated in either media only conditions (control) or with 1µM tBHP + 10µM HU (Treated) during the proliferation stage and for 7 days during the differentiation stage. Quantitative polymerase chain reaction (qPCR) was used to measure gene expression. Y-axis show the expression of each gene relative to control as calculated by the Pfaffl method. **FOXO3A** expression levels decreased as a result of passage number irrespective of treatment. **PTEN** expression levels showed decrease due to passage number only in treated cells. While **GRB10** expression levels decreased as a result of passage number both in control and treated conditions. **mTOR** showed significant variance as a result of passage number likely due to a decrease in expression levels in treated p26 when compared to treated p17 (p= 0.035) this variance however did not satisfy the significance threshold of 0.017. Significant results highlighted by green squares, all other genes (**SIRT1**, **IGF2R**, **ABTB1**, **NAMPT** and **UCP2**) showed no significant alterations in gene expression following treatment or passage number increase. Two-way ANOVAs, 3 biological replicates, 3 technical replicates. Error bars represent standard deviation. Y-axis is a log scale. Bonferroni correction to control for 3 multiple comparisons set significance threshold to p<0.017. Therefore, * symbolises p<0.017 and ** symbolises p<0.003.

Following the results above suggesting alterations in age-related nutrient sensing pathways due to passage number and treatment, mRNA levels of the known senescence markers NRF2 and p16 were tested by qPCR. Two-way ANOVAs revealed no significant changes in NRF2 expression following the proliferation or differentiation assay. NRF2 mRNA levels

following **proliferation** assay; Passage effect: F (1, 8) = 0.02 p=0.90, Treatment effect: F (1, 8) = 0.31 p=0.60, Interaction effect: F (1, 8) = 5e-005 p=0.99. NRF2 mRNA levels following **differentiation** assay: Passage effect: F (1, 8) = 0.31 p=0.59, Treatment effect: F (1, 8) = 0.59 p=0.46, Interaction effect: F (1, 8) = 0.070 p=080.

Similarly, p16 mRNA levels following both assays showed no significant alterations. p16 mRNA levels following the **proliferation** assay: Passage effect: F (1, 8) = 0.94 p=0.36, Treatment effect: F (1, 8) = 4.93 p=0.057. Interaction effect: F (1, 8) = 0.22 p=0.65.
Importantly however, the effect of treatment on p16 mRNA levels only marginally escaped significance. The two-way ANOVA results suggest it may indeed be responsible for 35% of the variance. Investigative post-hoc analysis was carried out which showed the comparisons of groups testing the effect of treatment, (i.e. comparing treated and untreated p17 cells (t (8) = 1.24 p= 0.25) and comparing treated and untreated p26 cells (t (8) = 1.90 p= 0.09)) also escaped significance. p16 mRNA levels following the differentiation however showed no variance between groups: Passage effect: F (1, 8) = 0.01 p=0.92, Treatment effect: F (1, 8) = 0.11 p=0.75, Interaction effect: F (1, 8) = 0.57 p=0.47.
See **Figure 48** for graphs showing the relative expression levels of NRF2 and p16 following the proliferation and the differentiation assays.

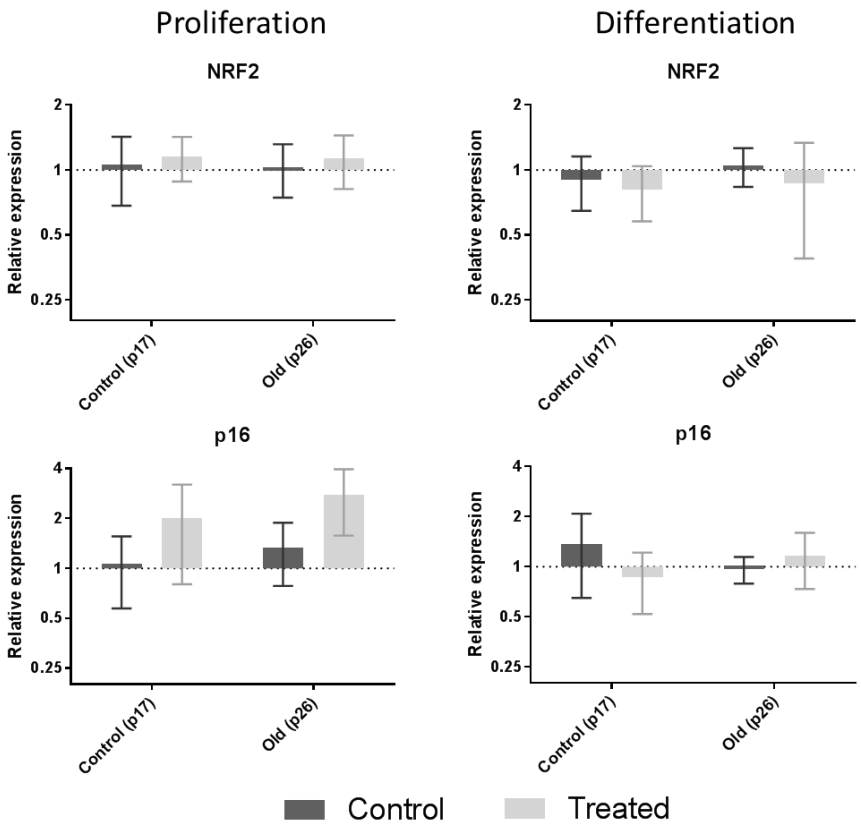

Figure 48 - Expression levels of senescence markers following proliferation and differentiation assays. HPC0A07/03A cells were incubated in either media only conditions (control) or with 1µM tBHP + 10µM HU (Treated) during the proliferation stage and for 7 days during the differentiation stage. Cells that provided the proliferation assay results (**left** column) only underwent the proliferation stage whilst cells that provided the differentiation assay results (**right** column) underwent both the proliferation and the differentiation stages. Quantitative polymerase chain reaction (qPCR) was used to measure gene expression. Y-axis show the expression of each gene relative to control as calculated by the Pfaffl method. **NRF2** and **p16** did not show significant gene expression alterations due to passage number or treatment. Two-way ANOVAs, 3 biological replicates, 3 technical replicates. Error bars represent standard deviation. Y-axis is a log scale.

4.4 Discussion

In this chapter, we assessed a novel multimodal ageing model of human NSC by identifying viable passage numbers and non-toxic concentrations of tBHP and HU. We also showed that while there were no alterations in the number of cells expressing each cellular marker, there were distinct morphological changes as a consequence of increased passage number. Finally, we showed that increased passage number and treatment induced gene-expression alterations of key molecules within the mTOR, IIS and sirtuin sensing pathways

4.4.1 Ageing model: chronic stressors on older cells

To establish the ageing model, appropriate components had to be selected. We aimed to model the OS, DNA damage and replicative senescence that usually accompany NSC ageing; we therefore selected treatment with tBHP, treatment with HU and increased passaging respectively.

Though H_2O_2 is more physiologically relevant, tBHP was chosen to induce OS due to its higher stability. H_2O_2 in fact, was shown to be unstable and affected by several factors such as the presence of solids, pH and temperature changes. In particular, the susceptibility to temperature increase causing a temperature-dependent decrease in concentration made H_2O_2 particularly unsuitable for culturing given the high temperatures needed to culture the cell line (Yazici and Deveci, 2010). tBHP instead, only begins undergoing thermolysis at 69.5°C, a temperature which is outside of the range used in cell culture (Liu et al., 2012). tBHP is a membrane permeable oxidant that has been previously used in *in vitro* models and shown to generate oxidative damage. It can be easily metabolised and, like H_2O_2, it causes ROS generation, lipid peroxidation, ATP synthesis impairments and DNA damage (Chen and Chen, 2011). Cells of diverse origins have been treated for varying treatment-periods at numerous peroxide concentration ranging from nanomolar to millimolar. This is not surprising as the effects of OS are dependent on cell type, experimental conditions and peroxide type (Bae et al., 2010; Harvey et al., 2012; Saffari and Sadrzadeh, 2004; Sée and Loeffler, 2001; Sun et al., 2010). In this chapter, we tested concentrations of 1µM, 10 µM and 100 µM and, to mimic chronic rather than acute OS, we opted for treatment duration similar to that used in the previous chapters of 48 hours during proliferation and 7 days

during differentiation. To our knowledge, such an extended treatment duration has not been tested on NSCs. We report tBHP to have considerable effects on cell number at higher concentrations but to only cause a modest decrease at the lowest concentration tested; 1µM was therefore selected for inducing OS in our model.

To induce DNA damage, another key feature of ageing NSCs, HU was used. This anti-neoplastic drug has been used by several groups to model ageing *in vitro*. By repressing ribonucleotide reductase, HU causes the accumulation of double stand breaks in both mitochondrial and nuclear DNA leading to cellular and mitochondrial stress and dysfunction (Dong et al., 2014). As for tBHP, several concentrations were tested to assess the most suitable one for the HPC model. Unlike tBHP however, varying treatment durations were also assessed, this was done both to replicate previous studies and to assess whether the anti-proliferative characteristics of HU meant longer treatments were not sustainable. So far, two other groups have used HU to model ageing in NSCs, both tested incubations of 1 to 16 hours and concentrations of 0.5µM, 8 µM, 20µM. Dong and colleagues report a small decrease in neurospheres as a consequence of 12-hour treatment with 8 µM HU while Daniele and colleagues report a decrease in cell number following 16-hour treatment with 20µM HU. Though our study was initially designed based on these studies, we report no change in cell number during short incubations (3 or 8 hours) at matching concentrations and a considerable reduction in cell number following longer incubations even at much lower concentrations. As Dong and Daniele do not report the effects of cell number following 3 or 8-hour incubation time and do not test longer incubations, it is difficult to compare the toxicity across assays (Daniele et al., 2016; Dong et al., 2014). Interestingly, experiments on foreskin fibroblasts showed only a mild effect of prolonged treatment with 100µM HU on cell number relative to controls, suggesting different cell types may be less susceptible to HU than NSCs (Yeo et al., 2000). Given our preliminary data showing similar variation in cellular markers irrespective of treatment duration, the lower doses but longer treatment periods were selected for both the proliferation and the differentiation assay to model the sub-toxic but chronic state of stress of aged cells *in vivo* in the absence of excessive cell loss. Though it is possible that higher concentrations may have induced more robust results, extensive cell loss, such as that seen

in response to the higher treatment concentrations, would not be representative of the *in vivo* ageing phenotype. Indeed, though there are reports of neuronal loss in ageing, this appears to be only minimal in non-pathological circumstances (de Magalhães and Passos, 2018; Dong et al., 2014; Price et al., 2001; Raz and Rodrigue, 2006).

The last component of the ageing model was replicative senescence, we modelled this *in vitro* by using cells with higher passage numbers. Though the HPCs used throughout this thesis are immortalised and are usually considered to be able to replicate indefinitely, they, like many other cell lines, show slight alterations with increased passage such as a slower duplication rate. Several groups have shown differences in morphology, development, gene expression and survival between high and low passage cell in a variety of cell lines (Briske-Anderson et al., 1997; Chang-Liu and Woloschak, 1997; Chen et al., 2015; Yu et al., 1997). In this chapter, we utilized this characteristic hypothesising that higher passage numbers would more closely resemble aged cells found *in vivo*. Therefore, we tested the survival, proliferative and differentiative abilities of passage 25 to passage 30 to assess whether higher passages could be used in future experiments. We show no obvious changes in cell number across passages and that cells at all passages expressed stemness and proliferation markers during the proliferation assay and markers for differentiation and reduced proliferation during the differentiation assay. As for OS, what is considered a high or low passage number varies considerably between cell lines as do its effects. For the cell line used here, experiments are usually carried out on cells at passage 16-20 (Anacker et al., 2013; Maruszak et al., 2014; Murphy et al., 2018). The pilot work outlined in section 4.3.1.2 suggested higher passage cells are proliferating and differentiating as expected and that there may be differences across passages in the number immature neurons. Passage 26 was selected as the passage number to be used as part of the ageing model as it showed similar properties in terms of proliferative and differentiative abilities to other higher passages but was faster to produce in terms of methodology.

4.4.2 Cellular consequences of the ageing model

After selecting viable treatment concentrations and durations, we assessed cellular readouts following each treatment, both individually and in combination, on 'young' passage 17 cells. The treatments discussed above, were combined to model several aspects of ageing and thereby replicate a more representative ageing environment. Surprisingly, we saw no effect on any of the cellular markers for proliferation, differentiation, apoptosis, DNA damage or oxidative response following individual or combination treatment except for treatment with 50µM HU only. 50µM HU in fact, caused a significant reduction in proliferation during the proliferation assay and an increase in DNA damage following the differentiation assay. These results are similar to those from Dong and Daniele showing HU dose-dependent increases in DNA damage as evidenced by increases in H2AX phosphorylation (Daniele et al., 2016; Dong et al., 2014). Our results however, differ from those of the two studies above in cell type and in HU treatment duration and concentration. In addition, we report this increase was accompanied by such strong toxicity and variability in cellular response, as evidenced by the large error bars, that further experiments would be necessary to assess whether these changes were simply driven by the resulting decline in cell density. Indeed, cells in culture are known to be strongly affected by cell density (Kim et al., 2017; Wilson et al., 2015). Besides the technical aspects, these results could also indicate hippocampal progenitor cells are less susceptible to these stressors. As reviewed by Wang and colleagues, different neuron cell types are affected by stress and damage in different ways. In particular, even within specific regions such as the hippocampus, each subfield experiences different susceptibilities. For example, dentate gyrus neurons were shown to be less susceptible to OS than CA1 neurons. These findings support the possibility that the cell type used here is more resistant than those used previously (Lee et al., 2015; Wang and Michaelis, 2010).

Given the toxicity of higher concentrations however, the lack of DNA damage seen in the treatment conditions involving HU remains unexpected. Suggesting that either HU concentrations that are higher than 10µM but lower than 50µM are necessary for a robust but sub-lethal effect or that H2AX quantification ought to be improved. Some groups in fact, quantify H2AX positive foci rather than H2AX positive cells, it may therefore be

interesting, to repeat these experiments with higher resolution microscopy to assess if different methodology yields different results (Kuo and Yang, 2008).

Similarly, quantification of cellular markers following combination treatment and higher passage number showed no change across experimental conditions. Interestingly, for some markers, higher passage numbers appeared to lead to increased variability in cellular markers. An explanation for this phenotype may be that increased passage causes a heterogeneous population of both damaged and healthy cells and that the proportion of each varies across biological replicates leading to the increased variability seen in the immunocytochemistry results. It is important to note the very high number of cells expressing nuclear NRF2 seen across all conditions, usually averaging around 90% of the total cell count. In unstressed conditions, NRF2 is typically anchored to the cytoplasm. Upon OS, NRF2 travels to the nucleus where it forms heterodimers with other transcription factors and initiates transcription of genes that code for proteins with cytoprotective effects (Bakunina et al., 2015). Therefore, this data suggests that though there is no change in NRF2 levels between conditions, all conditions show a high oxidative response. Thus, merely counting the number of cells positive for NRF2 may not be sufficient and instead, assessing the overall expression of NRF2 may be necessary. qPCR analysis of NRF2 mRNA levels however, showed no change across conditions suggesting the levels of NRF do indeed remain unchanged across treatment and passage number. To confirm this finding, it might be interesting to assess NRF2 translocation by cellular fractionation combined with western blots to determine whether there is indeed an increase in nuclear translocation in the stressed conditions. Currently, these results suggest that the lack of differences may instead be due to a ceiling effect in oxidative response; there is no visible difference between treatments because all groups are already undergoing the highest level of oxidative response. This hypothesis is in line with experts in the field of OS suggesting that cell culture imposes a constant state of OS on cells that is often ignored in studies (Halliwell, 2003; Wright and Shay, 2002). OS in culture is heavily dependent on cell type, isolation and culturing techniques but is likely due to an imbalance between ROS and anti-oxidant responses. Briefly, in comparison to *in vivo*, cultured cells tend to be exposed to higher levels of oxygen which promotes ROS generation. In addition, cell culture media is

frequently deficient in adequate levels of antioxidants and the presence of free metal ions can act as a pro-oxidant. Though this is not the case for every cell culture model, these aspects can all contribute to unusually high levels of OS in control conditions which may mask any further onset of OS (Halliwell, 2003). Future studies should therefore consider and minimise the impact of these aspects when assessing OS in culture.

Despite the lack of differences in the percentage positive cells for each marker, we report interesting alterations in neuronal morphology. Cells stained for MAP2 and DCX show a more rounded morphology with increasing passage number. This was present both in pilot work assessing the differentiation potential of cell from passage 25 to passage 30 as well as in finalised experiments validating the ageing model. This phenotype was driven by cell passage but appeared unaffected by treatment; both individual treatments and combination treatments on passage 17 cells in fact, showed no effect. These findings are in line with those by Knoth who reported dendritic alterations both when comparing DCX staining in young or aged mice and when comparing DCX staining on human post-mortem hippocampal tissue of individuals from 1 day to 100 years of age. The authors suggest DCX positive cells with no dendrites, which are more common in aged human and murine tissues, are cells in a more undifferentiated state (Knoth et al., 2010). Interestingly, our results show this phenotype was present both in DCX and MAP2 positive cells. As MAP2 expression occurs slightly later in the neuronal differentiation timeline, this data suggests that, if the rounded morphology is caused by a standstill in differentiation, this occurs after the cells begin to express MAP2. Furthermore, Knoth show these morphological alterations are accompanied by a large decline in DCX positive cells whereas our data suggests DCX and MAP2 expression remains stable across passages but the proportion of cells with an elongated morphology decreases whilst that with a rounded morphology increases. Older studies in rat tissues using 3,3'-Diaminobenzidine staining, also showed increases in soma area, perimeter and diameter of dorsal lateral geniculate nucleus neurons with age suggesting this age-related phenotype is not specific to the hippocampus alone (Villena et al., 1997).

We also report that the stunted morphology identified in higher passage numbers is characterised by increased cytoplasm width and cytoplasm width to length ratio as well as increased nuclear area and roundness. Importantly, nuclear and cellular enlargement are often reported as a recurring phenotype of senescence in a number of cell types ranging from fibroblasts to several cancer cell lines (Angello et al., 1989; Barascu et al., 2012; Sadaie et al., 2015; Sikora et al., 2016). This data therefore suggests HPCs that undergo repeated passaging exhibit phenotypes similar to those of senescent cells and may therefore be undergoing senescence. Despite this, as research into the senescent phenotypes of post-mitotic cells such as neurons is only just beginning, these phenotypes are yet to be explored in neurons and therefore a consensus on senescent phenotypes of neuronal cells is yet to be determined. Overall however, the morphological alterations reported here are a good indication that the model established in this chapter induces some aspects of ageing.

4.4.3 Molecular consequences of the ageing model

Finally, we evaluated whether the expression levels of the 9 candidate genes, identified in the previous chapter, varied following the ageing model. First, we assessed their expression following individual and combination treatment on 'young' passage 17 cells. This revealed that treatment during the proliferation or differentiation assay did not affect the expression level of our candidate genes. Next, we assessed the effect of combination treatment and increased passage number. We report variations due to passage number in the expression levels of several genes following both the proliferation and the differentiation assays.

We show that FOXO3A expression was significantly lower in cells with a higher passage. This was the case for experiments harvested both after the proliferation assay and after the differentiation assay, suggesting this change occurs in proliferating and differentiating cells alike. FOXO3A is a key molecule in NSC homeostasis that is frequently linked to ageing research as it is known to regulate the transcription of genes associated to OS response, DNA damage and to the repression of apoptosis (Fluteau et al., 2015; Paik et al., 2009; Renault et al., 2009; Stefanetti et al., 2018). FOXO3A has been linked to human longevity by several successful association studies: Willcox and colleagues initially tested 5 known

longevity genes for association in a sample of long-lived Japanese men and showed significant associations with 3 FOXO3A polymorphisms. This association was later confirmed by Flachsbart et al who replicated and extended Wilcox's results by showing these variations affected females and males alike in a German population. In line with this, associations between FOXO3A and longevity were also confirmed in a Han Chinese cohort (Flachsbart et al., 2009; Li et al., 2009; Willcox et al., 2008b).

Despite this, a link between its expression levels and ageing human brains is yet to be established Our results however, are in line with groups showing an age-dependent decrease in FOXO3A in mouse small-intestine cells and increased phosphorylation, and therefore inactivation, of FOXO3A in older mouse NSCs (Becker et al., 2018; Renault et al., 2009). In addition, experiments assessing the effects of the knockout and downregulation of FOXO3A in both mouse NSCs and human dermal fibroblasts, have reported the cells exhibited senescence and aged phenotypes therefore suggesting FOXO3A is indeed a driver of cellular ageing (Kyoung Kim et al., 2005; Renault et al., 2009). Given the important role in OS and DNA damage response, a decrease in the expression of FOXO3A in older cells may be indicative of poorer defence mechanisms. Interestingly, Fluteau and colleagues showed that while there was no association between FOXO3A expression and age in human lateral temporal cortex tissue, there was a significant correlation between FOXO3A expression and H2AX expression further supporting a role for FOXO3A in DNA damage response (Fluteau et al., 2015). While it is surprising that our results did not show accompanying alterations in DNA damage or apoptosis marker expression, this may be due to the assay length; a longer assay may in fact have allowed enough time for the gene expression alterations to be reflected by cellular outcomes.

We also report variation in the gene expression of mTOR pathway components due to passage number. mTOR, the key molecule within this signalling cascade, showed variation due to passage number following the differentiation assay but post-hoc analysis did not survive multiple correction testing suggesting a lack of power and possibly only a modest effect size. Though it is difficult to compare such data to previous findings, alterations in mTOR signalling are strongly associated to autophagy and stem cell maintenance and have

been repeatedly implicated in ageing. In general, attenuation of mTOR signalling either via rapamycin treatment or genetic intervention was shown to extend lifespan in yeast, worms, flies, and rodents as reviewed by Johnson (Johnson et al., 2013).

Interestingly, we also report higher passage number induced decreased expression of two negative regulators of the mTOR pathway; GRB10 and PTEN. As for FOXO3A, GRB10 showed a decrease in expression following both assays, again suggesting the alteration is a persistent change in response to passage number that is irrespective of the cell's differentiation state. This is particularly interesting as GRB10 is a known regulator of stem cells as evidenced by experiments investigating its role in hematopoetic stem cell regulation (Yan et al., 2016). Though its role in NSCs remains to be elucidated, alterations in its expression levels are indicative of mTOR signalling alterations as it is responsible for its regulation via negative feedback mechanisms. PTEN, the other negative regulator of mTOR investigated here, showed a significant decrease in expression level when comparing treated higher passage cells to treated lower passage cells but not when comparing untreated cells across passages. Our data shows treatment affects older cells more severely than younger cells. This suggests older cells are less equipped to deal with adverse environments; younger cells may thus be more efficient at dealing with OS and DNA damage and at returning to a normal state whilst older cells may have longer lasting alterations due to insults which is why the alterations are only detected in in the treated older cells. In line with this, the gene expression alterations in PTEN were only detectable following the differentiation assay. Given the differences in the assay length between the proliferation and differentiation assay, this data suggests either that tBHP and HU affect NSC progeny more harshly than their undifferentiated counterparts or that the differentiation assay is a more representative of chronic stress. Were the latter to be true, this result suggests older cells are more susceptible to prolonged periods of stress i.e. the differentiation assay. Regardless, previous findings have shown PTEN overexpression is linked to exceptional longevity in mice which is in line with our data showing decreased levels of PTEN in older cells (Ortega-Molina et al., 2012). In addition, PTEN has been linked to anti-oxidant activity and to apoptosis via PIP3 dependent and independent mechanisms respectively. The degree of damage was suggested to be a decisive factor as to whether

PTEN induces apoptosis or anti-oxidative response (Chen et al., 2005; Wan et al., 2007). Given the presence of PTEN expression alterations following the differentiation assay it would be interesting to prolong the assay and assess cellular changes pertaining to apoptosis and OS at a later timepoint. In summary, though the alterations in mTOR expression levels remain elusive, the lowered levels of negative regulators of the mTOR pathway are suggestive of a dysregulated signalling cascade which is likely to contribute to the altered phenotypes seen in cells with higher passage numbers.

NAMPT, the rate limiting enzyme essential for SIRT1 deacetylation activity showed very interesting alterations during the proliferation assay. We report higher expression levels of NAMPT in passage 26 cells when compared to passage 17 cells and a further increase in expression in treated passage 26 cells when compared to untreated passage 26 cells. Interestingly, there was no alteration in expression when comparing treated and untreated passage 17 cells. This data shows that while treatment alone is not able to cause alterations in low passage number cells, there is a cumulative effect of treatment and passage number that further exacerbates the phenotype seen in higher passage numbers. A possible explanation for these results is that cells with higher passage number have poorer, or at least different, resources to combat the oxidative and replicative stress caused by treatment, which result in an exacerbation of their 'aged' genetic signature. As for PTEN, it remains to be established whether the increase in NAMPT is a negative consequence or simply a compensatory mechanism. NAMPT overexpression in fact, was shown to rescue NAD+ depletion and mitochondrial dysfunction that accompany senescence by several groups. NAMPT expression was found to be lower in mesenchymal stem cells obtained from aged rats than in those obtained from younger rats. Notably, the aged phenotype found in older mesenchymal stem cells could be induced by inhibiting NAMPT function while NAMPT overexpression caused its attenuation (Ma et al., 2017). A marked decline in NAMPT expression and activity was also shown to precede senescence in human vascular smooth muscle cells which was delayed by NAMPT overexpression (van der Veer et al., 2007). In line with this, NAMPT ablation in mouse NSCs recapitulated ageing phenotypes (Stein and Imai, 2014). These reports suggest the increase in NAMPT seen in response to treatment and increased passage is likely a defence mechanism. Surprisingly, these

alterations were not accompanied by significant changes in Sirt1 expression. There was however, a trend in a similar direction to that of NAMPT suggesting SIRT1 expression may indeed be changing. Importantly, these alterations appear specific to the proliferation assay, suggesting either that increased NAMPT as a compensatory mechanism is specific to NSCs and not to differentiated cells or that the cells are unable to sustain increased NAMPT expression for an extended period of time such as the differentiation assay.

Finally, to assess whether these alterations were a consequence of senescence and to complement the NRF2 expression data discussed in the previous section, the expression levels of p16 were also assessed. p16 is a cyclin-dependent kinase inhibitor which is upregulated in senescent cells and is often used as a marker for senescence (Daniele et al., 2016). Though an interesting trend was shown, suggesting treatment but not passage number increases p16 expression this was not significant. This suggests that while these results may be indicative of ageing phenotypes they are likely not due to senescence. SA-βgal quantification was attempted to confirm this hypothesis, but components of the protocol appeared toxic, making the assay unreliable in this cell line (data not shown). Similarly, telomere length quantification by qPCR was attempted as described by Cawthon, but the resulting data was untrustworthy due to persistent variability across both technical and biological replicates (Cawthon, 2009). Further work optimising senescence readouts in this cell line is therefore necessary to clarify the state of these cells.

4.4.4 Summary and future directions

In summary, we identified viable concentrations for the chronic treatment of the HPCs with tBHP and HU. We also proved that cells with higher passage number retain all proliferative and differentiative abilities and that surprisingly, treatment and passage number do not affect the expression of cellular markers of neurogenesis except for possible alterations in DNA damage. Of note, we showed robust morphological alterations and interesting alterations in the expression levels of candidate nutrient-sensing genes in response to increased passage number. We initially aimed to establish a more robust and multimodal model of ageing. While increasing passage number showed robust morphological and molecular alterations, treatment did not obtain the same result. In addition, the

combination of both treatment and increased passage to obtain a multimodal ageing model also failed to show considerable differences from passage number alone. Though we still believe the development of multimodal ageing models would be beneficial for ageing research, our current data suggests the more robust experimental condition is simply increased passage.

Future experiments assessing post-translational modifications as well as the localization of these candidate molecules and epigenetic status would provide further insights on the alterations occurring in response to stress. Some of the genes that appear unaltered in response to stress may simply be undergoing different types of modifications. In addition, repeating these experiments and assessing both gene expression and cellular marker expression at varying timepoints throughout differentiation may uncover changes that have gone undetected in these assays. Specifically, extending the assay and assessing the electrophysiological properties of the resulting neurons would allow us to gain insight on the functionality of neurons that underwent chronic stress during both NSC and differentiated states. An unchanged number of progenitors, neuroblasts and immature neurons is not necessarily indicative of unaffected neurogenesis, a process that is dependent on a variety of other factors (Kempermann et al., 2004b). The altered morphology reported above in fact, may cause poorer integration and therefore poorer functionality. Finally, knockout and overexpression experiments targeting the altered genes would establish their contribution to the ageing phenotype and aid in understanding whether these changes are compensatory mechanisms or detrimental consequences contributing NSCs decline.

4.4.5 Limitations

Despite the interesting findings outlined above, this study had a number of limitations. Firstly, to induce sub-lethal chronic stress rather than acute stress, very low concentrations of the treatments had to be used to not bias the results with the use of cultures with extensive cell loss. As evidenced by the large variation in the treatment group using the higher dose of HU, similar treatment concentrations caused different levels of toxicity in different biological replicates suggesting other variables beyond our control affect

treatment susceptibility. It is therefore possible that ideal concentrations of tBHP and HU, that induce more robust OS, DNA damage and senescence but do not cause cell death, lie somewhere between those tested here. Identifying these might reveal changes which remained undetected in this study. In line with this, media components such as albumin and sodium selenite designed to prevent OS in culture may be interfering with the damage response to both passage number and treatment. Finally, while increased passage number has been used previously to model ageing, there is a possibility that this inadvertently selects for specific cell types.

5 Impact of Lifestyle and Genetics on Cognition: An Epidemiological Study.

5.1 Introduction

5.1.1 Lifestyle effects on healthspan and cognition

As discussed in chapter 1, increasing healthspan and thereby compressing morbidity is a major goal of current biogerontology research. Prolonging life is not a sustainable goal if it is not accompanied by an equal increase in healthspan. Currently, yet both lifespan and healthspan are increasing, healthspan is doing so at a slower rate. This has caused an increase in proportion of time spent in late-life morbidity which now consists of 16-20% of life (Oeppen and Vaupel, 2002). Though it is often debated whether one can reach end of life in a relatively healthy state, studies on centenarians have reported that those who live longer tend to do so with an accompanying reduction of time spent in late-life morbidity. These findings, together with work in animal models have shown it would indeed be possible to extend both life and healthspan if the underlying ageing mechanisms are identified (Fontana et al., 2010; Fontana and Partridge, 2015).

The steep increase in life expectancy over the last decades suggests only a minor role for genetic changes (Burger et al., 2012). Instead, lifestyle factors such as exercise, diet, education and social status appear to have greater effects than initially predicted. The hereditability of lifespan in fact, lies somewhere between 12% and 25% (Kaplanis et al., 2018; van den Berg et al., 2017) and only a few genetic loci have so far shown robust association with longevity (Joshi et al., 2017; Partridge et al., 2018). The effect of lifestyle on healthspan and longevity is further supported by lack of genetic differences between individuals from areas with very high life expectancy and their neighbours (Poulain et al., 2014). This has prompted the field to try and elucidate exactly how lifestyle can have such strong effects (Partridge et al., 2018). A major hurdle in biogerontology research however, is the heterogeneity with which ageing presents itself. Ageing is usually accompanied by multimorbidity i.e. the presence of two or more chronic health conditions, but these vary considerably between individuals. Therefore, whilst preventing each morbidity from

occurring in the first place may be a viable treatment option, it is difficult to predict which specific health conditions each person will be affected by (Partridge et al., 2018). This problem could be overcome if suitable and early biomarkers are developed to assess the risk of each age-associated condition. In an attempt to understand the mechanisms behind one of the most debilitating age-related morbidities, we focus on the age-related decline in cognitive function.

Diet and nutrition, as discussed in chapter 1 have been linked to longevity and cognition in a variety of animal models and human studies (Most et al., 2017). Together with this, exercise has been associated to improved cognitive abilities and a reduction in age-related decline in both animal models and human studies (Busse et al., 2009; Sujkowski et al., 2015; Vaynman et al., 2004; Vaynman and Gomez-Pinilla, 2006; Weuve et al., 2004). An increase in energy expenditure appears protective against cognitive decline. Interestingly, this is also the case in older adults (Mattson, 2012; Roig et al., 2013; Smith et al., 2010). In line with this, observational studies have shown aerobic fitness is associated with reduced brain tissue loss in ageing humans and increased physical activity is related to improved mental health and better performance on cognitive tasks (Chekroud et al., 2018; Colcombe et al., 2003; Hogan et al., 2013). In addition, several meta-analyses have been carried out assessing this relationship and have found aerobic exercise to be protective for cognitive function in the elderly, protective against dementia risk and also to be associated to lower risk of developing depression (Blondell et al., 2014; Northey et al., 2018; Schuch et al., 2018).

Following these findings, several intervention studies have tried elucidating the effects of diet and exercise on aspects of human ageing; the Mediterranean diet was shown to be protective against cardiovascular disease and cancer, while a combination of diet and exercise showed positive effects on diabetes and microvascular complications (Estruch et al., 2018; Nathan et al., 2015; Toledo et al., 2015). However, despite mounting evidence of the importance of diet and exercise in terms of cognition there are only limited and often contradicting human intervention studies assessing this relationship (Martin et al., 2007; Williams et al., 2010; Witte et al., 2009). One such study, is the ongoing FINGER intervention

study which focuses on 7 modifiable factors (low education, midlife hypertension, midlife obesity, diabetes, physical inactivity, smoking and depression) that greatly increase the risk of Alzheimer's disease. This double-blind randomised controlled trial recruited at-risk elderly individuals and assigned them a multidomain intervention including diet, exercise and cognitive training for two years. Results from this study showed an improvement in cognitive performance suggesting the combination of diet and exercise, as well as early intervention, is crucial for preventing age-related cognitive decline (Ngandu et al., 2015).

Despite this encouraging study, the exact lifestyle interventions that would benefit ageing and age-related cognitive decline the most are still unclear. In addition, dietary restriction, one of the most effective interventions, is notorious for its low compliancy rates suggesting lifestyle interventions as a whole may not be a realistic public health intervention (Moreira et al., 2011; Partridge et al., 2018). This, combined with the heterogeneity seen in ageing phenotypes and contradicting results from human interventions, suggests further research is needed to devise more targeted and effective interventions for specific subpopulations. To achieve this, it is necessary to understand what makes certain individuals more prone to certain age-related conditions and therefore more susceptible to certain lifestyle interventions. Though only a small proportion of longevity is hereditary, genetic polymorphisms may still have important functions in determining this susceptibility.

5.1.2 Gene environment interactions

Since the Human Genome Project was completed at the start of the century, increasing emphasis has been put on genetic studies. Projects such as the 100 genome project aimed at understanding genetic variation between individuals have provided new and exciting avenues for understanding the links between genotype and phenotype (Durbin et al., 2010). As more genomes are sequenced, our understanding of factors such as linkage disequilibrium and thereby the available techniques are undergoing steep improvements (Hinds et al., 2006; Reich et al., 2001).

These advances have allowed for the development of precision medicine, a field aimed at tailoring interventions to each patient in an attempt to decrease the number of failing

treatments. Often this tailoring is based upon the patient's genetic background and allows for a better targeting of both drugs and lifestyle interventions which is usually accompanied by decreased side effects and increased efficacy (Ginsburg and Phillips, 2018). Precision medicine has shown positive outcomes in several diseases such as certain types of cancer and cystic fibrosis and is currently being developed for a larger set of disorders such as dementias and ageing in general (Hampel et al., 2016; Reitz, 2016). It is indeed in pathologies such as ageing, where there is a lack of effective treatments and vast heterogeneity in between cases, where precision medicine could be most useful. Understanding which patients would benefit from specific interventions, whether these may be lifestyle-based, drug-based or a combination, would both improve the care given to patients and decrease the financial burden of healthcare caused by an ageing population (Wiener and Tilly, 2002). For such therapies to be developed however, the field must first identify which polymorphism make people more or less susceptible to faster age-related decline and to the lifestyle effects thereon. For this purpose, studies attempting to clarify gene environment interaction (GxE) in the context of age-related cognitive decline are a necessity.

5.1.3 CANTAB PAL© as a measure for hippocampal-dependent cognition

Biogerontology research is impaired by a lack of effective biomarkers to monitor disease progression in humans. Cambridge Cognition have therefore developed a battery of neuropsychological tests which can be used as early biomarkers of cognitive decline (Barnett et al., 2015). Cambridge Neuropsychological Test Automated Battery (CANTAB) was also designed with the aim to bridge the translational gap between animals and humans, another key issue in biogerontology research (Dutta and Sengupta, 2016; Murphy et al., 2014). Many of the tasks in the battery are based on animal paradigms and are adapted for human use. Equally, human neuropsychological assessments used in clinics were adapted to be used through touch screen devices and translated for use in both rodent and non-human primate models.

The CANTAB paired associates learning task in particular, was developed to help detect the prodromal stages of mild cognitive impairment and Alzheimer's disease. It is based on

episodic memory, which is the ability to store, learn and retrieve information about past experience. The spatial element of the task makes performance particularly dependent on the hippocampus and the entorhinal and transentorhinal cortex (Brown and Aggleton, 2001). The importance of the hippocampus in such tasks was initially suggested by case studies of patients with damaged hippocampi who performed badly on object-location tasks (Smith and Milner, 1981). Following this, Parkinson and colleagues reported that rhesus monkeys with large ablative legions in the hippocampal formation also reported significant impairments in object-location association tasks (Parkinson et al., 1988). Since then, the hippocampus has been further implicated in rodent-adapted versions of CANTAB PAL© performance; after muscimol (a GABA agonist) injection in the hippocampus in both rats and mice showed severe impairments in PAL task performance (Kim et al., 2015; Talpos et al., 2009; Yoon et al., 2012). Finally, functional MRI studies in humans showed the PAL task activates the hippocampus, interestingly, this occurred in a load-dependent manner whereby activation increased with PAL task difficulty (de Rover et al., 2011). Lesion studies have also confirmed PAL test performance is dependent on the functional integrity of the temporal lobe and specifically of the entorhinal cortex (Owen et al., 1995).

The PAL task was designed to be used within cognitively impaired and cognitively healthy populations alike, a graded adjustment was incorporated to help compare extreme performances. This graded nature means the task is subdivided into several stages and adjustments are applied to the participant's score if they do not reach the more difficult stages. The 6-pattern stage (the second hardest) has been extensively studied and showed a 100% sensitivity in distinguishing cases from controls in mild cognitive impairment and Alzheimer's studies (Barnett et al., 2015; Chandler et al., 2008). The more difficult 8-pattern PAL stage which is usually used in cognitively healthy populations instead, has no consensus on what score constitutes healthy or unhealthy cognition but is a valuable tool in assessing cognitive decline in the absence of pathology (Lee et al., 2013). In all stages, PAL is highly dependent on age owing to its reliance on episodic memory, making it a useful tool to study both healthy and pathology-driven cognitive ageing (Barnett et al., 2015; Lee et al., 2013; Soares et al., 2015). Finally, as discussed in section 3.1.1 the strong effect of age and dependence on hippocampal function combined with the emphasis on distinguishing

similar scenarios from one another highlights the possible involvement of pattern separation and therefore adult hippocampal neurogenesis in PAL tasks.

5.1.4 Aims of this chapter

As discussed above, interventions are needed to extend healthspan alongside lifespan and according to current research the most promising of these involve lifestyle interventions. However, no lifestyle intervention in humans has proven as efficient as those carried out in animal models, suggesting human heterogeneity may be an important factor to consider (Mitchell et al., 2015). In this chapter, we aimed the following. 1) To assess the impact of lifestyle factors such as diet and exercise on hippocampus-dependent cognition. 2) To assess the effect of genetic polymorphisms on hippocampus-dependent cognition and their interaction with lifestyle factors 3) To investigate methylation changes occurring as a result of age and lifestyle with the purpose to validate the importance of epigenetic alterations discussed in chapter 1. See **Figure 49** for the aims and hypothesis of this chapter.

We focus on polymorphisms related to the 9 candidate genes selected from the cellular and molecular *in vitro* work in previous chapters: mTOR, GRB10, IGF2R, PTEN, FOXO3A, UCP2, SIRT1, NAMPT and ABTB1. As discussed in chapter 3, these 9 genes all belong to pathways that have been associated to ageing, NSCs and cognitive decline. However, there are no previous studies linking polymorphisms in these regions with age-related cognitive decline or lifestyle interactions, making this an exciting and novel avenue.

With this study, we also hope to address the translational gap which has caused many interventions developed in animal and *in vitro* models to prove unsuccessful when translated to humans (Franco and Cedazo-Minguez, 2014; Mak et al., 2014; Medina and Avila, 2014). To this purpose, we validated these 9 candidate genes that were found to be associated to neural stem cell function *in vitro* (see chapter 3) for association to cognitive performance in a human cohort. The PAL task was selected as the cognitive task available in the cohort that was most closely related to hippocampal function and therefore likely to rely on neurogenesis and neural stem cell function. Making it a useful human-based cognitive task with which to validate our *in vitro* findings.

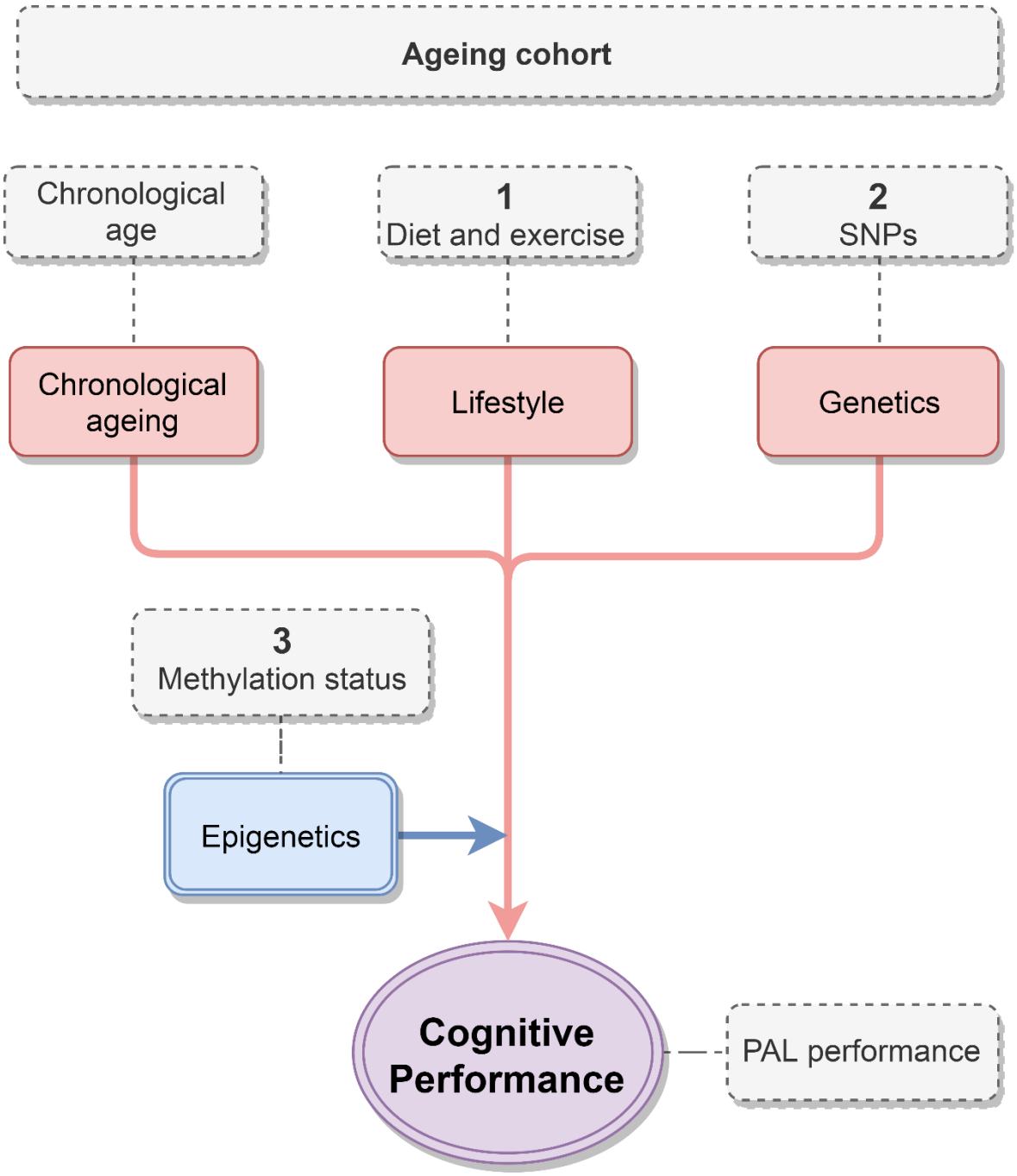

Figure 49 - Chapter 5 hypothesis. We hypothesis that chronological ageing, lifestyle and genetics impact on cognitive performance. We also hypothesise that these effects are in part, mediated by epigenetic alterations. Therefore, we aim to assess the effect of diet and exercise **(1)**, single nucleotide polymorphisms (SNP) **(2)** and methylation status **(3)** in relation to ageing and cognitive performance on the Paired Associates Learning (PAL) task.

5.2 Materials and methods

5.2.1 Programming software

All data cleaning, quality control, variable calculations, data merging, statistics and graphical representations outlined in this chapter were carried out in the Rstudio software (version 1.0.153) (RStudio Team, 2016).

5.2.2 Data request to access the TwinsUK cohort

The data used in this chapter was obtained by the Department of Twin Research at King's College London, as part of the TwinsUK cohort recruitment (Moayyeri et al., 2013). This cohort is comprised of over 12000 monozygotic and dizygotic twins between the ages of 16 and 95 with a wide range of demographic, cognitive, genetic and lifestyle data, making it an ideal cohort for this study. Data was requested through the data access request form available online at http://www.twinsuk.ac.uk/data-access/submission-procedure-2/ (accessed on 26th August 2018). To study the effect of genetic polymorphisms on hippocampus-related cognition, all available PAL result scores were requested along with the demographic and genotype information pertaining to the twins with available PAL scores. To investigate the effect of lifestyle on cognition, the most contiguous total energy intake, Healthy Eating Index (HEI) and physical activity measures to the PAL phenotype were also requested. Finally, DNA methylation data was requested to investigate any association between methylation intensity and performance on cognitive tasks.

5.2.3 CANTAB Paired Associates Learning Task

CANTAB includes a variety of digital cognitive tasks developed by the University of Cambridge aimed at assessing human brain function. In this study, we used CANTAB's Paired Associate Learning Task. The task is delivered on a touchscreen and has a duration of 8 minutes. It consists of 10 stages of increasing difficulty each comprised of 2 phases (acquisition and recall). During the acquisition phase 1,2,5,6, or, in the final stage, 8 patterns are shown in one of the 6 or, in the final stage, 8 boxes displayed on the screen. Following this initial acquisition phase, the patterns are shown one at a time in the middle of the screen and the participant is asked to place the patterns in the correct box. This

phase is known as the recall phase. During this phase, if the correct location of the patterns is given, the participant is allowed to proceed to the next stage, after an incorrect answer, all patterns are displayed again and the participant is prompted to provide the patterns' locations again. Screenshots from the task are shown in **Figure 50.**

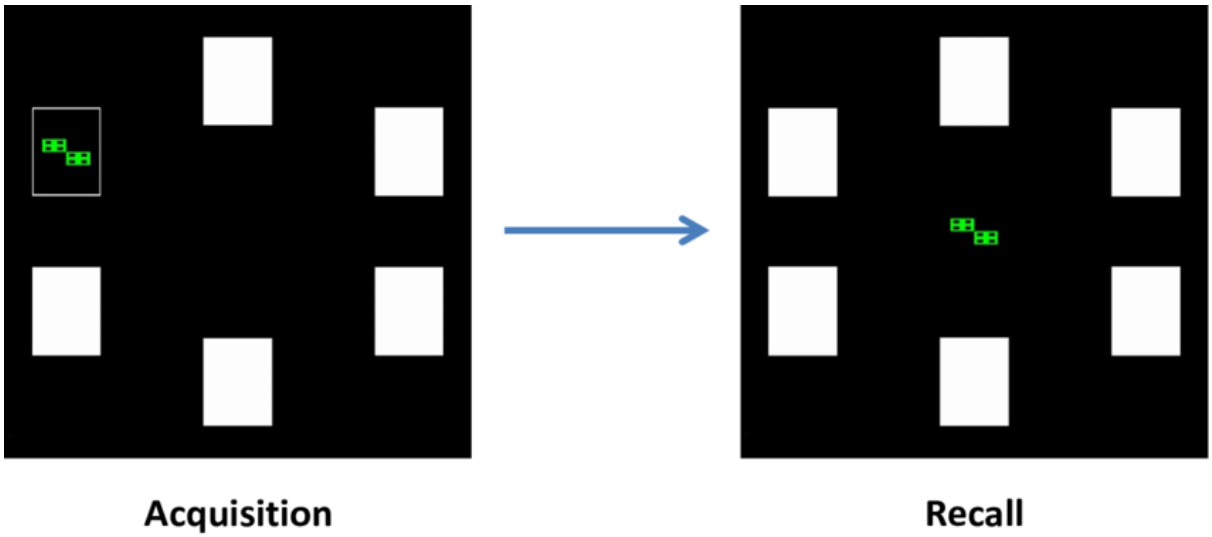

Figure 50 - CANTAB Paired Associates Learning task (PAL) Screenshot showing the acquisition and recall phases of the PAL task. The screenshots show the 6-boxstage. Participants are asked whether the image is in the correct box during the acquisition phase and asked to place the image in the correct box during the recall phase .Image from (Delotterie, 2014)

The outcome measure is the numbers of errors made by the participant adjusted for trials required and stages completed. Each stage allows a maximum of 10 errors before the participant is prevented from progressing and their adjusted score is calculated. The adjustment is calculated by summing the number of patterns not attempted and subtracting this number divided by the number of boxes from it. The result is then multiplied by the total number of possible trials. This adjustment is necessary to compare all participants irrespective of which stage of the test they have reached.

Results adjusted for the 6-pattern PAL, which only includes the first 9 stages, are usually used in cognitively-impaired populations, as this study was aimed at investigating cognition in a cognitively-healthy ageing population, the 8-pattern PAL adjustment was used. PAL scores of 2153 individuals were received from TwinsUK. Prior to analysis, the PAL data was inspected for normality, heteroscedasticity and for the presence of outliers via visual inspection of frequency distribution, residual vs fitted, quantile-quantile (Q-Q), scale-location and residual vs leverage plots.

5.2.4 Demographic information

Demographic factors such as date of birth, sex (female or male), zygosity (monozygotic or dizygotic), Mini Mental State Examination (MMSE) results, education and National Adult Reading Test (NART© Hazel E. Nelson) results were also received. TwinsUK is made up of predominantly white participants of European background.

Education was measured via an 8-question questionnaire (see **Table 29**). Participants were asked to tick the box with the qualification type most similar to their highest level of qualification.

Code	Qualification
1	No qualification
2	NVQ1/SVQ1
3	O-Level/GCSE/NVQ2/SVQ2/Scottish Intermediate
4	Scottish higher, NVQ3, city and qulds, Pitman
5	A Level, Scottish Advanced Higher
6	Higher Vocational training (e.g. Diploma, NVQ4, SVQ4)
7	University degree
8	Postgraduate degree (e.g. Masters or PhD), NVQ5, SVQ5

Table 29 - TwinsUK education questionnaire. Table reporting the method used to code education data throughout the TwinsUK cohort. The first column shows the numerical value given to the participant's answer (second column).

NART was carried out following the guidelines outlined by Nelson and Wilson (Nelson and Wilson, 1991). Briefly, English mother-tongue participants are given a list of 61 irregular and non-phonetic words (eg. "psalm", "ache", "depot" and asked to read each one out loud. Multiple responses are allowed as long as a final one is decided upon before proceeding to the next word. No time restriction is imposed and the participant is only given feedback as to the correct responses at the end of the task. The number of errors and correct responses is the summed to create the NART score. NART score is sometimes used as a proxy for education.

As multiple entries for both the education questionnaire and NART were available per participant, only the entries closest in time to the completion of the PAL task for each participant were used in this study. Despite this, some mismatch between questionnaire date of completion and PAL date was still present. Of the 1384 individuals with available education data, only 4 individuals answered the education questionnaire within 1 year of

undertaking PAL, while 643 answered the education questionnaire more than 1 year but less than 3 years before or after undertaking PAL and 737 answered the education questionnaire more than 3 years before or after undertaking the PAL task. Of the 1784 individuals with available NART data, 1708 underwent NART within 1 year or undergoing PAL, 0 individuals underwent the two tests within 3 years of each other and 76 individuals underwent NART more than 3 years before or after undergoing PAL. This is summarised in **Table 30**.

	Exact match to pal (<1 year)	Close match to pal (>1 but < 3 years)	Distant match to pal (>3 years)
Education (n=1384)	4	643	737
NART (n=1784)	1708	0	76

Table 30 - Table summarising the number of participants with exact, close or distant matches of education or NART entries in comparison to Paired associates learning test. An exact match means the participant underwent the education questionnaire or the NART test less than a year before or after undergoing the PAL task, a close match means they underwent the tests more than a year but less than 3 years before or after the PAL task and a distant match means the tests were carried out more than 3 years before or after the PAL task.

Time difference and age calculations were carried out using the "lubridate" package in R (Grolemund and Wickham, 2011). Due to missing and mismatched education data, NART was used as a proxy for education.

5.2.5 Lifestyle factors

To assess the effect of lifestyle on cognition, measures of nutritional habits and physical activity were requested from TwinsUK.

5.2.5.1 Nutrition: Calorie intake and Healthy Eating Index

Two measures of nutritional habits were available as part of this study: average daily calorie intake and Healthy Eating Index (HEI). Both were calculated from food frequency questionnaires (FFQ) collected following the EPIC-Norfolk guidelines (European Prospective Investigation of Cancer). The FFQ documented the participants eating habits over the previous year by assessing consumption of 290 foods (See appendix section 8.4.1.1). Jane Skinner at the University of East Anglia converted the FFQ data to nutritional information and estimated energy consumption in kcal, and Ruth C. E. Bowyer at King's College London

was responsible for converting the data to HEI. HEI was constructed following the guidelines described by Guenther and colleagues with the exception of the use of the UK based database "Composition of Foods integrated database" rather than an American based database (Bowyer et al., 2018; Guenther et al., 2013).

Briefly, food items are classified into "U.S. Department of Agriculture" subgroups (e.g. fruit, grains, dairy, etc.) (see **Table 31**) and then categorised into HEI components based on their predominant attributes (e.g. further subdivided into of lean and solid fat). Each subgroup has a maximum possible amount of HEI points that can be assigned to it, the FFQ data is first converted to equivalent cups or ounces from FFQ portion information and then to a measure of "nutritional component per 1000 kcal". Based on this ratio, a certain proportion of the possible HEI points for that subgroup is assigned to the participant. Out of the 12 subgroups, the first 9 are known as adequacy components which aim to quantify the amount of healthy foods consumed, the remaining 3 (refined grains, sodium and empty calories) were introduced to negatively weigh HEI when excessive amounts of non-healthy foods are consumed. (See **Table 31**)

Component	Maximum points	Standard for maximum score	Standard for minimum score of zero
Total fruit	5	≥0.8 cup equiv. per 1,000 kcal	No Fruit
Whole fruit	5	≥0.4 cup equiv. per 1,000 kcal	No Whole Fruit
Total vegetables	5	≥1.1 cup equiv. per 1,000 kcal	No Vegetables
Greens and beans	5	≥ 0.2 cup equiv. per 1,000 kcal	No Dark Green Vegetables or Beans and Peas
Whole grains	10	≥1.5 oz equiv. per 1,000 kcal	No Whole Grains
Dairy	10	≥1.3 cup equiv. per 1,000 kcal	No Dairy
Total protein foods	5	≥2.5 oz equiv. per 1,000 kcal	No Protein Foods
Seafood and plant proteins	5	≥0.8 oz equiv. per 1,000 kcal	No Seafood or Plant Proteins
Fatty acids	10	(PUFAs + MUFAs)/SFAs ≥2.5	(PUFAs + MUFAs)/SFAs ≤1.2
Refined grains	10	≤1.8 oz equiv. per 1,000 kcal	≥4.3 oz equiv. per 1,000 kcal
Sodium	10	≤1.1 gram per 1,000 kcal	≥2.0 grams per 1,000 kcal
Empty calories	20	≤19% of energy	≥50% of energy

Table 31 - Food subgroups and relative scoring included in the Healthy Eating Index (HEI). Food items are classified into subgroups (Component) and a maximum number of points (Max points) or a proportion thereof is assigned to contribute to the overall HEI score. Bottom two rows represent detrimental food items, therefore higher scores are obtained with lower intakes. Adapted from (Guenther et al., 2013)

HEI score can range from 0-100 points with the maximum achievable score indicating a diet that fulfils all health thresholds. The index was designed so that in a large enough population, 50 would be the mean HEI score and 1 and 99 would be the 1st and 99th percentile. Within the TwinsUK cohort we observe a mean of 60.03, a 1st percentile of 37 and a 99th percentile of 86 (Bowyer et al., 2018). Results from three batches of FFQ collections were received, as for the education questionnaires, the FFQ results collected closest in time to the PAL task results were used for each individual. Out of the 1567 individuals with available PAL and FFQ data, 437 individuals had PAL and FFQ data less than a year apart, 293 had a time interval of 1-3 years between the FFQ and PAL task and the remaining 800 had a time interval greater than 3 years.

5.2.5.2 Exercise

To investigate another aspect of lifestyle and its effects on cognition, physical activity data was collected via International Physical Activity Questionnaire (IPAQ) (Hagströmer et al., 2006), see section 8.4.1.2 for the IPAQ questionnaire.

IPAQ aims at assessing the types of physical activity done by the participants to estimate a total physical activity measure known as MET-minutes per week. The IPAQ short form questionnaire used here, consists of 7 questions about the previous 7 days, the questions are subdivided in 4 sections: vigorous physical activity (such as heavy lifting or fast cycling), moderate activity (such as carrying light loads or cycling at a regular pace), time spent walking and time spent sitting. For each of the 4 sections, the participant is asked to state the number of days a week as well as hours and minutes a day spent doing that specific type of physical activity. The participants are also able to indicate no time spent. From this, MET minutes are calculated: MET minutes represent the amount of energy expended when carrying out physical activity. 1 MET minute equals the amount of energy expended at rest. Therefore 2 MET minutes is double the resting energy expenditure.

Upon receiving the raw IPAQ data, MET minutes were calculated as per IPAQ guidelines, by first converting the time spent doing each form of activity to minutes and then multiplying that by a constant. The constant varied according to the form of activity: 3.3 for walking, 4 for moderate and 8 for vigorous physical activity. Only activities of 10 or more minutes are included in the calculations of MET minutes. Once MET minutes were calculated participants were split into high, moderate and low physical activity following guidelines outlined on the IPAQ website (www.ipaq.ki.se) (accessed on 1.10.18).

For a participant to be classified as high physical activity they must have had engaged in either of the following:

a) vigorous activity on at least 3 days achieving a minimum of 1500 MET minutes a week
b) 7 or more days of any combination of vigorous or moderate activity achieving a minimum of 3000 MET minutes a week.

For a participant to be classified as moderate physical activity they must have had engaged in any of the following:

a) 3 or more days of vigorous activity of at least 20 minutes a day
b) 5 or more days of moderate activity and/or walking at least 30 minutes a day
c) 5 more days of any combination of walking, moderate or vigorous activity achieving a minimum total physical activity of at least 600 MET minutes a week.

For a participant to be classified as low physical activity they must not have met any of the criteria for the other two groups.

Data cleaning was also carried out in accordance to IPAQ guidelines, this included removing participants with missing answers or with unreasonably high levels of activity, identifying possible human errors when completing the questionnaires and applying a truncation rule that converted all activity variables exceeding 180 minutes to equal 180 minutes. The truncation attempts to normalise the distribution of the activity levels and prevent misclassification of participants with very irregular exercise patterns into the "high activity" category. The data on time spent sitting was not used in this study. Of the participants with both IPAQ and PAL data, all those who declared a form of physical disability were explored to see whether the PAL task had been carried out prior to or following the disability onset. All those who underwent PAL before the onset of the disability, or underwent PAL less than a year following the disability's onset were excluded as their physical activity levels would not be representative of their physical activity levels at the time of PAL. All those with a disability of unknown duration were also excluded from analysis. Only one physical activity measure per participant was available. Out of the 846 participants with eligible PAL and IPAQ data, 473 had undergone the task and IPAQ within a year of one another, 34 within 1-3 years and 339 underwent the task and the IPAQ more than 3 years apart.

5.2.6 Genetic data

Single Nucleotide Polymorphisms (SNP) array analysis is typically used for the interrogation of genetic loci to obtain an individual's genotype. Oligonucelotide probes within the array hybridise with the fragmented DNA in the test sample and emit a fluorescent signal for each of the two alleles (e.g. allele A or allele B) at a given SNP. The signal abundance for each allele is then interpreted to identify the genotype as A, B or AB (i.e. homozygous for

A allele, homozygous for B allele or heterozygous). The signals emitted by the array are then normalised to a baseline to account for the overall brightness and to allow for comparisons between arrays, finally, several quality control (QC) steps carried out.

In our study, we focused on the SNPs present in and around our 9 genes of interest (FoxO3, Sirt1, IGF2R, ABTB1, NAMPT, PTEN, UCP2, GRB10 and mTOR). Therefore, the genotype information for all SNPs within the gene boundaries and 300 kb up and downstream was requested. The UCSC Genome Reference GRCh37 (assembly date 2009) was used to design the coordinates matching our areas of interest. **Table 32** shows the resulting coordinates for each of our genes of interest.

Gene	Coordinates
FoxO3	chr6: 108881026 - 109005971
Sirt1	chr10: 69644427 - 69678147
Igf2r	chr6: 160390131 - 160527583
ABTB1	chr3: 127391781 - 127399769
NAMPT	chr7: 105888732 - 106225638
PTEN	chr10: 89623195 - 89728532
UCP2	chr11: 73685716 - 73693889
GRB10	chr7: 50657760 - 50861159
mTOR	chr1: 11166588 -11322608

Table 32 - Table showing the gene coordinates for the genetic information request to TwinsUK. The coordinates for each gene contain the gene as well as 300KB up and downstream of the gene boundaries. All SNPs within these coordinates were requested for this study.

The genotyping was carried out by TwinsUK using a combination of Illumina arrays (HumanHap300, HumanHap610Q, 1M-Duo and 1.2MDuo 1M). The data for each array was normalised separately and then pooled. A visual inspection of 100 random shared SNPs across arrays was carried out to rule out any batch effects. Samples were excluded according to the following criteria: a sample call rate <98%, heterozygosity across all SNPs ≥2 SD from the sample mean, evidence of non-European ancestry (assessed by principal component analysis with HapMap3 populations) and possibility of sample identity errors as informed by the identity by descent probabilities. TwinsUK also carried out QC to select which SNPs should be included in the final data. The exclusion criteria included a Hardy-Weinberg p-value<10^{-6} (within unrelated individuals), a minor allele frequency (MAF) of <1% and a SNP call rate of <97% (SNPs with MAF ≥ 5%) or < 99% (for 1% ≤ MAF < 5%).

Upon receiving the data from TwinsUK, further QC was carried out. Due to our limited number of participants, MAF was restricted to 5% or more, and a minimum SNP call rate of 95% within our subset was applied. The area surrounding the gene boundaries was also reduced from 300kb to 100kb up and downstream. Following this last step of QC there were 4315 eligible SNPs. The number of SNPs per gene is summarised in **Table 33.**

Linkage disequilibrium (LD) was accounted for by creating tag SNPs with the Priority Pruner software. This software prunes SNPs by removing all those that are in LD with other SNPs in the dataset. As per convention, a SNPs with an $r^2 > 0.8$ and within 250KB was determined to be in LD. Based on MAF, one of the SNPs in LD is retained and named a 'tag SNPs' while all other SNPs are pruned. Following the creation of tag SNPs there were 482 eligible tag SNPs (see **Table 33**).

Gene	Raw SNPs	Tag SNPs
FoxO3	411	58
Sirt1	377	18
Igf2r	578	94
ABTB1	328	41
NAMPT	508	53
PTEN	423	66
UCP2	312	49
GRB10	1033	90
mTOR	345	13
TOTAL	4315	482

Table 33 - Pruning outcome. Table showing the 9 candidate genes investigated in this study (**Gene**), the number of single nucleotide polymorphisms (SNPs) per gene before (**Raw SNPs**) and after (**Tag SNPs**) pruning. Pruning was carried out to account for linkage disequilibrium between nearby SNPs

5.2.7 Methylation data

To assess whether DNA methylation of specific residues had an effect on PAL performance, DNA methylation intensity was requested. DNA methylation was measured using the Infinium HumanMethylation450 BeadChips and the results analysed in R. The signals were background corrected and those with a detection p value below 0.05 were set to missing. The BMIQ method (Teschendorff et al., 2013) was employed to carry out probe type correction and all probes with missing data were removed along with any probes mapping

to multiple locations of the genome. The resulting data were the methylation beta values, a measure of methylation intensity for a specific site, which can range from 0 to 1.

Only 288 participants had available data on methylation intensity, therefore we restricted the analysis to only 1 candidate residue. However, as seen in **Figure 52** only 73 participants had eligible PAL and methylation data, no analysis was carried out relating methylation intensity to cognitive performance. Instead, methylation intensity of the candidate residue and its association to lifestyle and age was investigated.

5.2.8 Descriptive statistics

Due to the interdisciplinary nature of this study, combining genetics, cognition and lifestyle, the number of eligible participants varied greatly across the different analyses. **Figure 51** and **Figure 52** show the number of participants when each new variable is included in the analysis. There was a large reduction in eligible participants due to large quantities of missing data for each variable. Due to this, it was not possible to use the same participants in all the analyses. Separate descriptive analyses were thus carried out to describe the sub cohorts used in each analysis.

Descriptive analysis of each of the sub cohorts is reported in **Table 34.** For all sub cohorts including SNP data, descriptive analysis was carried out on the maximum number of people included in regressions involving SNP data. This number varied according to which SNP was being analysed due to the SNP call rate ranging from 95% to 100% (as explained in 5.2.6). The “PAL with no dementia” subgroup was used in the analysis investigating the effects of age on PAL score. The “PAL, NART, SNPs” cohort was used in the analyses investigating the effects of SNPs on cognition. The “PAL, NART, SNPs, nutrition” and “PAL, NART, exercise” sub cohorts were used when investigating the interaction between SNP and lifestyle on cognition. The “methylation” sub cohort was used to assess whether methylation intensity of the ABTB1 methylation site cg03330058 varied with age. Finally, the “methylation, nutrition” and “methylation, exercise” sub cohorts were used to assess if there was an association between lifestyle and methylation of cg03330058.

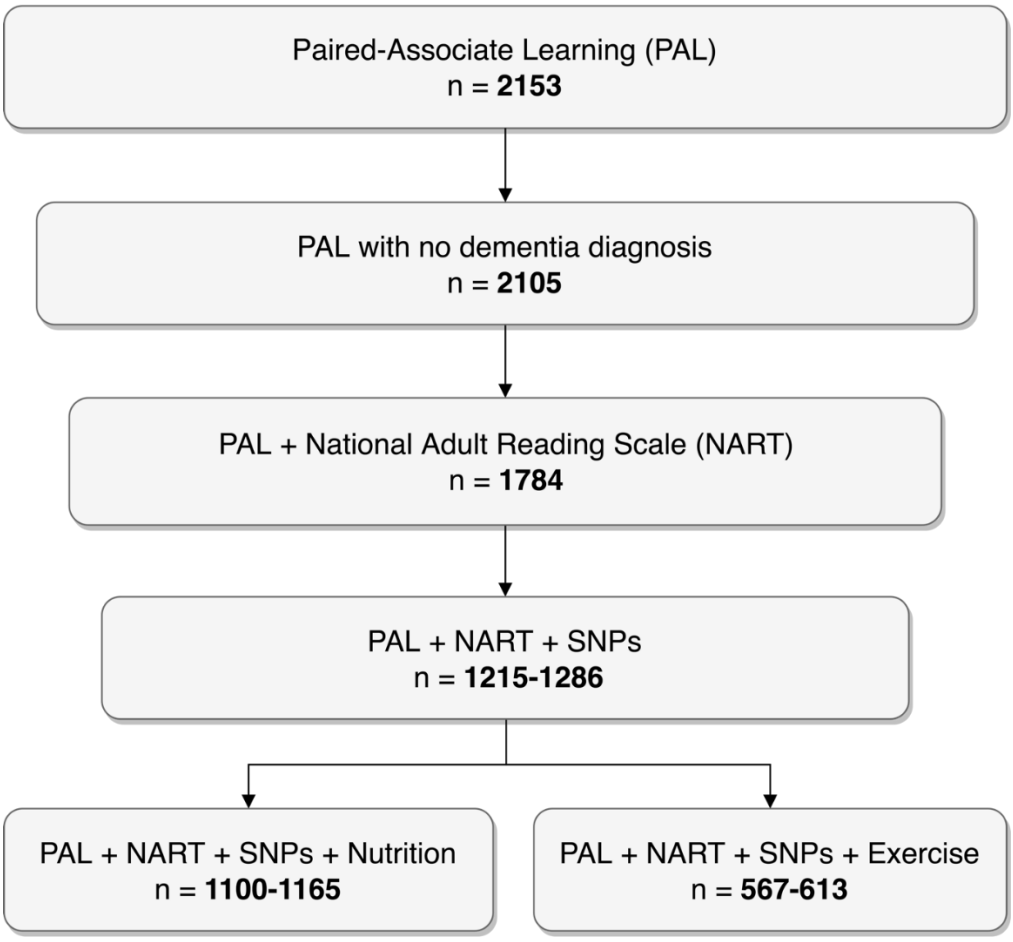

Figure 51 - Diagram showing the number of eligible participants with data for each variable combination in the study investigating Paired Associates Learning results (PAL), Single Nucleotide Polymorphisms (SNPs) and lifestyle (nutrition or exercise). NART: National Adult Reading Scale.

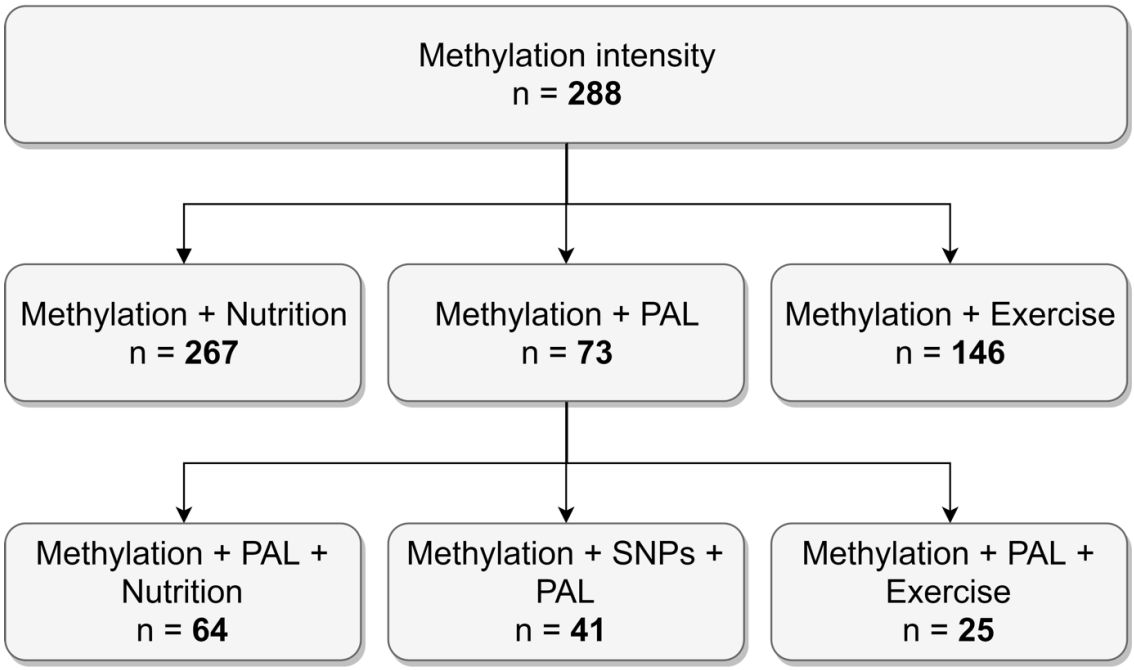

Figure 52 - Diagram showing the number of eligible participants with data for each variable combination when investigating ABTB1 residue cg03330058's methylation intensity and its relation to Paired Associates Learning results (PAL), Single Nucleotide Polymorphisms (SNPs) and lifestyle (nutrition or exercise). NART: National Adult Reading Scale.

Variables included and number of participants	Females : males	MZ : DZ	Min age - Max age Mean (sd)
PAL (no dementia) (2105)	1879:226	1185:906	16.13- 91.82 55.11 ± 14.9
PAL, NART, SNPs (1286)	1209:77	635:651	18.41-91.82 57.22 ± 12.97
PAL, NART, SNPs, nutrition (1165)	1104:61	548:617	18.41-91.82 57.77 ± 12.73
PAL, NART, SNPs, exercise (613)	568:45	321:294	22.52 – 91.82 60.23 ± 12.05
Methylation (288)	284:4	248:40	29.20 – 80.40 57.41 ± 9.30
Methylation, Nutrition (267)	265:2	229:38	29.20 – 80.90 57.68 ± 9.24
Methylation, Exercise (146)	144:2	127:19	29.20 – 80.90 56.74 ± 8.11

Table 34 - Descriptive statistics of cohort and subcohorts used in this chapter. Table showing the female to male ratio, Monozygotic (MZ) to Dizygotic (DZ) ratio and minimum, maximum and mean ± sd age for each of the sub cohorts. Age in the last 3 rows is the participant's age when the methylation array was carried out, in all other rows age equals to the participant's age at PAL.

5.2.9 General Estimating Equation model and statistics

To account for relatedness within the cohort, Generalised Estimating Equations (GEE) were used instead of linear regressions. The R package "geepack" was used for all analysis (Halekoh et al., 2006).

GEEs are a quasi-likelihood based statistical method that allow for clustering, they can be used to account for batch effects in large epidemiological studies, repeated measures within longitudinal studies or, as in this case, relatedness between individuals. In this study each twin pair, irrespective of zygosity, formed a cluster and their relatedness was therefore accounted for within the analysis. It is often debated whether monozygotic (MZ) twins should be treated differently owing to their identical genetic composition. One alternative is to use an average of the MZ twins' data. As a form of sensitivity analysis, part of the analysis was therefore repeated using averages of MZ data rather than individual values.

The assumptions when using GEE models include unrelated observations between clusters and adequately large sample size (usually around 50 clusters). There are no assumptions as to the normality of the data, though efficiency is improved when normally distributed data is used (Ghisletta and Spini, 2004). An exchangeable correlation structure was selected with the help of Quasi Information Criterion (QIC) and Correlation Information Criterion (CIC). The QIC is the quasi-likelihood counterpart of the Akaike information criterion. It is an estimator of the relative quality of a certain statistical model given the data it is based on. It is comprised of a trade-off between the goodness of fit of a model and a penalty for the model's over-complexity. CIC is a modified version of the QIC which was shown to have substantially improved. Therefore, smaller QIC and CIC are indicative of a better-fitted correlation structure, which is essentially a measure of correlation between observations within clusters performance (Barnett et al., 2010; Gosho et al., 2011). For all analysis involving PAL, age at PAL, NART score and gender were included in the model as covariates. Benjamini-Hochberg multiple correction was applied at each stage of the analysis p and q values are reported.

5.3 Results

In this chapter, we aimed to investigate the effects of genetic polymorphisms and lifestyle habits on PAL performance in a healthy population. We focused (on the 9 candidate genes selected in the previous sections and on diet and physical activity as lifestyle measures. In addition, we assessed the epigenetic changes occurring in ABTB1 as a function of age.

5.3.1 Mini Mental State Examination as an exclusion criteria

As a cognitively-healthy population was required for this study, MMSE results were used to exclude all participants with a known diagnosis of dementia. Dementia diagnosis was determined by an MMSE score of less than 27.

To test whether dementia diagnosis affected PAL score, and thus whether it was indeed necessary to exclude those with MMSE < 27, Welch's t-test was carried out to compare the mean PAL score of patients with and without a dementia diagnosis. Welch's t-test was chosen over the student's t-test due to the different variance and sample size across groups. As seen in **Figure 53,** participants with an MMSE value below 27 made more mistakes (mean of 50.5) on the PAL task when compared to those with an MMSE score of 27 or above (mean of 24.2); two-sample $t(48.1)= 4.5$, $p = 4 \times 10^{-5}$. All participants with MMSE scores below 27 were excluded from following analyses.

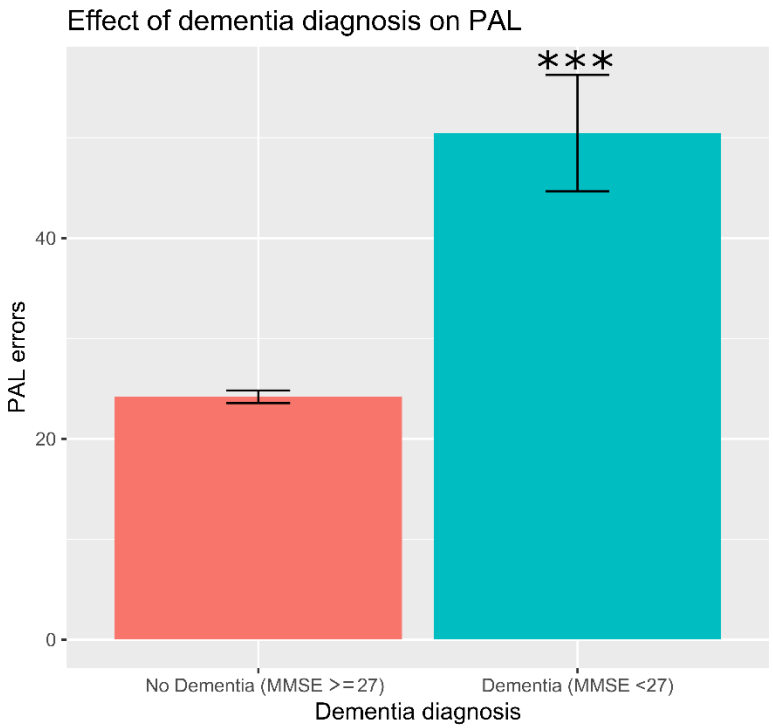

Figure 53 - Effect of Mini Mental State Examination (MMSE) score on Paired associates Learning (PAL) performance. Graph showing the mean errors made in PAL by participants with a MMSE score higher than or equal to 27 (No dementia) and those with an MMSE score lower than 27 (diagnosis).

5.3.2 Covariate selection; effect of age, education and gender on PAL

As PAL performance is known to be dependent on age, age was tested for correlation with PAL score within our cohort. Firstly, the frequency distribution plot for PAL values alone and for the resulting residuals showed a positive skew (**Figure 54** panel 1 A and F respectively). In line with this, the residual vs fitted value plot did not show a random distribution around the residual value of 0 but instead showed a propensity for larger PAL values to have greater residuals also suggesting a non-normal distribution (**Figure 54** panel 1 B). In addition, the Q-Q plot did not result in a straight line suggesting different distributions between PAL and age values (**Figure 54** panel 1 C). Furthermore, the scale-location plots used to see whether residuals were spread equally along the range of the predictor did not show a horizontal trend, this suggested that the assumption of equal variance was not met (**Figure 54** panel 1 D). Finally, residuals vs leverage plots were used to identify any influential outliers and 3 data points were identified, these however did not

exceed Cook's distance, meaning they were unlikely to be influential to regression results (**Figure 54** panel 1 E).

As the plots showed the data violated linear regression assumptions, a logarithmic transformation (Log_e(PAL score +1)) was applied onto the PAL values. The resulting frequency distribution plots of both the PAL values and the residual now followed a normal distribution as did the residual vs fitted value plot (**Figure 54** panel 2 A, F and B respecitvely). A straight line resulted from the Q-Q plot and a horizontal line with mostly equally spread values resulted from the scale-location plot (**Figure 54** panel 2 C and D). Finally, the residuals vs leverage plot showed 2 possible outliers, though as before, they did not exceed Cook's distance (**Figure 54** panel 2 E). The logarithmic+1 transformation was therefore selected. For the remainder of this study, the reported PAL errors will be the transformed values.

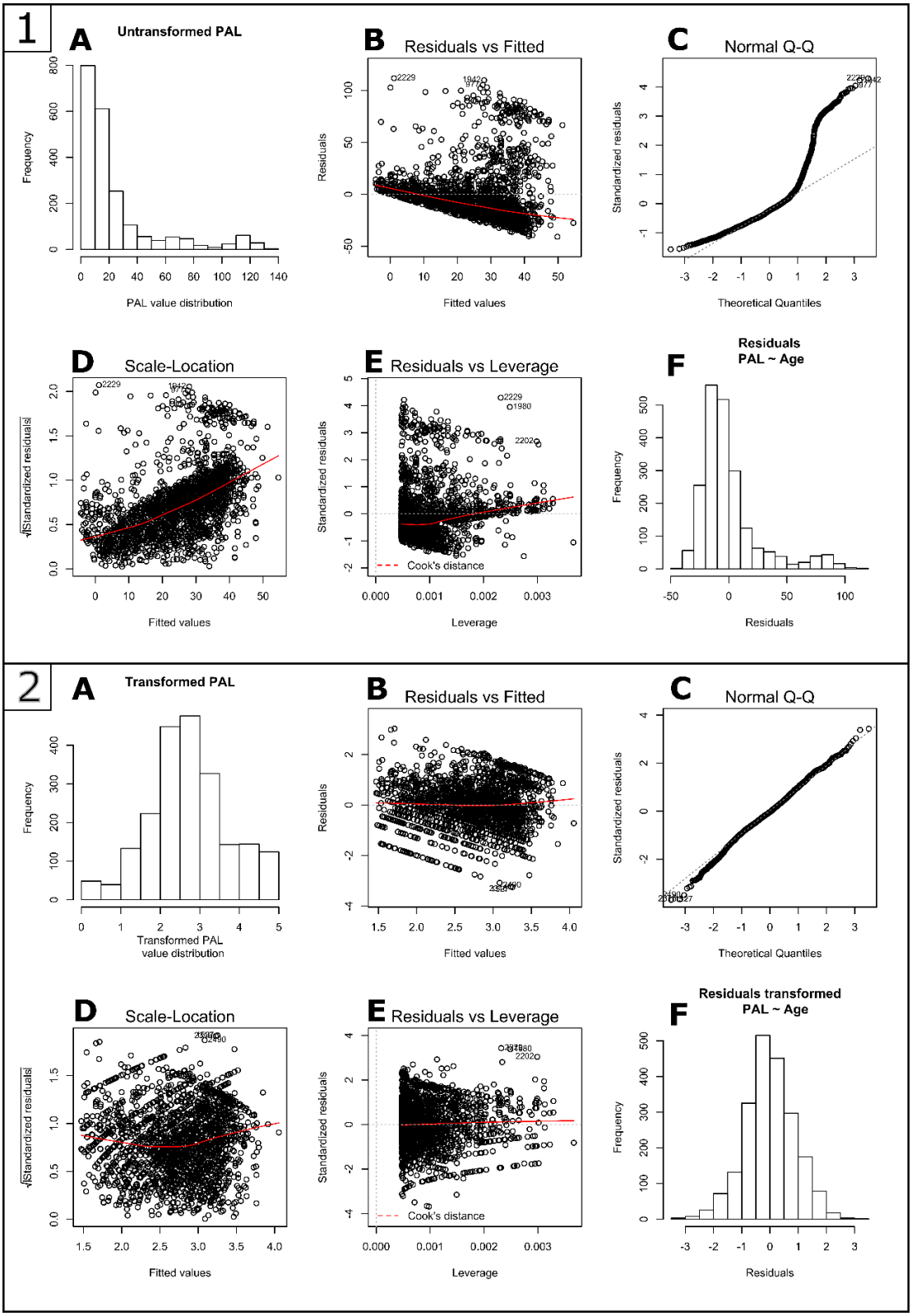

Figure 54 - Plots used to determine whether the data was normally distributed. **Panel** 1: Plots resulting from untransformed data. **Panel 2:** plots resulting from Log(PAL score +1) transformation. (A) Frequency plot of PAL values. (B) Residual vs fitted plot (C) Quantile-Quantile (Q-Q) plot. (D) Scale-location plot (E) residual vs leverage plot and (F) Frequency plot of the residuals of the correlation between Paired Associates Learning (PAL) and age.

Figure 55 shows the distribution of the data in a scatterplot showing the correlation between PAL and age before and after the transformation. A moderate correlation (Pearson's, r =0.50, p < 0.00001) was observed between age and PAL score. Age was therefore selected as a covariate for the models outlined in this chapter.

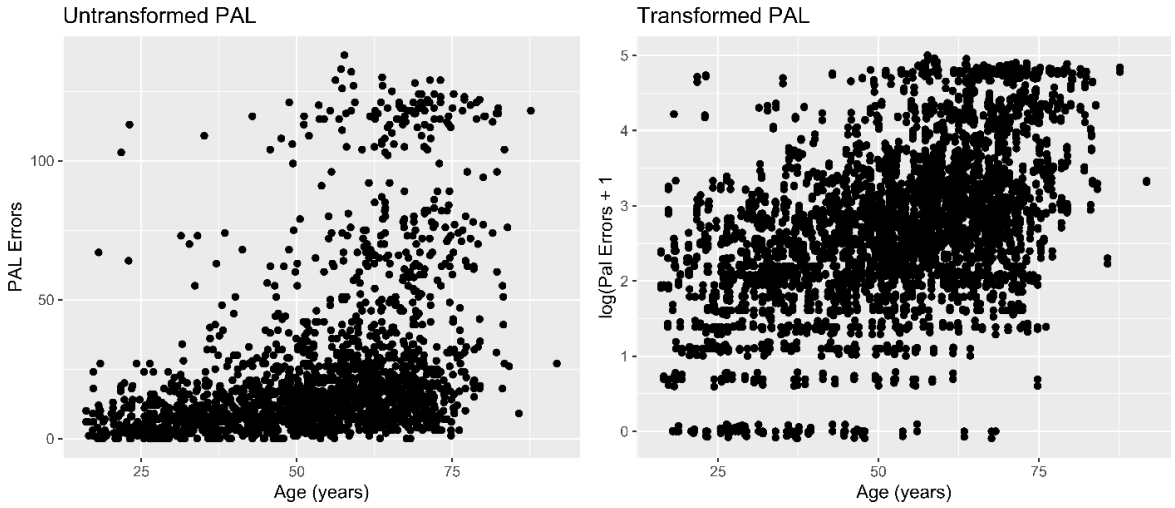

Figure 55 -Logarithmic transformation of Paired Associates Learning (PAL) variable. Graphs showing PAL errors against age in years before (**left**) and after logarithmic transformation (**right**). Each dot represents a participant.

PAL scores were also tested for correlation with education and gender to assess whether these would bias further analyses. PAL showed a weak but significant negative correlation with education (Spearman's, r = -0.29, p < 0.00001), suggesting higher education leads to better performance on the PAL task. As explained in section 5.2.4, NART data was available and was much completer and more accurate than the education data and was therefore tested for use as a proxy of education. As for education, NART showed a weak but significant correlation with PAL (Pearson's, r = 0.10, p < 0.00001), suggesting worse performance on the NART task correlates with worse performance on PAL. NART and education showed a moderate and significant negative correlation. (Spearman's, r= -0.43, p < 0.00001) suggesting higher education leads to better performance on the NART task. Following these comparisons, NART was selected as an important covariate for all models involving PAL. The effect of gender on PAL was tested via Welch's t-test and showed a non-significant (p = 0.1) increase of 2.3% in PAL errors in the male subgroup compared to the female subgroup. Due to the limited number of male participants within our cohort 1879:226 (F:M) and the varying number of participants in each model, gender was included

as a covariate to account for the possibility of an undetected effect of gender. The above correlations and t-test are displayed in **Figure 56.**

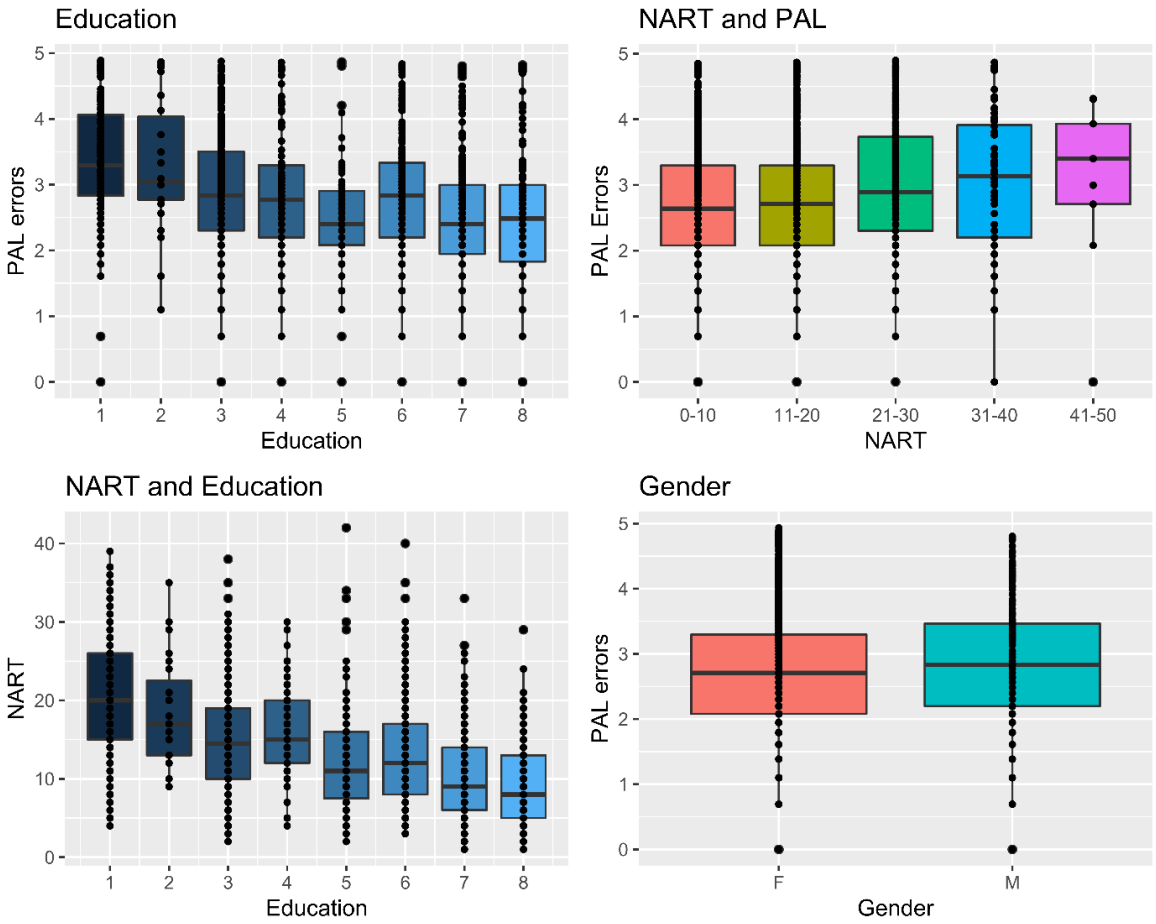

Figure 56 - Effect of education, National Adult Reading Test score (NART) and gender on Paired Associates Learning (PAL) performance. Graphs showing boxplots of the correlation and t-test carried out to assess the association of education, NART score and gender on PAL and the association between NART and education. The graph titled **Education** shows the negative correlation between PAL and level of education (higher education displayed by higher numbers, see methods for details). **NART and PAL** shows the positive correlation between PAL errors and NART, NART score was split into bins for ease of visualization due to the large number of data points**. NART and Education** shows the negative correlation between NART score and level of education. **Gender** shows the mean and distribution of PAL errors in females (F) and males (M). Each dot represents a participant. Data treated as continuous but graphed as categorical for ease of visualization

As lifestyle is known to change with age, associations between age and lifestyle were assessed. Interestingly, in this cohort age was not associated with calorie consumption (r =0.005, p = 0.8) or physical activity levels (r = 0.016, p= 0.6) as shown by Pearson's and Spearman's correlations respectively. Age showed a very weak but significant positive correlation with healthy eating (r = 0.08, p = 0.002) following the Pearson's correlation test. Though this suggests older participants ate more healthily, the very low r value suggests this association may be an artefact.

5.3.3 Association of cognition to lifestyle

The first hypothesis tested in this study was whether diet and physical activity can affect PAL score, irrespective of genotype (aim 1 in section 5.1.4). Firstly, correlations were carried out and residuals were inspected for normality, heteroscedasticity and for the presence of outliers via visual inspection of frequency distribution, residual vs fitted, quantile-quantile (Q-Q), scale-location and residual vs leverage plots as described in section 5.3.2, the plots showed the data did not require transformations (see appendix section 8.4.2.1 for plots).

GEE models were used to account for the relatedness of the individuals as explained in 5.2.9. No significant associations were seen between healthy eating and PAL, calorie intake and PAL or physical activity and PAL, suggesting dietary or exercise habits alone are not predictive of PAL score. This is shown by the scatterplot and box plots in **Figure 57.** All variables were used as continuous values. Interestingly however, there was a significant interaction between physical activity and calorie intake ($\beta = -0.0002$, $p = 0.0037$), suggesting a different association between calorie intake on PAL according to the participant's exercise level. This interaction is shown in **Figure 57E** where the intersecting lines show different slopes according to varying levels of activity. This result shows that for participants with low IPAQ, each Kcal consumed is predictive of a 0.0002 increase in PAL errors. For participants with moderate IPAQ levels, each Kcal consumed is predictive of a 0.00001 decrease in PAL errors. Finally, participants with high IPAQ levels show a decrease of 0.0002 PAL errors for each Kcal consumed. The interaction value, used in to calculate these slopes, is reported in **Table 35.** Following visual inspection of the scatterplot however, possible outliers were identified. As a form of sensitivity analysis, the interquartile range was used to set lower and upper limits to the Kcal variable. This excluded participants with calorie consumption greater than 3426, when the analysis was carried out on this new subset of participants the interaction effect was no longer significant ($p = 0.07$) but remained in the same direction.

There was no significant interaction between physical activity and healthy eating **Figure 57D**). The adjusted p values were obtained by carrying out Benjamini-Hochberg correction

to account for the 5 comparisons carried out in this analysis. See **Table 35** for beta coefficients, confidence intervals, p and q values and number of people in each linear model. The final two rows report the interaction values rather than marginal values.

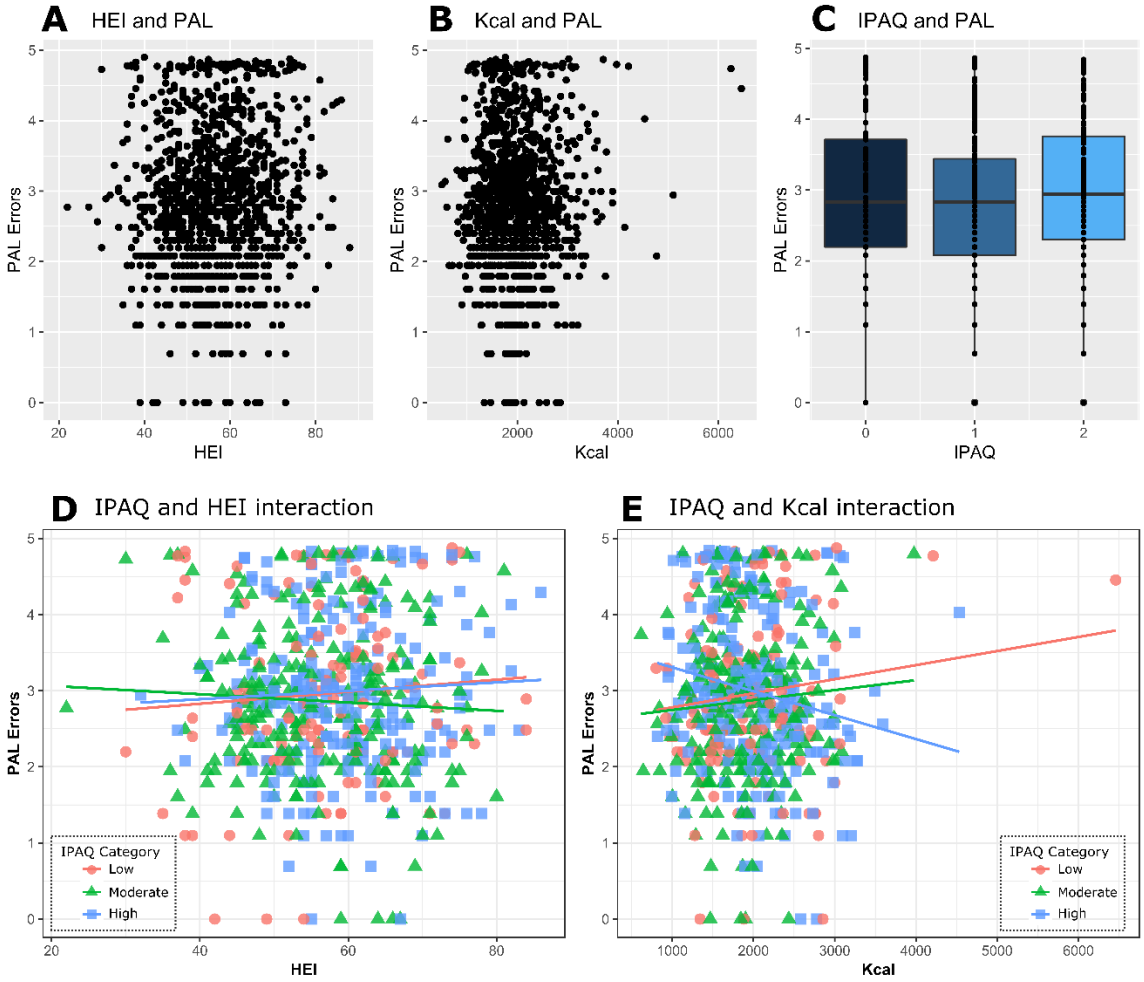

Figure 57 - Lifestyle effects on Paired Associates Learning (PAL) performance. Scatter plots showing the absence of significant association between PAL errors and (A) healthy eating and (B) calorie intake. (C) Boxplot showing no association between varying levels of physical activity and PAL performance. (D) Scatterplots showing there is no interaction between physical activity and healthy eating on PAL performance while (E) shows increased calorie intake is associated to better PAL performance in the subgroup of participants who are highly active (blue line) but not in the subgroups of participants with low and moderate exercise (orange and green lines respectively).In A,B,C each dot represents a participant. In D and E dots represent participants with low physical activity levels, triangles those with moderate activity levels and squares those with high physical activity levels. Data was analysed at continuous but plotted as categorical for ease of visualization.

PAL ~	β coefficient	L95	U95	p value	n	q value
HEI	0.0004	-0.004	0.005	0.87	1165	0.87
KCAL	0.00005	-0.00003	0.0001	0.21	1165	0.52
IPAQ	0.03	-0.06	0.005	0.56	613	0.87
IPAQ*HEI	-0.002	-0.02	0.013	0.81	605	0.87
IPAQ *KCAL	**-0.0002**	**-0.0004**	**-0.00001**	**0.0037**	**605**	**0.018**

Table 35 - Table showing the results of the linear models assessing the association between lifestyle and Paired Associates Learning (PAL) performance. β coefficient, lower (L95) and upper (U95) confidence intervals, unadjusted p value, number of people (n) and adjusted p value (q value) following Benjamini-Hochberg correction in each analysis. The first column reports which independent variable is tested for association with PAL errors: healthy eating index (HEI), calorie intake (Kcal), physical activity (IPAQ). The last two rows report the effect of the interaction between physical activity and healthy index (IPAQ*HEI) and between physical activity and calorie intake (IPAQ*Kcal) on PAL errors. Significant results in bold. " * " denotes interaction, " ~ " denotes correlation

5.3.4 Identifying tagging SNPs to account for linkage disequilibrium

Next, we investigated how genotype might affect PAL performance. To account for LD the Priority Pruner software was used to prune SNPs as explained in section 5.2.6. See appendix section 8.4.2.2 for a file containing all tagging and tagged genes.

To visualize the results of the SNP selection process, Locus Zoom plots were created. For each of the 9 candidate genes, a Locus Zoom plot was created before pruning and one after pruning, all 18 graphs are displayed below (**Figure 59** to **Figure 66**). The graphs titled raw SNPs are locus zoom plots of SNPs prior to pruning while those titled raw SNPs display SNPs after pruning. In each graph, the left y-axis shows the -log10 of the unadjusted p value obtained from the linear model testing the SNP for association to PAL score (as outlined in section 5.2.9). Dots closer to 0 represent least significant SNPs. A larger r^2 is indicative of a stronger disequilibrium. The right y-axis shows the recombination rate displayed on the graphs by the blue line whose peaks represent areas of the genome with higher-than-normal recombination rates. As can be seen in the ABTB1 graph prior to pruning, a high recombination rate essentially stops any LD past that point. As seen in the graphs below some of the SNPs in the tag SNP graph are in mild LD with each other but, as the $r^2 = 0.8$ cut-off was used, none of the remaining SNPs after pruning are in LD stronger than $r^2 = 0.8$.

Of note, in the graphs below are the high number of SNPs in ABTB1 and FOXO3 that were significantly associated to PAL errors as well as the absence of significant SNPs in mTOR. Furthermore, GRB10 showed near to no significant associations (except for rs189209677 which showed some association) despite the high density of SNPs. SNPs in IGF2R NAMPT, PTEN and UCP2 showed little to no association to PAL errors. Interestingly, the SIRT1 graph showed only one SNP (rs497849) to be significantly associated to PAL errors.

As the study was designed to include all SNPs within 100kb of the gene boundaries of each candidate gene, sometimes SNPs of interest appeared to overlap with other genes. This is seen clearly in the ABTB1 locus zoom where many significant SNPs are found within the MCM2 coding region and in the UCP2 locus zoom plot where some of the few significant SNPs appear to be in the coding region of the PAAF1 gene.

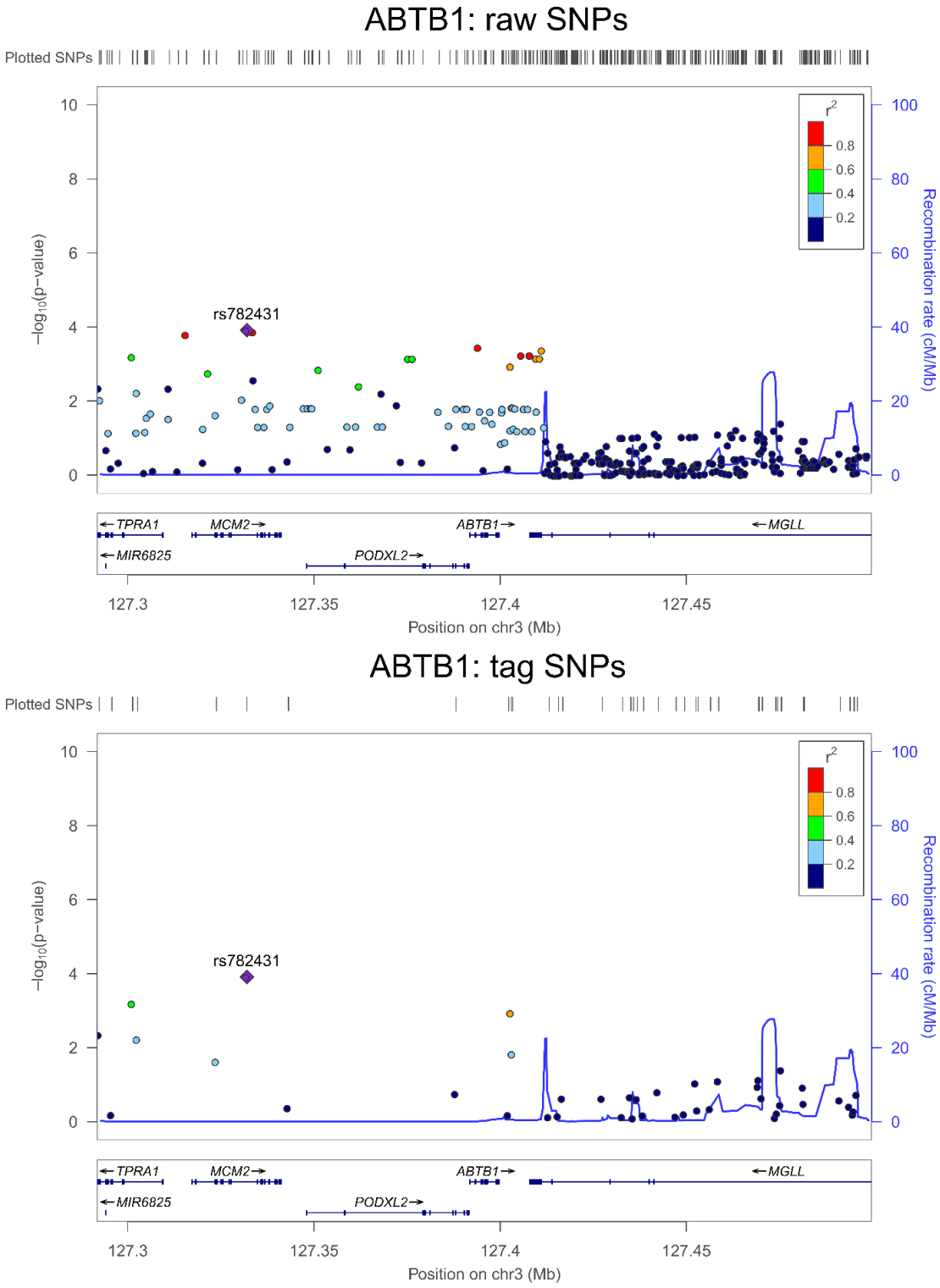

Figure 58 - Locus zoom plot of single nucleotide polymorphisms (SNPs) in ABTB1 Locus zoom plots showing the p-values (on the left y-axis) of the association between each SNP (shown as a dot) to performance in the paired associates learning (PAL) task. Peaks in the recombination rate of DNA (right y-axis) are shown by the blue line. Peaks mean higher recombination rate and therefore lower linkage disequilibrium. The top plot shows the locus zoom plot of all SNPs within 100KBb up and downstream of the gene boundaries, the bottom graph shows only a selection of these that survived pruning to account for linkage disequilibrium. For ease of visualization, the most significant SNP is highlighted in purple and its RS number is reported on the graph, the adjacent SNPs are then colour coded to show the degree of linkage disequilibrium to that SNP as show by the legend in the top right corner.

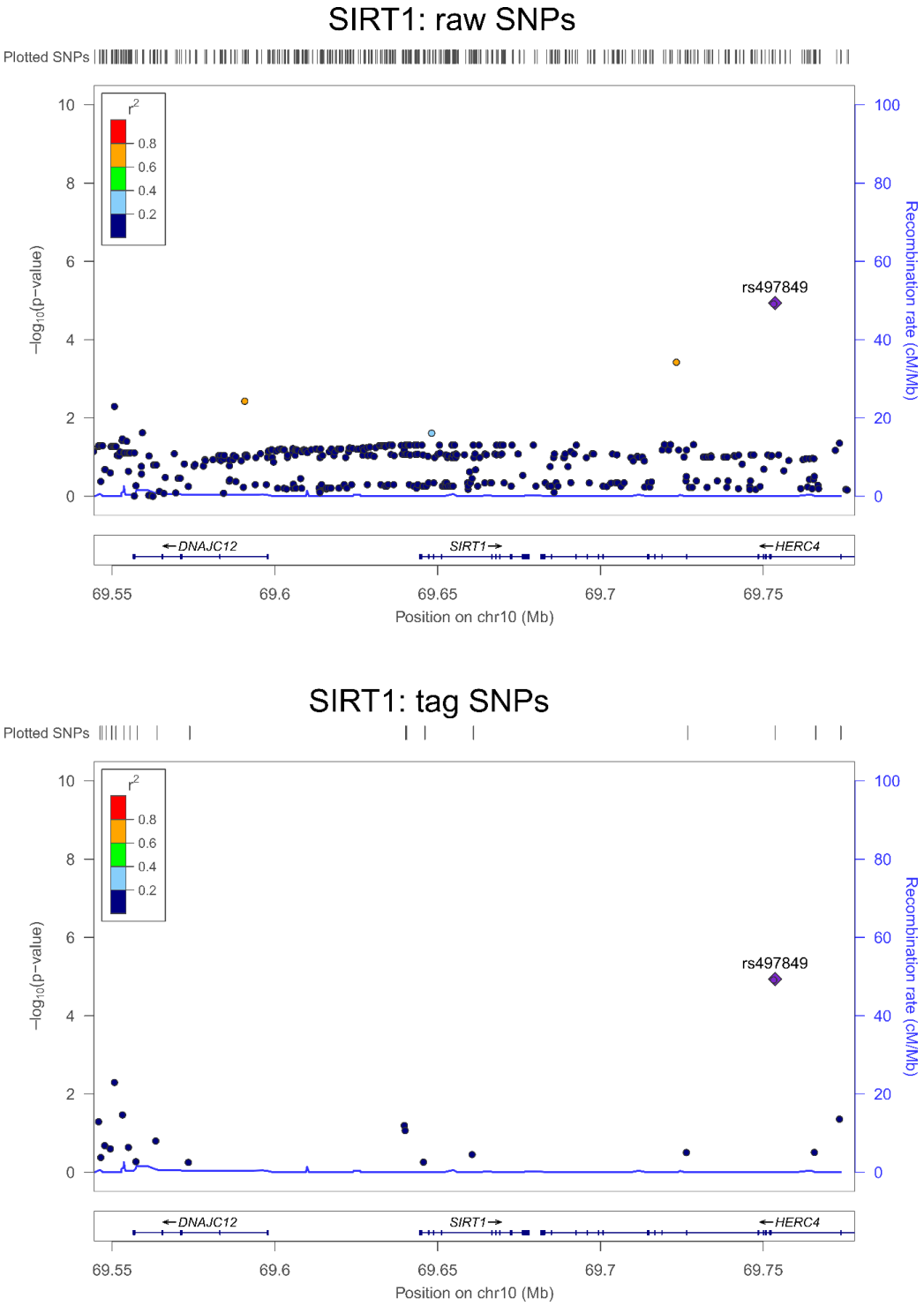

Figure 59 - Locus zoom plot of single nucleotide polymorphisms (SNPs) in SIRT1 Locus zoom plots showing the p-values (on the left y-axis) of the association between each SNP (shown as a dot) to performance in the paired associates learning (PAL) task. Peaks in the recombination rate of DNA (right y-axis) are shown by the blue line. Peaks mean higher recombination rate and therefore lower linkage disequilibrium. The top plot shows the locus zoom plot of all SNPs within 100KBb up and downstream of the gene boundaries, the bottom graph shows only a selection of these that survived pruning to account for linkage disequilibrium. For ease of visualization, the most significant SNP is highlighted in purple and its RS number is reported on the graph, the adjacent SNPs are then colour coded to show the degree of linkage disequilibrium to that SNP as show by the legend in the top right corner.

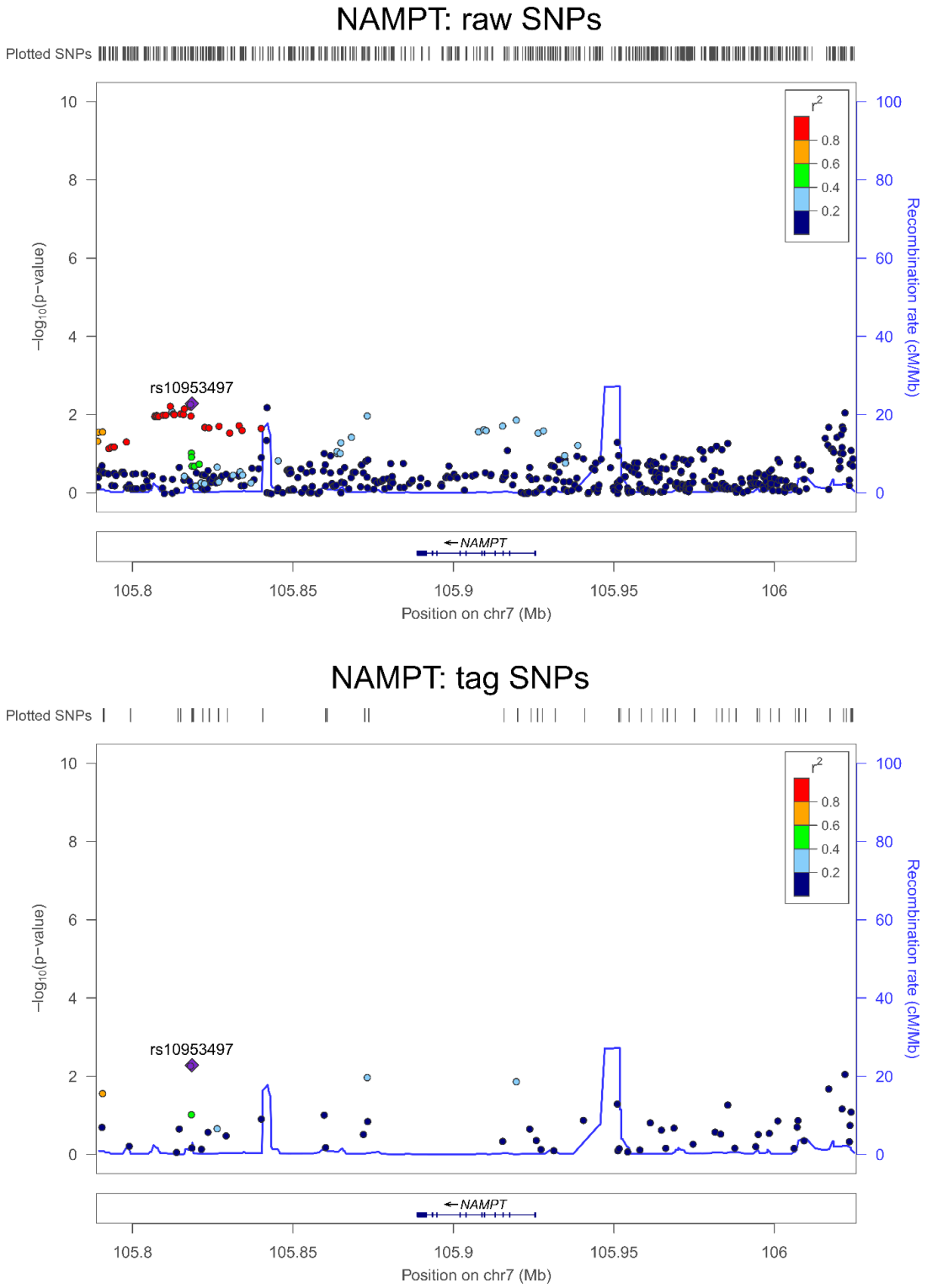

Figure 60 - Locus zoom plot of single nucleotide polymorphisms (SNPs) in NAMPT Locus zoom plots showing the p-values (on the left y-axis) of the association between each SNP (shown as a dot) to performance in the paired associates learning (PAL) task. Peaks in the recombination rate of DNA (right y-axis) are shown by the blue line. Peaks mean higher recombination rate and therefore lower linkage disequilibrium. The top plot shows the locus zoom plot of all SNPs within 100KBb up and downstream of the gene boundaries, the bottom graph shows only a selection of these that survived pruning to account for linkage disequilibrium. For ease of visualization, the most significant SNP is highlighted in purple and its RS number is reported on the graph, the adjacent SNPs are then colour coded to show the degree of linkage disequilibrium to that SNP as show by the legend in the top right corner.

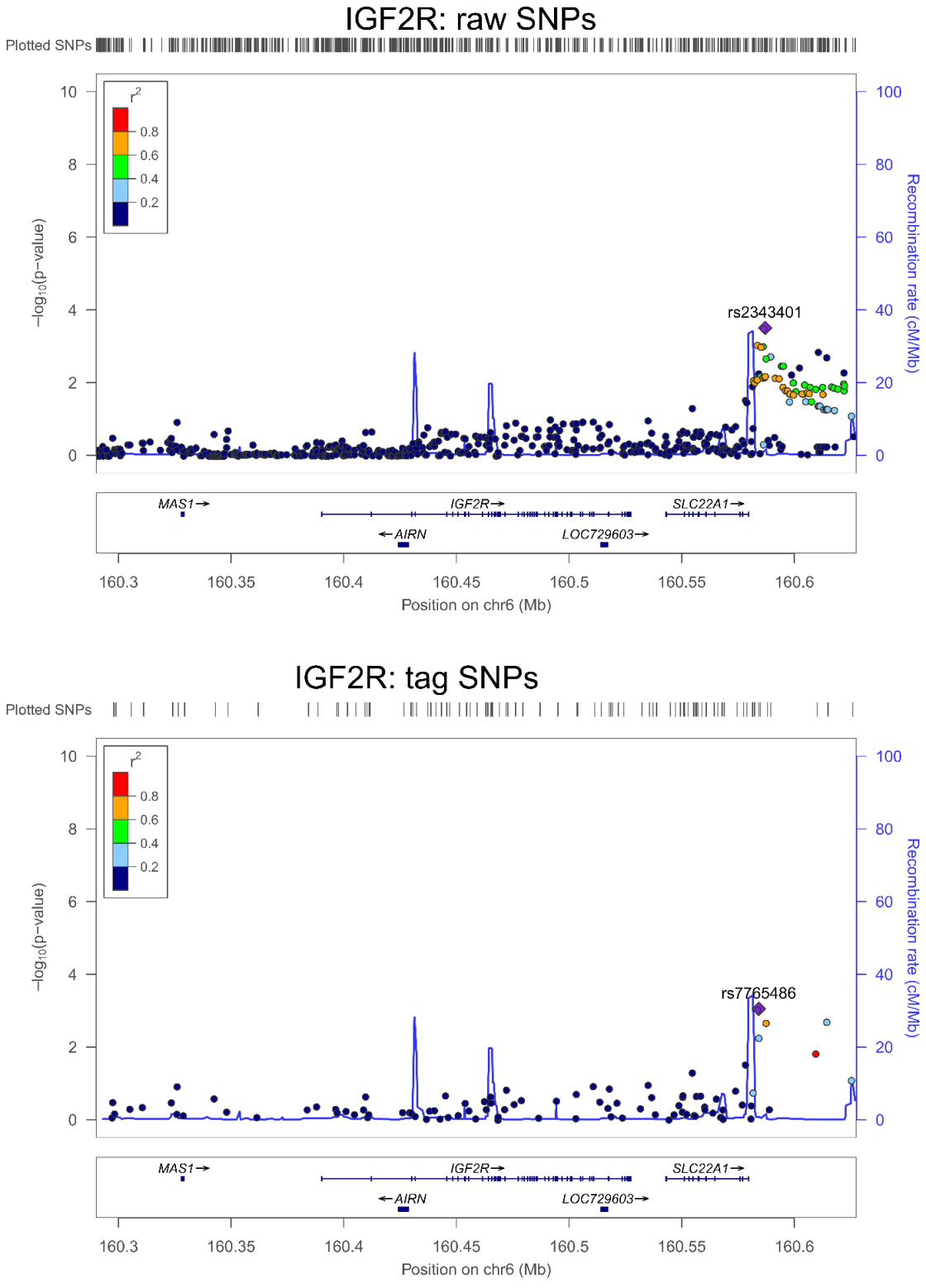

Figure 61 - Locus zoom plot of single nucleotide polymorphisms (SNPs) in IGF2R Locus zoom plots showing the p-values (on the left y-axis) of the association between each SNP (shown as a dot) to performance in the paired associates learning (PAL) task. Peaks in the recombination rate of DNA (right y-axis) are shown by the blue line. Peaks mean higher recombination rate and therefore lower linkage disequilibrium. The top plot shows the locus zoom plot of all SNPs within 100KBb up and downstream of the gene boundaries, the bottom graph shows only a selection of these that survived pruning to account for linkage disequilibrium. For ease of visualization, the most significant SNP is highlighted in purple and its RS number is reported on the graph, the adjacent SNPs are then colour coded to show the degree of linkage disequilibrium to that SNP as show by the legend in the top right corner.

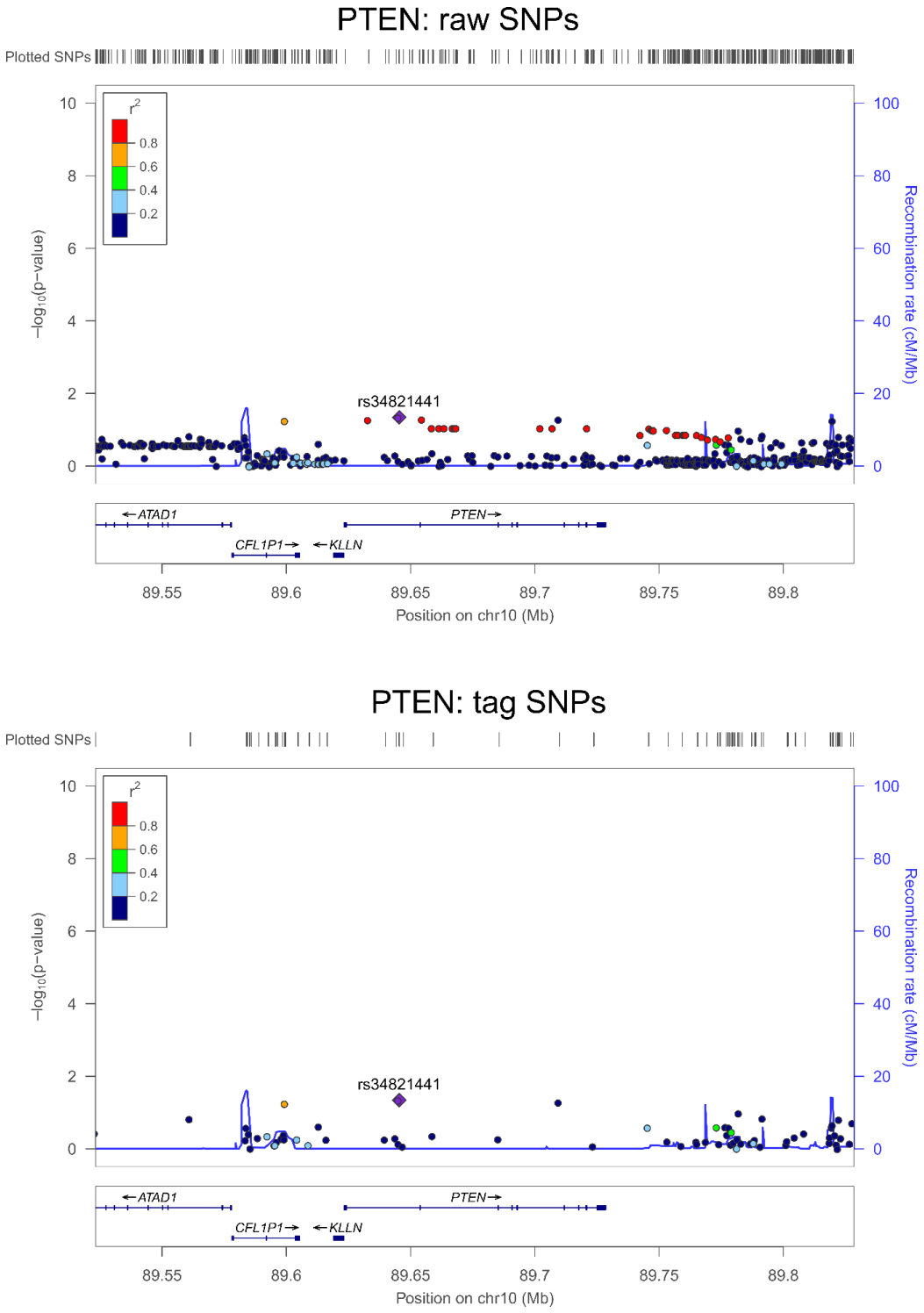

Figure 62 - Locus zoom plot of single nucleotide polymorphisms (SNPs) in PTEN Locus zoom plots showing the p-values (on the left y-axis) of the association between each SNP (shown as a dot) to performance in the paired associates learning (PAL) task. Peaks in the recombination rate of DNA (right y-axis) are shown by the blue line. Peaks mean higher recombination rate and therefore lower linkage disequilibrium. The top plot shows the locus zoom plot of all SNPs within 100KBb up and downstream of the gene boundaries, the bottom graph shows only a selection of these that survived pruning to account for linkage disequilibrium. For ease of visualization, the most significant SNP is highlighted in purple and its RS number is reported on the graph, the adjacent SNPs are then colour coded to show the degree of linkage disequilibrium to that SNP as show by the legend in the top right corner.

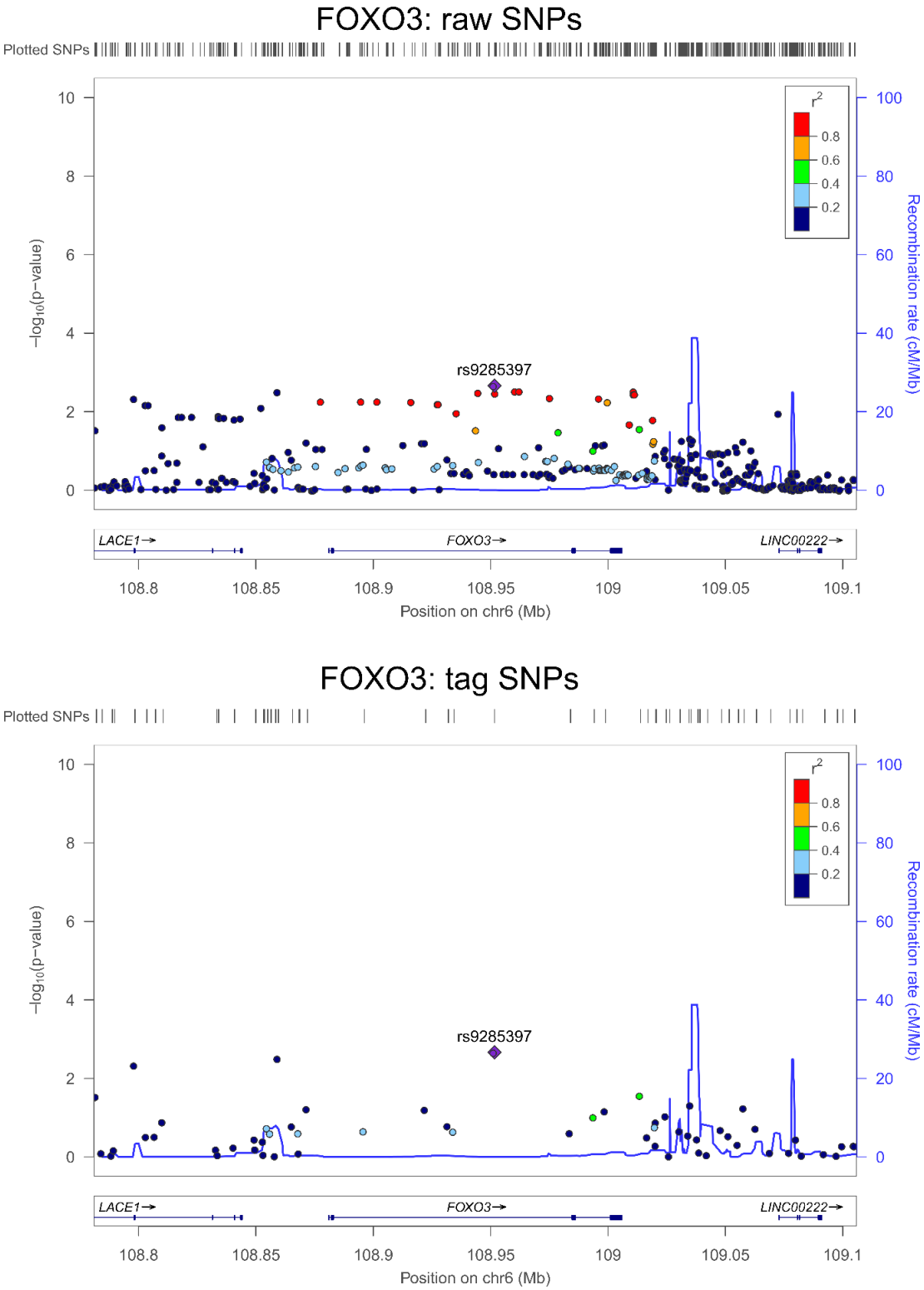

Figure 63 - Locus zoom plot of single nucleotide polymorphisms (SNPs) in FOXO3 Locus zoom plots showing the p-values (on the left y-axis) of the association between each SNP (shown as a dot) to performance in the paired associates learning (PAL) task. Peaks in the recombination rate of DNA (right y-axis) are shown by the blue line. Peaks mean higher recombination rate and therefore lower linkage disequilibrium. The top plot shows the locus zoom plot of all SNPs within 100KBb up and downstream of the gene boundaries, the bottom graph shows only a selection of these that survived pruning to account for linkage disequilibrium. For ease of visualization, the most significant SNP is highlighted in purple and its RS number is reported on the graph, the adjacent SNPs are then colour coded to show the degree of linkage disequilibrium to that SNP as show by the legend in the top right corner.

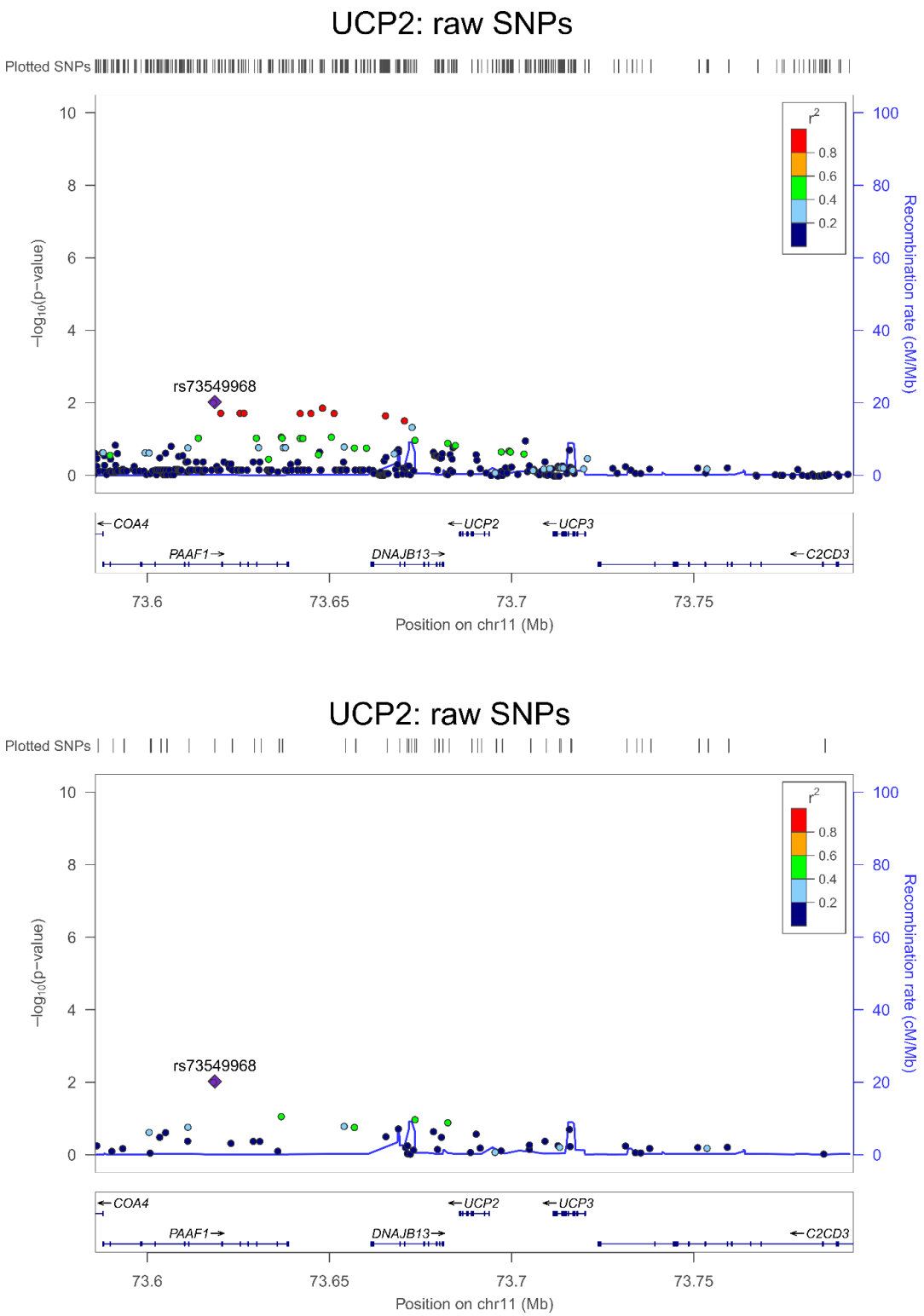

Figure 64 - Locus zoom plot of single nucleotide polymorphisms (SNPs) in UCP2 Locus zoom plots showing the p-values (on the left y-axis) of the association between each SNP (shown as a dot) to performance in the paired associates learning (PAL) task. Peaks in the recombination rate of DNA (right y-axis) are shown by the blue line. Peaks mean higher recombination rate and therefore lower linkage disequilibrium. The top plot shows the locus zoom plot of all SNPs within 100KBb up and downstream of the gene boundaries, the bottom graph shows only a selection of these that survived pruning to account for linkage disequilibrium. For ease of visualization, the most significant SNP is highlighted in purple and its RS number is reported on the graph, the adjacent SNPs are then colour coded to show the degree of linkage disequilibrium to that SNP as show by the legend in the top right corner.

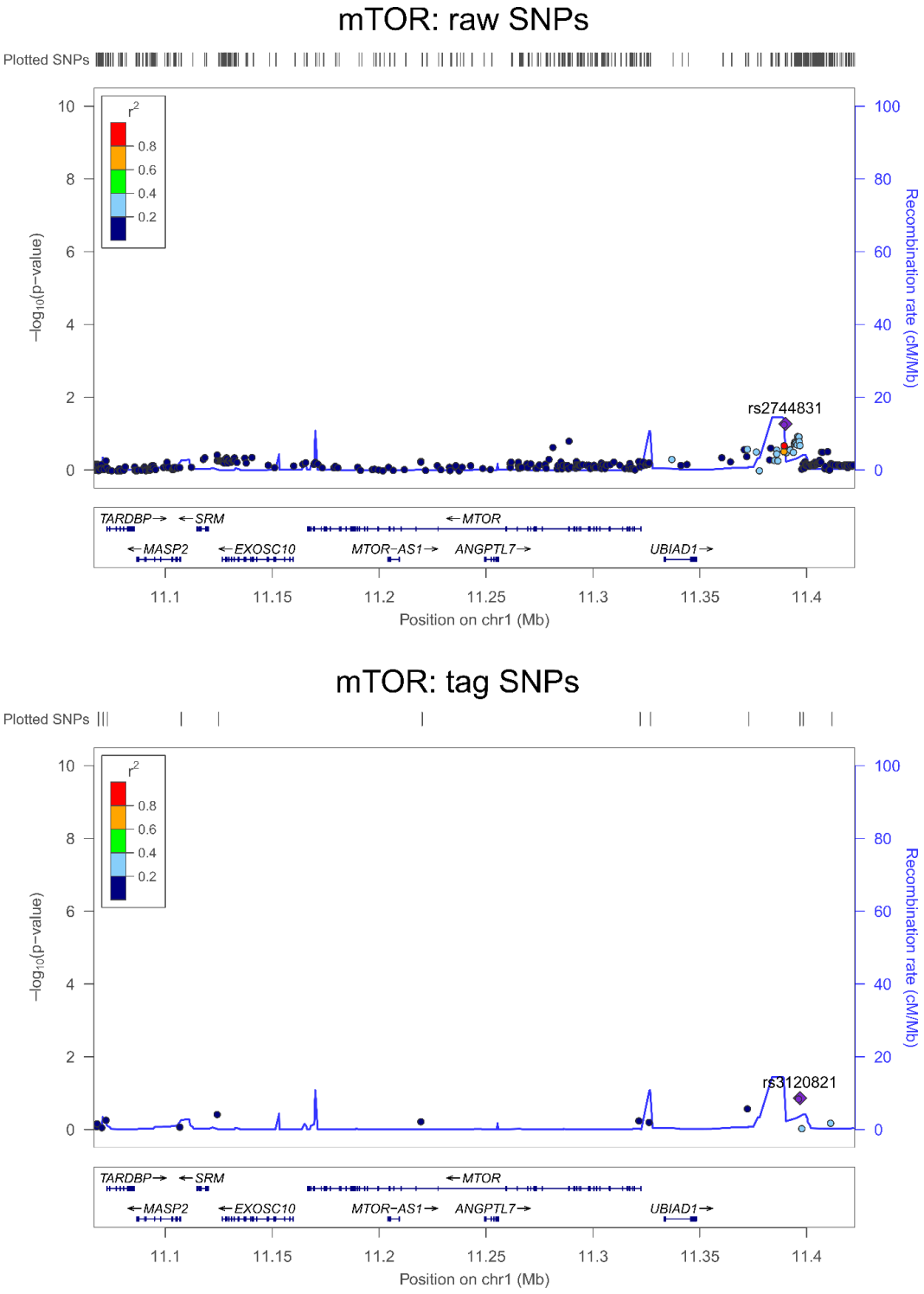

Figure 65 - Locus zoom plot of single nucleotide polymorphisms (SNPs) in mTOR Locus zoom plots showing the p-values (on the left y-axis) of the association between each SNP (shown as a dot) to performance in the paired associates learning (PAL) task. Peaks in the recombination rate of DNA (right y-axis) are shown by the blue line. Peaks mean higher recombination rate and therefore lower linkage disequilibrium. The top plot shows the locus zoom plot of all SNPs within 100KBb up and downstream of the gene boundaries, the bottom graph shows only a selection of these that survived pruning to account for linkage disequilibrium. For ease of visualization, the most significant SNP is highlighted in purple and its RS number is reported on the graph, the adjacent SNPs are then colour coded to show the degree of linkage disequilibrium to that SNP as show by the legend in the top right corner.

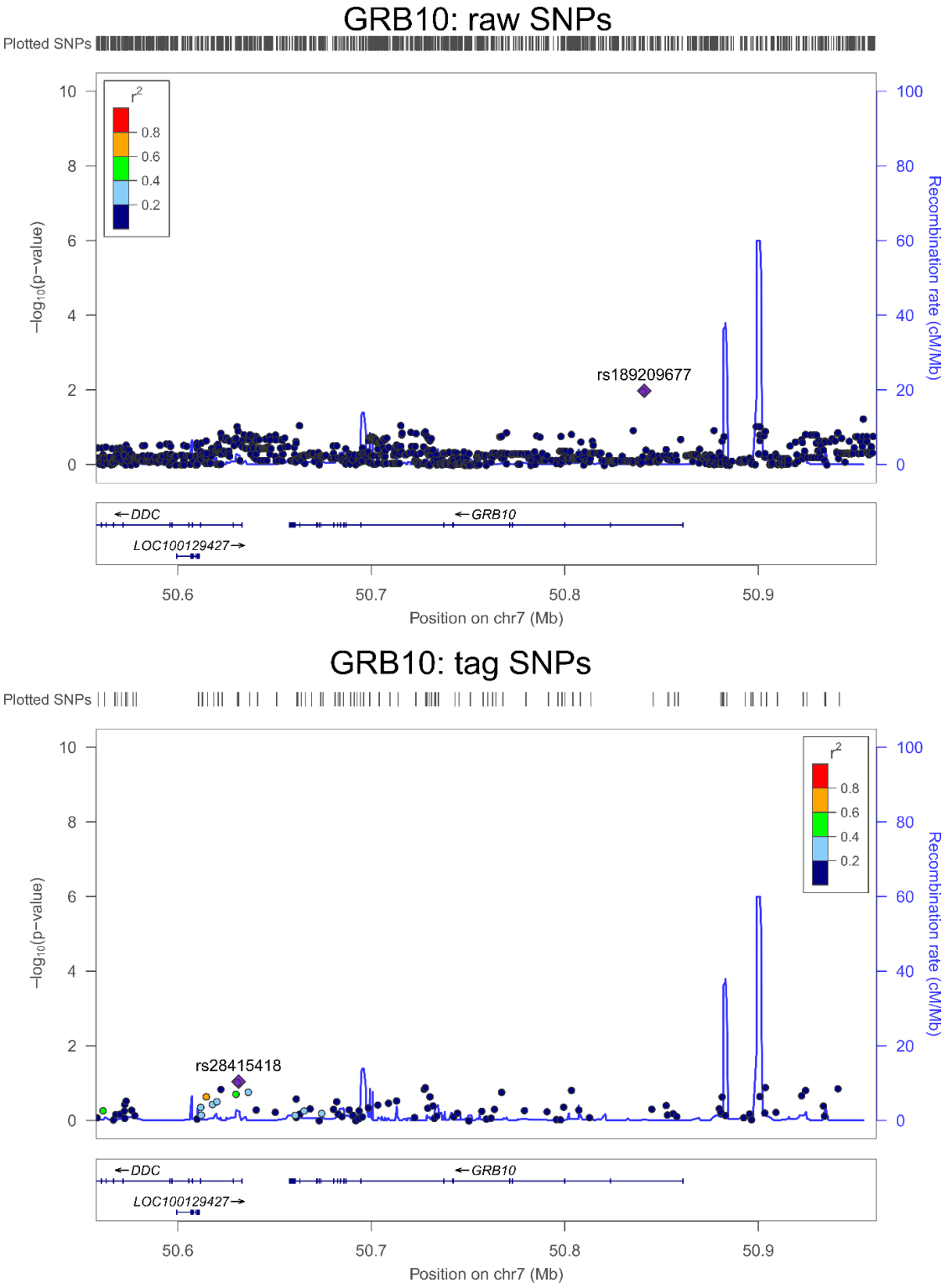

Figure 66 - Locus zoom plot of single nucleotide polymorphisms (SNPs) in GRB10 Locus zoom plots showing the p-values (on the left y-axis) of the association between each SNP (shown as a dot) to performance in the paired associates learning (PAL) task. Peaks in the recombination rate of DNA (right y-axis) are shown by the blue line. Peaks mean higher recombination rate and therefore lower linkage disequilibrium. The top plot shows the locus zoom plot of all SNPs within 100KBb up and downstream of the gene boundaries, the bottom graph shows only a selection of these that survived pruning to account for linkage disequilibrium. For ease of visualization, the most significant SNP is highlighted in purple and its RS number is reported on the graph, the adjacent SNPs are then colour coded to show the degree of linkage disequilibrium to that SNP as show by the legend in the top right corner.

5.3.5 SNPs in the proximity of Sirt1 and ABTB1 are associated to higher PAL errors

GEE linear models were used to investigate whether SNPs in the 9 candidate genes were associated to PAL errors. The 482 tag SNPs selected in the previous section were used and individual linear models were carried out for each SNP. As explained in section 5.2.9, each linear model included clusters to account for twin pairing and included age, gender and NART score as covariates owing to their effects on PAL performance as discussed in section 5.3.2.The results were then corrected for multiple testing (482 comparisons) using the Benjamini-Hochberg correction. **Table 36** reports the 5 most significantly associated SNPs to PAL errors along with the corresponding beta coefficients, confidence intervals, p and q values and number of people for each model. See section 8.4.2.3 for a file of all 482 association results.

SNP	Tagged SNPs	β coefficient	L95	U95	p value	n	q value
rs497849 (SIRT1)	-	**0.19**	**0.10**	**0.27**	**0.00001**	**1286**	**0.006**
rs782431 (ABTB1)	**rs2630213**	**0.14**	**0.07**	**0.22**	**0.0001**	**1277**	**0.029**
	rs2720262						
	rs782455						
rs6439080 (ABTB1)	rs4544568	-0.14	-0.21	-0.06	0.0006	1244	0.102
	rs4974412						
	rs13082666						
	rs13083682						
	rs13073911						
rs7765486 (IGF2r)	rs1094565	-0.12	-0.20	-0.05	0.0009	1269	0.108
	rs9689601						
	rs2083867						
rs782448 (ABTB1)	rs7578	0.12	0.05	0.20	0.001	1286	0.110
	rs813634						
	rs9383						
	rs782444						
	rs814131						
	rs812156						

Table 36 - Results of the linear models testing SNPs for association to Paired Associates Learning errors. β coefficient, lower (L95) and upper (U95) confidence intervals, unadjusted p value, number of people (n) and adjusted p value (q value) following Benjamini-Hochberg correction are reported for each model. The candidate gene closest to the single nucleotide polymorphism (SNP) being tested is reported in brackets in the first column. Tagged SNPs refer to the SNPs tagged by the SNP reported in the first column.

The association between SNPs rs497849 (a SNP in the proximity of SIRT1) and rs782431 (a SNP in the proximity of ABTB1) with PAL errors survived multiple testing correction, these graphical representations of these associations are shown in Figure 67. No other SNPs were in LD with rs497849 but 3 SNPs were in LD with rs782431: rs2630213, rs2720262 and rs782455, making them interesting candidates for effects on PAL. Of note, is the presence of a further 2 tag SNPs (rs6439080 and rs782448) related to ABTB1 appearing in the top 5 most significantly associated SNPs to PAL, though these did not survive multiple testing correction.

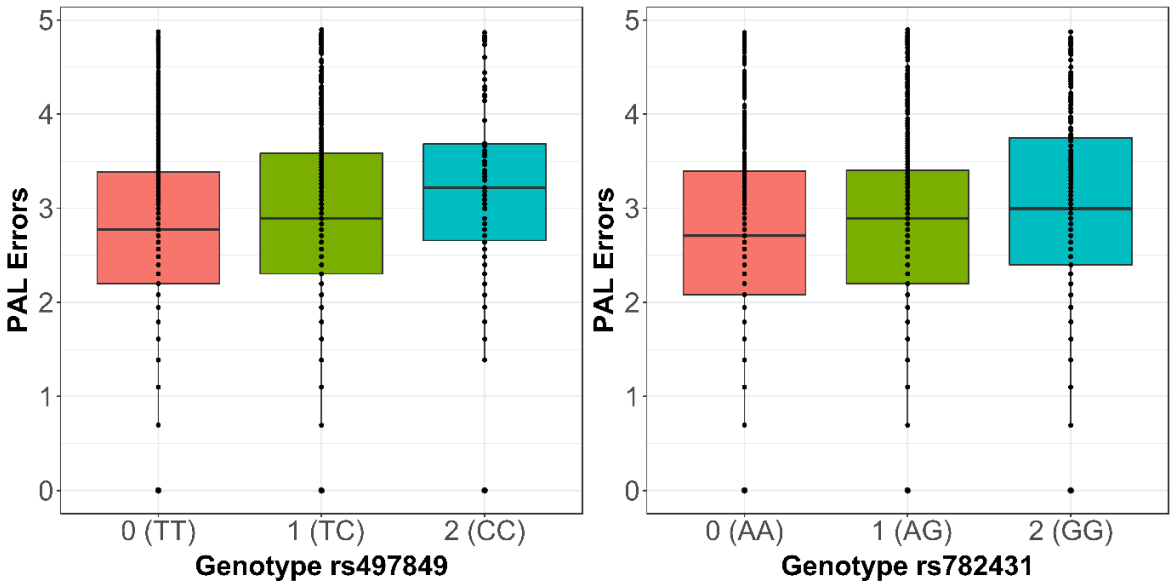

Figure 67 - Paired associates learning (PAL) task errors and genotype. Boxplots showing the association between rs497849 (**left**) and rs782431 (**right**) genotype with PAL errors. Genotypes are displayed as 0: homozygous for the major allele (orange), 1: heterozygous (green) and 2: homozygous for the minor allele (blue). Each dot represents a participant.

As the correct way to include MZ twins in epidemiological studies is often debated, sensitivity analysis was carried to see if different methods affected the results. The two other methods tested involved either averaging the MZ twins to form a single data point or including only one of the two MZ twins. These methods identified similar SNPs as when the analysis was carried out by using the chosen method detailed in section 5.2.9, which accounts for relatedness in MZ and DZ by using clusters within the GEE model. See appendix section 8.4.2.4 for the 5 most significant SNPs resulting from the other two methods.

5.3.6 Physical activity levels are differentially associated to PAL performance according to SIRT1 genotype.

The following analysis was carried out to investigate whether genotype affected the association between lifestyle habits and PAL errors. To do this, linear models testing the association between calorie intake, healthy eating and physical activity with PAL errors were carried out but the interaction with genotype was added into each model as well as the usual covariates (age, gender and NART score). All variables were continuous.
There were no significant interactions between genotype and healthy eating or genotype and calorie intake (see appendix section 8.4.2.5). However, physical activity levels showed significant interactions with rs10997817 (a SNP in the proximity of SIRT1) genotype (β= 0.30, p =0.0001), suggesting physical activity level may affect PAL performance differently according to genotype.

This result shows that for participants who are homozygous for the major allele (genotype 0), an increase in physical activity is predictive of a decrease of 0.054 in PAL errors. For those who are heterozygous (genotype 1) instead, increasing physical activity units were predictive of an average increase of 0.3 PAL errors. In contrast, participants who are homozygous for the minor allele (genotype 2) showed a large increase in PAL errors (0.56) with increased exercise. It is important to keep in mind that rs10997817 tags rs12220640 and rs77797709, meaning any of these 3 SNPs could be responsible for the interaction with physical activity.

The interaction coefficients of the 5 SNPS with the most significant interactions between physical activity and genotype are reported in **Table 37** along with the confidence intervals, p and q values and number of people for each interaction. As before, Benjamini-Hochberg correction was used to create the q values (482 comparisons). Though only one SNP survived FDR correction, the 4 most significant SNPs are all related to SIRT1.

SNP	Tagged SNPs	β coefficient	L95	U95	p value	n	q value
rs10997817 (SIRT1)	**rs77797709 rs12220640**	**0.30**	**0.07**	**0.54**	**0.0001**	**613**	**0.049**
rs866255 (SIRT1)	128+	0.22	0.03	0.41	0.0007	613	0.171
rs10997810 (SIRT1)	8+	0.29	0.03	0.55	0.001	605	0.224
rs4457643 (SIRT1)	43+	0.39	-0.05	0.79	0.002	607	0.261
rs6593185 (GRB10)	rs62447566	-0.19	-0.38	0.01	0.005	613	0.346

Table 37 - Results of linear models testing the interaction of genotype and physical activity levels on the association between physical activity and Paired Associates Learning task. β coefficient, lower (L95) and upper (U95) confidence intervals, unadjusted p value, number of people (n) and adjusted p value (q value) following Benjamini-Hochberg correction for each model are reported. The candidate gene closest to the SNP being tested is reported in brackets in the first column. Tagged SNPs refer to the SNPs tagged by the SNP reported in the first column, due to the high levels of LD in the SIRT genes, we do not report all tagged SNPS. See appendix section 8.4.2.2 for these SNPs.

Interestingly, the rs10997817 SNP showed no association with PAL performance when physical activity was excluded from the model (see **Table 38**), suggesting any association is dependent on the interaction between physical activity and genotype. The graphical representation of these comparisons in shown in Figure 68**.**

PAL ~ genotype	β coefficient	L95	U95	p value	n	q value
rs10997817 (SIRT1)	-0.08	-0.18	0.03	0.15	1286	0.773

Table 38 - Results of the linear model testing the association between rs10997817 and Paired Associates Learning (PAL) task . β coefficient, lower (L95) and upper (U95) confidence intervals, unadjusted p value, number of people (n) and adjusted p value (q value) following Benjamini-Hochberg correction are reported. " ~ " denotes test for association.

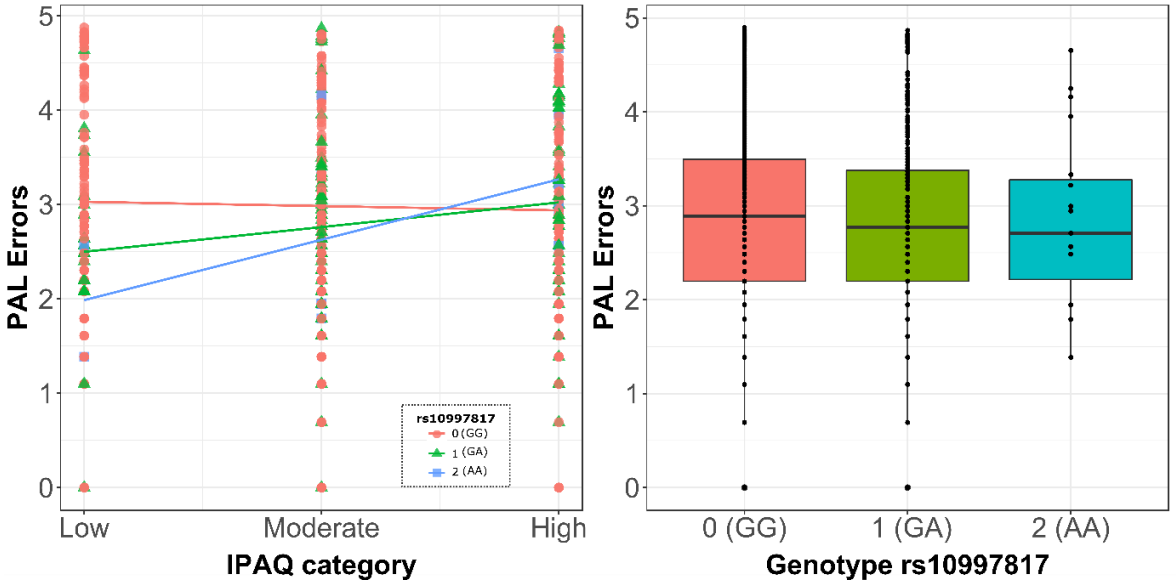

Figure 68 - Interaction between physical activity (IPAQ) and genotype on Paired Associates Learning (PAL) errors **Left**: Graph showing the effect of genotype on the association between physical activity (IPAQ on the x-axis) and PAL errors (y-axis). **Right**: Boxplot showing the lack of association between RS10997817 genotype with PAL errors. Genotypes are displayed as 0: homozygous for the major allele (orange), 1: heterozygous (green) and 2: homozygous for the minor allele (blue). Each dot represents a participant. Data was analysed as categorical but represented as continuous for ease of visualization.

5.3.7 Effects of age and lifestyle on methylation status

As both aging and lifestyle are likely to affect epigenetics, changes in methylation were also investigated. Due to the limited number of participants with available methylation data (n =288) however, the study was limited to assessing the methylation status of the cg03330058 residue. Assessing the methylation status of all sites in all 9 candidate genes, would have caused a loss of power due to a large number of multiple comparisons and only a small number of participants. Therefore, we approached a candidate approach and only investigated the cg03330058 in the ABTB1 gene which was previously highlighted by Horvath's clock (Horvath, 2013).

First, the methylation status of the residue was tested for association to gender. A Welch's two sample t-test showed a significant ($t(4)= 5$, $p = 0.007$) increase of 4.4% in methylation status of cg03330058 in males compared to females. However only 4 of 2888 patients were male making this result unreliable. Next, methylation status was tested for association to age with a GEE linear model. Clusters were used to control for the relatedness of the

participants and gender was included as a covariate. This showed a narrowly non-significant (p= 0.067) negative association between cg03330058 methylation and age, suggesting that in a larger sample, methylation at this residue may be decreased in older people (see **Table 39**). Graphs showing the correlation between age and methylation intensity of cg03330058 and the difference in methylation intensity of cg03330058 in male and female participants are shown in Figure 69**.**

	β coefficient	L95	U95	p value	n
Methylation ~ Age	-0.0009	-0.002	0.000006	0.0671	288

Table 39 Results of the linear model testing the association between methylation of the cg03330058 residue and age β coefficient, lower (L95) and upper (U95) confidence intervals, unadjusted p value, number of people (n) and adjusted p value (q value) following Benjamini-Hochberg correction are reported. " ~ " test for association.

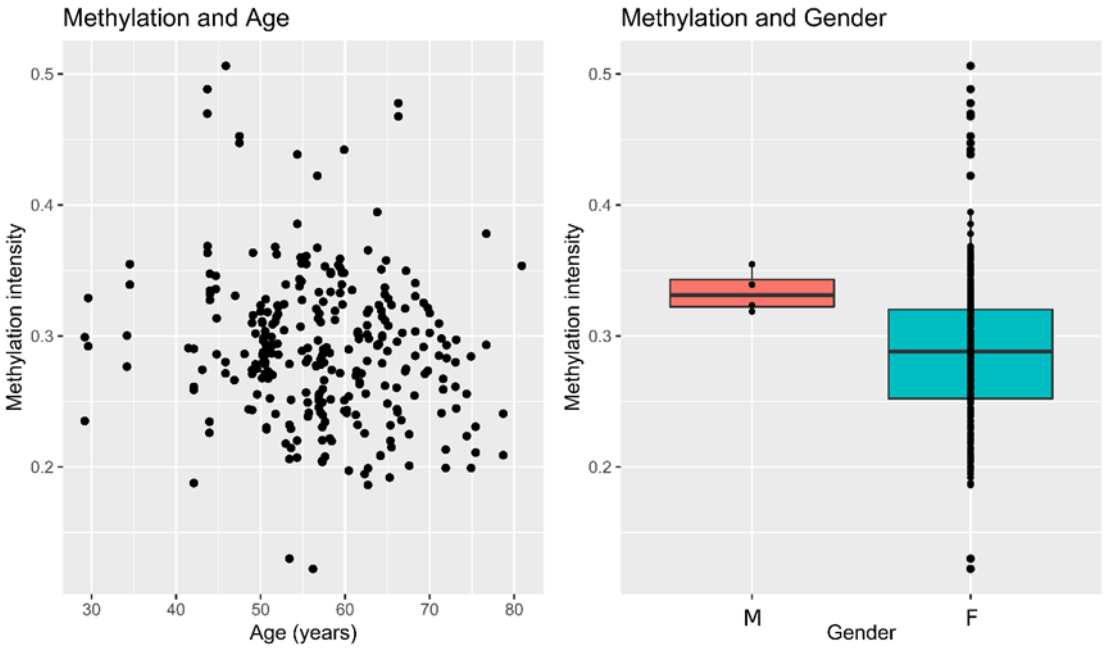

Figure 69 -Impact of age and gender on cg03330058 methylation. Scatter plot showing the correlation (p= 0.067) between age (x-axis) and methylation intensity of the cg03330058 residue (y-axis). Box plot showing the mean and the distribution of the methylation intensity of values of the cg03330058 residue in male (M) and female (F) participants.

To assess whether lifestyle affected methylation status, healthy eating, physical activity and calorie intake were regressed against methylation intensity. Age and gender were included as covariates and relatedness was controlled by clustering. This showed no association between any of the lifestyle measures and methylation intensity except for a possible weak association between healthy eating and methylation status. This association however, did

not survive multiple testing correction. See Table 40 for beta coefficients, confidence intervals, p and q values and number of people in each linear model. Graphical representations of these correlations are shown in **Figure 70.**

Methylation ~	β coefficient	L95	U95	p value	n	q value
HEI	**-0.0005**	**-0.001**	**-0.00003**	**0.0385**	**267**	0.116
Kcal	-0.0000008	-0.00001	0.000008	0.85	267	0.852
IPAQ	-0.007	-0.016	0.002	0.1264	146	0.190

Table 40 - Results of the analysis testing the association between methylation and healthy eating (HEI), methylation and calorie intake (Kcal) and methylation and physical activity and methylation status (IPAQ). Reported are the β coefficient, lower (L95) and upper (U95) confidence intervals, unadjusted p value, number of people (n) and adjusted p value (q value) following Benjamini-Hochberg correction for each linear model. " ~ " denotes correlation.

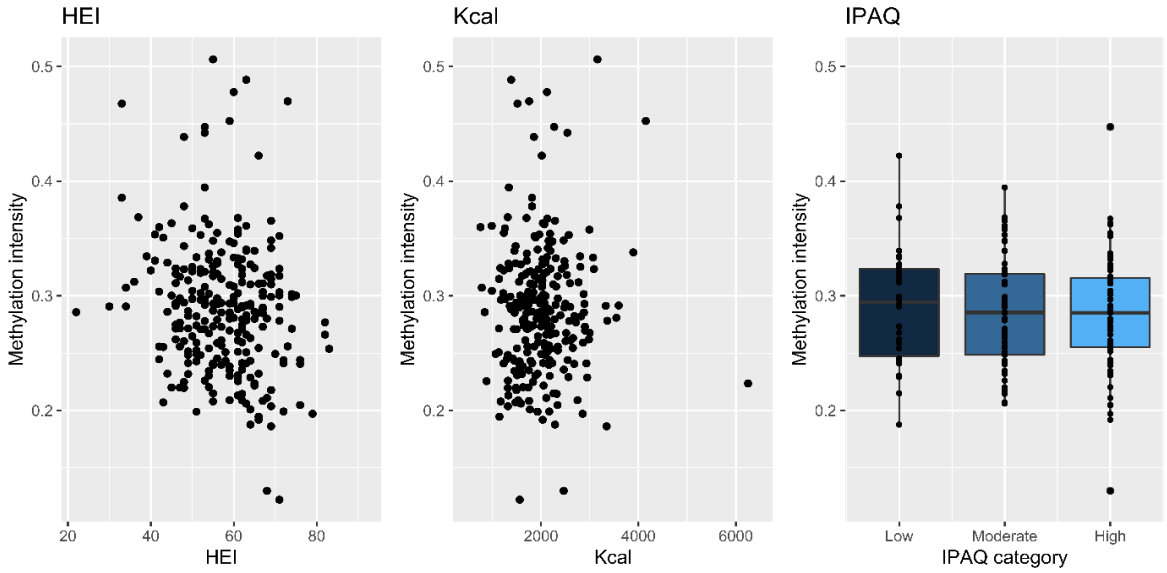

Figure 70 - Lifestyle effects on methylation. Scatterplots showing the association between healthy eating (HEI) and calorie intake (Kcal) with methylation intensity of the cg03330058 residue. Boxplot showing the association between varying levels of physical activity (IPAQ) and methylation intensity of cg03330058 residue. In all graphs methylation intensity is on the y-axis.

Due to the limited number of participants, there was a lack of power to carry out analyses testing the association between methylation status and cognition (n=64) or methylation and lifestyle (n=25). Data not shown.

5.4 Discussion

The data outlined in this chapter shows that while there is no significant effect on PAL performance of diet or exercise individually, an interaction of these two factors does impact PAL performance. In addition, this study reports interesting associations between genotype and hippocampal cognition and suggests possible epigenetic alterations as a function of age.

5.4.1 Preliminary data: Impact of dementia diagnosis on Paired Associates Learning performance

This study aimed to assess the association between lifestyle, genetic and epigenetic factors to cognition in a healthy population. To ensure this cohort only contained healthy participants a selection based on MMSE score was explored. To validate this decision and to assess whether MMSE score affected PAL performance, a preliminary study comparing participants with or without a MMSE-based dementia diagnosis was carried out.

We report worse performance on the PAL task by participants with a score lower than 27 on the MMSE. A cut-off of 27 was selected, over the more lenient and sometimes-used cut-off of 24, as TwinsUK is recruited as a healthy cohort and is formed largely by highly educated individuals. Therefore scores below 27 in the absence of dementia are not expected within this cohort (Kukull et al., 1994; O'Bryant et al., 2008). Our data suggests the possible presence of dementia (MMSE<27) negatively impacts PAL performance. This finding was not unexpected as associations between PAL performance and MMSE score have been reported before and as a decline in cognitive ability is likely to present itself as poorer performance in both the MMSE and the PAL task (Ito et al., 2010). It was interesting however, to witness this association in a healthy cohort.

The effectiveness of MMSE as a diagnostic tool and correct cut-off is often debated as is the effect of age, education and IQ on MMSE score (Butler et al., 1996; Dykiert et al., 2016; O'Bryant et al., 2008). Due to the exclusion of all participants with definite dementia diagnosis from the TwinsUK cohort however, this cohort was not appropriate to study these effects or the impact of MMSE score on PAL performance (Moayyeri et al., 2013).

Regardless, it is interesting to note that the maximum errors were not higher in the subgroup of participants with possible dementia (Maximum PAL errors =130) than in those with no dementia (Maximum PAL errors = 138), suggesting it was not outliers causing the mean of PAL errors to increase in this subgroup but an overall increase in PAL errors throughout participants.

Following this result, MMSE score was used to ensure a healthy population and to take into account any imminent dementia diagnoses. Though we believe this to be necessary to ensure no undiagnosed patients biased the data, it is possible this cut-off caused some older but healthy participants with borderline scores such as 26 to be mistakenly excluded.

5.4.2 Demographics effects on cognition: focus on age, education and gender

The data reported in this section shows a clear correlation between PAL performance and age. As PAL relies on episodic memory (Barnett et al., 2015) and episodic memory is known to decline with age (Friedman, 2013), this finding is in line with the existing literature and previous studies within this cohort (Barnett et al., 2015; Lee et al., 2013; Steves et al., 2013). CANTAB reports a steady performance until the 5th decade when participants start showing deterioration this trend is also reflected in our data as is the considerable interindividual variation in the extent of deterioration (Barnett et al., 2015). Part of this variation is likely to be explained by other confounding factors such as level of education, gender, lifestyle and genotype. Interestingly, the finding that PAL performance, which is highly dependent on hippocampal function, worsens with age is suggestive of a possible involvement of neurogenesis, which is also known to be strongly affected by age (Mathews et al., 2017).

To explain some of the interindividual variability, we assessed the effect of education on PAL performance; our results show increased education being associated to better performance. Though PAL is sometimes regarded as not being dependent on education, due to the use of pictures rather than words, several studies are now reporting an association between PAL performance and education, with more highly educated people making less errors (Blackwell et al., 2010; Lee et al., 2013). This was also supported by Bento-Torres and colleagues who found a similar association in a Brazilian cohort and

suggested early schooling as a preventative measure to fight age-related cognitive decline (Bento-Torres et al., 2017). This association is usually attributed to the cognitive reserve effect; people with higher IQs, education or participation in leisure activities show less severe signs of cognitive decline (both age and pathology related) despite the biological and histological deterioration of the brain. Cognitive reserve therefore refers to the ability of the individual to have a more flexible use of their cognitive resources allowing for better performance on tasks and a slower decline (Tucker and Stern, 2011). Knight and colleagues however, discuss that it may not be schooling itself that improves performance but rather that, people with lower cognitive abilities tend to collectively attain fewer educational qualifications, which might explain why higher educational levels appear to be associated to PAL performance (Knight et al., 2010). Another factor to take into account is that as the CANTAB PAL© is delivered on a touch screen, more educated people as well as younger people and those from higher socioeconomic background might have an advantage as they may be more accustomed to using such devices in their daily lives. The interaction between all these factors may contribute to the apparent effect of education on PAL.

We also report an association between NART and PAL performance and a strong association between NART and educational level. NART is usually used as a measure of intelligence but, as it relies on the participants reading irregular words, it is often associated to their educational levels (Kiely et al., 2011). Some studies however, have shown NART levels to remain unchanged from the age of 11 suggesting an effect irrespective of education (Suzanne Barker-Collo et al., 2008). In this case the relationship seen here between NART and education further supports Knight's notion that it may simply be the same participants, those with higher intelligence and therefore better NART scores, who perform better on PAL and opt for higher levels of education as opposed to an active effect of education level.

Finally, we report a non-significant trend of increased errors in the male subgroup compared to the female subgroup. This is in line with others finding female participants tend to have better performances on PAL compared to their male counterparts, though the reason behind this remains unknown (Blackwell et al., 2010). Due to the much larger

proportion of females compared to males within our cohort, it is difficult to discern whether this trend is a true effect or an artefact due to the small amount of variation in the male subgroup.

5.4.3 Lifestyle effects on cognition

This study aimed to assess the effect of lifestyle factors such as diet and exercise on cognitive performance. Our findings suggest no association between healthy eating and PAL performance. Though we hypothesised healthy eating impacted PAL performance, this result is supported by Tangney and colleagues who also failed to see an association between HEI and cognitive performance in individuals aged over 65 (Tangney et al., 2011). The authors did see an association between better adherence to the Mediterranean diet and slower cognitive decline, suggesting there was an effect of diet on cognition which was not detected by HEI. This is also further supported by studies using the recommended food score as a measure of diet quality reporting participants with the best diet qualities undergoing slower age-related cognitive decline (Wengreen et al., 2009).

In contrast, a more recent study showed positive associations to cognitive performance for both Mediterranean diet scores and HEI. The authors attributed the different results to a more comprehensive FFQ food list and a younger cohort (Ye et al., 2013). Our study however, is based on an even more comprehensive food list (290 foods vs 264) and wider age range, suggesting further reasons for this discrepancy may exist. Part of the discrepancy may be attributable to the different cognitive tests being used. No previous studies, including the two mentioned above, have focussed on the effect of HEI on hippocampal-dependent tasks, making our result a novel finding in the field. The hippocampus however was recently implicated by an interesting study showing an association between hippocampal volume and long-term high HEI (Akbaraly et al., 2018). Whether this would also relate to hippocampal-dependent tasks remains to be validated and would be an interesting addition to our study. The lack of association between HEI and PAL may indicate that HEI does not affect hippocampal-dependent tasks and that different diet measures may be more appropriate. For example, the Mediterranean diet has been robustly associated to slower cognitive decline making it a good candidate to study age-

related cognition (Féart et al., 2010; Scarmeas et al., 2009; Tangney et al., 2011; Valls-Pedret et al., 2012; Ye et al., 2013). Furthermore, the high levels of polyphenol rich foods in the Mediterranean diet are suggestive of an important role for the hippocampus and neurogenesis in this association (Fernández-Fernández et al., 2012; Shukitt-Hale et al., 2008; Valente et al., 2009; Valls-Pedret et al., 2012).

Surprisingly we saw no association between calorie intake and PAL score, this is in contrast to animal literature showing a relationship between calorie restriction and cognitive function or longevity. As discussed in chapter 1, several animal models have shown decreased calories to extend lifespan and improve cognitive abilities (Halagappa et al., 2007; Maalouf et al., 2009; Taormina and Mirisola, 2014). Recent experiments in rhesus monkeys suggested high translational potential for the benefits of calorie restriction in terms of longevity (Mattison et al., 2017). Interestingly, this group had previously failed to find significant associations between calorie restriction and longevity in rhesus monkeys. The authors suggested these results may be due to the standard lab diet already being healthier than normal, meaning calorie restriction did not cause considerable improvements (Mattison et al., 2012). These results highlight the importance of including other measures such as the HEI in dietary studies.

Human studies have also shown an increase in the incidence of mild cognitive impairment in people with high caloric intake suggesting an important role for calorie intake in cognitive function (Geda et al., 2013). Interestingly, results from the CALERIE clinical trial have shown several age-related benefits for calorie restriction but have failed to show an association with cognitive performance (Martin et al., 2007; Redman et al., 2018). Both our data and that from the CALERIE trial however, support the absence of adverse effects of calorie restriction on cognition which has been suggested in previous studies (Green and Saenz, 1995; Kemps and Tiggemann, 2005). To date, no studies have assessed the effect of calorie consumption on hippocampus-dependent tasks in a healthy population.

The surprising lack of association between both HEI and calorie intake with PAL performance reported in this study may be explained by the noise introduced in the

analysis by the large time differences between PAL assessment and FFQs. However, it may also be reflective of the need to account for other lifestyle aspects such as exercise and social status (Partridge et al., 2018). To assess if different exercise habits affected these associations, we tested for interactions between physical activity and dietary measures. We report physical activity modulates the association between calorie consumption and PAL performance. Individuals who undergo low or moderate levels of physical activity show an increase in PAL errors with an increase in calorie consumption. For individuals with high physical activity levels instead, an increase in calorie consumption appears related to fewer PAL errors. This result shows low calorie intake is unfavourable in highly active individuals suggesting a mismatch between energy intake and energy expenditure may be detrimental. It is interesting to note how data from low and moderately active individuals instead, shows positive effect of reduced calorie intake on cognitive performance, as per the literature discussed above. The different associations between calorie consumption and cognitive performance according to exercise levels, show the importance of factoring in lifestyle as a whole in such analyses. These differences are likely attributable to more or less favourable overall metabolic states as discussed by Picard and Turnbull (Picard and Turnbull, 2013). Due to possible influential outliers within our data, it would be interesting to repeat this analysis in a different cohort to validate this finding. Finally, we report no interaction between physical activity levels and the association between HEI and PAL performance, supporting either the possibility of diet not affecting hippocampal-cognition or the notion that other dietary indices may be more appropriate.

Interestingly we report no association between physical activity and PAL performance but show an interaction between exercise and diet. This result highlights the need to take into account all aspects of lifestyle and suggests this may be exceptionally important for hippocampus-related cognition (Lucassen et al., 2010).

The lack of association between physical activity and PAL was surprising due to the ever-increasing body of evidence showing a strong association between exercise and cognitive function (McNerney and Radvansky, 2015; Ngandu et al., 2015; Northey et al., 2018). The exact type of exercise and the pertaining mechanisms that are beneficial to human

cognition however have not yet been clarified (Kennedy et al., 2016; McNerney and Radvansky, 2015). Suggesting different types of exercise may have different outcomes on cognition. In addition, though animal studies suggest an important role for the hippocampus in exercise-associated cognitive benefits, no human study has focused specifically on hippocampal cognition but rather on related aspects such as depression and dementia onset (Blondell et al., 2014; Klempin et al., 2013; Schuch et al., 2018; van Praag et al., 2005). Our data suggests hippocampal cognition may not be as susceptible to exercise in humans as in animal models. Alternatively, it may be necessary to further subdivide the participants to distinguish those who are sedimentary from those with low levels of exercise and those with high exercise levels from those with excessively high exercise levels. Studies have in fact shown exercise benefits are already present in individuals with low to moderate exercise levels when compared to sedentary individuals (Sofi et al., 2011) and that extreme exercise ranges are associated to worse mental health (Chekroud et al., 2018).

5.4.4 SIRT1 and ABTB1 genotype effects on cognition

Following the results highlighting the importance of lifestyle on cognition, we attempted to explain some of the remaining part of interindividual variation. We report a significant association between rs497849 genotype (a polymorphism in the proximity of the SIRT1 gene) and PAL performance. Carriers of the minor allele “G” were more likely to perform worse on the PAL task than those carrying the major allele “T”. Accordingly, homozygous participants for this SNPs performed worse than those with a “TT” genotype but better than those with a “GG” genotype. This finding suggests an important role for SIRT1 in hippocampal cognition. As seen in **Figure 59** however, this SNP is not located in the SIRT1 coding region but further downstream closer to the HERC4 coding region in addition, the consequence of this mutation on SIRT1 one regulation remains unknown. Despite this, the rs497849 SNP is often used as a tag SNP in studies investigating SIRT1 as it is in strong LD with surrounding SNPs. Surprisingly and contrary to other studies, this SNP was not in LD with any other SNPs in our cohort. This may be due to the limited number of participants causing weaker r^2 values which do not survive the LD threshold of $r^2 = 0.8$.

Groups have reported associations between other SIRT1 polymorphisms and traits such as lung squamous cell carcinoma (Leng et al., 2013), body mass index (Zillikens et al., 2009), type 2 diabetes (Botden et al., 2012) and even cognitive performance (Kuningas et al., 2007). These links are supportive of a possible effect of SIRT1 on ageing, nutrition and cognition related phenotypes. Therefore, though no groups have reported direct associations of rs497849 to these specific traits before, our findings together with those mentioned above, support a promising role for SIRT1 in ageing.

The other polymorphism with a significant association to PAL performance was rs782431 which was included in our analysis due to its proximity to the ABTB1 gene. As above, the presence of the minor allele was predictive of increased errors in the PAL task. Accordingly, participants who were homozygous for the major allele showed lower PAL errors than their heterozygous and minor allele homozygous counterparts. This SNP was also in LD with three other SNPs (rs263021, rs2720262 and rs782455) suggesting any of these polymorphisms or combination could be affecting important molecular pathways relating to hippocampal cognition. The function of this gene, as discussed in chapter 3, remains largely unknown. It was however highlighted by unpublished work in our lab and Horvath's clock as an important gene in ageing and as a possible new gene involved in insulin-sensitivity (Horvath, 2013; Miranda et al., 2014; Murphy et al., 2018). No studies have so far identified phenotypes associated to polymorphisms in this gene. Interestingly, the rs782431SNP appears to be within the MCM2 coding region. This finding is particularly interesting given MCM2's function as DNA replication licensing factor and the use of MCM2 expression as a marker for slowly cycling NSCs in adult neurogenesis studies (Maslov et al., 2004; von Bohlen und Halbach, 2011). A polymorphism in this gene may therefore indicate alterations in NSC proliferation and NSC pool maintenance which would result in altered neurogenesis. Given the strong association between neurogenesis and hippocampus-dependent cognition, alterations in neurogenesis may be a possible explanation for the link seen between this SNP and PAL performance. Despite this, three of our top five most significantly associated SNPs were in proximity to ABTB1. This supports an important role for the gene in PAL performance rather than just an accidental proximity to the MCM2 gene. As seen in **Figure 71** in fact, the other SNPs are present further away from MCM2

with one (red dot in **Figure 71**) being within ABTB1's coding region. As each of these SNPs tags several other SNPs (**Table 36**) it would be interesting to elucidate whether these effects are synergistic and by which mechanism ABTB1 affects cognition.

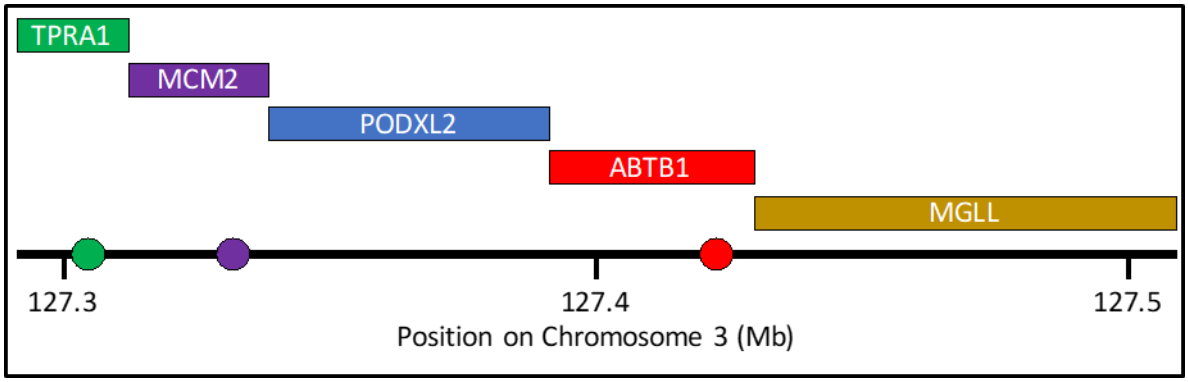

Figure 71 - SNPs in the proximity of ABTB1. Diagram highlighting the location of three SNPs in proximity to ABTB1 that showed likely associations to PAL performance. The black line at the bottom indicates the chromosome position in megabases (Mb). The SNPs are shown as coloured dots and the genes coded for by each section of the chromosome are shown as coloured squares. Though all SNPs are within 100KB of ABTB1's coding region, only rs782448 (red dot) is within ABTB1's coding region, whilst rs782431 (purple dot) is within the MCM2 gene coding region and RS6439080 (green dot) is further upstream within TPRA1's coding region. Each SNP shown also tags several other nearby SNPs.

Surprisingly, though the locus-zoom plots (see **Figure 63**) showed some association between SNPs in the proximity of FOXO3A and PAL performance, none of the SNPs survived multiple correction. As FOXO3A-related polymorphisms are some of the few polymorphisms successfully associated to human longevity, we had expected to see associations to cognitive performance for these polymorphisms (Joshi et al., 2017; Nygaard et al., 2014; Willcox et al., 2008a). Previous studies however have reported that while FOXO3A genotype is predictive of improved longevity and healthspan it is not associated to an accompanying superior cognitive performance (Willcox et al., 2008a; Zeng et al., 2015). Importantly, mTOR, a candidate gene in many ageing studies also showed no association to PAL performance suggesting it may not be involved in hippocampus dependent cognition (Harrison et al., 2009; Lamming et al., 2013). In line with this, several other candidate genes showed no association to cognitive performance despite previous studies reporting associations to other age-related declines. Indeed, genetic variations in mTOR and IGF2R have been associated to cancer (Xu et al. 2013; Shao et al. 2014; A. J. Yoon et al. 2012), those in GRB10 have been linked to increased risk of type II diabetes (Di Paola et al. 2010) and UCP2 polymorphisms have been correlated to physical ageing measures such as walking speed (Dato et al. 2014). As we employed an additive model to account for

the additive effect of the presence of the risk allele, it would be interesting to validate these findings by testing the association of haplotypes rather than individual SNPs.

5.4.5 Lifestyle and genotype interaction effects on cognition

As existing literature and our previous findings highlighted the importance of lifestyle when assessing factors affecting cognition, we investigated the possibility of a modulatory effect of genotype on the association between lifestyle and cognitive performance. Our study failed to identify any polymorphisms that affected susceptibility of either calorie intake or healthy eating on cognitive performance. It however highlighted an interaction between rs10997817 and physical activity levels affecting the association of physical activity with cognitive performance. As expected, participants who were homozygous for the major allele appeared to make less mistakes on the PAL task if they exercised more supporting the positive association between cognitive performance and exercise found in several studies (Chekroud et al., 2018; Colcombe et al., 2003; Hogan et al., 2013).

Surprisingly, those who were hetereozygous showed a minimal increase in PAL errors with increased exercise and those with the homozygous genotypes for the minor allele showed a strong increase in PAL errors with increased exercise. Besides Checkroud and colleagues finding an association between excessive exercise and poorer mental health, no other study has previously reported a negative effect of exercise on cognitive performance (Chekroud et al., 2018; Kennedy et al., 2016). To assess whether this was the case in our study, and whether participants with both risk alleles happened to undergo excessive amount of exercise and therefore have exceptionally detrimental outcomes on cognition, it would be interesting to repeat the study further subdividing the exercise categories to assess the effects of excessive exercise. Unfortunately, due to the low frequency of the minor allele larger cohorts are needed for such a study. Alternatively, this finding may simply highlight the importance of taking into account both genotype and lifestyle; the fact that most studies have highlighted a positive effect of exercise may be due to most participants having the major allele genotype. The minor allele may therefore be associated to poorer cognition but this association is usually harder to detect.

In addition, the finding that the rs10997817 genotype is not on its own associated to PAL performance once again highlights the importance of a holistic approach to ageing

research. Interestingly, other studies have selected SIRT1 polymorphisms to assess associations with longevity but have failed to find any links, our results suggest this may be due to factoring in aspects such as lifestyle (Flachsbart et al., 2005). One study however, found a significant association between rs10997870, a SNP in LD with rs866255, and suicidal behaviour in patients with bipolar syndrome, implicating the SIRT1 polymorphisms in mental health. The rs866255 polymorphism, was the SNP with the second most significant interaction with physical activity on PAL performance but did not survive multiple testing correction. It is also in LD with rs1467568 a SNP which was associated to BMI at baseline (Zillikens et al., 2009). If the association between rs866255 and PAL performance is not a false positive as FDR correction implies, this association combined with the findings above, suggests an important role for this area of SIRT1 in the interplay between genotype, cognition and lifestyle. Accordingly, as four of the five SNPs with most significant modulatory effects on the association between exercise and PAL performance are related to the SIRT1 gene, our findings support a role for this gene in this interplay. It is interesting to note that SIRT1 is known to have functions in energy metabolism in animal models making it a perfect candidate for convergent effects of both exercise and nutrition (Boily et al., 2008). Though dietary habits showed no interaction with SIRT1 genotype in our study, one could speculate that analyses assessing a three-way interaction between exercise, diet and genotype could identify interesting associations with respect to cognition. This analysis however, would require larger cohorts.

5.4.6 Lifestyle effects on ABTB1 methylation

Following results highlighting an interesting role for in ABTB1 in hippocampal cognition, the methylation status of this gene was investigated. This gene and residue were selected due to exciting findings by the Horvath group highlighting this residue in the ABTB1 gene as one of the 353 methylation sites constituting the “Methylation clock”. The methylation clock is essentially a methylation signature that provides information on the biological, rather than chronological age of a tissue. Specifically, the cg03330058 residue in the ABTB1 gene has been highlighted, alongside other methylation sites, as undergoing a decrease in methylation intensity with age (Horvath, 2013). Therefore, we assessed the association of ABTB1 methylation, age and lifestyle within our cohort.

We report a non-significant but interesting negative trend between cg03330058's methylation intensity and age, this observation is line with Horvath's clock data (Horvath, 2013). Recently, in an effort to explain some of the heterogeneity of ageing, groups have focused on trying to distinguish what makes biological age differ from the chronological one. This has given rise to several human and animal methylation clocks aimed at understanding the methylation changes that occur in response to both chronological and biological age (Hannum et al., 2013; Levine et al., 2018). These are of great use in biogerontology research as they have strong correlations with both age of death, a measure of lifespan, and age-related disease onset and progression which can be used as a measure of healthspan (Horvath and Raj, 2018; Levine et al., 2018). Though our finding of a possible correlation between age and ABTB1 relates to those of Horvath's, it is not supported by Hannum's findings which do not highlight ABTB1 in the set of genes used to calculate the methylation clock (Hannum et al., 2013; Horvath, 2013).

We also report an increase in methylation intensity in males compared to females, though this is based on only five male participants. This finding is not in line with previous findings by Horvath suggesting men tend to appear epigenetically older than their female counterparts. Horvath's findings however, are based on the entire methylation clock and not exclusively on the cg03330058 residue like ours, suggesting there may be different gender effects on each residue. Regardless, given the very limited number of males and variation in the female subgroup, it is likely this result would change if more male participants were added to the analysis.

We report no significant associations between lifestyle measures and methylation intensity of the cg03330058 residue besides a possible association with healthy eating, which does not survive multiple testing correction. Prior to Benjamini-Hochberg correction, our results show healthier eating is predictive of lower methylation intensity of the candidate residue. Should this finding to be confirmed, it would indicate an interesting association between healthier eating and an "epigenetically older" methylation status of this residue. As discussed in the chapter 1, diet is known to affect epigenetic status, however, to our

knowledge this is the first time it has been associated to methylation changes in the ABTB1 gene. Interestingly, we did not see any associations with calorie consumption, suggesting the diet's effects are likely due to specific, healthier nutrients being consumed rather than an effect of calorie reduction. To further understand and confirm this association, it would be interesting to look at the specific nutrients consumed by participants with varying amount of methylation intensities. In addition, for this to be relevant at an organismal level, it would be necessary to test if the association between healthy eating and methylation status is still present when all 353 CpG sites that form Horvath's clock are taken into account.

There was no correlation between physical activity levels and methylation status of the candidate residue, suggesting the reported effects of physical activity on epigenetics may act on other residues or on the overall methylation status rather than individual residues. Interestingly, the same study that reported an effect of physical activity on methylation, also reported an association with cognitive health (Marioni et al., 2015). Supporting this, studies have confirmed the validity of the methylation clocks in terms of cognitive ageing, finding associations between methylation status and the number of neurons, Alzheimer's disease and neuropathology such as amyloid plaques (Horvath and Raj, 2018; Levine et al., 2015; Lu et al., 2017). Unfortunately, due to limited power in our cohort we were not able to test the association between methylation and cognitive performance, we believe this to be an interesting and necessary next step for this analysis. Alongside this, it would be interesting to test whether genotype is correlated to methylation status as studies are suggesting accelerated epigenetic ageing has hereditary components. Finally, testing the interaction between lifestyle, genotype and methylation status on cognitive performance would provide interesting answers within ageing research the ageing phenotype is likely a combination of all these factors.

Though this study was limited by power, elucidating the effects of lifestyle on methylation status and the association between methylation and cognitive ageing is an interesting avenue. Epigenetic clocks have been suggested as useful tools in ageing research and age-related healthcare as they can efficiently detect phenotypic age with minimal invasion

(Levine et al., 2018). Further research is needed to assess the validity of such clocks as a measure of age-related cognitive decline due to the differences between blood and brain methylation statuses (Walton et al., 2016).

5.4.7 Summary and future directions

In summary, we report an interesting interaction between different aspects of lifestyle on their association to hippocampus dependent cognition. We also report an important function for both SIRT1 and ABTB1 polymorphisms in cognitive performance and highlight SIRT1 as a possible mediator of the effects of physical activity on cognition. Finally, we also suggest an age-relate association for ABTB1 methylation. Future studies validating these findings in independent longitudinal cohorts or cohorts comparing young and old participants are necessary to understand the impact of age on these associations. In addition, it will be interesting to assess the impact of genome-wide methylation status on PAL and other cognitive tasks and to relate this to lifestyle habits and genetic polymorphisms. Finally, future studies incorporating using the recently developed phenome-wide methodology, to compare genotype-to-phenotype via the use of electronic health records, may provide interesting information on the phenotypic relevance of these SNPs.

5.4.8 Limitations

Despite interesting findings, this study has a number of limitations. Firstly, the variables pertaining to lifestyle are the result of self-report questionnaires which are known to suffer from errors and over reporting (Heesch et al., 2010; National Cancer Institute.; Rzewnicki et al., 2003). One study even suggested that older individuals may make more errors on the IPAQ (Heesch et al., 2010). In addition, as the population was not recruited for this particular study, the timings and nature of the measures may have impacted the results. For example, measures such as the Mediterranean diet score may have been more appropriate than HEI in this study and more consistent time differences in between questionnaires and the PAL task may have reduced noise.

Additionally, the study was limited by missing data across participants, particularly the lack of data on education and the considerable reduction in power when assessing lifestyle as

opposed to genotype alone. This reduction in number of participants for example, prevented us from assessing a possible interplay between nutrition, exercise and genotype on cognition. Furthermore, in spite of the cohort being free of illness it may be more accurate to correct for medication, especially when thinking about the rising problem of polypharmacy in ageing populations (Guthrie et al., 2015). Also, while CANTAB PAL© provided an easy way to deliver a standardised cognitive task to a large number of participants, the use of technology may have hindered older people more than their younger counterparts. In addition, though the use of PAL was chosen to select for age-related hippocampal cognition, a wider battery of tests may have provided better insights into ageing cognition as a whole. Furtheremore, it would be interesting to validate these findings on pattern separation tasks such as the Mnemonic Similarity Task developed by the Stark and colleagues (Stark et al., 2015). Authors have in fact suggested that while PAL is hippocampal dependent it might not be specifically dependent on neurogenesis (Déry et al., 2013).

In terms of study design, as for any genetic study, the present one lacks power to detect associations with very rare variants. Also, the decision to test several genes and to include 100kb up and downstream of the coding regions allowed us to find novel polymorphisms but also caused a loss of power due to the large number of multiple comparisons. Finally, though it was interesting to assess the effect of each SNP on cognition, it may be necessary to also assess the synergistic function of several SNPs or several genes as the interplay between lifestyle and cognition is likely to be affected by a number of related pathways.

6 General Conclusions

6.1 Summary of key findings and future directions

With this project, we aimed to evaluate the role of the mTOR, insulin and insulin-like signalling and sirtuin pathway in human NSC regulation and cognition. In particular, we evaluated the effect of ageing human serum, tert-Butyl hydroperoxide, hydroxyurea and increased passage number on NSC regulation and on the expression levels of candidate genes to mimic an aged systemic environment, oxidative stress, DNA damage and replicative senescence respectively. We also investigated associations between genetic polymorphisms in candidate genes within these pathways and cognitive performance as well as the effects of lifestyle on this association.

Firstly, we report that serum from human donors elicits alterations in NSC regulation that are associated to *in vivo* phenotypes such as cognitive performance and hippocampal volumes. In addition, we show that while gene expression alterations are not associated to the serum-donor's age, the expression levels of nine candidate genes are strongly correlated to cellular phenotype. We hypothesise that this result is representative of biological ageing and that the lack of association to serum donor's age is due to the discrepancies between chronological and biological age, a known characteristic of human ageing. Focusing on this and adopting an endophenotype approach we show that four of these nine genes (NAMPT, FOXO3A, mTOR and PTEN) show significant expression alterations in response to replicative senescence and that PTEN is also susceptible to treatment with tert-Butyl hydroperoxide and hydroxyurea. Importantly, we report that the molecular alterations following increased passage number are also accompanied by dramatic morphological alterations reminiscent of senescence. Finally, we report significant associations between genetic polymorphisms in two of the nine candidate genes identified by the endophenotype approach (ABTB1 and SIRT1) and cognitive performance in a human cohort. Our results also emphasise the effect of lifestyle in mediating this association.

Throughout this thesis we investigated nutrient-sensing pathways using a multidisciplinary approach. The collective interpretation of these findings not only provides support for a role of these pathways in human ageing but also highlights the advantages and limitations of each approach. In chapter 4, we aimed to establish a more controlled model of ageing that was less susceptible to human heterogeneity in comparison to the *in vitro* parabiosis model used in chapter 3. While passage number showed interesting alterations in both gene expression and morphology, pharmacological treatment showed little effect on both cellular and molecular aspects of the hippocampal progenitor cells. Therefore, our results suggest a more representative and robust ageing model might involve combining the use of serum and that of higher passage cells. However, given the importance of diet and exercise highlighted in chapter 5 and the human heterogeneity reported in chapter 3, such experiments would benefit from the use of serum from a human cohort with lifestyle information.

As discussed in previous sections, future research can build upon these findings in several ways. Firstly, findings from the epidemiological study in the TwinsUK cohort could be mimicked in *in vivo* and *in vitro* models to identify the mechanisms affected by each polymorphism. Next, assessing expression levels of the candidate genes and resulting proteins *in vivo* would provide clearer information on the validity of the *in vitro* models and the discrepancies between the two approaches. In addition, further analysis of the effects of epigenetic alterations, such as methylation, on identified and novel genes will no doubt provide interesting information on the regulatory mechanism of these pathways.

6.2 Considerations on methodological approach

This study employed several noteworthy techniques. Firstly, the use of human serum, human cells and a human cohort enabled the investigation of ageing mechanisms in an entirely “human” context. As discussed throughout this thesis, the differences between humans and model organisms are becoming increasingly evident for several aspects of ageing. These are especially pronounced when evaluating the contribution of uniquely-human aspects such as the inter-individual variability in response to genetic variation, diet and exercise. The work presented here is one of the very few studies investigating nutrient-sensing pathways in NSC ageing in a human context. The use of an immortalised embryonic

cell line was selected over other human-based *in vitro* approaches such as induced pluripotent stem cells (iPSC) and induced neurons (iN). When compared to iPSCs, the HPC model faced similar drawbacks such as the "young" epigenetic and proteomic signatures but enabled a much more cost and time-efficient *in vitro* platform. In addition, a specific genetic composition was not necessary in this exploratory project making iPSCs unnecessary, given their methodological complexity. Though the use of iN would have overcome the rejuvenation drawbacks of iPSCs, the directed differentiation methodology would have hindered the assessment of NSC maintenance and differentiation, which was a key aspect of this research. To our knowledge, these other cellular models have not yet been employed in studies like the present one. Both iPSCs and iN however, would be extremely valuable platforms for future experiments combining findings from different chapters of this thesis. Both methods could be employed to assess the effect of an ageing environment and lifestyle in neurons with specific SNP combinations from individuals with accelerated or delayed cognitive decline.

In addition, by using the systemic environment in chapter 3 and a combination of ageing characteristics in chapter 4, we modelled ageing in a more comprehensive manner than is usually done. Other studies in fact, tend to focus on a specific ageing aspect to determine its contribution to the overall ageing phenotype (Daniele et al., 2016; Le Belle et al., 2011; Walton et al., 2012). While this comes with obvious benefits for understanding the specific mechanisms responsible for each phenotype, it does not recapitulate the multifaceted nature of the ageing process. Authors have in fact described the variety a co-occurrence of processes involved in ageing and suggested approaches focused on understanding their interaction are necessary (López-Otín et al., 2013; Schubert et al., 2018). Though our models do not completely recapitulate all nine commonly accepted hallmarks of ageing they do aim towards this goal. Throughout this thesis in fact, we directly or indirectly assess five of these hallmarks, namely: deregulated nutrient-sensing pathways, mitochondrial dysfunction, cellular senescence and stem cell exhaustion.

Furthermore, this thesis adopts a back-translation approach to usual studies involving epidemiological analysis. Normally, epidemiological studies are used to inform *in vitro* work. Instead, here we used results from our *in vitro* models to select the candidate genes

to be targeted by the epidemiological study. We believe this approach enables for the validation of *in vitro* work and at the same time allows for a more targeted approach to epidemiological research which is less susceptible to the statistical hindrance of multiple comparisons. As discussed throughout this thesis, validation of *in vitro* and *in vivo* work is essential to contest the replicability crisis currently affecting most of biomedical research (Begley and Ioannidis, 2015). As evidenced by our results, some genes that appeared to be essential regulators in both *in vitro* models, did not present with genotypic alterations associated to cognitive phenotypes in the epidemiological portion of this study. While an association between SNP and cognition is by no means the only proof for the involvement of a specific gene in NSC regulation. Such results do suggest further research is needed to elucidate the mechanisms responsible for the gene expression alterations in the *in vitro* models and both their impact and implications for human ageing.

Finally, rapid advances in technology over the last two decades have enabled the collection and distribution of an overwhelming amount of data in a variety of disciplines. Much of this data however is not used to its full potential. Because of this, the analysis of pre-existing data has been suggested as a cost and time efficient way to address important scientific questions (Cheng and Phillips, 2014; Greenhoot and Dowsett, 2012). This increase in data availability however, has not yet been met by a shift in the research mentality where data collection is still regarded as a necessary part of most studies (Anderson et al., 2007). By using a pre-existing cohort, we hope to show how existing data can be shared across biomedical fields and incorporated to complement ongoing research. In line with this, large public cohorts are now being established to facilitate this kind of research (Khoury and Evans, 2015; Trehearne, 2016).

6.3 Impact on biogerontology

We believe the research outlined in this thesis contributes to advancing knowledge in the field of biogerontology. Of note, we confirm several genes identified by animal studies are involved in human ageing. We also provide evidence reinforcing the role for nutrient-sensing-genes in ageing and in particular, highlight key molecules shared among several pathways. In addition, we emphasise the role of novel ageing molecules such as ABTB1 and suggest future research should focus on determining their biological function. Importantly,

we address the inter-individual variability often discussed in the field and show it is due, at least in part, to genetics and lifestyle. We also demonstrate that there are interesting interactions between lifestyle and nutrient-sensing gene genotype thereby providing further support for the development of precision medicine. We believe tailoring interventions to appropriate times and populations will improve the effectiveness of any intervention, be it pharmaceutical or environmental, and that studies such as the one outlined in this thesis will help achieve this goal. Importantly, our study can be used as a basis for future research into both pharmacological and environmental interventions due to the strong focus on both genetics and lifestyle.

6.4 Conclusion

In conclusion, using distinct methodologies, this thesis demonstrates an important role for nutrient-sensing pathways in both NSC regulation and cognitive ageing. In addition, it provides novel *in vitro* models of NSC ageing and delivers interesting candidates for future *in vivo* and *in vitro* studies aimed at developing pharmacological and lifestyle interventions to slow the ageing process and the concomitant development of age-related pathologies. Importantly, our study also emphasises the inter-individual variability of ageing and highlights the need for targeted therapies.

7 References

Åberg, M. A., Aberg, N. D., Hedbacker, H., Oscarsson, J., Eriksson, P. S., Aberg, M. A. I., et al. (2000). Peripheral infusion of IGF-I selectively induces neurogenesis in the adult rat hippocampus. *J. Neurosci.* 20, 2896–2903.

Åberg, M. A., Åberg, N. D., Palmer, T. D., Alborn, A.-M., Carlsson-Skwirut, C., Bang, P., et al. (2003). IGF-I has a direct proliferative effect in adult hippocampal progenitor cells. *Mol. Cell. Neurosci.* 24, 23–40. doi:10.1016/S1044-7431(03)00082-4.

Aguilaniu, H., Gustafsson, L., Rigoulet, M., and Nyström, T. (2003). Asymmetric inheritance of oxidatively damaged proteins during cytokinesis. *Science* 299, 1751–3. doi:10.1126/science.1080418.

Akbaraly, T., Sexton, C., Zsoldos, E., Mahmood, A., Filippini, N., Kerleau, C., et al. (2018). Association of Long-Term Diet Quality with Hippocampal Volume: Longitudinal Cohort Study. *Am. J. Med.* doi:10.1016/j.amjmed.2018.07.001.

Albagli, O., Dhordain, P., Deweindt, C., Lecocq, G., and Leprince, D. (1995). The BTB/POZ domain: a new protein-protein interaction motif common to DNA- and actin-binding proteins. *Cell Growth Differ.* 6, 1193–8.

Altman, J., and Das, G. D. (1965a). Autoradiographic and histological evidence of postnatal hippocampal neurogenesis in rats. *J. Comp. Neurol.* 124, 319–335. doi:10.1002/cne.901240303.

Altman, J., and Das, G. D. (1965b). Post-natal origin of microneurones in the rat brain. *Nature* 207, 953–6.

Anacker, C., Cattaneo, A., Luoni, A., Musaelyan, K., Zunszain, P. A., Milanesi, E., et al. (2013). Glucocorticoid-Related Molecular Signaling Pathways Regulating Hippocampal Neurogenesis. *Neuropsychopharmacology* 38, 872–883. doi:10.1038/npp.2012.253.

Anacker, C., Zunszain, P. A., Cattaneo, A., Carvalho, L. A., Garabedian, M. J., Thuret, S., et al. (2011). Antidepressants increase human hippocampal neurogenesis by activating the glucocorticoid receptor. *Mol. Psychiatry* 16, 738–50. doi:10.1038/mp.2011.26.

Anderson, N. R., Lee, E. S., Brockenbrough, J. S., Minie, M. E., Fuller, S., Brinkley, J., et al.

(2007). Issues in Biomedical Research Data Management and Analysis: Needs and Barriers. *J. Am. Med. Informatics Assoc.* 14, 478–488. doi:10.1197/jamia.M2114.

Angello, J. C., Pendergrass, W. R., Norwood, T. H., and Prothero, J. (1989). Cell enlargement: One possible mechanism underlying cellular senescence. *J. Cell. Physiol.* 140, 288–294. doi:10.1002/jcp.1041400214.

Araki, T., Sasaki, Y., and Milbrandt, J. (2004). Increased nuclear NAD biosynthesis and SIRT1 activation prevent axonal degeneration. *Science* 305, 1010–3. doi:10.1126/science.1098014.

Arruda-Carvalho, M., Sakaguchi, M., Akers, K. G., Josselyn, S. A., and Frankland, P. W. (2011). Posttraining ablation of adult-generated neurons degrades previously acquired memories. *J. Neurosci.* 31, 15113–27. doi:10.1523/JNEUROSCI.3432-11.2011.

Arsenijevic, Y., Weiss, S., Schneider, B., and Aebischer, P. (2001). Insulin-like growth factor-I is necessary for neural stem cell proliferation and demonstrates distinct actions of epidermal growth factor and fibroblast growth factor-2. *J. Neurosci.* 21, 7194–202.

Bae, S. J., Lee, J. S., Kim, J. M., Lee, E. K., Han, Y. K., Kim, H. J., et al. (2010). 5-Hydroxytrytophan Inhibits tert-Butylhydroperoxide (t-BHP)-Induced Oxidative Damage via the Suppression of Reactive Species (RS) and Nuclear Factor-κB (NF-κB) Activation on Human Fibroblast. *J. Agric. Food Chem.* 58, 6387–6394. doi:10.1021/jf904201h.

Bakunina, N., Pariante, C. M., and Zunszain, P. A. (2015). Immune mechanisms linked to depression via oxidative stress and neuroprogression. *Immunology* 144, 365–373. doi:10.1111/imm.12443.

Banerjee, S. (2015). Multimorbidity--older adults need health care that can count past one. *Lancet (London, England)* 385, 587–589. doi:10.1016/S0140-6736(14)61596-8.

Barascu, A., Le Chalony, C., Pennarun, G., Genet, D., Imam, N., Lopez, B., et al. (2012). Oxidative stress induces an ATM-independent senescence pathway through p38 MAPK-mediated lamin B1 accumulation. *EMBO J.* 31, 1080–94. doi:10.1038/emboj.2011.492.

Barnett, A. G., Koper, N., Dobson, A. J., Schmiegelow, F., and Manseau, M. (2010). Using information criteria to select the correct variance-covariance structure for longitudinal data in ecology. *Methods Ecol. Evol.* 1, 15–24. doi:10.1111/j.2041-210X.2009.00009.x.

Barnett, J. H., Blackwell, A. D., Sahakian, B. J., and Robbins, T. W. (2015). "The Paired

Associates Learning (PAL) Test: 30 Years of CANTAB Translational Neuroscience from Laboratory to Bedside in Dementia Research," in (Springer, Cham), 449–474. doi:10.1007/7854_2015_5001.

Bartke, A., Sun, L. Y., and Longo, V. (2013). Somatotropic signaling: trade-offs between growth, reproductive development, and longevity. *Physiol. Rev.* 93, 571–98. doi:10.1152/physrev.00006.2012.

Becker, L., Nguyen, L., Gill, J., Kulkarni, S., Pasricha, P. J., and Habtezion, A. (2018). Age-dependent shift in macrophage polarisation causes inflammation-mediated degeneration of enteric nervous system. *Gut* 67, 827–836. doi:10.1136/gutjnl-2016-312940.

Beerman, I., and Rossi, D. J. (2015). Epigenetic Control of Stem Cell Potential during Homeostasis, Aging, and Disease. *Cell Stem Cell* 16, 613–625. doi:10.1016/j.stem.2015.05.009.

Begley, C. G., and Ioannidis, J. P. A. (2015). Reproducibility in Science. *Circ. Res.* 116, 116–126. doi:10.1161/CIRCRESAHA.114.303819.

Behrens, A., van Deursen, J. M., Rudolph, K. L., and Schumacher, B. (2014). Impact of genomic damage and ageing on stem cell function. *Nat. Cell Biol.* 16, 201–7. doi:10.1038/ncb2928.

Ben Abdallah, N. M.-B., Slomianka, L., Vyssotski, A. L., and Lipp, H.-P. (2010). Early age-related changes in adult hippocampal neurogenesis in C57 mice. *Neurobiol. Aging* 31, 151–161. doi:10.1016/j.neurobiolaging.2008.03.002.

Bento-Torres, N. V. O., Bento-Torres, J., Tomás, A. M., Costa, V. O., Corrêa, P. G. R., Costa, C. N. M., et al. (2017). Influence of schooling and age on cognitive performance in healthy older adults. *Brazilian J. Med. Biol. Res. = Rev. Bras. Pesqui. medicas e Biol.* 50, e5892. doi:10.1590/1414-431X20165892.

Berg, U., and Bang, P. (2004). Exercise and circulating insulin-like growth factor I. *Horm. Res.* 62 Suppl 1, 50–8. doi:10.1159/000080759.

Bergmann, O., Spalding, K. L., and Frisén, J. (2015). Adult Neurogenesis in Humans. *Cold Spring Harb. Perspect. Biol.* 7. doi:10.1101/cshperspect.a018994.

Berron, D., Schütze, H., Maass, A., Cardenas-Blanco, A., Kuijf, H. J., Kumaran, D., et al. (2016). Strong Evidence for Pattern Separation in Human Dentate Gyrus. *J. Neurosci.* 36, 7569–

79. doi:10.1523/JNEUROSCI.0518-16.2016.

Bigarella, C. L., Liang, R., and Ghaffari, S. (2014). Stem cells and the impact of ROS signaling. *Development* 141, 4206–18. doi:10.1242/dev.107086.

Blackwell, A. D., Barnett, J. H., Hayat, S., Luben, R., Moore, S., Dalzell, N., et al. (2010). The effect of age, sex and education on visuospatial paired associates learning ability: Preliminary data from a British population study. *Alzheimer's Dement.* 6, S485. doi:10.1016/j.jalz.2010.05.1617.

Blagosklonny, M. V (2008). Aging, stem cells, and mammalian target of rapamycin: a prospect of pharmacologic rejuvenation of aging stem cells. *Rejuvenation Res.* 11, 801–8. doi:10.1089/rej.2008.0722.

Blagosklonny, M. V (2010). Calorie restriction: Decelerating mTOR-driven aging from cells to organisms (including humans). *Cell Cycle*, 683–688.

Blondell, S. J., Hammersley-Mather, R., and Veerman, J. L. (2014). Does physical activity prevent cognitive decline and dementia?: A systematic review and meta-analysis of longitudinal studies. *BMC Public Health* 14, 510. doi:10.1186/1471-2458-14-510.

Blüher, M., Kahn, B. B., and Kahn, C. R. (2003). Extended longevity in mice lacking the insulin receptor in adipose tissue. *Science* 299, 572–4. doi:10.1126/science.1078223.

Boekhoorn, K., Joels, M., and Lucassen, P. J. (2006). Increased proliferation reflects glial and vascular-associated changes, but not neurogenesis in the presenile Alzheimer hippocampus. *Neurobiol. Dis.* 24, 1–14. doi:10.1016/J.NBD.2006.04.017.

Boily, G., Seifert, E. L., Bevilacqua, L., He, X. H., Sabourin, G., Estey, C., et al. (2008). SirT1 Regulates Energy Metabolism and Response to Caloric Restriction in Mice. *PLoS One* 3, e1759. doi:10.1371/journal.pone.0001759.

Boldrini, M., Fulmore, C. A., Tartt, A. N., Simeon, L. R., Pavlova, I., Poposka, V., et al. (2018). Human Hippocampal Neurogenesis Persists throughout Aging. *Cell Stem Cell* 22, 589–599.e5. doi:10.1016/j.stem.2018.03.015.

Bolijn, S., and Lucassen, P. J. (2015). How the Body Talks to the Brain; Peripheral Mediators of Physical Activity-Induced Proliferation in the Adult Hippocampus. *Brain Plast.* 1, 5–27. doi:10.3233/BPL-150020.

Bonafè, M., Barbieri, M., Marchegiani, F., Olivieri, F., Ragno, E., Giampieri, C., et al. (2003). Polymorphic variants of insulin-like growth factor I (IGF-I) receptor and phosphoinositide 3-kinase genes affect IGF-I plasma levels and human longevity: cues for an evolutionarily conserved mechanism of life span control. *J. Clin. Endocrinol. Metab.* 88, 3299–304. doi:10.1210/jc.2002-021810.

Bondolfi, L., Ermini, F., Long, J. M., Ingram, D. K., and Jucker, M. (2004). Impact of age and caloric restriction on neurogenesis in the dentate gyrus of C57BL/6 mice. *Neurobiol. Aging* 25, 333–40. doi:10.1016/S0197-4580(03)00083-6.

Bonnet, E., Touyarot, K., Alfos, S., Pallet, V., Higueret, P., and Abrous, D. N. (2008). Retinoic Acid Restores Adult Hippocampal Neurogenesis and Reverses Spatial Memory Deficit in Vitamin A Deprived Rats. *PLoS One* 3, e3487. doi:10.1371/journal.pone.0003487.

Bordone, L., Motta, M. C., Picard, F., Robinson, A., Jhala, U. S., Apfeld, J., et al. (2005). Sirt1 Regulates Insulin Secretion by Repressing UCP2 in Pancreatic β Cells. *PLoS Biol.* 4, e31. doi:10.1371/journal.pbio.0040031.

Botden, I. P. G., Carola Zillikens, M., De Rooij, S. R., Langendonk, J. G., Danser, A. H. J., Sijbrands, E. J. G., et al. (2012). Variants in the SIRT1 Gene May Affect Diabetes Risk in Interaction With Prenatal Exposure to Famine. doi:10.2337/dc11-1203.

Bowyer, R. C. E., Jackson, M. A., Pallister, T., Skinner, J., Spector, T. D., Welch, A. A., et al. (2018). Use of dietary indices to control for diet in human gut microbiota studies. *Microbiome* 6, 77. doi:10.1186/s40168-018-0455-y.

Bracko, O., Singer, T., Aigner, S., Knobloch, M., Winner, B., Ray, J., et al. (2012). Gene Expression Profiling of Neural Stem Cells and Their Neuronal Progeny Reveals IGF2 as a Regulator of Adult Hippocampal Neurogenesis. *J. Neurosci.* 32, 3376–3387. doi:10.1523/JNEUROSCI.4248-11.2012.

Brandhorst, S., Choi, I. Y., Wei, M., Cheng, C. W., Sedrakyan, S., Navarrete, G., et al. (2015). A Periodic Diet that Mimics Fasting Promotes Multi-System Regeneration, Enhanced Cognitive Performance, and Healthspan. *Cell Metab.* 22, 86–99. doi:10.1016/j.cmet.2015.05.012.

Briske-Anderson, M. J., Finley, J. W., and Newman, S. M. (1997). The influence of culture time and passage number on the morphological and physiological development of Caco-2 cells. *Proc. Soc. Exp. Biol. Med.* 214, 248–57.

Brown, M. W., and Aggleton, J. P. (2001). Recognition memory: What are the roles of the

perirhinal cortex and hippocampus? *Nat. Rev. Neurosci.* 2, 51–61. doi:10.1038/35049064.

Burger, O., Baudisch, A., and Vaupel, J. W. (2012). Human mortality improvement in evolutionary context. *Proc. Natl. Acad. Sci.* 109, 18210–18214. doi:10.1073/pnas.1215627109.

Burgess, N., Maguire, E. A., and O'Keefe, J. (2002). The Human Hippocampus and Spatial and Episodic Memory. *Neuron* 35, 625–641. doi:10.1016/S0896-6273(02)00830-9.

Busse, A. L., Gil, G., Santarém, J. M., and Jacob Filho, W. (2009). Physical activity and cognition in the elderly: A review. *Dement. Neuropsychol.* 3, 204–208. doi:10.1590/S1980-57642009DN30300005.

Butler, D. (2008). Translational research: Crossing the valley of death. *Nature* 453, 840–842. doi:10.1038/453840a.

Butler, S. M., Ashford, J. W., and Snowdon, D. A. (1996). Age, education, and changes in the Mini-Mental State Exam scores of older women: findings from the Nun Study. *J. Am. Geriatr. Soc.* 44, 675–81.

Cai, N., Bigdeli, T. B., Kretzschmar, W., Li, Y., Liang, J., Song, L., et al. (2015). Sparse whole-genome sequencing identifies two loci for major depressive disorder. *Nature* 523, 588–591. doi:10.1038/nature14659.

Campisi, J., and d'Adda di Fagagna, F. (2007). Cellular senescence: when bad things happen to good cells. *Nat. Rev. Mol. Cell Biol.* 8, 729–40. doi:10.1038/nrm2233.

Cantó, C., and Auwerx, J. (2009). Caloric restriction, SIRT1 and longevity. *Trends Endocrinol. Metab.* 20, 325–31. doi:10.1016/j.tem.2009.03.008.

Carpentier, P. A., and Palmer, T. D. (2009). Immune influence on adult neural stem cell regulation and function. *Neuron* 64, 79–92. doi:10.1016/j.neuron.2009.08.038.

Carson, M. J., Behringer, R. R., Brinster, R. L., and McMorris, F. A. (1993). Insulin-like growth factor I increases brain growth and central nervous system myelination in tTransgenic mice. *Neuron* 10, 729–740. doi:10.1016/0896-6273(93)90173-O.

Castilho, R. M., Squarize, C. H., Chodosh, L. A., Williams, B. O., and Gutkind, J. S. (2009). mTOR mediates Wnt-induced epidermal stem cell exhaustion and aging. *Cell Stem Cell* 5, 279–

89. doi:10.1016/j.stem.2009.06.017.

Cawthon, R. M. (2009). Telomere length measurement by a novel monochrome multiplex quantitative PCR method. *Nucleic Acids Res.* 37, e21. doi:10.1093/nar/gkn1027.

Cès, A., Burg, T., Herbeaux, K., Héraud, C., Bott, J.-B., Mensah-Nyagan, A. G., et al. (2018). Age-related vulnerability of pattern separation in C57BL/6J mice. *Neurobiol. Aging* 62, 120–129. doi:10.1016/j.neurobiolaging.2017.10.013.

Chaker, Z., Aïd, S., Berry, H., and Holzenberger, M. (2015). Suppression of IGF-I signals in neural stem cells enhances neurogenesis and olfactory function during aging. *Aging Cell* 14, 847–56. doi:10.1111/acel.12365.

Chaker, Z., George, C., Petrovska, M., Caron, J.-B., Lacube, P., Caillé, I., et al. (2016). Hypothalamic neurogenesis persists in the aging brain and is controlled by energy-sensing IGF-I pathway. *Neurobiol. Aging* 41, 64–72. doi:10.1016/j.neurobiolaging.2016.02.008.

Chandler, J. M., Marsico, M., Harper-Mozley, L., Vogt, R., Peng, Y., Lesk, V., et al. (2008). P3-111: Cognitive assessment: Discrimination of impairment and detection of decline in Alzheimer's disease and mild cognitive impairment. *Alzheimer's Dement.* 4, T551–T552. doi:10.1016/J.JALZ.2008.05.1676.

Chang-Liu, C. M., and Woloschak, G. E. (1997). Effect of passage number on cellular response to DNA-damaging agents: cell survival and gene expression. *Cancer Lett.* 113, 77–86.

Check, E. (2003). NIH "roadmap" charts course to tackle big research issues. *Nature* 425, 438–438. doi:10.1038/425438b.

Check Hayden, E. (2014). Pet dogs set to test anti-ageing drug. *Nature* 514, 546. doi:10.1038/514546a.

Chekroud, S. R., Gueorguieva, R., Zheutlin, A. B., Paulus, M., Krumholz, H. M., Krystal, J. H., et al. (2018). Association between physical exercise and mental health in 1·2 million individuals in the USA between 2011 and 2015: a cross-sectional study. *The Lancet Psychiatry* 5, 739–746. doi:10.1016/S2215-0366(18)30227-X.

Chen, D., Steele, A. D., Hutter, G., Bruno, J., Govindarajan, A., Easlon, E., et al. (2008). The role of calorie restriction and SIRT1 in prion-mediated neurodegeneration. *Exp. Gerontol.* 43, 1086–93. doi:10.1016/j.exger.2008.08.050.

Chen, D. Y., Stern, S. A., Garcia-Osta, A., Saunier-Rebori, B., Pollonini, G., Bambah-Mukku, D., et al. (2011). A critical role for IGF-II in memory consolidation and enhancement. *Nature* 469, 491–497. doi:10.1038/nature09667.

Chen, J., Du, X., Chen, Q., and Xiang, C. (2015). Effects of donors' age and passage number on the biological characteristics of menstrual blood-derived stem cells. *Int. J. Clin. Exp. Pathol.* 8, 14584.

Chen, Y., and Chen, C. (2011). Corilagin prevents tert-butyl hydroperoxide-induced oxidative stress injury in cultured N9 murine microglia cells. *Neurochem. Int.* 59, 290–296. doi:10.1016/j.neuint.2011.05.020.

Chen, Z., Trotman, L. C., Shaffer, D., Lin, H.-K., Dotan, Z. A., Niki, M., et al. (2005). Crucial role of p53-dependent cellular senescence in suppression of Pten-deficient tumorigenesis. *Nature* 436, 725–730. doi:10.1038/nature03918.

Cheng, H. G., and Phillips, M. R. (2014). Secondary analysis of existing data: opportunities and implementation. *Shanghai Arch. psychiatry* 26, 371–5. doi:10.11919/j.issn.1002-0829.214171.

Chigogora, S., Zaninotto, P., Kivimaki, M., Steptoe, A., and Batty, G. D. (2016). Insulin-like growth factor 1 and risk of depression in older people: the English Longitudinal Study of Ageing. *Transl. Psychiatry* 6, e898. doi:10.1038/tp.2016.167.

Chiu, J., and Dawes, I. W. (2012). Redox control of cell proliferation. *Trends Cell Biol.* 22, 592–601. doi:10.1016/J.TCB.2012.08.002.

Choi, S.-W., and Friso, S. (2010). Epigenetics: A New Bridge between Nutrition and Health. *Adv. Nutr.* 1, 8–16. doi:10.3945/an.110.1004.

Chung, J., Kuo, C. J., Crabtree, G. R., and Blenis, J. (1992). Rapamycin-FKBP specifically blocks growth-dependent activation of and signaling by the 70 kd S6 protein kinases. *Cell* 69, 1227–1236. doi:10.1016/0092-8674(92)90643-Q.

Clayton, R. N. (2003). Cardiovascular function in acromegaly. *Endocr. Rev.* 24, 272–7. doi:10.1210/er.2003-0009.

Clelland, C. D., Choi, M., Romberg, C., Clemenson, G. D., Fragniere, A., Tyers, P., et al. (2009). A functional role for adult hippocampal neurogenesis in spatial pattern separation. *Science* 325, 210–3. doi:10.1126/science.1173215.

Cohen, H. Y., Miller, C., Bitterman, K. J., Wall, N. R., Hekking, B., Kessler, B., et al. (2004). Calorie Restriction Promotes Mammalian Cell Survival by Inducing the SIRT1 Deacetylase. *Science (80-.).* 305, 390–392. doi:10.1126/science.1099196.

Colcombe, S. J., Erickson, K. I., Raz, N., Webb, A. G., Cohen, N. J., McAuley, E., et al. (2003). Aerobic fitness reduces brain tissue loss in aging humans. *J. Gerontol. A. Biol. Sci. Med. Sci.* 58, 176–80.

Conboy, I. M., and Rando, T. A. (2012). Heterochronic parabiosis for the study of the effects of aging on stem cells and their niches. *Cell Cycle* 11, 2260–7. doi:10.4161/cc.20437.

Conrad, M., Schothorst, J., Kankipati, H. N., Van Zeebroeck, G., Rubio-Texeira, M., and Thevelein, J. M. (2014). Nutrient sensing and signaling in the yeast *Saccharomyces cerevisiae*. *FEMS Microbiol. Rev.* 38, 254–299. doi:10.1111/1574-6976.12065.

Cooney, C. A. (1993). Are somatic cells inherently deficient in methylation metabolism? A proposed mechanism for DNA methylation loss, senescence and aging. *Growth. Dev. Aging* 57, 261–73.

Corniola, R. S., Tassabehji, N. M., Hare, J., Sharma, G., and Levenson, C. W. (2008). Zinc deficiency impairs neuronal precursor cell proliferation and induces apoptosis via p53-mediated mechanisms. *Brain Res.* 1237, 52–61. doi:10.1016/j.brainres.2008.08.040.

Costa-Mattioli, M., and Monteggia, L. M. (2013). mTOR complexes in neurodevelopmental and neuropsychiatric disorders. *Nat. Neurosci.* 16, 1537–43. doi:10.1038/nn.3546.

Cuervo, A. M. (2008). Autophagy and aging: keeping that old broom working. *Trends Genet.* 24, 604–12. doi:10.1016/j.tig.2008.10.002.

Curtis, M. A., Penney, E. B., Pearson, A. G., van Roon-Mom, W. M. C., Butterworth, N. J., Dragunow, M., et al. (2003). Increased cell proliferation and neurogenesis in the adult human Huntington's disease brain. *Proc. Natl. Acad. Sci. U. S. A.* 100, 9023–7. doi:10.1073/pnas.1532244100.

Daniele, S., Da Pozzo, E., Iofrida, C., and Martini, C. (2016). Human neural stem cell ageing is counteracted by α-glyceryl-phosphoryl-ethanolamine. *ACS Chem. Neurosci.* doi:10.1021/acschemneuro.6b00078.

Datan, E., Shirazian, A., Benjamin, S., Matassov, D., Tinari, A., Malorni, W., et al. (2014). mTOR/p70S6K signaling distinguishes routine, maintenance-level autophagy from autophagic cell death during influenza A infection. *Virology* 452–453, 175–190.

doi:10.1016/j.virol.2014.01.008.

Daugherty, A. M., Bender, A. R., Raz, N., and Ofen, N. (2016). Age differences in hippocampal subfield volumes from childhood to late adulthood. *Hippocampus* 26, 220–8. doi:10.1002/hipo.22517.

Day, K., Shefer, G., Shearer, A., and Yablonka-Reuveni, Z. (2010). The depletion of skeletal muscle satellite cells with age is concomitant with reduced capacity of single progenitors to produce reserve progeny. *Dev. Biol.* 340, 330–43. doi:10.1016/j.ydbio.2010.01.006.

de Lucia, C., Murphy, T., and Thuret, S. (2017). Emerging Molecular Pathways Governing Dietary Regulation of Neural Stem Cells during Aging. *Front. Physiol.* 8, 17. doi:10.3389/fphys.2017.00017.

De Lucia, C., Rinchon, A., Olmos-Alonso, A., Riecken, K., Fehse, B., Boche, D., et al. (2016). Microglia regulate hippocampal neurogenesis during chronic neurodegeneration. *Brain. Behav. Immun.* 55, 179–190. doi:10.1016/j.bbi.2015.11.001.

de Magalhães, J. P., and Passos, J. F. (2018). Stress, cell senescence and organismal ageing. *Mech. Ageing Dev.* 170, 2–9. doi:10.1016/J.MAD.2017.07.001.

de Rover, M., Pironti, V. A., McCabe, J. A., Acosta-Cabronero, J., Arana, F. S., Morein-Zamir, S., et al. (2011). Hippocampal dysfunction in patients with mild cognitive impairment: A functional neuroimaging study of a visuospatial paired associates learning task. *Neuropsychologia* 49, 2060–2070. doi:10.1016/J.NEUROPSYCHOLOGIA.2011.03.037.

Delotterie, D. (2014). Translational potential of the touchscreen-based methodology to assess cognitive abilities in mice.

Deng, B. (2017). Mouse models and induced pluripotent stem cells in researching psychiatric disorders. *Stem cell Investig.* 4, 62. doi:10.21037/sci.2017.06.10.

Deng, W., Aimone, J. B., and Gage, F. H. (2010). New neurons and new memories: how does adult hippocampal neurogenesis affect learning and memory? *Nat. Rev. Neurosci.* 11, 339–350. doi:10.1038/nrn2822.

Dennis, C. V., Suh, L. S., Rodriguez, M. L., Kril, J. J., and Sutherland, G. T. (2016a). Human adult neurogenesis across the ages: An immunohistochemical study. *Neuropathol. Appl. Neurobiol.* 42, 621–638. doi:10.1111/nan.12337.

Dennis, C. V., Suh, L. S., Rodriguez, M. L., Kril, J. J., and Sutherland, G. T. (2016b). Human adult neurogenesis across the ages: An immunohistochemical study. *Neuropathol. Appl. Neurobiol.* 42, 621–638. doi:10.1111/nan.12337.

Déry, N., Pilgrim, M., Gibala, M., Gillen, J., Wojtowicz, J. M., MacQueen, G., et al. (2013). Adult hippocampal neurogenesis reduces memory interference in humans: opposing effects of aerobic exercise and depression. *Front. Neurosci.* 7, 66. doi:10.3389/fnins.2013.00066.

Di Micco, R., Cicalese, A., Fumagalli, M., Dobreva, M., Verrecchia, A., Pelicci, P. G., et al. (2008). DNA damage response activation in mouse embryonic fibroblasts undergoing replicative senescence and following spontaneous immortalization. *Cell Cycle* 7, 3601–3606. doi:10.4161/cc.7.22.7152.

Dickinson, B. C., Peltier, J., Stone, D., Schaffer, D. V, and Chang, C. J. (2011). Nox2 redox signaling maintains essential cell populations in the brain. *Nat. Chem. Biol.* 7, 106–112. doi:10.1038/nchembio.497.

Doetsch, F., and Hen, R. (2005). Young and excitable: the function of new neurons in the adult mammalian brain. *Curr. Opin. Neurobiol.* 15, 121–8. doi:10.1016/j.conb.2005.01.018.

Dong, C.-M., Wang, X.-L., Wang, G.-M., Zhang, W.-J., Zhu, L., Gao, S., et al. (2014). A stress-induced cellular aging model with postnatal neural stem cells. *Cell Death Dis.* 5, e1116. doi:10.1038/cddis.2014.82.

Dong, W., Cheng, S., Huang, F., Fan, W., Chen, Y., Shi, H., et al. (2011). Mitochondrial dysfunction in long-term neuronal cultures mimics changes with aging. *Med. Sci. Monit.* 17, BR91-6.

Donmez, G., and Outeiro, T. F. SIRT1 and SIRT2: emerging targets in neurodegeneration. doi:10.1002/emmm.201302451.

Driscoll, I., Howard, S. R., Stone, J. C., Monfils, M. H., Tomanek, B., Brooks, W. M., et al. (2006). The aging hippocampus: A multi-level analysis in the rat. *Neuroscience* 139, 1173–1185. doi:10.1016/j.neuroscience.2006.01.040.

Dröge, W., and Schipper, H. M. (2007). Oxidative stress and aberrant signaling in aging and cognitive decline. *Aging Cell* 6, 361–370. doi:10.1111/j.1474-9726.2007.00294.x.

Durbin, R. M., Altshuler, D. L., Durbin, R. M., Abecasis, G. R., Bentley, D. R., Chakravarti, A.,

et al. (2010). A map of human genome variation from population-scale sequencing. *Nature* 467, 1061–1073. doi:10.1038/nature09534.

Dutta, S., and Sengupta, P. (2016). Men and mice: Relating their ages. *Life Sci.* 152, 244–248. doi:10.1016/j.lfs.2015.10.025.

Dykiert, D., Der, G., Starr, J. M., and Deary, I. J. (2016). Why is Mini-Mental state examination performance correlated with estimated premorbid cognitive ability? *Psychol. Med.* 46, 2647–54. doi:10.1017/S0033291716001045.

Elorza, A., Hyde, B., Mikkola, H. K., Collins, S., and Shirihai, O. S. (2008). UCP2 modulates cell proliferation through the MAPK/ERK pathway during erythropoiesis and has no effect on heme biosynthesis. *J. Biol. Chem.* 283, 30461–70. doi:10.1074/jbc.M805400200.

Enwere, E., Shingo, T., Gregg, C., Fujikawa, H., Ohta, S., and Weiss, S. (2004). Aging results in reduced epidermal growth factor receptor signaling, diminished olfactory neurogenesis, and deficits in fine olfactory discrimination. *J. Neurosci.* 24, 8354–65. doi:10.1523/JNEUROSCI.2751-04.2004.

Epp, J. R., Silva Mera, R., Köhler, S., Josselyn, S. A., and Frankland, P. W. (2016). Neurogenesis-mediated forgetting minimizes proactive interference. *Nat. Commun.* 7, 10838. doi:10.1038/ncomms10838.

Eriksson, P. S., Perfilieva, E., Björk-Eriksson, T., Alborn, A. M., Nordborg, C., Peterson, D. A., et al. (1998). Neurogenesis in the adult human hippocampus. *Nat. Med.* 4, 1313–7. doi:10.1038/3305.

Ernst, A., Alkass, K., Bernard, S., Salehpour, M., Perl, S., Tisdale, J., et al. (2014). Neurogenesis in the striatum of the adult human brain. *Cell* 156, 1072–83. doi:10.1016/j.cell.2014.01.044.

Estruch, R., Ros, E., Salas-Salvadó, J., Covas, M.-I., Corella, D., Arós, F., et al. (2018). Primary Prevention of Cardiovascular Disease with a Mediterranean Diet Supplemented with Extra-Virgin Olive Oil or Nuts. *N. Engl. J. Med.* 378, e34. doi:10.1056/NEJMoa1800389.

European Prospective Investigation of Cancer EPIC-Norfolk nutritional methods: food frequency questionnaire. Available at: http://www.srl.cam.ac.uk/epic/nutmethod/FFQ.shtml [Accessed October 12, 2018].

Fan, G., Martinowich, K., Chin, M. H., He, F., Fouse, S. D., Hutnick, L., et al. (2005). DNA methylation controls the timing of astrogliogenesis through regulation of JAK-STAT

signaling. *Development* 132, 3345–56. doi:10.1242/dev.01912.

Féart, C., Samieri, C., and Barberger-Gateau, P. (2010). Mediterranean diet and cognitive function in older adults. *Curr. Opin. Clin. Nutr. Metab. Care* 13, 14–8. doi:10.1097/MCO.0b013e3283331fe4.

Fernández-Fernández, L., Comes, G., Bolea, I., Valente, T., Ruiz, J., Murtra, P., et al. (2012). LMN diet, rich in polyphenols and polyunsaturated fatty acids, improves mouse cognitive decline associated with aging and Alzheimer's disease. *Behav. Brain Res.* 228, 261–271. doi:10.1016/j.bbr.2011.11.014.

Ferrón, S. R., Marqués-Torrejón, M. A., Mira, H., Flores, I., Taylor, K., Blasco, M. A., et al. (2009). Telomere shortening in neural stem cells disrupts neuronal differentiation and neuritogenesis. *J. Neurosci.* 29, 14394–407. doi:10.1523/JNEUROSCI.3836-09.2009.

Flachsbart, F., Caliebe, A., Kleindorp, R., Blanché, H., von Eller-Eberstein, H., Nikolaus, S., et al. (2009). Association of FOXO3A variation with human longevity confirmed in German centenarians. *Proc. Natl. Acad. Sci.* 106, 2700–2705. doi:10.1073/pnas.0809594106.

Flachsbart, F., Croucher, P. J., Nikolaus, S., Hampe, J., Cordes, C., Schreiber, S., et al. (2005). Sirtuin 1 (SIRT1) sequence variation is not associated with exceptional human longevity. doi:10.1016/j.exger.2005.09.008.

Fluteau, A., Ince, P. G., Minett, T., Matthews, F. E., Brayne, C., Garwood, C. J., et al. (2015). The nuclear retention of transcription factor FOXO3a correlates with a DNA damage response and increased glutamine synthetase expression by astrocytes suggesting a neuroprotective role in the ageing brain. *Neurosci. Lett.* 609, 11–17. doi:10.1016/J.NEULET.2015.10.001.

Fok, W. C., Chen, Y., Bokov, A., Zhang, Y., Salmon, A. B., Diaz, V., et al. (2014). Mice fed rapamycin have an increase in lifespan associated with major changes in the liver transcriptome. *PLoS One* 9, e83988. doi:10.1371/journal.pone.0083988.

Fontana, L., and Partridge, L. (2015). Promoting Health and Longevity through Diet: From Model Organisms to Humans. *Cell* 161, 106–118. doi:10.1016/j.cell.2015.02.020.

Fontana, L., Partridge, L., and Longo, V. D. (2010). Extending healthy life span--from yeast to humans. *Science* 328, 321–6. doi:10.1126/science.1172539.

Franco, R., and Cedazo-Minguez, A. (2014). Successful therapies for Alzheimer's disease: why so many in animal models and none in humans? *Front. Pharmacol.* 5, 146.

doi:10.3389/fphar.2014.00146.

Franklin, N. C., and Tate, C. A. (2008). Lifestyle and Successful Aging: An Overview. *Am. J. Lifestyle Med.* 3, 6–11. doi:10.1177/1559827608326125.

Friedman, D. (2013). The cognitive aging of episodic memory: a view based on the event-related brain potential. *Front. Behav. Neurosci.* 7, 111. doi:10.3389/fnbeh.2013.00111.

Galán, L., Gómez-Pinedo, U., Guerrero, A., García-Verdugo, J. M., and Matías-Guiu, J. (2017). Amyotrophic lateral sclerosis modifies progenitor neural proliferation in adult classic neurogenic brain niches. *BMC Neurol.* 17, 173. doi:10.1186/s12883-017-0956-5.

Galasko, D., and Golde, T. E. (2013). Biomarkers for Alzheimer's disease in plasma, serum and blood - conceptual and practical problems. *Alzheimers. Res. Ther.* 5, 10. doi:10.1186/alzrt164.

Gao, A., Xia, F., Guskjolen, A. J., Ramsaran, A. I., Santoro, A., Josselyn, S. A., et al. (2018). Elevation of Hippocampal Neurogenesis Induces a Temporally Graded Pattern of Forgetting of Contextual Fear Memories. *J. Neurosci.* 38, 3190–3198. doi:10.1523/JNEUROSCI.3126-17.2018.

Garner, J. P. (2014). The significance of meaning: why do over 90% of behavioral neuroscience results fail to translate to humans, and what can we do to fix it? *ILAR J.* 55, 438–56. doi:10.1093/ilar/ilu047.

Geda, Y. E., Ragossnig, M., Roberts, L. A., Roberts, R. O., Pankratz, V. S., Christianson, T. J. H., et al. (2013). Caloric intake, aging, and mild cognitive impairment: a population-based study. *J. Alzheimers. Dis.* 34, 501–7. doi:10.3233/JAD-121270.

Geekiyanage, H., Jicha, G. A., Nelson, P. T., and Chan, C. (2012). Blood serum miRNA: non-invasive biomarkers for Alzheimer's disease. *Exp. Neurol.* 235, 491–6. doi:10.1016/j.expneurol.2011.11.026.

Gems, D., and de la Guardia, Y. (2013). Alternative Perspectives on Aging in Caenorhabditis elegans: Reactive Oxygen Species or Hyperfunction? *Antioxid. Redox Signal.* 19, 321–9. doi:10.1089/ars.2012.4840.

Gems, D., and Partridge, L. (2013). Genetics of Longevity in Model Organisms: Debates and Paradigm Shifts. *Annu. Rev. Physiol.* 75, 621–644. doi:10.1146/annurev-physiol-030212-183712.

Geyer, R., Wee, S., Anderson, S., Yates, J., and Wolf, D. A. (2003). BTB/POZ Domain Proteins Are Putative Substrate Adaptors for Cullin 3 Ubiquitin Ligases. However.

Ghisletta, P., Rabbitt, P., Lunn, M., and Lindenberger, U. (2012). Two thirds of the age-based changes in fluid and crystallized intelligence, perceptual speed, and memory in adulthood are shared. *Intelligence* 40, 260–268. doi:10.1016/J.INTELL.2012.02.008.

Ghisletta, P., and Spini, D. (2004). An Introduction to Generalized Estimating Equations and an Application to Assess Selectivity Effects in a Longitudinal Study on Very Old Individuals. Winter.

Gingras, A. C., Raught, B., Gygi, S. P., Niedzwiecka, A., Miron, M., Burley, S. K., et al. (2001). Hierarchical phosphorylation of the translation inhibitor 4E-BP1. *Genes Dev.* 15, 2852–64. doi:10.1101/gad.912401.

Ginsburg, G. S., and Phillips, K. A. (2018). Precision Medicine: From Science To Value. *Health Aff. (Millwood).* 37, 694–701. doi:10.1377/hlthaff.2017.1624.

Gomez-Nicola, D., Suzzi, S., Vargas-Caballero, M., Fransen, N. L., Al-Malki, H., Cebrian-Silla, A., et al. (2014). Temporal dynamics of hippocampal neurogenesis in chronic neurodegeneration. *Brain* 137, 2312–28. doi:10.1093/brain/awu155.

Gosho, M., Hamada, C., and Yoshimura, I. (2011). Criterion for the Selection of a Working Correlation Structure in the Generalized Estimating Equation Approach for Longitudinal Balanced Data. *Commun. Stat. - Theory Methods* 40, 3839–3856. doi:10.1080/03610926.2010.501938.

Gould, E., Reeves, A. J., Fallah, M., Tanapat, P., Gross, C. G., and Fuchs, E. (1999). Hippocampal neurogenesis in adult Old World primates. *Proc. Natl. Acad. Sci. U. S. A.* 96, 5263–7. doi:10.1073/PNAS.96.9.5263.

Gräff, J., Kahn, M., Samiei, A., Gao, J., Ota, K. T., Rei, D., et al. (2013). A dietary regimen of caloric restriction or pharmacological activation of SIRT1 to delay the onset of neurodegeneration. *J. Neurosci.* 33, 8951–60. doi:10.1523/JNEUROSCI.5657-12.2013.

Green, B., and Saenz, D. (1995). Tests of a Mediational Model of Restrained Eating: The Role of Dieting Self-Efficacy and Social Comparisons. *J. Soc. Clin. Psychol.* 14, 1–22.

Greenhoot, A. F., and Dowsett, C. J. (2012). Secondary Data Analysis: An Important Tool for Addressing Developmental Questions. *J. Cogn. Dev.* 13, 2–18. doi:10.1080/15248372.2012.646613.

Grolemund, G., and Wickham, H. (2011). Dates and Times Made Easy with lubridate. *J. Stat. Softw.* 40, 1–25. doi:10.18637/jss.v040.i03.

Guarente, L. (2007). Sirtuins in aging and disease. *Cold Spring Harb. Symp. Quant. Biol.* 72, 483–8. doi:10.1101/sqb.2007.72.024.

Guarente, L. (2014). Linking DNA damage, NAD(+)/SIRT1, and aging. *Cell Metab.* 20, 706–7. doi:10.1016/j.cmet.2014.10.015.

Guenther, P. M., Casavale, K. O., Reedy, J., Kirkpatrick, S. I., Hiza, H. A. B., Kuczynski, K. J., et al. (2013). Update of the Healthy Eating Index: HEI-2010. *J. Acad. Nutr. Diet.* 113, 569–580. doi:10.1016/J.JAND.2012.12.016.

Guthrie, B., Makubate, B., Hernandez-Santiago, V., and Dreischulte, T. (2015). The rising tide of polypharmacy and drug-drug interactions: population database analysis 1995–2010. *BMC Med.* 13, 74. doi:10.1186/s12916-015-0322-7.

Hagströmer, M., Oja, P., and Sjöström, M. (2006). The International Physical Activity Questionnaire (IPAQ): a study of concurrent and construct validity. *Public Health Nutr.* 9, 755–62.

Halagappa, V. K. M., Guo, Z., Pearson, M., Matsuoka, Y., Cutler, R. G., LaFerla, F. M., et al. (2007). Intermittent fasting and caloric restriction ameliorate age-related behavioral deficits in the triple-transgenic mouse model of Alzheimer's disease. *Neurobiol. Dis.* 26, 212–220. doi:10.1016/J.NBD.2006.12.019.

Halekoh, U., Højsgaard, S., and Yan, J. (2006). The R Package geepack for Generalized Estimating Equations. *J. Stat. Softw.* 15, 1–11. doi:10.18637/jss.v015.i02.

Hall, B. M., Balan, V., Gleiberman, A. S., Strom, E., Krasnov, P., Virtuoso, L. P., et al. (2016). Aging of mice is associated with p16(Ink4a)- and β-galactosidase-positive macrophage accumulation that can be induced in young mice by senescent cells. *Aging (Albany. NY).* 8, 1294–1315. doi:10.18632/aging.100991.

Halliwell, B. (2003). Oxidative stress in cell culture: an under-appreciated problem? *FEBS Lett.* 540, 3–6.

Halliwell, B. (2006). Reactive species and antioxidants. Redox biology is a fundamental theme of aerobic life. *Plant Physiol.* 141, 312–22. doi:10.1104/pp.106.077073.

Hampel, H., O'Bryant, S. E., Castrillo, J. I., Ritchie, C., Rojkova, K., Broich, K., et al. (2016). PRECISION MEDICINE - The Golden Gate for Detection, Treatment and Prevention of Alzheimer's Disease. *J. Prev. Alzheimer's Dis.* 3, 243–259. doi:10.14283/jpad.2016.112.

Han, J., Wang, B., Xiao, Z., Gao, Y., Zhao, Y., Zhang, J., et al. (2008). Mammalian target of rapamycin (mTOR) is involved in the neuronal differentiation of neural progenitors induced by insulin. *Mol. Cell. Neurosci.* 39, 118–24. doi:10.1016/j.mcn.2008.06.003.

Hannum, G., Guinney, J., Zhao, L., Zhang, L., Hughes, G., Sadda, S., et al. (2013). Genome-wide Methylation Profiles Reveal Quantitative Views of Human Aging Rates. *Mol. Cell* 49, 359–367. doi:10.1016/J.MOLCEL.2012.10.016.

Harman, D. (1956). Aging: a theory based on free radical and radiation chemistry. *J. Gerontol.* 11, 298–300.

Harrison, D. E., Strong, R., Sharp, Z. D., Nelson, J. F., Astle, C. M., Flurkey, K., et al. (2009). Rapamycin fed late in life extends lifespan in genetically heterogeneous mice. *Nature* 460, 392–5. doi:10.1038/nature08221.

Hartopp, N., Wright, P., J Ray, N., Evans, T. E., Metzler-Baddeley, C., Aggleton, J. P., et al. (2018). A key role for subiculum-fornix connectivity in recollection in older age. *In prep.*

Harvey, B. S., Ohlsson, K. S., Mååg, J. L. V., Musgrave, I. F., and Smid, S. D. (2012). Contrasting protective effects of cannabinoids against oxidative stress and amyloid-β evoked neurotoxicity in vitro. *Neurotoxicology* 33, 138–146. doi:10.1016/J.NEURO.2011.12.015.

Hasselmo, M. E. (2005). The Role of Hippocampal Regions CA3 and CA1 in Matching Entorhinal Input With Retrieval of Associations Between Objects and Context: Theoretical Comment on Lee et al. (2005). *Behav. Neurosci.* 119, 342–345. doi:10.1037/0735-7044.119.1.342.

Hayes, S. M., Ryan, L., Schnyer, D. M., and Nadel, L. (2004). An fMRI study of episodic memory: retrieval of object, spatial, and temporal information. *Behav. Neurosci.* 118, 885–96. doi:10.1037/0735-7044.118.5.885.

Hedden, T., and Gabrieli, J. D. E. (2004). Insights into the ageing mind: a view from cognitive neuroscience. *Nat. Rev. Neurosci.* 5, 87–96. doi:10.1038/nrn1323.

Heesch, K. C., van Uffelen, J. G., Hill, R. L., and Brown, W. J. (2010). What do IPAQ questions mean to older adults? Lessons from cognitive interviews. *Int. J. Behav. Nutr. Phys. Act.*

7, 35. doi:10.1186/1479-5868-7-35.

Heine, V. M., Maslam, S., Joëls, M., and Lucassen, P. J. (2004). Prominent decline of newborn cell proliferation, differentiation, and apoptosis in the aging dentate gyrus, in absence of an age-related hypothalamus–pituitary–adrenal axis activation. *Neurobiol. Aging* 25, 361–375. doi:10.1016/S0197-4580(03)00090-3.

Hernandez-Segura, A., Nehme, J., and Demaria, M. (2018). Hallmarks of Cellular Senescence. *Trends Cell Biol.* 28, 436–453. doi:10.1016/j.tcb.2018.02.001.

Herskind, A. M., McGue, M., Holm, N. V, Sørensen, T. I., Harvald, B., and Vaupel, J. W. (1996). The heritability of human longevity: a population-based study of 2872 Danish twin pairs born 1870-1900. *Hum. Genet.* 97, 319–23.

Hill, A. S., Sahay, A., and Hen, R. (2015). Increasing Adult Hippocampal Neurogenesis is Sufficient to Reduce Anxiety and Depression-Like Behaviors. *Neuropsychopharmacology*. doi:10.1038/npp.2015.85.

Hill, M. J., Donocik, J. G., Nuamah, R. A., Mein, C. A., Sainz-Fuertes, R., and Bray, N. J. (2014). Transcriptional consequences of schizophrenia candidate miR-137 manipulation in human neural progenitor cells. *Schizophr. Res.* 153, 225–230. doi:10.1016/j.schres.2014.01.034.

Hinds, D. A., Kloek, A. P., Jen, M., Chen, X., and Frazer, K. A. (2006). Common deletions and SNPs are in linkage disequilibrium in the human genome. *Nat. Genet.* 38, 82–85. doi:10.1038/ng1695.

Hochmuth, C. E., Biteau, B., Bohmann, D., and Jasper, H. (2011). Redox Regulation by Keap1 and Nrf2 Controls Intestinal Stem Cell Proliferation in Drosophila. *Cell Stem Cell* 8, 188–199. doi:10.1016/j.stem.2010.12.006.

Hogan, C. L., Mata, J., and Carstensen, L. L. (2013). Exercise Holds Immediate Benefits for Affect and Cognition in Younger and Older Adults. *Psychol. Aging* 28, 587. doi:10.1037/A0032634.

Hornsby, A. K. E., Redhead, Y. T., Rees, D. J., Ratcliff, M. S. G., Reichenbach, A., Wells, T., et al. (2016). Short-term calorie restriction enhances adult hippocampal neurogenesis and remote fear memory in a Ghsr-dependent manner. *Psychoneuroendocrinology* 63, 198–207. doi:10.1016/j.psyneuen.2015.09.023.

Horvath, S. (2013). DNA methylation age of human tissues and cell types. *Genome Biol.* 14,

R115. doi:10.1186/gb-2013-14-10-r115.

Horvath, S., and Raj, K. (2018). DNA methylation-based biomarkers and the epigenetic clock theory of ageing. *Nat. Rev. Genet.* 19, 371–384. doi:10.1038/s41576-018-0004-3.

Howitz, K. T., Bitterman, K. J., Cohen, H. Y., Lamming, D. W., Lavu, S., Wood, J. G., et al. (2003). Small molecule activators of sirtuins extend Saccharomyces cerevisiae lifespan. *Nature* 425, 191–6. doi:10.1038/nature01960.

Hunsaker, M. R., and Kesner, R. P. (2008). Evaluating the differential roles of the dorsal dentate gyrus, dorsal CA3, and dorsal CA1 during a temporal ordering for spatial locations task. *Hippocampus* 18, 955–964. doi:10.1002/hipo.20455.

Huttner, H. B., Bergmann, O., Salehpour, M., Rácz, A., Tatarishvili, J., Lindgren, E., et al. (2014). The age and genomic integrity of neurons after cortical stroke in humans. *Nat. Neurosci.* 17, 801–803. doi:10.1038/nn.3706.

Hye, A., Riddoch-Contreras, J., Baird, A. L., Ashton, N. J., Bazenet, C., Leung, R., et al. (2014). Plasma proteins predict conversion to dementia from prodromal disease. *Alzheimer's Dement.* doi:10.1016/j.jalz.2014.05.1749.

Iglesias, J. E., Augustinack, J. C., Nguyen, K., Player, C. M., Player, A., Wright, M., et al. (2015). A computational atlas of the hippocampal formation using ex vivo, ultra-high resolution MRI: Application to adaptive segmentation of in vivo MRI. *Neuroimage* 115, 117–137.

Iglesias, J. E., Van Leemput, K., Augustinack, J., Insausti, R., Fischl, B., and Reuter, M. (2016). Bayesian longitudinal segmentation of hippocampal substructures in brain MRI using subject-specific atlases. *Neuroimage* 141, 542–555. doi:10.1016/J.NEUROIMAGE.2016.07.020.

Imayoshi, I., Sakamoto, M., Ohtsuka, T., Takao, K., Miyakawa, T., Yamaguchi, M., et al. (2008). Roles of continuous neurogenesis in the structural and functional integrity of the adult forebrain. *Nat. Neurosci.* 11, 1153–1161. doi:10.1038/nn.2185.

Ingram, D. K., Weindruch, R., Spangler, E. L., Freeman, J. R., and Walford, R. L. (1987). Dietary Restriction Benefits Learning and Motor Performance of Aged Mice. *J. Gerontol.* 42, 78–81. doi:10.1093/geronj/42.1.78.

Ito, K., Ahadieh, S., Corrigan, B., French, J., Fullerton, T., Tensfeldt, T., et al. (2010). Disease progression meta-analysis model in Alzheimer's disease. *Alzheimer's Dement.* 6, 39–53. doi:10.1016/j.jalz.2009.05.665.

Itoh, T., Imano, M., Nishida, S., Tsubaki, M., Mizuguchi, N., Hashimoto, S., et al. (2012). Epigallocatechin-3-gallate increases the number of neural stem cells around the damaged area after rat traumatic brain injury. *J. Neural Transm.* 119, 877–90. doi:10.1007/s00702-011-0764-9.

Janzen, V., Forkert, R., Fleming, H. E., Saito, Y., Waring, M. T., Dombkowski, D. M., et al. (2006). Stem-cell ageing modified by the cyclin-dependent kinase inhibitor p16INK4a. *Nature* 443, 421–426. doi:10.1038/nature05159.

Jiménez-Moreno, N., Stathakos, P., Caldwell, M. A., and Lane, J. D. (2017). Induced Pluripotent Stem Cell Neuronal Models for the Study of Autophagy Pathways in Human Neurodegenerative Disease. *Cells* 6. doi:10.3390/cells6030024.

Johansson, S., Price, J., and Modo, M. (2008). Effect of Inflammatory Cytokines on Major Histocompatibility Complex Expression and Differentiation of Human Neural Stem/Progenitor Cells. *Stem Cells* 26, 2444–2454. doi:10.1634/stemcells.2008-0116.

Johnson, S. C., Rabinovitch, P. S., and Kaeberlein, M. (2013). mTOR is a key modulator of ageing and age-related disease. *Nature* 493, 338–45. doi:10.1038/nature11861.

Joshi, P. K., Pirastu, N., Kentistou, K. A., Fischer, K., Hofer, E., Schraut, K. E., et al. (2017). Genome-wide meta-analysis associates HLA-DQA1/DRB1 and LPA and lifestyle factors with human longevity. *Nat. Commun.* 8, 910. doi:10.1038/s41467-017-00934-5.

Jurk, D., Wang, C., Miwa, S., Maddick, M., Korolchuk, V., Tsolou, A., et al. (2012). Postmitotic neurons develop a p21-dependent senescence-like phenotype driven by a DNA damage response. *Aging Cell* 11, 996–1004. doi:10.1111/j.1474-9726.2012.00870.x.

Kalichman, L., Rodrigues, B., Gurvich, D., Israelov, Z., and Spivak, E. (2007). Impact of patient's weight on stroke rehabilitation results. *Am. J. Phys. Med. Rehabil.* 86, 650–5. doi:10.1097/PHM.0b013e318115f41b.

Kapahi, P., Chen, D., Rogers, A. N., Katewa, S. D., Li, P. W.-L., Thomas, E. L., et al. (2010). With TOR, Less Is More: A Key Role for the Conserved Nutrient-Sensing TOR Pathway in Aging. *Cell Metab.* 11, 453–465. doi:10.1016/J.CMET.2010.05.001.

Kaplanis, J., Gordon, A., Shor, T., Weissbrod, O., Geiger, D., Wahl, M., et al. (2018). Quantitative analysis of population-scale family trees with millions of relatives. *Science (80-.).* 360, 171–175. doi:10.1126/science.aam9309.

Katsimpardi, L., Litterman, N. K., Schein, P. A., Miller, C. M., Loffredo, F. S., Wojtkiewicz, G.

R., et al. (2014). Vascular and neurogenic rejuvenation of the aging mouse brain by young systemic factors. *Science* 344, 630–4. doi:10.1126/science.1251141.

Kawakita, E., Hashimoto, M., and Shido, O. (2006). Docosahexaenoic acid promotes neurogenesis in vitro and in vivo. *Neuroscience* 139, 991–997. doi:10.1016/j.neuroscience.2006.01.021.

Keenan, K. P., Smith, P. F., Hertzog, P., Soper, K., Ballam, G. C., and Clark, R. L. (1994). The effects of overfeeding and dietary restriction on Sprague-Dawley rat survival and early pathology biomarkers of aging. *Toxicol. Pathol.* 22, 300–15.

Kempermann, G., Gage, F. H., Aigner, L., Song, H., Curtis, M. A., Thuret, S., et al. (2018). Human Adult Neurogenesis: Evidence and Remaining Questions. *Cell Stem Cell* 0. doi:10.1016/j.stem.2018.04.004.

Kempermann, G., Jessberger, S., Steiner, B., and Kronenberg, G. (2004a). Milestones of neuronal development in the adult hippocampus. *Trends Neurosci.* 27, 447–452. doi:10.1016/J.TINS.2004.05.013.

Kempermann, G., Wiskott, L., and Gage, F. H. (2004b). Functional significance of adult neurogenesis. *Curr. Opin. Neurobiol.* 14, 186–191. doi:10.1016/J.CONB.2004.03.001.

Kemps, E., and Tiggemann, M. (2005). Working memory performance and preoccupying thoughts in female dieters: Evidence for a selective central executive impairment. *Br. J. Clin. Psychol.* 44, 357–366. doi:10.1348/014466505X35272.

Kennedy, G., Hardman, R. J., Macpherson, H., Scholey, A. B., and Pipingas, A. (2016). How Does Exercise Reduce the Rate of Age-Associated Cognitive Decline? A Review of Potential Mechanisms. *J. Alzheimer's Dis.* 55, 1–18. doi:10.3233/JAD-160665.

Khoury, M. J., and Evans, J. P. (2015). A Public Health Perspective on a National Precision Medicine Cohort. *JAMA* 313, 2117. doi:10.1001/jama.2015.3382.

Kiely, K. M., Luszcz, M. A., Piguet, O., Christensen, H., Bennett, H., and Anstey, K. J. (2011). Functional equivalence of the National Adult Reading Test (NART) and Schonell reading tests and NART norms in the Dynamic Analyses to Optimise Ageing (DYNOPTA) project. *J. Clin. Exp. Neuropsychol.* 33, 410–421. doi:10.1080/13803395.2010.527321.

Kim, C. H., Heath, C. J., Kent, B. A., Bussey, T. J., and Saksida, L. M. (2015). The role of the dorsal hippocampus in two versions of the touchscreen automated paired associates learning (PAL) task for mice. *Psychopharmacology (Berl).* 232, 3899–3910.

doi:10.1007/s00213-015-3949-3.

Kim, D., Nguyen, M. D., Dobbin, M. M., Fischer, A., Sananbenesi, F., Rodgers, J. T., et al. (2007). SIRT1 deacetylase protects against neurodegeneration in models for Alzheimer's disease and amyotrophic lateral sclerosis. *EMBO J.* 26, 3169–79. doi:10.1038/sj.emboj.7601758.

Kim, D. S., Lee, M. W., Lee, T.-H., Sung, K. W., Koo, H. H., and Yoo, K. H. (2017). Cell culture density affects the stemness gene expression of adipose tissue-derived mesenchymal stem cells. *Biomed. reports* 6, 300–306. doi:10.3892/br.2017.845.

Kimura, K. D., Tissenbaum, H. A., Liu, Y., and Ruvkun, G. (1997). daf-2, an insulin receptor-like gene that regulates longevity and diapause in Caenorhabditis elegans. *Science* 277, 942–6.

Kirkwood, T. B. L. (2005). Understanding the Odd Science of Aging. *Cell* 120, 437–447. doi:10.1016/j.cell.2005.01.027.

Kitamura, T., Mishina, M., and Sugiyama, H. (2006). Dietary restriction increases hippocampal neurogenesis by molecular mechanisms independent of NMDA receptors. *Neurosci. Lett.* 393, 94–96. doi:10.1016/j.neulet.2005.08.073.

Klempin, F., Beis, D., Mosienko, V., Kempermann, G., Bader, M., and Alenina, N. (2013). Serotonin Is Required for Exercise-Induced Adult Hippocampal Neurogenesis. *J. Neurosci.* 33, 8270–8275. doi:10.1523/JNEUROSCI.5855-12.2013.

Knight, H. M., Brown, M., Dodgeon, B., Maughan, B., Richards, M., Elliott, J., et al. (2010). *Understanding Individual Behaviours Exploratory Networks*.

Knoth, R., Singec, I., Ditter, M., Pantazis, G., Capetian, P., Meyer, R. P., et al. (2010). Murine Features of Neurogenesis in the Human Hippocampus across the Lifespan from 0 to 100 Years. *PLoS One* 5, e8809. doi:10.1371/journal.pone.0008809.

Kojima, T., Kamei, H., Aizu, T., Arai, Y., Takayama, M., Nakazawa, S., et al. (2004). Association analysis between longevity in the Japanese population and polymorphic variants of genes involved in insulin and insulin-like growth factor 1 signaling pathways. *Exp. Gerontol.* 39, 1595–8. doi:10.1016/j.exger.2004.05.007.

Koutsakis, C., and Kazanis, I. (2016). How Necessary is the Vasculature in the Life of Neural Stem and Progenitor Cells? Evidence from Evolution, Development and the Adult Nervous System. *Front. Cell. Neurosci.* 10, 35. doi:10.3389/fncel.2016.00035.

Kuhn, H. G., Dickinson-Anson, H., and Gage, F. H. (1996). Neurogenesis in the dentate gyrus of the adult rat: age-related decrease of neuronal progenitor proliferation. *J. Neurosci.* 16, 2027–2033. doi:10.1523/JNEUROSCI.16-06-02027.1996.

Kuhn, H. G., Palmer, T. D., and Fuchs, E. (2001). Adult neurogenesis: a compensatory mechanism for neuronal damage. *Eur. Arch. Psychiatry Clin. Neurosci.* 251, 152–158. doi:10.1007/s004060170035.

Kukull, W. A., Larson, E. B., Teri, L., Bowen, J., McCormick, W., and Pfanschmidt, M. L. (1994). The Mini-Mental State Examination score and the clinical diagnosis of dementia. *J. Clin. Epidemiol.* 47, 1061–7.

Kumar, S., Parkash, J., Kataria, H., and Kaur, G. (2009). Interactive effect of excitotoxic injury and dietary restriction on neurogenesis and neurotrophic factors in adult male rat brain. *Neurosci. Res.* 65, 367–74. doi:10.1016/j.neures.2009.08.015.

Kuningas, M., Putters, M., Westendorp, R. G. J., Slagboom, P. E., and van Heemst, D. (2007). SIRT1 Gene, Age-Related Diseases, and Mortality: The Leiden 85-Plus Study. *Journals Gerontol. Ser. A Biol. Sci. Med. Sci.* 62, 960–965. doi:10.1093/gerona/62.9.960.

Kuo, L. J., and Yang, L.-X. (2008). Gamma-H2AX - a novel biomarker for DNA double-strand breaks. *In Vivo* 22, 305–9.

Kyoung Kim, H., Kyoung Kim, Y., Song, I.-H., Baek, S.-H., Lee, S.-R., Hye Kim, J., et al. (2005). Down-Regulation of a Forkhead Transcription Factor, FOXO3a, Accelerates Cellular Senescence in Human Dermal Fibroblasts. *Journals Gerontol. Ser. A Biol. Sci. Med. Sci.* 60, 4–9. doi:10.1093/gerona/60.1.4.

Lamming, D. W., Ye, L., Sabatini, D. M., and Baur, J. A. (2013). Rapalogs and mTOR inhibitors as anti-aging therapeutics. *J. Clin. Invest.* 123, 980–9. doi:10.1172/JCI64099.

Laplante, M., and Sabatini, D. M. (2012). mTOR signaling in growth control and disease. *Cell* 149, 274–93. doi:10.1016/j.cell.2012.03.017.

Lara, J., Cooper, R., Nissan, J., Ginty, A. T., Khaw, K.-T., Deary, I. J., et al. (2015). A proposed panel of biomarkers of healthy ageing. *BMC Med.* 13, 222. doi:10.1186/s12916-015-0470-9.

Larsson, L.-G. (2011). Oncogene- and tumor suppressor gene-mediated suppression of cellular senescence. *Semin. Cancer Biol.* 21, 367–376. doi:10.1016/j.semcancer.2011.10.005.

Le Belle, J. E., Orozco, N. M., Paucar, A. A., Saxe, J. P., Mottahedeh, J., Pyle, A. D., et al. (2011). Proliferative Neural Stem Cells Have High Endogenous ROS Levels that Regulate Self-Renewal and Neurogenesis in a PI3K/Akt-Dependant Manner. *Cell Stem Cell* 8, 59–71. doi:10.1016/j.stem.2010.11.028.

Lee, A., Archer, J., Wong, C. K. Y., Chen, S.-H. A., and Qiu, A. (2013). Age-Related Decline in Associative Learning in Healthy Chinese Adults. *PLoS One* 8, e80648. doi:10.1371/journal.pone.0080648.

Lee, H., and Thuret, S. (2018). Adult Human Hippocampal Neurogenesis: Controversy and Evidence. *Trends Mol. Med.* 24, 521–522. doi:10.1016/J.MOLMED.2018.04.002.

Lee, J., Duan, W., Long, J. M., Ingram, D. K., and Mattson, M. P. (2000). Dietary restriction increases the number of newly generated neural cells, and induces BDNF expression, in the dentate gyrus of rats. *J. Mol. Neurosci.* 15, 99–108. doi:10.1385/JMN:15:2:99.

Lee, J. E., Lim, M. S., Park, J. H., Park, C. H., and Koh, H. C. (2016). S6K Promotes Dopaminergic Neuronal Differentiation Through PI3K/Akt/mTOR-Dependent Signaling Pathways in Human Neural Stem Cells. *Mol. Neurobiol.* 53, 3771–3782. doi:10.1007/s12035-015-9325-9.

Lee, J., Seroogy, K. B., and Mattson, M. P. (2002). Dietary restriction enhances neurotrophin expression and neurogenesis in the hippocampus of adult mice. *J. Neurochem.* 80, 539–547. doi:10.1046/j.0022-3042.2001.00747.x.

Lee, S. G., Yoo, D. Y., Jung, H. Y., Nam, S. M., Kim, J. W., Choi, J. H., et al. (2015). Neurons in the hippocampal CA1 region, but not the dentate gyrus, are susceptible to oxidative stress in rats with streptozotocin-induced type 1 diabetes. *Neural Regen. Res.* 10, 451–6. doi:10.4103/1673-5374.153695.

Lees, H., Walters, H., and Cox, L. S. (2016). Animal and human models to understand ageing. *Maturitas* 93, 18–27. doi:10.1016/j.maturitas.2016.06.008.

Lehtinen, M. K., Zappaterra, M. W., Chen, X., Yang, Y. J., Hill, A. D., Lun, M., et al. (2011). The cerebrospinal fluid provides a proliferative niche for neural progenitor cells. *Neuron* 69, 893–905. doi:10.1016/j.neuron.2011.01.023.

Leng, S., Picchi, M. A., Liu, Y., Thomas, C. L., Willis, D. G., Bernauer, A. M., et al. (2013). Genetic variation in SIRT1 affects susceptibility of lung squamous cell carcinomas in former uranium miners from the Colorado plateau. *Carcinogenesis* 34, 1044–50. doi:10.1093/carcin/bgt024.

Levine, M. E., Lu, A. T., Bennett, D. A., and Horvath, S. (2015). Epigenetic age of the pre-frontal cortex is associated with neuritic plaques, amyloid load, and Alzheimer's disease related cognitive functioning. *Aging (Albany. NY).* 7, 1198–1211. doi:10.18632/aging.100864.

Levine, M. E., Lu, A. T., Quach, A., Chen, B., Assimes, T. L., Bandinelli, S., et al. (2018). An epigenetic biomarker of aging for lifespan and healthspan. *bioRxiv*, 276162. doi:10.1101/276162.

Li, Y., Cao, J., Chen, M., Li, J., Sun, Y., Zhang, Y., et al. (2017). Abnormal Neural Progenitor Cells Differentiated from Induced Pluripotent Stem Cells Partially Mimicked Development of TSC2 Neurological Abnormalities. *Stem Cell Reports* 8, 883–893. doi:10.1016/J.STEMCR.2017.02.020.

Li, Y., Wang, W.-J., Cao, H., Lu, J., Wu, C., Hu, F.-Y., et al. (2009). Genetic association of FOXO1A and FOXO3A with longevity trait in Han Chinese populations. *Hum. Mol. Genet.* 18, 4897–4904. doi:10.1093/hmg/ddp459.

Libert, S., Pointer, K., Bell, E. L., Das, A., Cohen, D. E., Asara, J. M., et al. (2011). SIRT1 activates MAO-A in the brain to mediate anxiety and exploratory drive. *Cell* 147, 1459–72. doi:10.1016/j.cell.2011.10.054.

Lin, S. J., Defossez, P. A., and Guarente, L. (2000). Requirement of NAD and SIR2 for life-span extension by calorie restriction in Saccharomyces cerevisiae. *Science* 289, 2126–8.

Liu, B., and Liu, F. (2014). Feedback regulation of mTORC1 by Grb10 in metabolism and beyond. *Cell Cycle* 13, 2643–4. doi:10.4161/15384101.2014.954221.

Liu, H., Gu, L., Zhu, P., Liu, Z., and Zhou, B. (2012). Evaluation on Thermal Hazard of Ter-Butyl Hydroperoxide by Using Accelerating Rate Calorimeter. *Procedia Eng.* 45, 574–579. doi:10.1016/J.PROENG.2012.08.206.

Liu, Y. W. J., Curtis, M. A., Gibbons, H. M., Mee, E. W., Bergin, P. S., Teoh, H. H., et al. (2008). Doublecortin expression in the normal and epileptic adult human brain. *Eur. J. Neurosci.* 28, 2254–2265. doi:10.1111/j.1460-9568.2008.06518.x.

Loffredo, F. S., Steinhauser, M. L., Jay, S. M., Gannon, J., Pancoast, J. R., Yalamanchi, P., et al. (2013). Growth differentiation factor 11 is a circulating factor that reverses age-related cardiac hypertrophy. *Cell* 153, 828–39. doi:10.1016/j.cell.2013.04.015.

Logan, J. M., Sanders, A. L., Snyder, A. Z., Morris, J. C., and Buckner, R. L. (2002). Under-

Recruitment and Nonselective Recruitment: Dissociable Neural Mechanisms Associated with Aging. *Neuron* 33, 827–840. doi:10.1016/S0896-6273(02)00612-8.

Lombard, D. B., Tishkoff, D. X., and Bao, J. (2011). Mitochondrial sirtuins in the regulation of mitochondrial activity and metabolic adaptation. *Handb. Exp. Pharmacol.* 206, 163–88. doi:10.1007/978-3-642-21631-2_8.

López-Otín, C., Blasco, M. A., Partridge, L., Serrano, M., and Kroemer, G. (2013). The hallmarks of aging. *Cell* 153, 1194–217. doi:10.1016/j.cell.2013.05.039.

López-Toledano, Michael L, M. A. S., López-Toledano, M. A., and Shelanski, M. L. (2004). Neurogenic effect of beta-amyloid peptide in the development of neural stem cells. *J. Neurosci.* 24, 5439–44. doi:10.1523/JNEUROSCI.0974-04.2004.

López-Toledano, M. A., Shelanski, Shelanski, M. L., and Shelanski (2007). Increased neurogenesis in young transgenic mice overexpressing human APP(Sw, Ind). *J. Alzheimers. Dis.* 12, 229–40.

Lovestone, S., Francis, P., Kloszewska, I., Mecocci, P., Simmons, A., Soininen, H., et al. (2009). AddNeuroMed--the European collaboration for the discovery of novel biomarkers for Alzheimer's disease. *Ann. N. Y. Acad. Sci.* 1180, 36–46. doi:10.1111/j.1749-6632.2009.05064.x.

Lowndes, G. J., Saling, M. M., Ames, D., Chiu, E., Gonzalez, L. M., and G.R., S. (2008). Recall and recognition of verbal paired associates in early Alzheimer's disease. *J. Int. Neuropsychol. Soc.* 14, 591–600. doi:10.1017/S1355617708080806.

Lu, A. T., Hannon, E., Levine, M. E., Crimmins, E. M., Lunnon, K., Mill, J., et al. (2017). Genetic architecture of epigenetic and neuronal ageing rates in human brain regions. *Nat. Commun.* 8, 15353. doi:10.1038/ncomms15353.

Lucassen, P. J., Meerlo, P., Naylor, A. S., van Dam, A. M., Dayer, A. G., Fuchs, E., et al. (2010). Regulation of adult neurogenesis by stress, sleep disruption, exercise and inflammation: Implications for depression and antidepressant action. *Eur. Neuropsychopharmacol.* 20, 1–17. doi:10.1016/J.EURONEURO.2009.08.003.

Lucassen, P. J., Oomen, C. A., Naninck, E. F. G., Fitzsimons, C. P., van Dam, A.-M., Czeh, B., et al. (2015). Regulation of Adult Neurogenesis and Plasticity by (Early) Stress, Glucocorticoids, and Inflammation. *Cold Spring Harb. Perspect. Biol.* 7, a021303. doi:10.1101/cshperspect.a021303.

Lucassen, P. J., Toni, N., Kempermann, G., Frisen, J., Gage, F. H., and Swaab, D. F. (2019). Limits to human neurogenesis—really? *Mol. Psychiatry*, 1. doi:10.1038/s41380-018-0337-5.

Ma, C., Pi, C., Yang, Y., Lin, L., Shi, Y., Li, Y., et al. (2017). Nampt Expression Decreases Age-Related Senescence in Rat Bone Marrow Mesenchymal Stem Cells by Targeting Sirt1. *PLoS One* 12, e0170930. doi:10.1371/journal.pone.0170930.

Maalouf, M., Rho, J. M., and Mattson, M. P. (2009). The neuroprotective properties of calorie restriction, the ketogenic diet, and ketone bodies. *Brain Res. Rev.* 59, 293–315. doi:10.1016/J.BRAINRESREV.2008.09.002.

Maestas, N., Mullen, K., and Powell, D. (2016). *The Effect of Population Aging on Economic Growth, the Labor Force and Productivity*. RAND Corporation doi:10.7249/WR1063-1.

Magri, L., and Galli, R. (2013). mTOR signaling in neural stem cells: from basic biology to disease. *Cell. Mol. Life Sci.* 70, 2887–98. doi:10.1007/s00018-012-1196-x.

Mak, I. W., Evaniew, N., and Ghert, M. (2014). Lost in translation: animal models and clinical trials in cancer treatment. *Am. J. Transl. Res.* 6, 114–8.

Malberg, J. E. (2004). Implications of adult hippocampal neurogenesis in antidepressant action. *J. Psychiatry Neurosci.* 29, 196–205.

Malley, C. O., and Pidgeon, G. P. (2016). The mTOR pathway in obesity driven gastrointestinal cancers: Potential targets and clinical trials. *BBA Clin.* 5, 29–40. doi:10.1016/J.BBACLI.2015.11.003.

Marioni, R. E., Shah, S., McRae, A. F., Ritchie, S. J., Muniz-Terrera, G., Harris, S. E., et al. (2015). The epigenetic clock is correlated with physical and cognitive fitness in the Lothian Birth Cohort 1936. *Int. J. Epidemiol.* 44, 1388–1396. doi:10.1093/ije/dyu277.

Martin, C. K., Anton, S. D., Han, H., York-Crowe, E., Redman, L. M., Ravussin, E., et al. (2007). Examination of cognitive function during six months of calorie restriction: results of a randomized controlled trial. *Rejuvenation Res.* 10, 179–90. doi:10.1089/rej.2006.0502.

Martínez-Cisuelo, V., Gómez, J., García-Junceda, I., Naudí, A., Cabré, R., Mota-Martorell, N., et al. (2016). Rapamycin reverses age-related increases in mitochondrial ROS production at complex I, oxidative stress, accumulation of mtDNA fragments inside nuclear DNA, and lipofuscin level, and increases autophagy, in the liver of middle-aged mice. *Exp. Gerontol.* 83, 130–8. doi:10.1016/j.exger.2016.08.002.

Maruszak, A., Murphy, T., Liu, B., Lucia, C. de, Douiri, A., Nevado, A. J., et al. (2017). Cellular phenotyping of hippocampal progenitors exposed to patient serum predicts conversion to Alzheimer's Disease. *bioRxiv*, 175604. doi:10.1101/175604.

Maruszak, A., Pilarski, A., Murphy, T., Branch, N., and Thuret, S. (2014). Hippocampal neurogenesis in Alzheimer's disease: is there a role for dietary modulation? *J. Alzheimers. Dis.* 38, 11–38. doi:10.3233/JAD-131004.

Maslov, A. Y., Barone, T. A., Plunkett, R. J., and Pruitt, S. C. (2004). Neural Stem Cell Detection, Characterization, and Age-Related Changes in the Subventricular Zone of Mice. *J. Neurosci.* 24, 1726–1733. doi:10.1523/JNEUROSCI.4608-03.2004.

Mathers, C. D., Stevens, G. A., Boerma, T., White, R. A., and Tobias, M. I. (2015). Causes of international increases in older age life expectancy. *Lancet* 385, 540–548. doi:10.1016/S0140-6736(14)60569-9.

Mathers, J. c., and Ford, D. (2009). "Nutrition, epigenetics, and ageing," in *Nutrients and Epigenetics*, eds. S.-W. Choi and S. Frisio, 175–196.

Mathews, K. J., Allen, K. M., Boerrigter, D., Ball, H., Shannon Weickert, C., and Double, K. L. (2017). Evidence for reduced neurogenesis in the aging human hippocampus despite stable stem cell markers. 16, 1195–1199. doi:10.1111/acel.12641.

Mattison, J. A., Colman, R. J., Beasley, T. M., Allison, D. B., Kemnitz, J. W., Roth, G. S., et al. (2017). Caloric restriction improves health and survival of rhesus monkeys. *Nat. Commun.* 8, 14063. doi:10.1038/ncomms14063.

Mattison, J. A., Roth, G. S., Beasley, T. M., Tilmont, E. M., Handy, A. M., Herbert, R. L., et al. (2012). Impact of caloric restriction on health and survival in rhesus monkeys from the NIA study. *Nature* 489, 318–321. doi:10.1038/nature11432.

Mattson, M. P. (2012). Energy intake and exercise as determinants of brain health and vulnerability to injury and disease. *Cell Metab.* 16, 706–22. doi:10.1016/j.cmet.2012.08.012.

McAvoy, K., Besnard, A., and Sahay, A. (2015). Adult hippocampal neurogenesis and pattern separation in DG: a role for feedback inhibition in modulating sparseness to govern population-based coding. *Front. Syst. Neurosci.* 9, 120. doi:10.3389/fnsys.2015.00120.

McNerney, M. W., and Radvansky, G. A. (2015). Mind racing: The influence of exercise on long-term memory consolidation. *Memory* 23, 1140–1151.

doi:10.1080/09658211.2014.962545.

Medina, M., and Avila, J. (2014). The need for better AD animal models. *Front. Pharmacol.* 5, 227. doi:10.3389/fphar.2014.00227.

Meng, D., Frank, A. R., and Jewell, J. L. (2018). mTOR signaling in stem and progenitor cells. doi:10.1242/dev.152595.

Merksamer, P. I., Liu, Y., He, W., Hirschey, M. D., Chen, D., and Verdin, E. (2013). The sirtuins, oxidative stress and aging: an emerging link. *Aging (Albany. NY).* 5, 144–150. doi:10.18632/aging.100544.

Merrill, D. A., Karim, R., Darraq, M., Chiba, A. A., and Tuszynski, M. H. (2003). Hippocampal cell genesis does not correlate with spatial learning ability in aged rats. *J. Comp. Neurol.* 459, 201–207. doi:10.1002/cne.10616.

Mihaylova, M. M., Sabatini, D. M., and Yilmaz, Ö. H. (2014). Dietary and metabolic control of stem cell function in physiology and cancer. *Cell Stem Cell* 14, 292–305. doi:10.1016/j.stem.2014.02.008.

Miranda, D. N., Coletta, D. K., Mandarino, L. J., and Shaibi, G. Q. (2014). Increases in insulin sensitivity among obese youth are associated with gene expression changes in whole blood. *Obesity* 22, 1337–1344. doi:10.1002/oby.20711.

Mirescu, C., Peters, J. D., Noiman, L., and Gould, E. (2006). Sleep deprivation inhibits adult neurogenesis in the hippocampus by elevating glucocorticoids. *Proc. Natl. Acad. Sci. U. S. A.* 103, 19170–5. doi:10.1073/pnas.0608644103.

Mitchell, K. J., Johnson, M. K., Raye, C. L., and D'Esposito, M. (2000). fMRI evidence of age-related hippocampal dysfunction in feature binding in working memory. *Cogn. Brain Res.* 10, 197–206. doi:10.1016/S0926-6410(00)00029-X.

Mitchell, S. J., Scheibye-Knudsen, M., Longo, D. L., and De Cabo, R. (2015). Animal Models of Aging Research: Implications for Human Aging and Age-Related Diseases Ã. doi:10.1146/annurev-animal-022114-110829.

Moayyeri, A., Hammond, C. J., Valdes, A. M., and Spector, T. D. (2013). Cohort Profile: TwinsUK and Healthy Ageing Twin Study. *Int. J. Epidemiol.* 42, 76–85. doi:10.1093/ije/dyr207.

Molofsky, A. V., Slutsky, S. G., Joseph, N. M., He, S., Pardal, R., Krishnamurthy, J., et al. (2006). Increasing p16 INK4a expression decreases forebrain progenitors and neurogenesis during ageing. *Nature* 443, 448–452. doi:10.1038/nature05091.

Monteiro, B. M. M., Moreira, F. A., Massensini, A. R., Moraes, M. F. D., and Pereira, G. S. (2014). Enriched environment increases neurogenesis and improves social memory persistence in socially isolated adult mice. *Hippocampus* 24, 239–248. doi:10.1002/hipo.22218.

Moreira, E. A. M., Most, M., Howard, J., and Ravussin, E. (2011). Dietary adherence to long-term controlled feeding in a calorie-restriction study in overweight men and women. *Nutr. Clin. Pract.* 26, 309–15. doi:10.1177/0884533611405992.

Morgan, A. H., Andrews, Z. B., and Davies, J. S. (2017). Less is more: Caloric regulation of neurogenesis and adult brain function. *J. Neuroendocrinol.* 29, e12512. doi:10.1111/jne.12512.

Mori, M., Higuchi, K., Sakurai, A., Tabara, Y., Miki, T., and Nose, H. (2009). Genetic basis of inter-individual variability in the effects of exercise on the alleviation of lifestyle-related diseases. *J. Physiol.* 587, 5577–5584. doi:10.1113/jphysiol.2009.179283.

Most, J., Tosti, V., Redman, L. M., and Fontana, L. (2017). Calorie restriction in humans: An update. *Ageing Res. Rev.* 39, 36–45. doi:10.1016/j.arr.2016.08.005.

Mueller, S. G., Chao, L. L., Berman, B., and Weiner, M. W. (2011). Evidence for functional specialization of hippocampal subfields detected by MR subfield volumetry on high resolution images at 4 T. *Neuroimage* 56, 851–7. doi:10.1016/j.neuroimage.2011.03.028.

Mueller, S. G., Stables, L., Du, A. T., Schuff, N., Truran, D., Cashdollar, N., et al. (2007). Measurement of hippocampal subfields and age-related changes with high resolution MRI at 4T. *Neurobiol. Aging* 28, 719–26. doi:10.1016/j.neurobiolaging.2006.03.007.

Mueller, S. G., and Weiner, M. W. (2009). Selective effect of age, Apo e4, and Alzheimer's disease on hippocampal subfields. *Hippocampus* 19, 558–564. doi:10.1002/hipo.20614.

Murphy, T., Dias, G. P., and Thuret, S. (2014). Effects of diet on brain plasticity in animal and human studies: mind the gap. *Neural Plast.* 2014, 563160. doi:10.1155/2014/563160.

Murphy, T., Maruszak, A., Powell, T. R., de Lucia, C., Price, J., Lovestone, S., et al. (2018).

Older Human Serum Increases Apoptosis and Molecular Ageing Markers in Human Hippocampal Progenitor Cells. *In prep.*

Murphy, T., and Thuret, S. (2015). The systemic milieu as a mediator of dietary influence on stem cell function during ageing. *Ageing Res. Rev.* 19, 53–64. doi:10.1016/j.arr.2014.11.004.

Myant, K. B., Cammareri, P., McGhee, E. J., Ridgway, R. A., Huels, D. J., Cordero, J. B., et al. (2013). ROS Production and NF-κB Activation Triggered by RAC1 Facilitate WNT-Driven Intestinal Stem Cell Proliferation and Colorectal Cancer Initiation. *Cell Stem Cell* 12, 761–773. doi:10.1016/j.stem.2013.04.006.

Myzak, M. C., Ho, E., and Dashwood, R. H. (2006). Dietary agents as histone deacetylase inhibitors. *Mol. Carcinog.* 45, 443–6. doi:10.1002/mc.20224.

Nagai, M., Kuriyama, S., Kakizaki, M., Ohmori-Matsuda, K., Sone, T., Hozawa, A., et al. (2012). Impact of obesity, overweight and underweight on life expectancy and lifetime medical expenditures: the Ohsaki Cohort Study. *BMJ Open* 2, e000940-. doi:10.1136/bmjopen-2012-000940.

Nathan, D. M., Barrett-Connor, E., Crandall, J. P., Edelstein, S. L., Goldberg, R. B., Horton, E. S., et al. (2015). Long-term effects of lifestyle intervention or metformin on diabetes development and microvascular complications over 15-year follow-up: the Diabetes Prevention Program Outcomes Study. *lancet. Diabetes Endocrinol.* 3, 866–75. doi:10.1016/S2213-8587(15)00291-0.

National Cancer Institute. The Healthy Eating Index-Overview of the Methods & Calculations. Available at: https://epi.grants.cancer.gov/hei/hei-methods-and-calculations.html [Accessed October 11, 2018].

Nelson, H., and Wilson, J. (1991). *National adult reading test (NART).* Windsor: Nfer-Nelson.

Ngandu, T., Lehtisalo, J., Solomon, A., Levälahti, E., Ahtiluoto, S., Antikainen, R., et al. (2015). A 2 year multidomain intervention of diet, exercise, cognitive training, and vascular risk monitoring versus control to prevent cognitive decline in at-risk elderly people (FINGER): a randomised controlled trial. *Lancet* 385, 2255–2263. doi:10.1016/S0140-6736(15)60461-5.

Ngwenya, L. B., Peters, A., and Rosene, D. L. (2006). Maturational sequence of newly generated neurons in the dentate gyrus of the young adult rhesus monkey. *J. Comp. Neurol.* 498, 204–216. doi:10.1002/cne.21045.

Niccoli, T., and Partridge, L. (2012). Ageing as a risk factor for disease. *Curr. Biol.* 22, R741-52. doi:10.1016/j.cub.2012.07.024.

Niculescu, M. D., Craciunescu, C. N., and Zeisel, S. H. (2006). Dietary choline deficiency alters global and gene-specific DNA methylation in the developing hippocampus of mouse fetal brains. *FASEB J.* 20, 43–9. doi:10.1096/fj.05-4707com.

Norden, D. M., and Godbout, J. P. (2013). Review: microglia of the aged brain: primed to be activated and resistant to regulation. *Neuropathol. Appl. Neurobiol.* 39, 19–34. doi:10.1111/j.1365-2990.2012.01306.x.

Northey, J. M., Cherbuin, N., Pumpa, K. L., Smee, D. J., and Rattray, B. (2018). Exercise interventions for cognitive function in adults older than 50: a systematic review with meta-analysis. *Br. J. Sports Med.* 52, 154–160. doi:10.1136/bjsports-2016-096587.

Nygaard, M., Lindahl-Jacobsen, R., Soerensen, M., Mengel-From, J., Andersen-Ranberg, K., Jeune, B., et al. (2014). Birth cohort differences in the prevalence of longevity-associated variants in APOE and FOXO3A in Danish long-lived individuals. *Exp. Gerontol.* 57, 41–46. doi:10.1016/j.exger.2014.04.018.

O' Neill, C. (2013). PI3-kinase/Akt/mTOR signaling: impaired on/off switches in aging, cognitive decline and Alzheimer's disease. *Exp. Gerontol.* 48, 647–53. doi:10.1016/j.exger.2013.02.025.

O'Bryant, S. E., Humphreys, J. D., Smith, G. E., Ivnik, R. J., Graff-Radford, N. R., Petersen, R. C., et al. (2008). Detecting dementia with the mini-mental state examination in highly educated individuals. *Arch. Neurol.* 65, 963–7. doi:10.1001/archneur.65.7.963.

O'Bryant, S. E., Xiao, G., Barber, R., Huebinger, R., Wilhelmsen, K., Edwards, M., et al. (2011). A blood-based screening tool for Alzheimer's disease that spans serum and plasma: findings from TARC and ADNI. *PLoS One* 6, e28092. doi:10.1371/journal.pone.0028092.

Ochocki, J. D., and Simon, M. C. (2013). Nutrient-sensing pathways and metabolic regulation in stem cells. *J. Cell Biol.* 203, 23–33. doi:10.1083/jcb.201303110.

Oellerich, M. F., and Potente, M. (2012). FOXOs and sirtuins in vascular growth, maintenance, and aging. *Circ. Res.* 110, 1238–51. doi:10.1161/CIRCRESAHA.111.246488.

Oeppen, J., and Vaupel, J. W. (2002). DEMOGRAPHY: Enhanced: Broken Limits to Life Expectancy. *Science (80-.).* 296, 1029–1031. doi:10.1126/science.1069675.

Ortega-Molina, A., Efeyan, A., Lopez-Guadamillas, E., Muñoz-Martin, M., Gómez-López, G., Cañamero, M., et al. (2012). Pten Positively Regulates Brown Adipose Function, Energy Expenditure, and Longevity. *Cell Metab.* 15, 382–394. doi:10.1016/j.cmet.2012.02.001.

Owen, A. M., Sahakian, B. J., Semple, J., Polkey, C. E., and Robbins, T. W. (1995). Visuo-spatial short-term recognition memory and learning after temporal lobe excisions, frontal lobe excisions or amygdalo-hippocampectomy in man. *Neuropsychologia* 33, 1–24.

Paik, J., Ding, Z., Narurkar, R., Ramkissoon, S., Muller, F., Kamoun, W. S., et al. (2009). FoxOs cooperatively regulate diverse pathways governing neural stem cell homeostasis. *Cell Stem Cell* 5, 540–53. doi:10.1016/j.stem.2009.09.013.

Paliouras, G. N., Hamilton, L. K., Aumont, A., Joppé, S. E., Barnabé-Heider, F., and Fernandes, K. J. L. (2012). Mammalian target of rapamycin signaling is a key regulator of the transit-amplifying progenitor pool in the adult and aging forebrain. *J. Neurosci.* 32, 15012–26. doi:10.1523/JNEUROSCI.2248-12.2012.

Palmer, T. D., Schwartz, P. H., Taupin, P., Kaspar, B., Stein, S. A., and Gage, F. H. (2001). Progenitor cells from human brain after death. *Nature* 411, 42–43. doi:10.1038/35075141.

Panossian, L., Fenik, P., Zhu, Y., Zhan, G., McBurney, M. W., and Veasey, S. (2011). SIRT1 regulation of wakefulness and senescence-like phenotype in wake neurons. *J. Neurosci.* 31, 4025–36. doi:10.1523/JNEUROSCI.5166-10.2011.

Papenberg, G., Lindenberger, U., and Bäckman, L. (2015). Aging-related magnification of genetic effects on cognitive and brain integrity. *Trends Cogn. Sci.* 19, 506–514. doi:10.1016/j.tics.2015.06.008.

Park, D., Yang, Y.-H., Bae, D. K., Lee, S. H., Yang, G., Kyung, J., et al. (2013). Improvement of cognitive function and physical activity of aging mice by human neural stem cells over-expressing choline acetyltransferase. *Neurobiol. Aging* 34, 2639–46. doi:10.1016/j.neurobiolaging.2013.04.026.

Parkinson, J. K., Murray, E. A., and Mishkin, M. (1988). A selective mnemonic role for the hippocampus in monkeys: memory for the location of objects. *J. Neurosci.* 8, 4159–67. doi:10.1523/JNEUROSCI.08-11-04159.1988.

Parrella, E., Maxim, T., Maialetti, F., Zhang, L., Wan, J., Wei, M., et al. (2013). Protein restriction cycles reduce IGF-1 and phosphorylated Tau, and improve behavioral performance in an Alzheimer's disease mouse model. *Aging Cell* 12, 257–68.

doi:10.1111/acel.12049.

Partridge, L., Deelen, J., and Slagboom, P. E. (2018). Facing up to the global challenges of ageing. *Nature* 561, 45–56. doi:10.1038/s41586-018-0457-8.

Pencea, V., Bingaman, K. D., Freedman, L. J., and Luskin, M. B. (2001). Neurogenesis in the subventricular zone and rostral migratory stream of the neonatal and adult primate forebrain. *Exp. Neurol.* 172, 1–16. doi:10.1006/exnr.2001.7768.

Pereira, J. B., Valls-Pedret, C., Ros, E., Palacios, E., Falcón, C., Bargalló, N., et al. (2014). Regional vulnerability of hippocampal subfields to aging measured by structural and diffusion MRI. *Hippocampus* 24, 403–414. doi:10.1002/hipo.22234.

Perera, F., and Herbstman, J. (2011). Prenatal environmental exposures, epigenetics, and disease. *Reprod. Toxicol.* 31, 363–73. doi:10.1016/j.reprotox.2010.12.055.

Perry, H. V., Cunningham, C., and Boche, D. (2002). Atypical inflammation in the central nervous system in prion disease. *Curr. Opin. Neurol.* 15, 349–354.

Peters, R. (2006). Ageing and the brain. *Postgrad. Med. J.* 82, 84–8. doi:10.1136/pgmj.2005.036665.

Picard, M., and Turnbull, D. M. (2013). Linking the Metabolic State and Mitochondrial DNA in Chronic Disease, Health, and Aging. *Diabetes* 62, 672–678. doi:10.2337/db12-1203.

Plancher, G., Gyselinck, V., Nicolas, S., and Piolino, P. (2010). Age effect on components of episodic memory and feature binding: A virtual reality study. *Neuropsychology* 24, 379–390. doi:10.1037/a0018680.

Pollock, K., Stroemer, P., Patel, S., Stevanato, L., Hope, A., Miljan, E., et al. (2006). A conditionally immortal clonal stem cell line from human cortical neuroepithelium for the treatment of ischemic stroke. *Exp. Neurol.* 199, 143–155. doi:10.1016/j.expneurol.2005.12.011.

Porstmann, T., Santos, C. R., Griffiths, B., Cully, M., Wu, M., Leevers, S., et al. (2008). SREBP activity is regulated by mTORC1 and contributes to Akt-dependent cell growth. *Cell Metab.* 8, 224–36. doi:10.1016/j.cmet.2008.07.007.

Poulain, M., Herm, A., and Pes, G. (2014). The Blue Zones: areas of exceptional longevity around the world. *Vienna Yearb. Popul. Res.* Volume 11, 87–108.

doi:10.1553/populationyearbook2013s87.

Powell, T. R., Murphy, T., Lee, S. H., Price, J., Thuret, S., and Breen, G. (2017). Transcriptomic profiling of human hippocampal progenitor cells treated with antidepressants and its application in drug repositioning. *J. Psychopharmacol.*, 026988111769146. doi:10.1177/0269881117691467.

Price, J. L., Ko, A. I., Wade, M. J., Tsou, S. K., McKeel, D. W., and Morris, J. C. (2001). Neuron number in the entorhinal cortex and CA1 in preclinical Alzheimer disease. *Arch. Neurol.* 58, 1395–402.

Prozorovski, T., Schulze-Topphoff, U., Glumm, R., Baumgart, J., Schröter, F., Ninnemann, O., et al. (2008). Sirt1 contributes critically to the redox-dependent fate of neural progenitors. *Nat. Cell Biol.* 10, 385–94. doi:10.1038/ncb1700.

Radford, E. J., Ito, M., Shi, H., Corish, J. A., Yamazawa, K., Isganaitis, E., et al. (2014). In utero undernourishment perturbs the adult sperm methylome and intergenerational metabolism. *Science (80-.).* 345, 1255903-. doi:10.1126/science.1255903.

Rafalski, V. A., and Brunet, A. (2011). Energy metabolism in adult neural stem cell fate. *Prog. Neurobiol.* 93, 182–203. doi:10.1016/j.pneurobio.2010.10.007.

Rafalski, V. A., Ho, P. P., Brett, J. O., Ucar, D., Dugas, J. C., Pollina, E. A., et al. (2013). Expansion of oligodendrocyte progenitor cells following SIRT1 inactivation in the adult brain. *Nat. Cell Biol.* 15, 614–24. doi:10.1038/ncb2735.

Rafalski, V. A., Mancini, E., and Brunet, A. (2012). Energy metabolism and energy-sensing pathways in mammalian embryonic and adult stem cell fate. *J. Cell Sci.* 125, 5597–608. doi:10.1242/jcs.114827.

Ramon y Cajal, S. (1928). *Degeneration and regeneration of the nervous system.* Oxford: Clarendon Press.

Rando, T. A., and Chang, H. Y. (2012). Aging, rejuvenation, and epigenetic reprogramming: resetting the aging clock. *Cell* 148, 46–57. doi:10.1016/j.cell.2012.01.003.

Raz, N., and Rodrigue, K. M. (2006). Differential aging of the brain: Patterns, cognitive correlates and modifiers. *Neurosci. Biobehav. Rev.* 30, 730–748. doi:10.1016/J.NEUBIOREV.2006.07.001.

Rea, I. M., Dellet, M., and Mills, K. I. (2015). Living long and ageing well: is epigenomics the missing link between nature and nurture? *Biogerontology* 17, 33–54. doi:10.1007/s10522-015-9589-5.

Redman, L. M., Smith, S. R., Burton, J. H., Martin, C. K., Il'yasova, D., and Ravussin, E. (2018). Metabolic Slowing and Reduced Oxidative Damage with Sustained Caloric Restriction Support the Rate of Living and Oxidative Damage Theories of Aging. *Cell Metab.* 27, 805–815.e4. doi:10.1016/j.cmet.2018.02.019.

Reed, M. J., Penn, P. E., Li, Y., Birnbaum, R., Vernon, R. B., Johnson, T. S., et al. (1996). Enhanced cell proliferation and biosynthesis mediate improved wound repair in refed, caloric-restricted mice. *Mech. Ageing Dev.* 89, 21–43. doi:10.1016/0047-6374(96)01737-X.

Reich, D. E., Cargill, M., Bolk, S., Ireland, J., Sabeti, P. C., Richter, D. J., et al. (2001). Linkage disequilibrium in the human genome. *Nature* 411, 199–204. doi:10.1038/35075590.

Reitz, C. (2016). Toward precision medicine in Alzheimer's disease. *Ann. Transl. Med.* 4, 107–107. doi:10.21037/atm.2016.03.05.

Renault, V. M., Rafalski, V. A., Morgan, A. A., Salih, D. A. M., Brett, J. O., Webb, A. E., et al. (2009). FoxO3 regulates neural stem cell homeostasis. *Cell Stem Cell* 5, 527–39. doi:10.1016/j.stem.2009.09.014.

Ries, W., and Pöthig, D. (1984). Chronological and biological age. *Exp. Gerontol.* 19, 211–216. doi:10.1016/0531-5565(84)90041-X.

Rinaldi, P., Polidori, M. C., Metastasio, A., Mariani, E., Mattioli, P., Cherubini, A., et al. (2003). Plasma antioxidants are similarly depleted in mild cognitive impairment and in Alzheimer's disease. *Neurobiol. Aging* 24, 915–9.

Rodier, F., and Campisi, J. (2011). Four faces of cellular senescence. *J. Cell Biol.* 192, 547–556. doi:10.1083/jcb.201009094.

Roig, M., Nordbrandt, S., Geertsen, S. S., and Nielsen, J. B. (2013). The effects of cardiovascular exercise on human memory: A review with meta-analysis. *Neurosci. Biobehav. Rev.* 37, 1645–1666. doi:10.1016/j.neubiorev.2013.06.012.

Romine, J., Gao, X., Xu, X.-M., So, K. F., and Chen, J. (2015). The proliferation of amplifying neural progenitor cells is impaired in the aging brain and restored by the mTOR pathway activation. *Neurobiol. Aging* 36, 1716–26.

doi:10.1016/j.neurobiolaging.2015.01.003.

RStudio Team (2016). RStudio: Integrated Development for R.

Rupprecht, A., Sittner, D., Smorodchenko, A., Hilse, K. E., Goyn, J., Moldzio, R., et al. (2014). Uncoupling Protein 2 and 4 Expression Pattern during Stem Cell Differentiation Provides New Insight into Their Putative Function. *PLoS One* 9, e88474. doi:10.1371/journal.pone.0088474.

Rzewnicki, R., Auweele, Y. Vanden, and Bourdeaudhuij, I. De (2003). Addressing overreporting on the International Physical Activity Questionnaire (IPAQ) telephone survey with a population sample. *Public Health Nutr.* 6, 299–305. doi:10.1079/PHN2002427.

Sadaie, M., Dillon, C., Narita, M., Narita, M., Young, A. R. J., Cairney, C. J., et al. (2015). Cell-based screen for altered nuclear phenotypes reveals senescence progression in polyploid cells after Aurora kinase B inhibition. *Mol. Biol. Cell* 26, 2971–85. doi:10.1091/mbc.E15-01-0003.

Saffari, Y., and Sadrzadeh, S. M. H. (2004). Green tea metabolite EGCG protects membranes against oxidative damage in vitro. *Life Sci.* 74, 1513–8.

Sahay, A., Scobie, K. N., Hill, A. S., O'Carroll, C. M., Kheirbek, M. A., Burghardt, N. S., et al. (2011). Increasing adult hippocampal neurogenesis is sufficient to improve pattern separation. *Nature* 472, 466–470. doi:10.1038/nature09817.

Samanez-Larkin, G. R., and Knutson, B. (2015). Decision making in the ageing brain: changes in affective and motivational circuits. *Nat. Rev. Neurosci.* 16, 278–289. doi:10.1038/nrn3917.

Sarbassov, D. D., Ali, M., and Sabatini, D. M. (2005). Growing roles for the mTOR pathway. *Curr. Opin. Cell Biol.* 17, 596–603. doi:10.1016/j.ceb.2005.09.009.

Sato, A., Sunayama, J., Matsuda, K., Tachibana, K., Sakurada, K., Tomiyama, A., et al. (2010). Regulation of neural stem/progenitor cell maintenance by PI3K and mTOR. *Neurosci. Lett.* 470, 115–20. doi:10.1016/j.neulet.2009.12.067.

Satoh, A., Brace, C. S., Rensing, N., Cliften, P., Wozniak, D. F., Herzog, E. D., et al. (2013). Sirt1 extends life span and delays aging in mice through the regulation of Nk2 homeobox 1 in the DMH and LH. *Cell Metab.* 18, 416–30. doi:10.1016/j.cmet.2013.07.013.

Scarmeas, N., Stern, Y., Mayeux, R., Manly, J. J., Schupf, N., and Luchsinger, J. A. (2009). Mediterranean Diet and Mild Cognitive Impairment. *Arch. Neurol.* 66, 216–225. doi:10.1001/archneurol.2008.536.

Scheibye-Knudsen, M., Mitchell, S. J., Fang, E. F., Iyama, T., Ward, T., Wang, J., et al. (2014). A high-fat diet and NAD(+) activate Sirt1 to rescue premature aging in cockayne syndrome. *Cell Metab.* 20, 840–55. doi:10.1016/j.cmet.2014.10.005.

Schmidt-Hieber, C., Jonas, P., and Bischofberger, J. (2004). Enhanced synaptic plasticity in newly generated granule cells of the adult hippocampus. *Nature* 429, 184–7. doi:10.1038/nature02553.

Schmitt, T. L., Hotz-Wagenblatt, A., Klein, H., and Dröge, W. (2005). Interdependent regulation of insulin receptor kinase activity by ADP and hydrogen peroxide. *J. Biol. Chem.* 280, 3795–801. doi:10.1074/jbc.M410352200.

Schubert, D., Currais, A., Goldberg, J., Finley, K., Petrascheck, M., and Maher, P. (2018). Geroneuroprotectors: Effective Geroprotectors for the Brain. *Trends Pharmacol. Sci.* 39, 1004–1007. doi:10.1016/j.tips.2018.09.008.

Schuch, F. B., Vancampfort, D., Firth, J., Rosenbaum, S., Ward, P. B., Silva, E. S., et al. (2018). Physical Activity and Incident Depression: A Meta-Analysis of Prospective Cohort Studies. *Am. J. Psychiatry* 175, 631–648. doi:10.1176/appi.ajp.2018.17111194.

Sée, V., and Loeffler, J. P. (2001). Oxidative stress induces neuronal death by recruiting a protease and phosphatase-gated mechanism. *J. Biol. Chem.* 276, 35049–59. doi:10.1074/jbc.M104988200.

Seidenfaden, R., Desoeuvre, A., Bosio, A., Virard, I., and Cremer, H. (2006). Glial conversion of SVZ-derived committed neuronal precursors after ectopic grafting into the adult brain. *Mol. Cell. Neurosci.* 32, 187–198. doi:10.1016/j.mcn.2006.04.003.

Shihabuddin, L. S., Horner, P. J., Ray, J., and Gage, F. H. (2000). Adult spinal cord stem cells generate neurons after transplantation in the adult dentate gyrus. *J. Neurosci.* 20, 8727–35.

Shing, Y. L., Rodrigue, K. M., Kennedy, K. M., Fandakova, Y., Bodammer, N., Werkle-Bergner, M., et al. (2011). Hippocampal Subfield Volumes: Age, Vascular Risk, and Correlation with Associative Memory. *Front. Aging Neurosci.* 3, 2. doi:10.3389/fnagi.2011.00002.

Shors, T. J., Townsend, D. A., Zhao, M., Kozorovitskiy, Y., And, and Gould, E. (2002).

Neurogenesis May Relate to Some But Not All Types of Hippocampal-Dependent Learning. *Hippocampus* 12, 578–584. Available at: http://aks.rutgers.edu/articles/Memory/Priming/EyeBlink_Delay_Trace/Shors_Gould02.pdf [Accessed March 20, 2013].

Shukitt-Hale, B., Bielinski, D. F., Lau, F. C., Willis, L. M., Carey, A. N., Joseph, J. A., et al. (2015). The beneficial effects of berries on cognition, motor behaviour and neuronal function in ageing. *Br. J. Nutr.* 114, 1542–1549. doi:10.1017/S0007114515003451.

Shukitt-Hale, B., Lau, F. C., Carey, A. N., Galli, R. L., Spangler, E. L., Ingram, D. K., et al. (2008). Blueberry polyphenols attenuate kainic acid-induced decrements in cognition and alter inflammatory gene expression in rat hippocampus. *Nutr. Neurosci.* 11, 172–182. doi:10.1179/147683008X301487.

Sierra, A., Encinas, J. M., and Maletic-Savatic, M. (2011). Adult human neurogenesis: from microscopy to magnetic resonance imaging. *Front. Neurosci.* 5, 47. doi:10.3389/fnins.2011.00047.

Signer, R. A. J., and Morrison, S. J. (2013). Mechanisms that regulate stem cell aging and life span. *Cell Stem Cell* 12, 152–65. doi:10.1016/j.stem.2013.01.001.

Sikora, E., Mosieniak, G., and Sliwinska, M. A. (2016). Morphological and Functional Characteristic of Senescent Cancer Cells. *Curr. Drug Targets* 17, 377–87.

Sizemore, G. M., Pitarresi, J. R., Balakrishnan, S., and Ostrowski, M. C. (2017). The ETS family of oncogenic transcription factors in solid tumours. *Nat. Rev. Cancer* 17, 337–351. doi:10.1038/nrc.2017.20.

Skalecka, A., Liszewska, E., Bilinski, R., Gkogkas, C., Khoutorsky, A., Malik, A. R., et al. (2016). mTOR kinase is needed for the development and stabilization of dendritic arbors in newly born olfactory bulb neurons. *Dev. Neurobiol.* 76, 1308–1327. doi:10.1002/dneu.22392.

Small, S. A. (2014). Isolating Pathogenic Mechanisms Embedded within the Hippocampal Circuit through Regional Vulnerability. *Neuron* 84, 32–39. doi:10.1016/j.neuron.2014.08.030.

Smith, J. J., Kenney, R., Gagne, D. J., Frushour, B. P., Ladd, W., Galonek, H. L., et al. (2009). Small molecule activators of SIRT1 replicate signaling pathways triggered by calorie restriction in vivo. *BMC Syst. Biol.* 3, 31. doi:10.1186/1752-0509-3-31.

Smith, M. Lou, and Milner, B. (1981). The role of the right hippocampus in the recall of spatial location. *Neuropsychologia* 19, 781–793. doi:10.1016/0028-3932(81)90090-7.

Smith, P. J., Blumenthal, J. A., Hoffman, B. M., Cooper, H., Strauman, T. A., Welsh-Bohmer, K., et al. (2010). Aerobic Exercise and Neurocognitive Performance: A Meta-Analytic Review of Randomized Controlled Trials. *Psychosom. Med.* 72, 239–252. doi:10.1097/PSY.0b013e3181d14633.

Snyder, J. S., Soumier, A., Brewer, M., Pickel, J., and Cameron, H. A. (2011). Adult hippocampal neurogenesis buffers stress responses and depressive behaviour. *Nature* 476, 458–461. doi:10.1038/nature10287.

Soares, F. C., de Oliveira, T. C. G., de Macedo, L. D. e D., Tomás, A. M., Picanço-Diniz, D. L. W., Bento-Torres, J., et al. (2015). CANTAB object recognition and language tests to detect aging cognitive decline: an exploratory comparative study. *Clin. Interv. Aging* 10, 37–48. doi:10.2147/CIA.S68186.

Sofi, F., Valecchi, D., Bacci, D., Abbate, R., Gensini, G. F., Casini, A., et al. (2011). Physical activity and risk of cognitive decline: a meta-analysis of prospective studies. *J. Intern. Med.* 269, 107–117. doi:10.1111/j.1365-2796.2010.02281.x.

Solon-Biet, S. M., McMahon, A. C., Ballard, J. W. O., Ruohonen, K., Wu, L. E., Cogger, V. C., et al. (2014). The ratio of macronutrients, not caloric intake, dictates cardiometabolic health, aging, and longevity in ad libitum-fed mice. *Cell Metab.* 19, 418–30. doi:10.1016/j.cmet.2014.02.009.

Solon-Biet, S. M., Mitchell, S. J., Coogan, S. C. P., Cogger, V. C., Gokarn, R., McMahon, A. C., et al. (2015). Dietary Protein to Carbohydrate Ratio and Caloric Restriction: Comparing Metabolic Outcomes in Mice. *Cell Rep.* 11, 1529–34. doi:10.1016/j.celrep.2015.05.007.

Song, F., Poljak, A., Smythe, G. A., and Sachdev, P. (2009). Plasma biomarkers for mild cognitive impairment and Alzheimer's disease. *Brain Res. Rev.* 61, 69–80. doi:10.1016/j.brainresrev.2009.05.003.

Song, T.-Y., Yeh, S.-L., Hu, M.-L., Chen, M.-Y., and Yang, N.-C. (2015). A Nampt inhibitor FK866 mimics vitamin B3 deficiency by causing senescence of human fibroblastic Hs68 cells via attenuation of NAD(+)-SIRT1 signaling. *Biogerontology* 16, 789–800. doi:10.1007/s10522-015-9605-9.

Sorrells, S. F., Paredes, M. F., Cebrian-Silla, A., Sandoval, K., Qi, D., Kelley, K. W., et al. (2018). Human hippocampal neurogenesis drops sharply in children to undetectable levels in

adults. *Nature* 555, 377–381. doi:10.1038/nature25975.

Spalding, K. L., Bergmann, O., Alkass, K., Bernard, S., Salehpour, M., Huttner, H. B., et al. (2013). Dynamics of hippocampal neurogenesis in adult humans. *Cell* 153, 1219–27. doi:10.1016/j.cell.2013.05.002.

Squire, L. R., Stark, C. E. L., and Clark, R. E. (2004). The Medial Temporal Lobe. *Annu. Rev. Neurosci.* 27, 279–306. doi:10.1146/annurev.neuro.27.070203.144130.

Stangl, D., and Thuret, S. (2009). Impact of diet on adult hippocampal neurogenesis. *Genes Nutr.* 4, 271–82. doi:10.1007/s12263-009-0134-5.

Stark, S. M., Stevenson, R., Wu, C., Rutledge, S., and Stark, C. E. L. (2015). Stability of age-related deficits in the mnemonic similarity task across task variations. *Behav. Neurosci.* 129, 257–68. doi:10.1037/bne0000055.

Stark, S. M., Yassa, M. A., Lacy, J. W., and Stark, C. E. L. (2013). A task to assess behavioral pattern separation (BPS) in humans: Data from healthy aging and mild cognitive impairment. *Neuropsychologia* 51, 2442–9. doi:10.1016/j.neuropsychologia.2012.12.014.

Stark, S. M., Yassa, M. A., and Stark, C. E. L. (2010). Individual differences in spatial pattern separation performance associated with healthy aging in humans. *Learn. Mem.* 17, 284–8. doi:10.1101/lm.1768110.

Stefanetti, R. J., Voisin, S., Russell, A., and Lamon, S. (2018). Recent advances in understanding the role of FOXO3. *F1000Research* 7, 1372. doi:10.12688/f1000research.15258.1.

Stein, L. R., and Imai, S. (2014). Specific ablation of Nampt in adult neural stem cells recapitulates their functional defects during aging. *EMBO J.* 33, 1321–40. doi:10.1002/embj.201386917.

Steinmetz, A. B., Johnson, S. A., Iannitelli, D. E., Pollonini, G., and Alberini, C. M. (2016). Insulin-like growth factor 2 rescues aging-related memory loss in rats. *Neurobiol. Aging* 44, 9–21. doi:10.1016/j.neurobiolaging.2016.04.006.

Steves, C. J., Jackson, S. H. D., and Spector, T. D. (2013). Cognitive change in older women using a computerised battery: a longitudinal quantitative genetic twin study. *Behav. Genet.* 43, 468–79. doi:10.1007/s10519-013-9612-z.

Suh, Y., Atzmon, G., Cho, M.-O., Hwang, D., Liu, B., Leahy, D. J., et al. (2008). Functionally significant insulin-like growth factor I receptor mutations in centenarians. *Proc. Natl. Acad. Sci. U. S. A.* 105, 3438–42. doi:10.1073/pnas.0705467105.

Sujkowski, A., Bazzell, B., Carpenter, K., Arking, R., and Wessells, R. J. (2015). Endurance exercise and selective breeding for longevity extend Drosophila healthspan by overlapping mechanisms. *Aging (Albany. NY).* 7, 535–52. doi:10.18632/aging.100789.

Sun, H., Xu, L., Yu, P., Jiang, J., Zhang, G., and Wang, Y. (2010). Synthesis and preliminary evaluation of neuroprotection of celastrol analogues in PC12 cells. *Bioorg. Med. Chem. Lett.* 20, 3844–3847. doi:10.1016/j.bmcl.2010.05.066.

Suzanne Barker-Collo, Hamish Bartle, Annabel Clarke, Annik van Toledo, Helen Vykopal, and Amanda Willetts (2008). Premorbid Estimations in New Zealand.

Taguchi, A., Wartschow, L. M., and White, M. F. (2007). Brain IRS2 signaling coordinates life span and nutrient homeostasis. *Science* 317, 369–72. doi:10.1126/science.1142179.

Talpos, J. C., Winters, B. D., Dias, R., Saksida, L. M., and Bussey, T. J. (2009). A novel touchscreen-automated paired-associate learning (PAL) task sensitive to pharmacological manipulation of the hippocampus: a translational rodent model of cognitive impairments in neurodegenerative disease. *Psychopharmacology (Berl).* 205, 157–168. doi:10.1007/s00213-009-1526-3.

Tan, F. C. C., Hutchison, E. R., Eitan, E., and Mattson, M. P. (2014). Are there roles for brain cell senescence in aging and neurodegenerative disorders? *Biogerontology* 15, 643–60. doi:10.1007/s10522-014-9532-1.

Tan, P., Wang, Y.-J., Li, S., Wang, Y., He, J.-Y., Chen, Y.-Y., et al. (2016). The PI3K/Akt/mTOR pathway regulates the replicative senescence of human VSMCs. *Mol. Cell. Biochem.* 422, 1–10. doi:10.1007/s11010-016-2796-9.

Tangney, C. C., Kwasny, M. J., Li, H., Wilson, R. S., Evans, D. A., and Morris, M. C. (2011). Adherence to a Mediterranean-type dietary pattern and cognitive decline in a community population. *Am. J. Clin. Nutr.* 93, 601–607. doi:10.3945/ajcn.110.007369.

Taormina, G., and Mirisola, M. G. (2014). Calorie restriction in mammals and simple model organisms. *Biomed Res. Int.* 2014, 308690. doi:10.1155/2014/308690.

Tashiro, A., Makino, H., and Gage, F. H. (2007). Experience-specific functional modification of the dentate gyrus through adult neurogenesis: a critical period during an immature

stage. *J. Neurosci.* 27, 3252–9. doi:10.1523/JNEUROSCI.4941-06.2007.

Teschendorff, A. E., Marabita, F., Lechner, M., Bartlett, T., Tegner, J., Gomez-Cabrero, D., et al. (2013). A beta-mixture quantile normalization method for correcting probe design bias in Illumina Infinium 450 k DNA methylation data. *Bioinformatics* 29, 189–196. doi:10.1093/bioinformatics/bts680.

Teumer, A., Qi, Q., Nethander, M., Aschard, H., Bandinelli, S., Beekman, M., et al. (2016). Genomewide meta-analysis identifies loci associated with IGF-I and IGFBP-3 levels with impact on age-related traits. *Aging Cell* 15, 811–24. doi:10.1111/acel.12490.

Thoreen, C. C., Kang, S. A., Chang, J. W., Liu, Q., Zhang, J., Gao, Y., et al. (2009). An ATP-competitive Mammalian Target of Rapamycin Inhibitor Reveals Rapamycin-resistant Functions of mTORC1. *J. Biol. Chem.* 284, 8023–8032. doi:10.1074/jbc.M900301200.

Toledo, E., Salas-Salvadó, J., Donat-Vargas, C., Buil-Cosiales, P., Estruch, R., Ros, E., et al. (2015). Mediterranean Diet and Invasive Breast Cancer Risk Among Women at High Cardiovascular Risk in the PREDIMED Trial. *JAMA Intern. Med.* 175, 1752. doi:10.1001/jamainternmed.2015.4838.

Trehearne, A. (2016). Genetics, lifestyle and environment. UK Biobank is an open access resource following the lives of 500,000 participants to improve the health of future generations. *Bundesgesundheitsblatt - Gesundheitsforsch. - Gesundheitsschutz* 59, 361–367. doi:10.1007/s00103-015-2297-0.

Tucker, A. M., and Stern, Y. (2011). Cognitive reserve in aging. *Curr. Alzheimer Res.* 8, 354–60.

Tuohimaa, P. (2009). Vitamin D and aging. *J. Steroid Biochem. Mol. Biol.* 114, 78–84.

Uday Bhanu, M., Mandraju, R. K., Bhaskar, C., and Kondapi, A. K. (2010). Cultured cerebellar granule neurons as an in vitro aging model: Topoisomerase IIβ as an additional biomarker in DNA repair and aging. *Toxicol. Vitr.* 24, 1935–1945. doi:10.1016/J.TIV.2010.08.003.

Unoki, M., and Nakamura, Y. (2001). Growth-suppressive effects of BPOZ and EGR2, two genes involved in the PTEN signaling pathway. *Oncogene* 20, 4457–4465. doi:10.1038/sj.onc.1204608.

Valente, T., Hidalgo, J., Bolea, I., Ramirez, B., Anglés, N., Reguant, J., et al. (2009). A Diet Enriched in Polyphenols and Polyunsaturated Fatty Acids, LMN Diet, Induces

Neurogenesis in the Subventricular Zone and Hippocampus of Adult Mouse Brain. *J. Alzheimer's Dis.* 18, 849–865. doi:10.3233/JAD-2009-1188.

Valls-Pedret, C., Lamuela-Raventós, R. M., Medina-Remón, A., Quintana, M., Corella, D., Pintó, X., et al. (2012). Polyphenol-Rich Foods in the Mediterranean Diet are Associated with Better Cognitive Function in Elderly Subjects at High Cardiovascular Risk. *J. Alzheimer's Dis.* 29, 773–782. doi:10.3233/JAD-2012-111799.

van den Berg, N., Beekman, M., Smith, K. R., Janssens, A., and Slagboom, P. E. (2017). Historical demography and longevity genetics: Back to the future. *Ageing Res. Rev.* 38, 28–39. doi:10.1016/j.arr.2017.06.005.

van der Flier, W. M., and Scheltens, P. (2005). Epidemiology and risk factors of dementia. *J. Neurol. Neurosurg. Psychiatry* 76 Suppl 5, v2-7. doi:10.1136/jnnp.2005.082867.

van der Spoel, E., Jansen, S. W., Akintola, A. A., Ballieux, B. E., Cobbaert, C. M., Slagboom, P. E., et al. (2016). Growth hormone secretion is diminished and tightly controlled in humans enriched for familial longevity. *Aging Cell* 15, 1126–1131. doi:10.1111/acel.12519.

van der Veer, E., Ho, C., O'Neil, C., Barbosa, N., Scott, R., Cregan, S. P., et al. (2007). Extension of human cell lifespan by nicotinamide phosphoribosyltransferase. *J. Biol. Chem.* 282, 10841–5. doi:10.1074/jbc.C700018200.

van Heemst, D. (2010). Insulin, IGF-1 and longevity. *Aging Dis.* 1, 147–57.

Van Petten, C. (2004). Relationship between hippocampal volume and memory ability in healthy individuals across the lifespan: review and meta-analysis. *Neuropsychologia* 42, 1394–1413. doi:10.1016/J.NEUROPSYCHOLOGIA.2004.04.006.

van Praag, H., Shubert, T., Zhao, C., and Gage, F. H. (2005). Exercise enhances learning and hippocampal neurogenesis in aged mice. *J. Neurosci.* 25, 8680–5. doi:10.1523/JNEUROSCI.1731-05.2005.

Van Rooij, J. G. M., Veeger, M. M. S., Bodelier-Bade, M. M., Scheepers, P. T. J., and Jongeneelen, F. J. (1994). Smoking and dietary intake of polycyclic aromatic hydrocarbons as sources of interindividual variability in the baseline excretion of 1-hydroxypyrene in urine. *Int. Arch. Occup. Environ. Health* 66, 55–65. doi:10.1007/BF00386580.

Vaynman, S., and Gomez-Pinilla, F. (2006). Revenge of the "Sit": How lifestyle impacts

neuronal and cognitive health through molecular systems that interface energy metabolism with neuronal plasticity. *J. Neurosci. Res.* 84, 699–715. doi:10.1002/jnr.20979.

Vaynman, S., Ying, Z., and Gomez-Pinilla, F. (2004). Hippocampal BDNF mediates the efficacy of exercise on synaptic plasticity and cognition. *Eur. J. Neurosci.* 20, 2580–2590. doi:10.1111/j.1460-9568.2004.03720.x.

Verburgh, K. (2015). Nutrigerontology: why we need a new scientific discipline to develop diets and guidelines to reduce the risk of aging-related diseases. *Aging Cell* 14, 17–24. doi:10.1111/acel.12284.

Villeda, S. A., Luo, J., Mosher, K. I., Zou, B., Britschgi, M., Bieri, G., et al. (2011). The ageing systemic milieu negatively regulates neurogenesis and cognitive function. *Nature* 477, 90–4. doi:10.1038/nature10357.

Villeda, S. A., Plambeck, K. E., Middeldorp, J., Castellano, J. M., Mosher, K. I., Luo, J., et al. (2014). Young blood reverses age-related impairments in cognitive function and synaptic plasticity in mice. *Nat. Med.* 20, 659–663. doi:10.1038/nm.3569.

Villena, A., Díaz, F., Requena, V., Chavarría, I., Rius, F., and Perez de Vargas, I. (1997). Quantitative morphological changes in neurons from the dorsal lateral geniculate nucleus of young and old rats. *Anat. Rec.* 248, 137–141. doi:10.1002/(SICI)1097-0185(199705)248:1<137::AID-AR16>3.0.CO;2-Q.

Vomund, S., Schäfer, A., Parnham, M. J., Brüne, B., and von Knethen, A. (2017). Nrf2, the Master Regulator of Anti-Oxidative Responses. *Int. J. Mol. Sci.* 18. doi:10.3390/ijms18122772.

von Bohlen und Halbach, O. (2011). Immunohistological markers for proliferative events, gliogenesis, and neurogenesis within the adult hippocampus. *Cell Tissue Res.* 345, 1–19. doi:10.1007/s00441-011-1196-4.

Walker, G., Houthoofd, K., Vanfleteren, J. R., and Gems, D. (2005). Dietary restriction in C. elegans: From rate-of-living effects to nutrient sensing pathways. *Mech. Ageing Dev.* 126, 929–937. doi:10.1016/J.MAD.2005.03.014.

Wallace, D. C. (2005). A Mitochondrial Paradigm of Metabolic and Degenerative Diseases, Aging, and Cancer: A Dawn for Evolutionary Medicine. *Annu. Rev. Genet.* 39, 359–407. doi:10.1146/annurev.genet.39.110304.095751.

Walton, E., Hass, J., Liu, J., Roffman, J. L., Bernardoni, F., Roessner, V., et al. (2016). Correspondence of DNA Methylation Between Blood and Brain Tissue and Its Application to Schizophrenia Research. *Schizophr. Bull.* 42, 406–414. doi:10.1093/schbul/sbv074.

Walton, N. M., Shin, R., Tajinda, K., Heusner, C. L., Kogan, J. H., Miyake, S., et al. (2012). Adult Neurogenesis Transiently Generates Oxidative Stress. *PLoS One* 7, e35264. doi:10.1371/journal.pone.0035264.

Wan, H., Aggleton, J. P., and Brown, M. W. (1999). Different contributions of the hippocampus and perirhinal cortex to recognition memory. *J. Neurosci.* 19, 1142–8.

Wan, X., Li, J., Xie, X., and Lu, W. (2007). PTEN augments doxorubicin-induced apoptosis in PTEN-null Ishikawa cells. *Int. J. Gynecol. Cancer* 17, 808–812. doi:10.1111/j.1525-1438.2007.00890.x.

Wang, X., and Michaelis, E. K. (2010). Selective neuronal vulnerability to oxidative stress in the brain. *Front. Aging Neurosci.* 2, 12. doi:10.3389/fnagi.2010.00012.

Wanke, V., Cameroni, E., Uotila, A., Piccolis, M., Urban, J., Loewith, R., et al. (2008). Caffeine extends yeast lifespan by targeting TORC1. *Mol. Microbiol.* 69, 277–85. doi:10.1111/j.1365-2958.2008.06292.x.

Warner-Schmidt, J. L., and Duman, R. S. (2006). Hippocampal neurogenesis: Opposing effects of stress and antidepressant treatment. *Hippocampus* 16, 239–249. doi:10.1002/hipo.20156.

Warr, M. R., Binnewies, M., Flach, J., Reynaud, D., Garg, T., Malhotra, R., et al. (2013). FOXO3A directs a protective autophagy program in haematopoietic stem cells. *Nature* 494, 323–7. doi:10.1038/nature11895.

Waterland, R. A., and Jirtle, R. L. (2003). Transposable elements: targets for early nutritional effects on epigenetic gene regulation. *Mol. Cell. Biol.* 23, 5293–300.

Waterland, R. A., Travisano, M., and Tahiliani, K. G. (2007). Diet-induced hypermethylation at agouti viable yellow is not inherited transgenerationally through the female. *FASEB J.* 21, 3380–5. doi:10.1096/fj.07-8229com.

Watts, G. (2011). Leonard Hayflick and the limits of ageing. *Lancet* 377, 2075. doi:10.1016/S0140-6736(11)60908-2.

Wengreen, H. J., Neilson, C., Munger, R., and Corcoran, C. (2009). Diet quality is associated with better cognitive test performance among aging men and women. *J. Nutr.* 139, 1944–9. doi:10.3945/jn.109.106427.

Weuve, J., Kang, J. H., Manson, J. E., Breteler, M. M. B., Ware, J. H., and Grodstein, F. (2004). Physical Activity, Including Walking, and Cognitive Function in Older Women. *JAMA* 292, 1454. doi:10.1001/jama.292.12.1454.

White, M. F. (2015). Mapping the path to a longer life. *Nature* 524, 170–171. doi:10.1038/524170a.

Wiener, J. M., and Tilly, J. (2002). Population ageing in the United States of America: implications for public programmes. *Int. J. Epidemiol.* 31, 776–781. doi:10.1093/ije/31.4.776.

Willcox, B. J., Donlon, T. A., He, Q., Chen, R., Grove, J. S., Yano, K., et al. (2008a). FOXO3A genotype is strongly associated with human longevity. *Proc. Natl. Acad. Sci. U. S. A.* 105, 13987–92. doi:10.1073/pnas.0801030105.

Willcox, B. J., Donlon, T. A., He, Q., Chen, R., Grove, J. S., Yano, K., et al. (2008b). FOXO3A genotype is strongly associated with human longevity. *Proc. Natl. Acad. Sci.* 105, 13987–13992. doi:10.1073/pnas.0801030105.

Williams, J. W., Plassman, B. L., Burke, J., and Benjamin, S. (2010). Preventing Alzheimer's disease and cognitive decline. *Evid. Rep. Technol. Assess. (Full. Rep).*, 1–727.

Wilson, H. K., Canfield, S. G., Hjortness, M. K., Palecek, S. P., and Shusta, E. V (2015). Exploring the effects of cell seeding density on the differentiation of human pluripotent stem cells to brain microvascular endothelial cells. *Fluids Barriers CNS* 12, 13. doi:10.1186/s12987-015-0007-9.

Wilson, I. A., Ikonen, S., Gallagher, M., Eichenbaum, H., and Tanila, H. (2005). Age-Associated Alterations of Hippocampal Place Cells Are Subregion Specific. *J. Neurosci.* 25, 6877–6886. doi:10.1523/JNEUROSCI.1744-05.2005.

Wilson, I. A., Ikonen, S., Gureviciene, I., McMahan, R. W., Gallagher, M., Eichenbaum, H., et al. (2004). Cognitive Aging and the Hippocampus: How Old Rats Represent New Environments. *J. Neurosci.* 24, 3870–3878. doi:10.1523/JNEUROSCI.5205-03.2004.

Wilson, V., and Jones, P. (1983). DNA methylation decreases in aging but not in immortal cells. *Science (80-.).* 220, 1055–1057. doi:10.1126/science.6844925.

Wimmer, M. E., Hernandez, P. J., Blackwell, J., and Abel, T. (2012). Aging impairs hippocampus-dependent long-term memory for object location in mice. *Neurobiol. Aging* 33, 2220–2224. doi:10.1016/J.NEUROBIOLAGING.2011.07.007.

Winner, B., Kohl, Z., and Gage, F. H. (2011). Neurodegenerative disease and adult neurogenesis. *Eur. J. Neurosci.* 33, 1139–51. doi:10.1111/j.1460-9568.2011.07613.x.

Witte, A. V, Fobker, M., Gellner, R., Knecht, S., and Flöel, A. (2009). Caloric restriction improves memory in elderly humans. *Proc. Natl. Acad. Sci. U. S. A.* 106, 1255–60. doi:10.1073/pnas.0808587106.

Wright, W. E., and Shay, J. W. (2002). Historical claims and current interpretations of replicative aging. *Nat. Biotechnol.* 20, 682–688. doi:10.1038/nbt0702-682.

Wu, H., Coskun, V., Tao, J., Xie, W., Ge, W., Yoshikawa, K., et al. (2010). Dnmt3a-dependent nonpromoter DNA methylation facilitates transcription of neurogenic genes. *Science* 329, 444–8. doi:10.1126/science.1190485.

Yan, X., Himburg, H. A., Pohl, K., Quarmyne, M., Tran, E., Zhang, Y., et al. (2016). Deletion of the Imprinted Gene Grb10 Promotes Hematopoietic Stem Cell Self-Renewal and Regeneration. *Cell Rep.* 17, 1584–1594. doi:10.1016/j.celrep.2016.10.025.

Yang, T.-T., Lo, C.-P., Tsai, P.-S., Wu, S.-Y., Wang, T.-F., Chen, Y.-W., et al. (2015). Aging and Exercise Affect Hippocampal Neurogenesis via Different Mechanisms. *PLoS One* 10, e0132152. doi:10.1371/journal.pone.0132152.

Yankner, B. A., Lu, T., and Loerch, P. (2008). The Aging Brain. *Annu. Rev. Pathol. Mech. Dis.* 3, 41–66. doi:10.1146/annurev.pathmechdis.2.010506.092044.

Yassa, M. A., and Stark, C. E. L. (2011). Pattern separation in the hippocampus. *Trends Neurosci.* 34, 515–25. doi:10.1016/j.tins.2011.06.006.

Yazici, E., and Deveci, H. (2010). Factors Affecting Decomposition of Hydrogen Peroxide. in *Proceedings of the XIIth. International Mineral Processing Symposium.*

Ye, P., Li, L., Richards, R. G., DiAugustine, R. P., and D'Ercole, A. J. (2002). Myelination is altered in insulin-like growth factor-I null mutant mice. *J. Neurosci.* 22, 6041–51. doi:20026581.

Ye, X., Scott, T., Gao, X., Maras, J. E., Bakun, P. J., and Tucker, K. L. (2013). Mediterranean

Diet, Healthy Eating Index-2005, and Cognitive Function in Middle-Aged and Older Puerto Rican Adults. *J Acad Nutr Diet* 113, 276–81. doi:10.1016/j.jand.2012.10.014.

Yeo, E. . J., Hwang, Y. . C., Kang, C.-M. M., Kim, I. . H., Kim, D. . I., Parka, J. . S., et al. (2000). Senescence-like changes induced by hydroxyurea in human diploid firbroblasts. 35. doi:10.1016/S0531-5565(00)00108-X.

Yoon, J., Seo, Y., Kim, J., and Lee, I. (2012). Hippocampus is required for paired associate memory with neither delay nor trial uniqueness. *Learn. Mem.* 19, 1–8. doi:10.1101/lm.024554.111.

Yu, H., Cook, T. J., and Sinko, P. J. (1997). Evidence for diminished functional expression of intestinal transporters in Caco-2 cell monolayers at high passages. *Pharm. Res.* 14, 757–62.

Yu, K., Toral-Barza, L., Shi, C., Zhang, W.-G., Lucas, J., Shor, B., et al. (2009). Biochemical, Cellular, and In vivo Activity of Novel ATP-Competitive and Selective Inhibitors of the Mammalian Target of Rapamycin. *Cancer Res.* 69, 6232–6240. doi:10.1158/0008-5472.CAN-09-0299.

Yu, S.-W., Baek, S.-H., Brennan, R. T., Bradley, C. J., Park, S. K., Lee, Y. S., et al. (2008). Autophagic death of adult hippocampal neural stem cells following insulin withdrawal. *Stem Cells* 26, 2602–10. doi:10.1634/stemcells.2008-0153.

Yu, Y., Yoon, S.-O., Poulogiannis, G., Yang, Q., Ma, X. M., Villen, J., et al. (2011). Phosphoproteomic Analysis Identifies Grb10 as an mTORC1 Substrate That Negatively Regulates Insulin Signaling. *Science (80-.).* 332, 1322–1326. doi:10.1126/science.1199484.

Yuan, R., Tsaih, S.-W., Petkova, S. B., Marin de Evsikova, C., Xing, S., Marion, M. A., et al. (2009). Aging in inbred strains of mice: study design and interim report on median lifespans and circulating IGF1 levels. *Aging Cell* 8, 277–87. doi:10.1111/j.1474-9726.2009.00478.x.

Zeng, Y., Chen, H., Ni, T., Ruan, R., Feng, L., Nie, C., et al. (2015). GxE Interactions between FOXO Genotypes and Tea Drinking Are Significantly Associated with Cognitive Disability at Advanced Ages in China. *Journals Gerontol. Ser. A Biol. Sci. Med. Sci.* 70, 426–433. doi:10.1093/gerona/glu060.

Zhang, J., Ji, F., Liu, Y., Lei, X., Li, H., Ji, G., et al. (2014). Ezh2 regulates adult hippocampal neurogenesis and memory. *J. Neurosci.* 34, 5184–99. doi:10.1523/JNEUROSCI.4129-

13.2014.

Zhang, Y., Pak, C., Han, Y., Ahlenius, H., Zhang, Z., Chanda, S., et al. (2013). Rapid single-step induction of functional neurons from human pluripotent stem cells. *Neuron* 78, 785–98. doi:10.1016/j.neuron.2013.05.029.

Zhao, N., Zhong, C., Wang, Y., Zhao, Y., Gong, N., Zhou, G., et al. (2008). Impaired hippocampal neurogenesis is involved in cognitive dysfunction induced by thiamine deficiency at early pre-pathological lesion stage. *Neurobiol. Dis.* 29, 176–185. doi:10.1016/j.nbd.2007.08.014.

Ziegler, A. N., Levison, S. W., and Wood, T. L. (2015). Insulin and IGF receptor signalling in neural-stem-cell homeostasis. *Nat. Rev. Endocrinol.* 11, 161–70. doi:10.1038/nrendo.2014.208.

Ziegler, A. N., Schneider, J. S., Qin, M., Tyler, W. A., Pintar, J. E., Fraidenraich, D., et al. (2012). IGF-II promotes stemness of neural restricted precursors. *Stem Cells* 30, 1265–76. doi:10.1002/stem.1095.

Zillikens, M. C., van Meurs, J. B. J., Rivadeneira, F., Amin, N., Hofman, A., Oostra, B. A., et al. (2009). SIRT1 genetic variation is related to BMI and risk of obesity. *Diabetes* 58, 2828–34. doi:10.2337/db09-0536.

Zupanc, G. K. (2001). A comparative approach towards the understanding of adult neurogenesis. *Brain. Behav. Evol.* 58, 246–9. doi:10.1159/000057568.

8 Appendix

8.1 Chapter 2 appendix

8.1.1 CellInsight Parameters

Below are the tables summarising the parameters used throughout the *in vitro* experiments.

Marker	DAPI
Exposure	0.04
Smoothing	1
Thresholding	1
Segmentation	1
Object Area	30-290

Table 41 - Table showing CellInsight parameters used to select cells via DAPI staining. Nuclei stains that satisfied these parameters were selected as cells.

Marker	Exposure	Average Intensity Threshold	Mask value: Ring/ Circle
Ki67 (555 wavelength)	0.1	50	Circle = 0
Ki67 (488 wavelength)	0.03	60	Circle = 0
CC3	0.1	160	Circle = 1
SOX2	0.02	40	Circle = 0
Nestin	0.03	55	Ring = -1, 3
H2ax	0.1	100	Circle = 0
NRF2	0.08	50	Circle = 1

Table 42 - Table showing CellInsight parameters used throughout in vitro studies on proliferating cells.

Marker	Exposure	Average Intensity Threshold	Mask value: Ring/ Circle
KI67 (555 wavelength)	0.1	60	Circle = 0
Ki67 (488 wavelength)	0.06	60	Circle = 0
CC3	0.1	20	Circle = 1
MAP2	0.2	200	Ring = -1, 3
DCX	0.1	40	Circle = 3
H2AX	0.2	100	Circle = 0
NRF2	0.08	20	Circle = 1

Table 43 - Table showing CellInsight parameters used throughout *in vitro* studies on differentiating cells.

8.2 Chapter 3 appendix

8.2.1 Correlation matrix of PAL performance, cellular markers and hippocampal volumes

Below is the correlation matrix used to analyse which correlations showed significant association.

Score	Stat	CC3	Ki67	Map2	H2AX	Dcx	CellNo	Subiculum	CA1	GCLDG	CA3	CA4	Whole hippocampus
PAL1n10 recognition	Correlation (con age & edu)	0.388	-0.151	-0.510	-0.339	-0.259	0.179	-0.391	-0.554	-0.603	-0.488	-0.585	-0.621
PAL1n10 recall	Correlation (con age & edu)	0.378	-0.291	-0.311	0.083	-0.033	0.536	0.060	-0.383	-0.313	-0.277	-0.303	-0.320
CC3	Correlation (con age)							0.038	-0.256	-0.312	-0.322	-0.270	-0.216
Ki67	Correlation (con age)							-0.042	0.127	0.112	0.214	0.152	0.121
Map2	Correlation (con age)							0.079	0.107	-0.017	-0.204	-0.057	0.056
H2AX	Correlation (con age)							0.447	0.392	0.380	0.415	0.438	0.440
Dcx	Correlation (con age)							0.375	0.235	0.478	0.544	0.526	0.424
CellNo	Correlation (con age)							0.293	-0.068	-0.036	-0.240	-0.091	-0.033
Subiculum	Correlation (con age)	0.038	-0.042	0.079	0.447	0.375	0.293						
CA1	Correlation (con age)	-0.256	0.127	0.107	0.392	0.235	-0.068						
GCLDG	Correlation (con age)	-0.312	0.112	-0.017	0.380	0.478	-0.036						
CA3	Correlation (con age)	-0.322	0.214	-0.204	0.415	0.544	-0.240						
CA4	Correlation (con age)	-0.270	0.152	-0.057	0.438	0.526	-0.091						
Whole hippocampus	Correlation (con age)	-0.216	0.121	0.056	0.440	0.424	-0.033						

Legend:
p value < 0.05
p value < 0.01

Figure 72- Screenshot of correlation matrix used to summarise relevant correlations. The first column reports the first variable and columns 3-14 show the other variable being tested for association during each correlation. The second column indicates the corrections applied to each correlation: correlations involving Paired Associates Learning (PAL) were corrected for both age and education while all others were only corrected for age.

8.2.2 Non-significant associations between gene expression and cellular markers

Tables reporting the p and R values for the non-significant correlations carried out in **section 943.3.3.3**

MASH	r	p value
MASH and Ki67	0.10	0.58
MASH and CC3%	-0.342	0.075
MASH and MAP2%	0.210	0.294
MASH and DCX%	-0.008	0.969
MASH and cells/field	0.197	0.298

ETV6	r	p value
ETV6 and Ki67	0.086	0.662
ETV6 and CC3%	0.341	0.088
ETV6 and MAP2%	-0.201	0.336
ETV6 and DCX%	0.357	0.074
ETV6 and cells/field	-0.316	0.101

S6K	r	p value
S6K and Ki67	-0.067	0.734
S6K and CC3%	-0.003	0.990
S6K and MAP2%	0.181	0.386
S6K and DCX%	0.028	0.892
S6K and cells/field	0.173	0.379

EIF4E	r	p value
EIF4E and Ki67	-0.001	0.992
EIF4E and CC3%	0.029	0.887
EIF4E and MAP2%	0.265	0.200
EIF4E and DCX%	0.073	0.725
EIF4E and cells/field	0.207	0.291

4EBP1	r	p value
4EBP1 and Ki67	0.236	0.228
4EBP1 and CC3%	0.079	0.701
4EBP1 and MAP2%	-0.046	0.828
4EBP1 and DCX%	-0.221	0.279
4EBP1 and cells/field	-0.038	0.846

IRS2	r	p value
IRS2 and Ki67	-0.0003	0.999
IRS2 and CC3%	0.089	0.664
IRS2 and MAP2%	-0.113	0.592
IRS2 and DCX%	-0.052	0.801
IRS2 and cells/field	-0.341	0.076

NRIP	r	p value
NRIP and Ki67	-0.09	0.656
NRIP and CC3%	0.002	0.991
NRIP and MAP2%	-0.104	0.622
NRIP and DCX%	0.192	0.348
NRIP and cells/field	-0.190	0.333

8.2.3 Correlation of expression levels of related genes

The expression levels of genes with direct or indirect effects on each other's activity or expression were assessed for associations. Besides several interesting trends, the association of the expression levels of PTEN and GRB10 and those of mTOR and GRB10 showed significant negative and positive correlations respectively. In line with our results, GRB10 is believed to be under positive regulation by mTOR and PTEN is believed to negatively regulate mTOR activity. Though there was no significant association between PTEN and mTOR there is a clear trend towards a negative association providing further support for PTEN's negative control of the mTOR pathway and, ultimately, of GRB10.

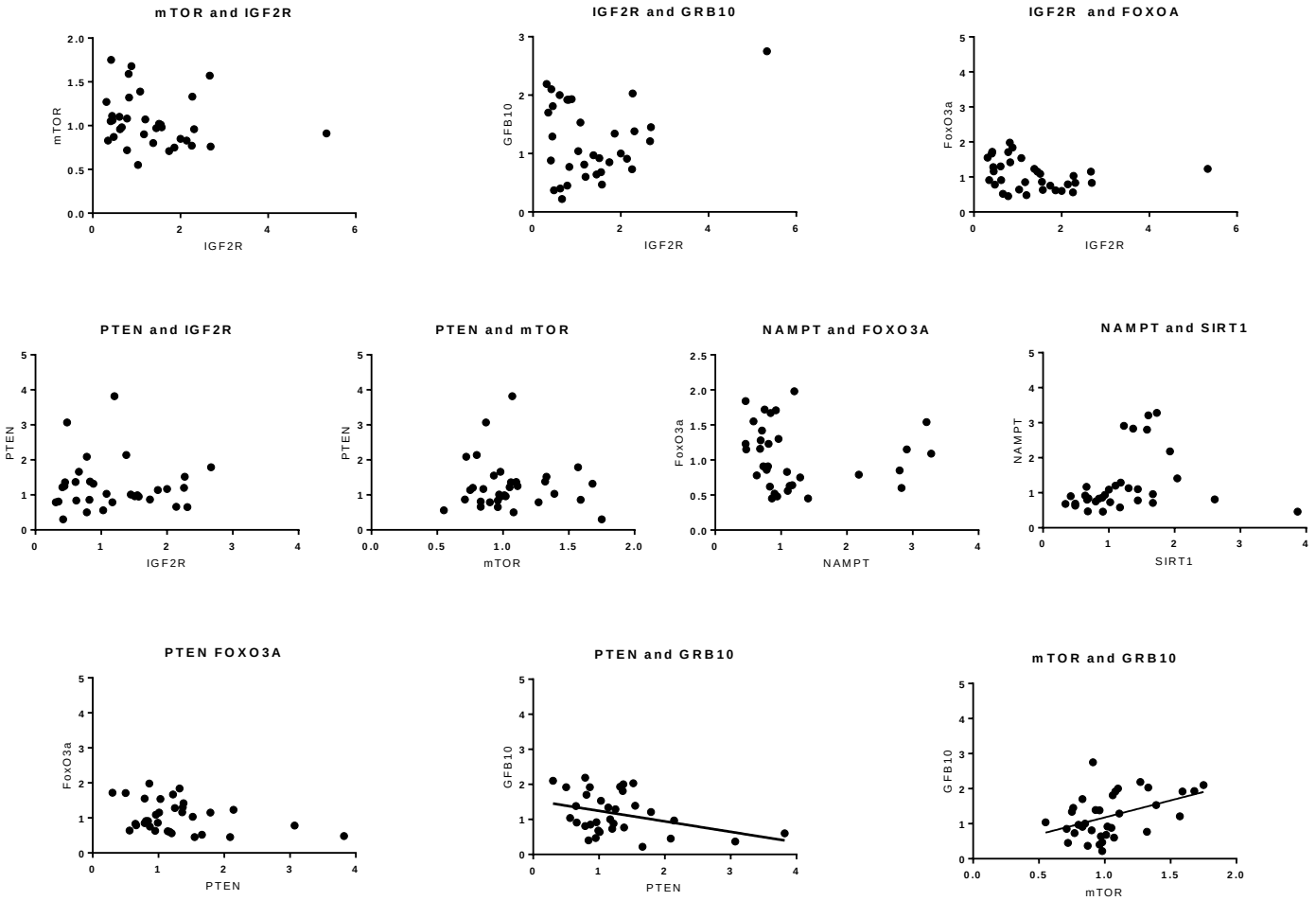

Figure 73 – Correlations between related genes. Figure showing the relationship between expression levels of genes known to alter each other's function or expression. Each dot represents the average expression levels of the genes in HPCOA07 cells after treatment with a single serum sample. Experiments were carried out in duplicates and correlation analysis was used to check for significant associations. Line of best fit indicates significant result PTEN and GRB10 expression levels were negatively correlated ($p = 0.037$, $r = -0.36$). mTOR and GRB10 expression levels instead, showed positive correlations ($p = 0.007$, $r = 0.44$)

8.3 Chapter 4 appendix

8.3.1 Methods

8.3.1.1 Machine learning methods and scripts

The scripts used for carrying out machine learning on the Columbus software can be found at the following links:

- **MAP2 machine learning script:**
  https://drive.google.com/open?id=1ZKycgPevBd1VF-OPXYAZvikF1hCXt1jr

- **DCX machine learning script:**
  https://drive.google.com/open?id=1aoNKyHhUn0q3FthzuR0CWTSirKdjLxjB

Below are the summaries of the scripts outlined in the links above.

Map2 protocol parameters summary:

Find Nuclei	**Channel :** Channel1 **ROI :** None	**Method :** M Diameter : 13 µm Splitting Coefficient : 0.4 Common Threshold : 0.4	Output Population : Nuclei
Calculate Morphology Properties	**Population :** Nuclei **Region :** Nucleus	**Method :** Standard Area Roundness	Output Properties : Nucleus
Select Population	**Population :** Nuclei	**Method :** Filter by Property Nucleus Area [µm²] : > 30	Output Population : Real Nuclei
Find Cytoplasm	**Channel :** Channel3 **Nuclei :** Real Nuclei	**Method :** A Individual Threshold : 0.15	
Calculate Intensity Properties	**Channel :** Channel3 **Population :** Real Nuclei **Region :** Cytoplasm	**Method :** Standard Mean Standard Deviation	Output Properties : Intensity map2
Select Population (2)	**Population :** Real Nuclei	**Method :** Filter by Property Intensity map2 Mean : > 160	Output Population : Selected map2 +ve
Calculate Morphology Properties (2)	**Population :** Selected map2 +ve **Region :** Cytoplasm	**Method :** Standard Area Roundness Width Length Ratio Width to Length	Output Properties : Cytoplasm
Select Population (3)	**Population :** Selected map2 +ve	**Method :** Linear Classifier Number of Classes : 2 Nucleus Area [µm²] Nucleus Roundness Intensity map2 Mean Intensity map2 StdDev Cytoplasm Area [µm²] Cytoplasm Roundness Cytoplasm Width [µm] Cytoplasm Length [µm] Cytoplasm Ratio Width to Length	Output Population A : thin Output Population B : short and round

DCX protocol parameters summary:

Find Nuclei	**Channel :** Channel1 **ROI :** None	**Method :** M Diameter : 13 µm Splitting Coefficient : 0.4 Common Threshold : 0.4	Output Population : Nuclei
Calculate Morphology Properties	**Population :** Nuclei **Region :** Nucleus	**Method :** Standard Area Roundness	Output Properties : Nucleus
Select Population	**Population :** Nuclei	**Method :** Filter by Property Nucleus Area [µm²] : > 30	Output Population : Real Nuclei
Find Cytoplasm	**Channel :** Channel2 **Nuclei :** Real Nuclei	**Method :** A Individual Threshold : 0.15	
Calculate Intensity Properties	**Channel :** Channel2 **Population :** Real Nuclei **Region :** Cytoplasm	**Method :** Standard Mean Standard Deviation	Output Properties : Intensity DCX
Select Population (2)	**Population :** Real Nuclei	**Method :** Filter by Property Intensity DCX Mean : > 95	Output Population : Selected DCX +ve
Calculate Morphology Properties (2)	**Population :** Selected DCX +ve **Region :** Cytoplasm	**Method :** Standard Area Roundness Width Length Ratio Width to Length	Output Properties : Cytoplasm
Select Population (3)	**Population :** Selected DCX +ve	**Method :** Linear Classifier Number of Classes : 2 Nucleus Area [µm²] Nucleus Roundness Intensity DCX Mean Intensity DCX StdDev Cytoplasm Area [µm²] Cytoplasm Roundness Cytoplasm Width [µm] Cytoplasm Length [µm] Cytoplasm Ratio Width to Length	Output Population A : Elongated Output Population B : Stubby

8.3.2 Results

8.3.2.1 Cellular marker expression after varying treatment concentrations

8.3.2.1.1 Proliferation

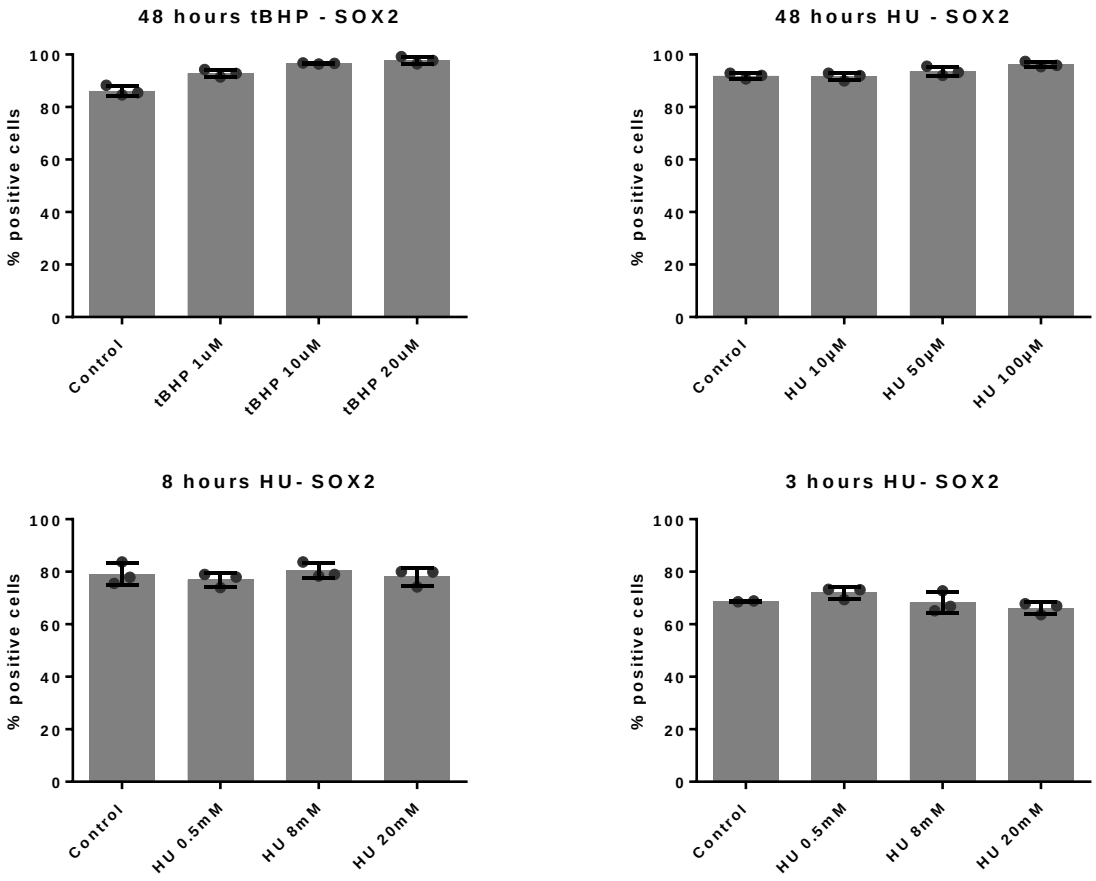

Figure 74 - Proliferation assay: Percentage of SOX2 positive cells with varying tert-Butyl hydroperoxide (tBHP) and hydroxyurea (HU) concentrations. Graphs showing the resulting percentage of SOX2 positive cells following various treatments during the human progenitor cell proliferation assay. The top row shows standard incubation periods of 48 hours. The left graph shows the percentage of SOX2 positive cells with increasing tBHP concentrations (1µM, 10µM and 20 µM) compared to controls treated with media only. The graph on the right shows the percentage of SOX2 positive cells with increasing HU concentrations (10µM, 50 µM, 100µM). The bottom row shows the percentage of SOX2 positive cells following shorter incubation periods with HU; 8-hour incubation on the left and 3-hour incubation on the right. In all cases, cells were fixed 72 hours after seeding. Standard deviation is reported as error bars. Each dot represents a technical replicate. 3 technical replicates are shown.

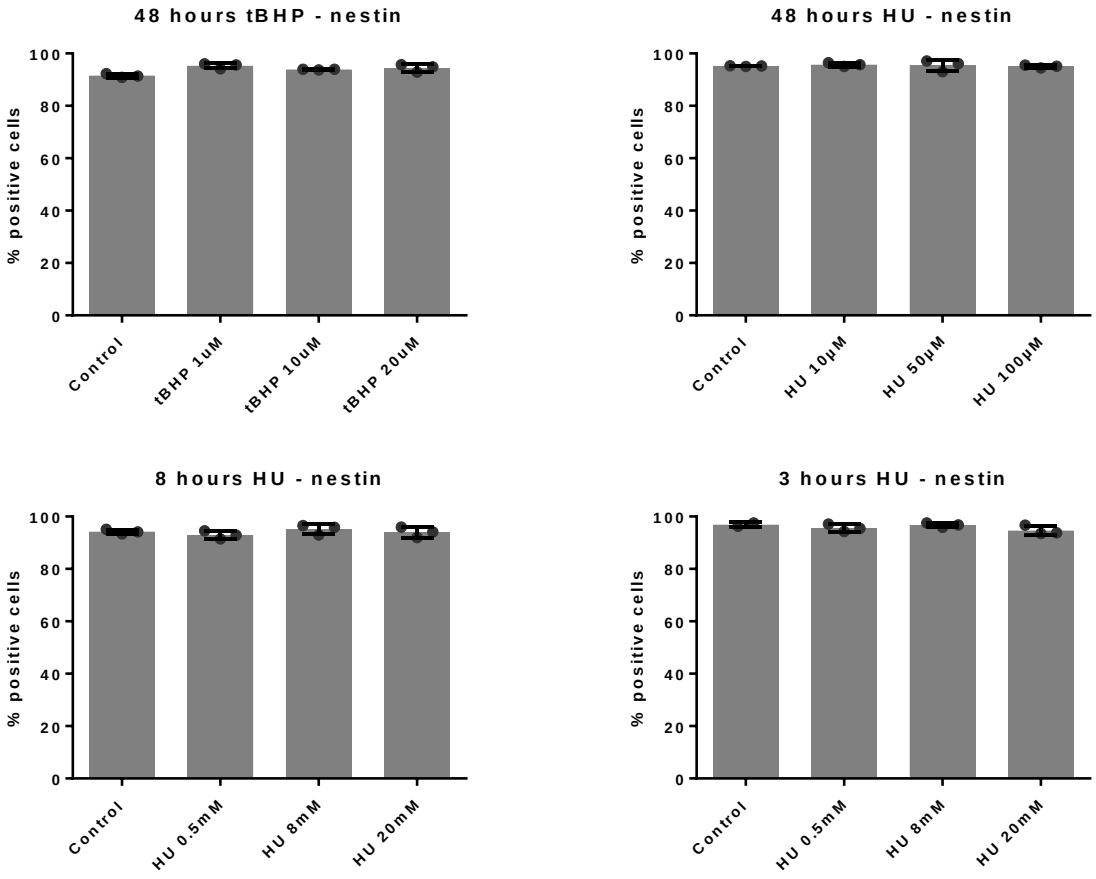

Figure 75 - Proliferation assay: Percentage of nestin positive cells with varying tert-Butyl hydroperoxide (tBHP) and hydroxyurea (HU) concentrations. Graphs showing the resulting percentage of nestin positive cells following various treatments during the human progenitor cell proliferation assay. The top row shows standard incubation periods of 48 hours. The left graph shows the percentage of nestin positive cells with increasing tBHP concentrations (1µM, 10µM and 20 µM) compared to controls treated with media only. The graph on the right shows the percentage of nestin positive cells with increasing HU concentrations (10µM, 50 µM, 100µM). The bottom row shows the percentage of nestin positive cells following shorter incubation periods with HU; 8-hour incubation on the left and 3-hour incubation on the right. In all cases, cells were fixed 72 hours after seeding. Standard deviation is reported as error bars. Each dot represents a technical replicate. 3 technical replicates are shown.

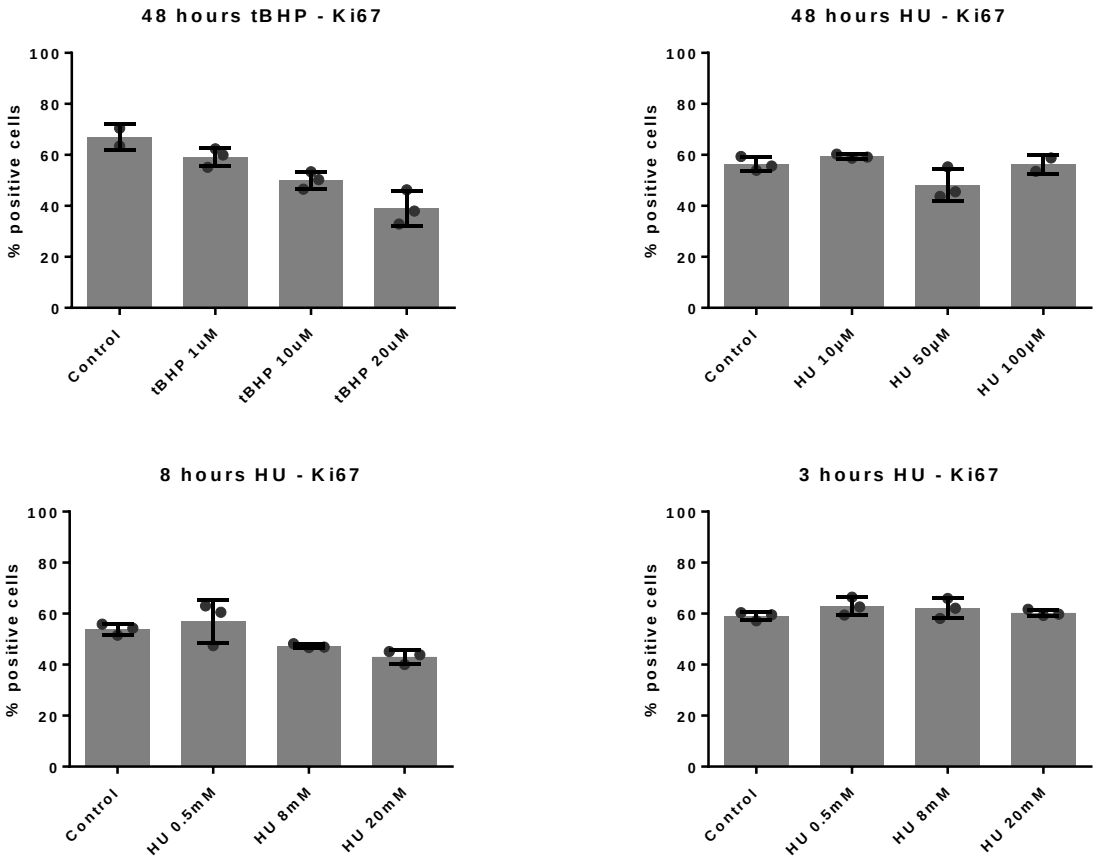

Figure 76 - Proliferation assay: Percentage of Ki67 positive cells with varying tert-Butyl hydroperoxide (tBHP) and hydroxyurea (HU) concentrations. Graphs showing the resulting percentage of Ki67 positive cells following various treatments during the human progenitor cell proliferation assay. The top row shows standard incubation periods of 48 hours. The left graph shows the percentage of Ki67 positive cells with increasing tBHP concentrations (1µM, 10µM and 20 µM) compared to controls treated with media only. The graph on the right shows the percentage of Ki67 positive cells with increasing HU concentrations (10µM, 50 µM, 100µM). The bottom row shows the percentage of Ki67 positive cells following shorter incubation periods with HU; 8-hour incubation on the left and 3-hour incubation on the right. In all cases, cells were fixed 72 hours after seeding. Standard deviation is reported as error bars. Each dot represents a technical replicate. 3 technical replicates are shown.

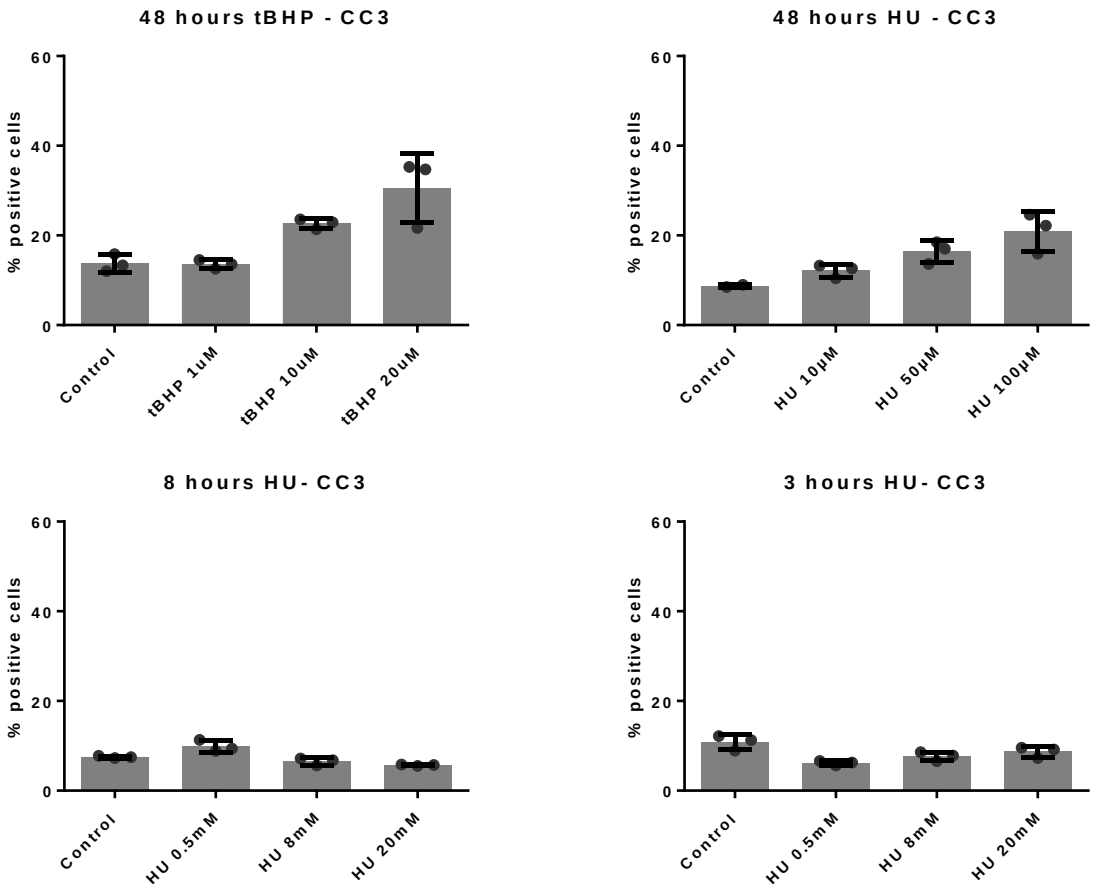

Figure 77 - **Proliferation assay: Percentage of CC3 positive cells with varying tert-Butyl hydroperoxide (tBHP) and hydroxyurea (HU) concentrations.** Graphs showing the resulting percentage of CC3 positive cells following various treatments during the human progenitor cell proliferation assay. The top row shows standard incubation periods of 48 hours. The left graph shows the percentage of CC3 positive cells with increasing tBHP concentrations (1µM, 10µM and 20 µM) compared to controls treated with media only. The graph on the right shows the percentage of CC3 positive cells with increasing HU concentrations (10µM, 50 µM, 100µM). The bottom row shows the percentage of CC3 positive cells following shorter incubation periods with HU; 8-hour incubation on the left and 3-hour incubation on the right. In all cases, cells were fixed 72 hours after seeding. Standard deviation is reported as error bars. Each dot represents a technical replicate. 3 technical replicates are shown.

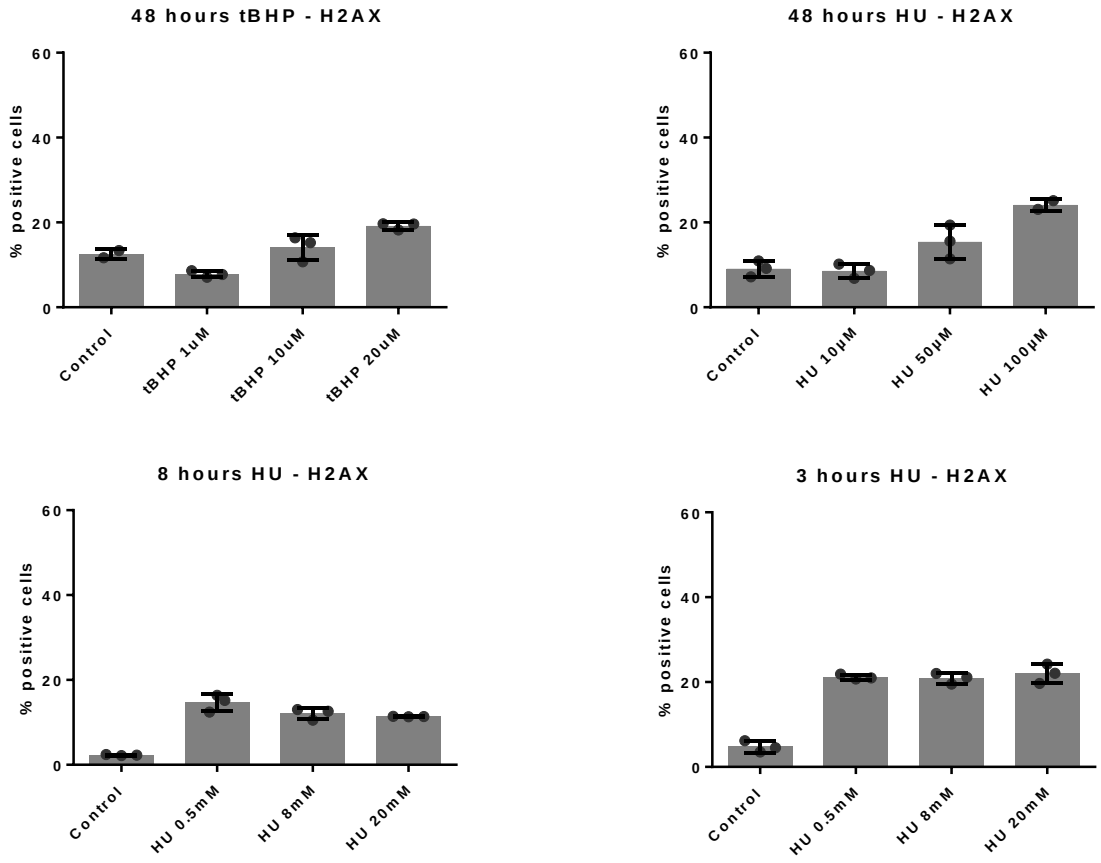

Figure 78 - Proliferation assay: Percentage of H2AX positive cells with varying tert-Butyl hydroperoxide (tBHP) and hydroxyurea (HU) concentrations. Graphs showing the resulting percentage of H2AX positive cells following various treatments during the human progenitor cell proliferation assay. The top row shows standard incubation periods of 48 hours. The left graph shows the percentage of H2AX positive cells with increasing tBHP concentrations (1µM, 10µM and 20 µM) compared to controls treated with media only. The graph on the right shows the percentage of H2AX positive cells with increasing HU concentrations (10µM, 50 µM, 100µM). The bottom row shows the percentage of H2AX positive cells following shorter incubation periods with HU; 8-hour incubation on the left and 3-hour incubation on the right. In all cases, cells were fixed 72 hours after seeding. Standard deviation is reported as error bars. Each dot represents a technical replicate. 3 technical replicates are shown.

8.3.2.1.2 Differentiation

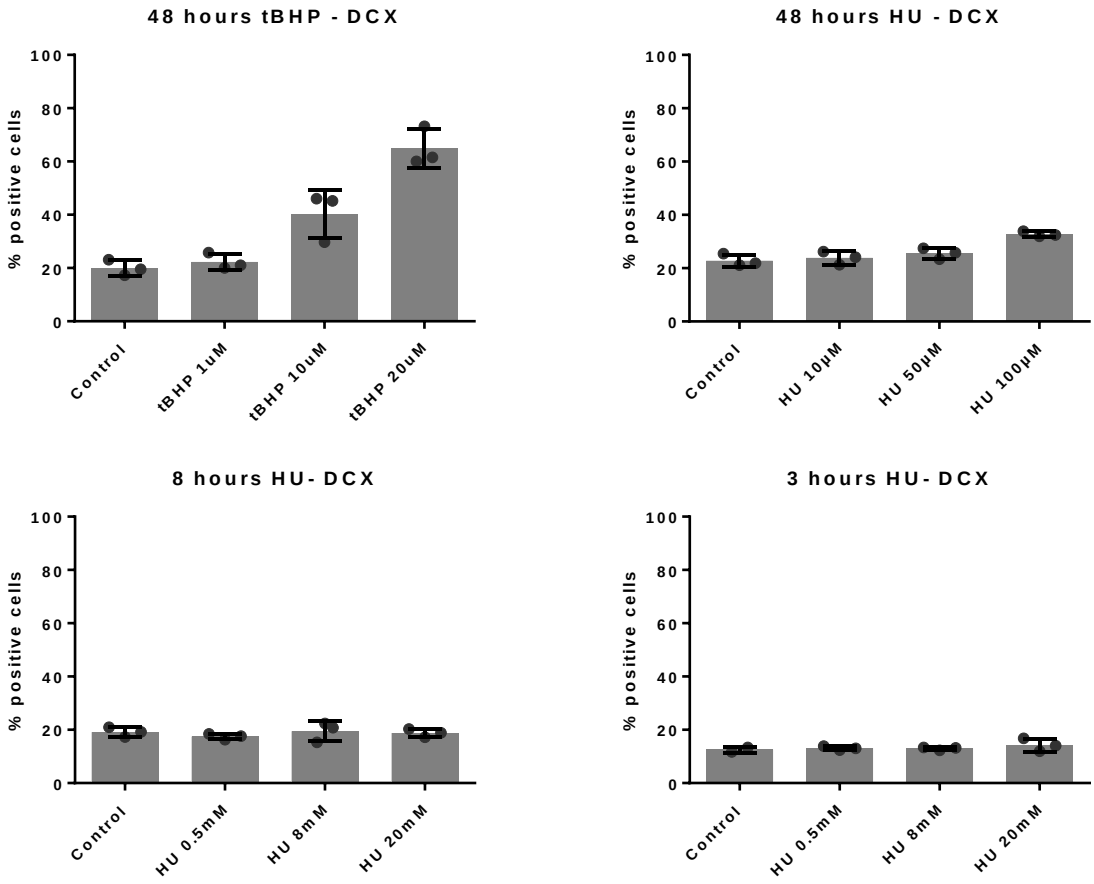

Figure 79 - Differentiation assay: Percentage of DCX positive cells with varying tert-Butyl hydroperoxide (tBHP) and hydroxyurea (HU) concentrations Graphs showing the resulting percentage of DCX positive cells following various treatments during the human progenitor cell differentiation assay. The top row shows standard incubation periods of 48 hours. The left graph shows the percentage of DCX positive cells with increasing tBHP concentrations (1µM, 10µM and 20 µM) compared to controls treated with media only. The graph on the right shows the percentage of DCX positive cells with increasing HU concentrations (10µM, 50 µM, 100µM). The bottom row shows the percentage of DCX positive cells following shorter incubation periods with HU; 8-hour incubation on the left and 3-hour incubation on the right. In all cases, cells were not treated during the proliferation assay (72 hours). They were then either washed and treated at the 72 hour timepoint and left to differentiate for a further 7 days or washed at the 72 hour timepoint and allowed to differentiate in media only conditions until treatment 8 or 3 hours prior to fixing. Cells were always fixed 9 days after seeding. Standard deviation is reported as error bars. Each dot represents a technical replicate. 12 technical replicates are shown.

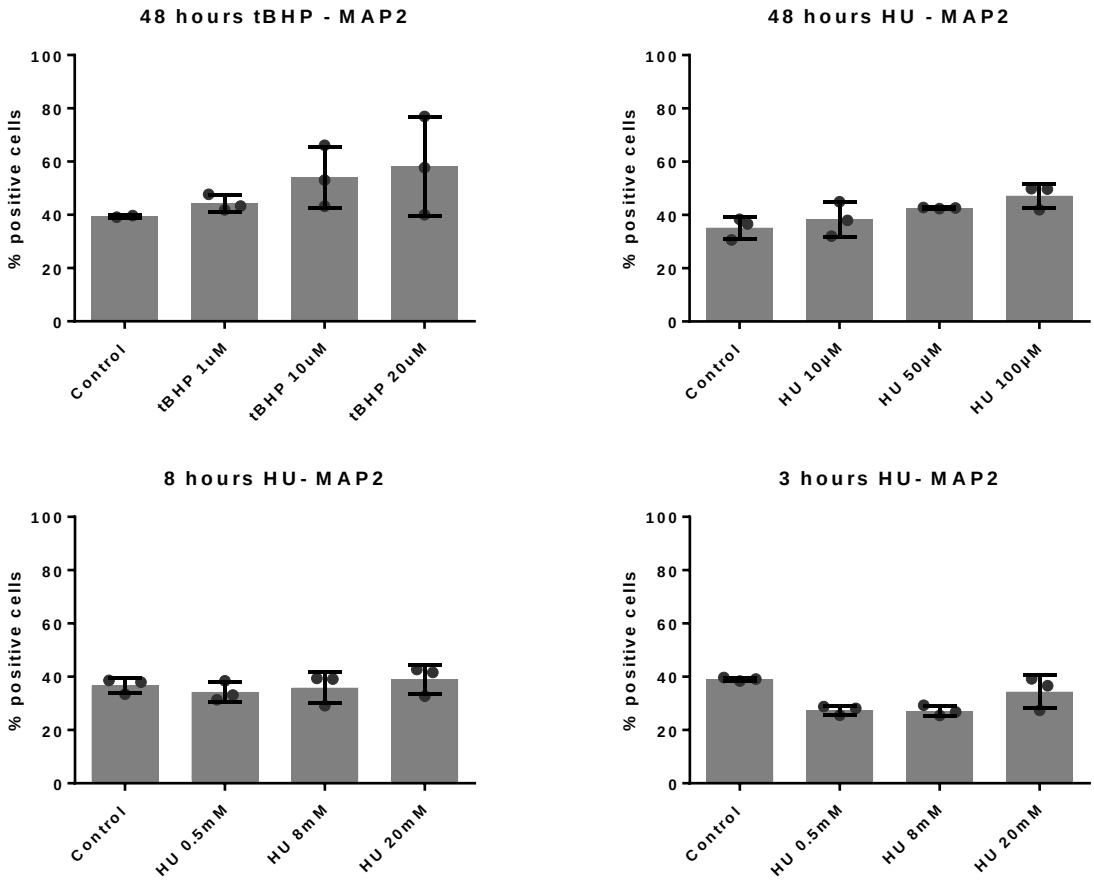

Figure 80- Differentiation assay: Percentage of MAP2 positive cells with varying tert-Butyl hydroperoxide (tBHP) and hydroxyurea (HU) concentrations Graphs showing the resulting percentage of MAP2 positive cells following various treatments during the human progenitor cell differentiation assay. The top row shows standard incubation periods of 48 hours. The left graph shows the percentage of MAP2 positive cells with increasing tBHP concentrations (1µM, 10µM and 20 µM) compared to controls treated with media only. The graph on the right shows the percentage of MAP2 positive cells with increasing HU concentrations (10µM, 50 µM, 100µM). The bottom row shows the percentage of MAP2 positive cells following shorter incubation periods with HU; 8-hour incubation on the left and 3-hour incubation on the right. In all cases, cells were not treated during the proliferation assay (72 hours). They were then either washed and treated at the 72 hour timepoint and left to differentiate for a further 7 days or washed at the 72 hour timepoint and allowed to differentiate in media only conditions until treatment 8 or 3 hours prior to fixing. Cells were always fixed 9 days after seeding. Standard deviation is reported as error bars. Each dot represents a technical replicate. 12 technical replicates are shown.

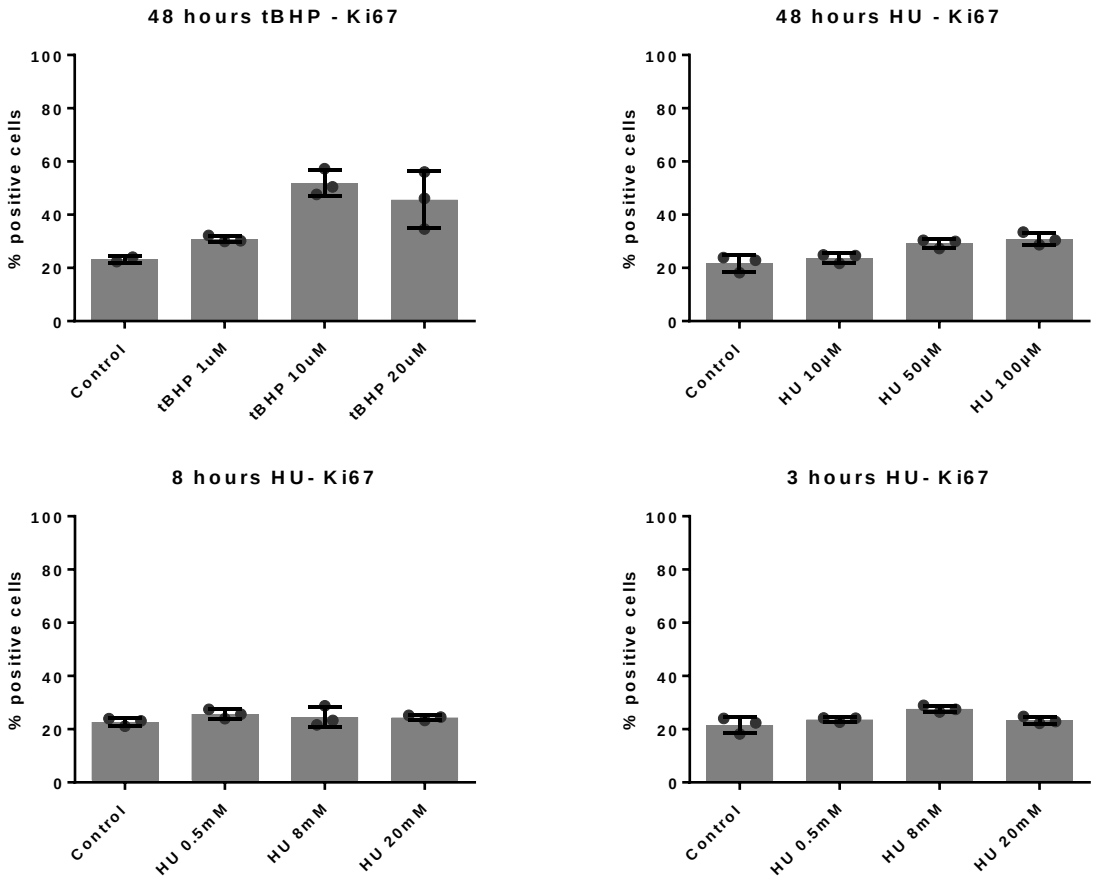

Figure 81 - Differentiation assay: Percentage of Ki67 positive cells with varying tert-Butyl hydroperoxide (tBHP) and hydroxyurea (HU) concentrations Graphs showing the resulting percentage of Ki67 positive cells following various treatments during the human progenitor cell differentiation assay. The top row shows standard incubation periods of 48 hours. The left graph shows the percentage of Ki67 positive cells with increasing tBHP concentrations (1µM, 10µM and 20 µM) compared to controls treated with media only. The graph on the right shows the percentage of Ki67 positive cells with increasing HU concentrations (10µM, 50 µM, 100µM). The bottom row shows the percentage of Ki67 positive cells following shorter incubation periods with HU; 8-hour incubation on the left and 3-hour incubation on the right. In all cases, cells were not treated during the proliferation assay (72 hours). They were then either washed and treated at the 72 hour timepoint and left to differentiate for a further 7 days or washed at the 72 hour timepoint and allowed to differentiate in media only conditions until treatment 8 or 3 hours prior to fixing. Cells were always fixed 9 days after seeding. Standard deviation is reported as error bars. Each dot represents a technical replicate. 12 technical replicates are shown.

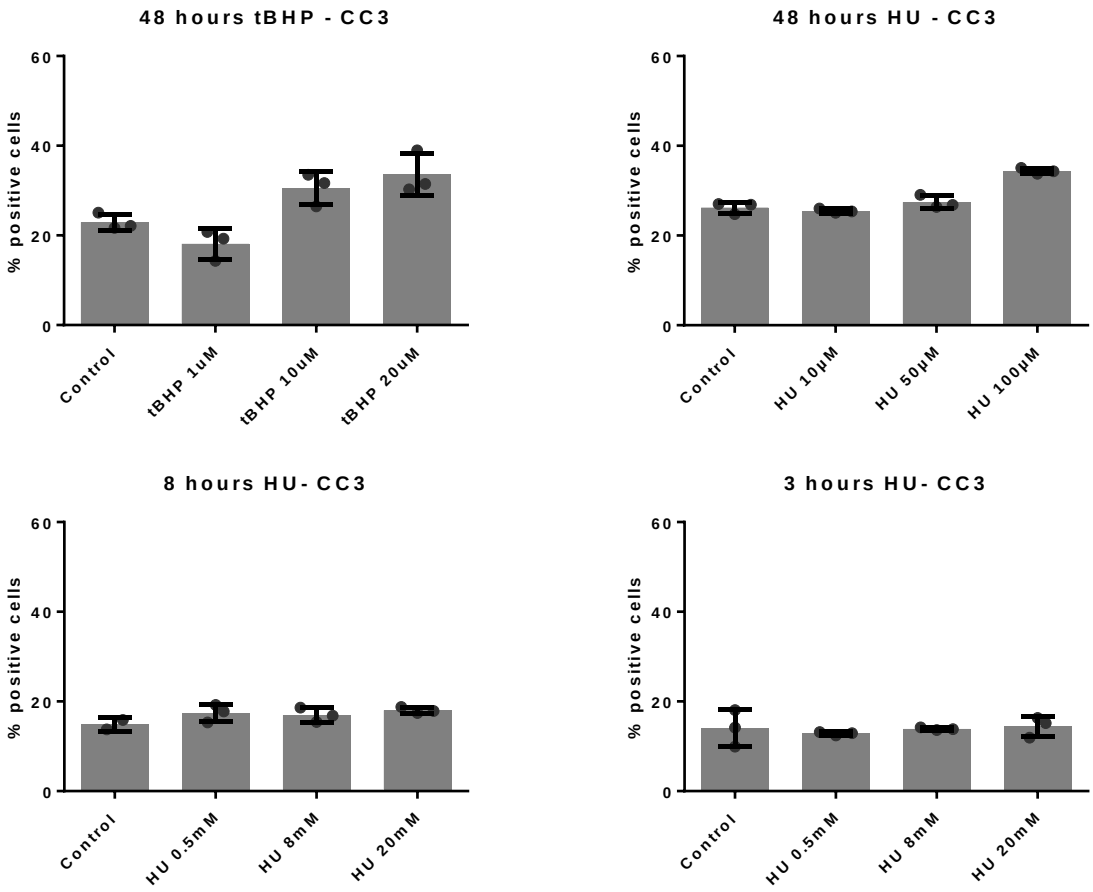

Figure 82 - Differentiation assay: Percentage of CC3 positive cells with varying tert-Butyl hydroperoxide (tBHP) and hydroxyurea (HU) concentrations Graphs showing the resulting percentage of CC3 positive cells following various treatments during the human progenitor cell differentiation assay. The top row shows standard incubation periods of 48 hours. The left graph shows the percentage of CC3 positive cells with increasing tBHP concentrations (1µM, 10µM and 20 µM) compared to controls treated with media only. The graph on the right shows the percentage of CC3 positive cells with increasing HU concentrations (10µM, 50 µM, 100µM). The bottom row shows the percentage of CC3 positive cells following shorter incubation periods with HU; 8-hour incubation on the left and 3-hour incubation on the right. In all cases, cells were not treated during the proliferation assay (72 hours). They were then either washed and treated at the 72 hour timepoint and left to differentiate for a further 7 days or washed at the 72 hour timepoint and allowed to differentiate in media only conditions until treatment 8 or 3 hours prior to fixing. Cells were always fixed 9 days after seeding. Standard deviation is reported as error bars. Each dot represents a technical replicate. 12 technical replicates are shown.

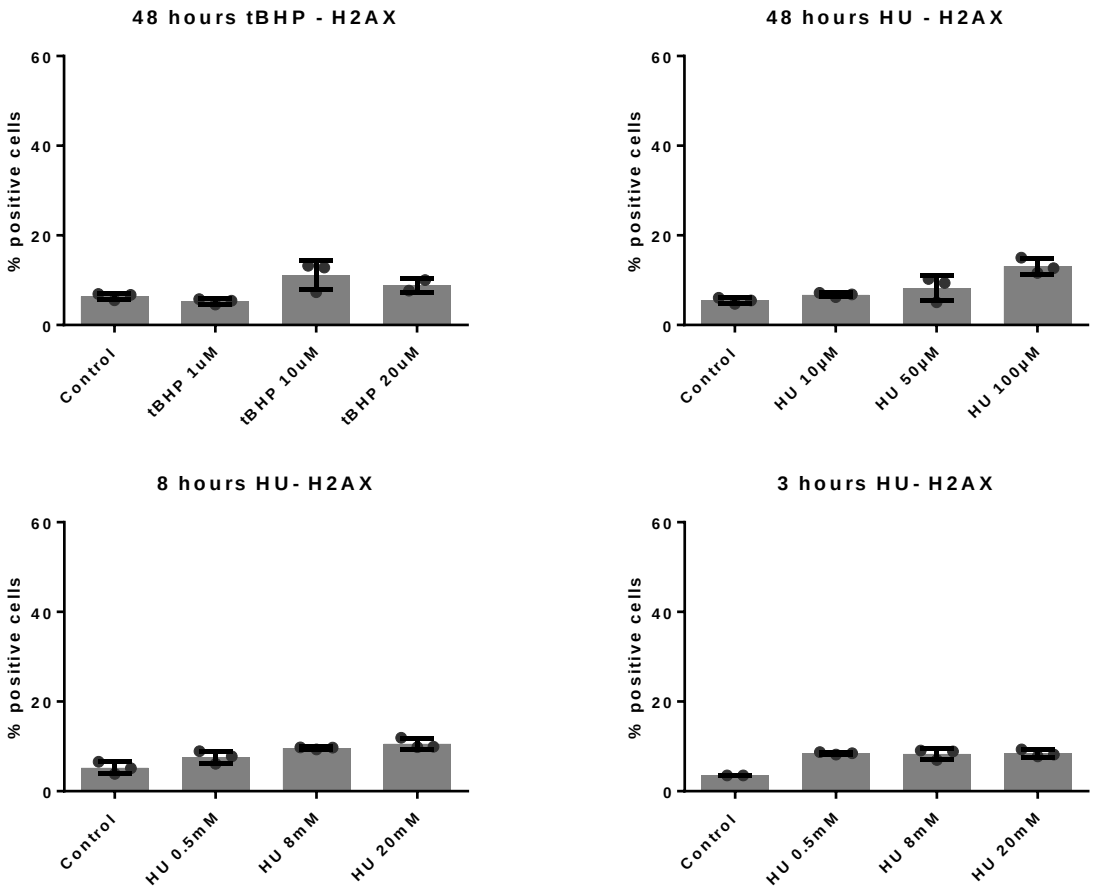

Figure 83 - Differentiation assay: Percentage of H2AX positive cells with varying tert-Butyl hydroperoxide (tBHP) and hydroxyurea (HU) concentrations Graphs showing the resulting percentage of H2AX positive cells following various treatments during the human progenitor cell differentiation assay. The top row shows standard incubation periods of 48 hours. The left graph shows the percentage of H2AX positive cells with increasing tBHP concentrations (1µM, 10µM and 20 µM) compared to controls treated with media only. The graph on the right shows the percentage of H2AX positive cells with increasing HU concentrations (10µM, 50 µM, 100µM). The bottom row shows the percentage of H2AX positive cells following shorter incubation periods with HU; 8-hour incubation on the left and 3-hour incubation on the right. In all cases, cells were not treated during the proliferation assay (72 hours). They were then either washed and treated at the 72 hour timepoint and left to differentiate for a further 7 days or washed at the 72 hour timepoint and allowed to differentiate in media only conditions until treatment 8 or 3 hours prior to fixing. Cells were always fixed 9 days after seeding. Standard deviation is reported as error bars. Each dot represents a technical replicate. 12 technical replicates are shown.

8.3.2.2 Morphology alterations across passages

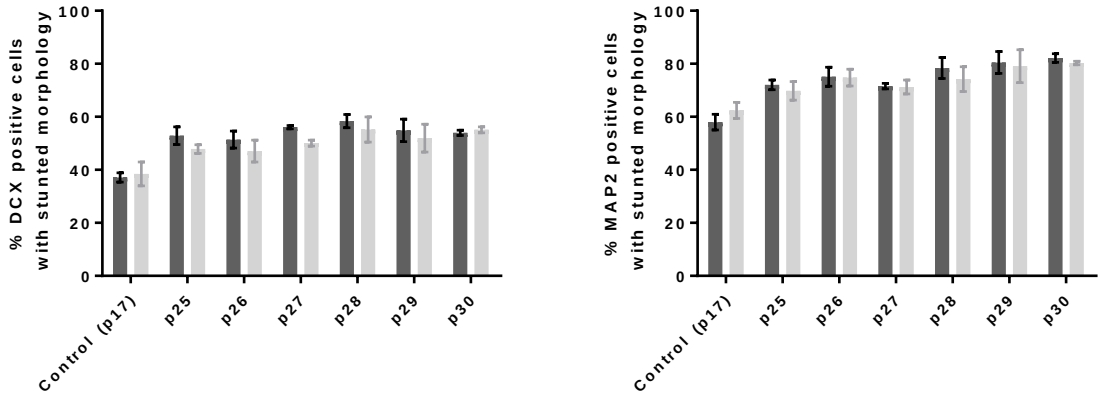

Figure 84 - Morphology of DCX and MAP2 positive cells at different passage number. Differentiation assay results, cells at different passage numbers were incubated in either media only conditions or with 1µM tert-Butyl hydroperoxide (tBHP) + 10µM hydroxyurea (HU) for 48 hours during the proliferation stage and for 7 days during the differentiation stage. Passage numbers included 17 (p17) as a control and several higher passages ranging from passage 25 (p25) to passage 30 (p30). The proportion of cells with a more rounded morphology (stunted) and the proportion of cells with an elongated morphology for each group was quantified by machine learning. Treatment does not appear to have an effect on morphology but higher passage numbers appear to have a greater proportion of stunted cells than lower passage cells. 2 technical replicates, 3 technical replicates. Error bars display standard deviation.

8.3.2.3 Parameters used by machine learning scripts to distinguish between morphology types

Using these scripts above, the following parameters were selected as important in distinguishing between the stunted and elongated morphologies.

The Columbus software used linear classifiers to establish the class of each cell positive for either DCX or MAP2 staining. Briefly, this entails using a set of parameters and pertinent linear coefficients (detailed below) to inform on the most likely class (i.e. stunted or elongated). In both tables, the properties (1st column) are ordered by relevance to the model. The second column shows the linear coefficient for each property used to in the linear classifier models.

MAP2:

Properties (ordered by relevance)	Linear coefficient
Cytoplasm Ratio Width to Length	10.54928
Nucleus Area [µm²]	0.010956
Cytoplasm Width [µm]	-0.10162
Nucleus Roundness	2.345629

DCX:

Properties (ordered by relevance)	Linear Coefficient
Cytoplasm Roundness	3.354727
Cytoplasm Ratio Width to Length	3.403816
Nucleus Roundness	5.174257
Nucleus Area [µm²]	0.004966

8.4 Chapter 5 appendix

8.4.1 Methods

8.4.1.1 Food Frequency Questionnaire

Below are screenshots of the food frequency questionnaires used in the TwinsUK cohort.

1. **YOUR DIET LAST YEAR**

For each food there is an amount shown, either a "medium serving" or a common household unit such as a slice or teaspoon. Please put a tick (✓) in the box to indicate how often, **on average**, you have eaten the specified amount of each food **during the past year**.

EXAMPLES:

For white bread the amount is one slice, so if you ate 4 or 5 slices a day, you should put a tick in the column headed "4-5 per day".

FOODS AND AMOUNTS	AVERAGE USE LAST YEAR								
BREAD AND SAVOURY BISCUITS (one slice or biscuit)	Never or less than once/month	1-3 per month	Once a week	2-4 per week	5-6 per week	Once a day	2-3 per day	4-5 per day	6+ per day
White bread and rolls								✓	

For chips, the amount is a "medium serving", so if you had a helping of chips twice a week you should put a tick in the column headed "2-4 per week".

FOODS AND AMOUNTS	AVERAGE USE LAST YEAR								
POTATOES, RICE AND PASTA (medium serving)	Never or less than once/month	1-3 per month	Once a week	2-4 per week	5-6 per week	Once a day	2-3 per day	4-5 per day	6+ per day
Chips				✓					

For very seasonal fruits such as strawberries and raspberries you should estimate your average use when the fruits are in season, so if you ate strawberries or raspberries about once a week when they were in season you should put a tick in the column headed "once a week"

FOODS AND AMOUNTS	AVERAGE USE LAST YEAR								
FRUIT (1 fruit or medium serving)	Never or less than once/month	1-3 per month	Once a week	2-4 per week	5-6 per week	Once a day	2-3 per day	4-5 per day	6+ per day
Strawberries, raspberries, kiwi fruit			✓						

Please estimate your average food use as best you can, and please answer every question - do not leave ANY lines blank. PLEASE PUT A TICK (✓) ON EVERY LINE

FOODS AND AMOUNTS	AVERAGE USE LAST YEAR								
MEAT AND FISH (medium serving)	Never or less than once/month	1-3 per month	Once a week	2-4 per week	5-6 per week	Once a day	2-3 per day	4-5 per day	6+ per day
Beef: roast, steak, mince, stew or casserole									
Beefburgers									
Pork: roast, chops, stew or slices									
Lamb: roast, chops or stew									
Chicken or other poultry eg. turkey									
Bacon									
Ham									
Corned beef, Spam, luncheon meats									
Sausages									
Savoury pies, eg. meat pie, pork pie, pasties, steak & kidney pie, sausage rolls									
Liver, liver paté, liver sausage									
Fried fish in batter, as in fish and chips									
Fish fingers, fish cakes									
Other white fish, fresh or frozen, eg. cod, haddock, plaice, sole, halibut									
Oily fish, fresh or canned, eg. mackerel, kippers, tuna, salmon, sardines, herring									
Shellfish, eg. crab, prawns, mussels									
Fish roe, taramasalata									
	Never or less than once/month	1-3 per month	Once a week	2-4 per week	5-6 per week	Once a day	2-3 per day	4-5 per day	6+ per day

Please check that you have a tick (✓) on EVERY line

PLEASE PUT A TICK (✓) ON EVERY LINE

FOODS AND AMOUNTS	AVERAGE USE LAST YEAR								
BREAD AND SAVOURY BISCUITS (one slice or biscuit)	Never or less than once/month	1-3 per month	Once a week	2-4 per week	5-6 per week	Once a day	2-3 per day	4-5 per day	6+ per day
White bread and rolls									
Brown bread and rolls									
Wholemeal bread and rolls									
Cream crackers, cheese biscuits									
Crispbread, eg. Ryvita									
CEREALS (one bowl)									
Porridge, Readybrek									
Breakfast cereal such as cornflakes, muesli etc.									
POTATOES, RICE AND PASTA (medium serving)									
Boiled, mashed, instant or jacket potatoes									
Chips									
Roast potatoes									
Potato salad									
White rice									
Brown rice									
White or green pasta, eg. spaghetti, macaroni, noodles									
Wholemeal pasta									
Lasagne, moussaka									
Pizza									
	Never or less than once/month	1-3 per month	Once a week	2-4 per week	5-6 per week	Once a day	2-3 per day	4-5 per day	6+ per day

Please check that you have a tick (✓) on EVERY line

PLEASE PUT A TICK (✓) ON EVERY LINE

FOODS AND AMOUNTS	AVERAGE USE LAST YEAR								
DAIRY PRODUCTS AND FATS	Never or less than once/month	1-3 per month	Once a week	2-4 per week	5-6 per week	Once a day	2-3 per day	4-5 per day	6+ per day
Single or sour cream (tablespoon)									
Double or clotted cream (tablespoon)									
Low fat yogurt, fromage frais (125g carton)									
Full fat or Greek yogurt (125g carton)									
Dairy desserts (125g carton)									
Cheese, eg. Cheddar, Brie, Edam (medium serving)									
Cottage cheese, low fat soft cheese (medium serving)									
Eggs as boiled, fried, scrambled, etc. (one)									
Quiche (medium serving)									
Low calorie, low fat salad cream(tablespoon)									
Salad cream, mayonnaise (tablespoon)									
French dressing (tablespoon)									
Other salad dressing (tablespoon)									
The following on bread or vegetables									
Butter (teaspoon)									
Block margarine, eg. Stork, Krona (teaspoon)									
Polyunsaturated margarine (tub), eg. Flora, sunflower (teaspoon)									
Other soft margarine,dairy spreads (tub), eg. Blue Band, Clover (teaspoon)									
Low fat spread (tub), eg. Outline, Gold (teaspoon)									
Very low fat spread (tub) (teaspoon)									
	Never or less than once/month	1-3 per month	Once a week	2-4 per week	5-6 per week	Once a day	2-3 per day	4-5 per day	6+ per day

Please check that you have a tick (✓) on EVERY line

PLEASE PUT A TICK (✓) ON EVERY LINE

FOODS AND AMOUNTS	AVERAGE USE LAST YEAR								
SWEETS AND SNACKS (medium serving)	Never or less than once/month	1-3 per month	Once a week	2-4 per week	5-6 per week	Once a day	2-3 per day	4-5 per day	6+ per day
Sweet biscuits, chocolate , eg. digestive (one)									
Sweet biscuits, plain, eg. Nice, ginger (one)									
Cakes eg. fruit, sponge, home baked									
Cakes eg. fruit, sponge, ready made									
Buns, pastries eg. scones, flapjacks, home baked									
Buns, pastries eg. croissants, doughnuts, ready made									
Fruit pies, tarts, crumbles, home baked									
Fruit pies, tarts, crumbles, ready made									
Sponge puddings, home baked									
Sponge puddings, ready made									
Milk puddings, eg. rice, custard, trifle									
Ice cream, choc ices									
Chocolates, single or squares									
Chocolate snack bars eg. Mars, Crunchie									
Sweets, toffees, mints									
Sugar added to tea, coffee, cereal (teaspoon)									
Crisps or other packet snacks, eg. Wotsits									
Peanuts or other nuts									
SOUPS, SAUCES, AND SPREADS									
Vegetable soups (bowl)									
Meat soups (bowl)									
Sauces, eg. white sauce, cheese sauce, gravy (tablespoon)									
Tomato ketchup (tablespoon)									
Pickles, chutney (tablespoon)									
Marmite, Bovril (teaspoon)									
Jam, marmalade, honey (teaspoon)									
Peanut butter (teaspoon)									
	Never or less than once/month	1-3 per month	Once a week	2-4 per week	5-6 per week	Once a day	2-3 per day	4-5 per day	6+ per day

Please check that you have a tick (✓) on EVERY line

PLEASE PUT A TICK (✓) ON EVERY LINE

FOODS AND AMOUNTS	AVERAGE USE LAST YEAR								
DRINKS	Never or less than once/month	1-3 per month	Once a week	2-4 per week	5-6 per week	Once a day	2-3 per day	4-5 per day	6+ per day
Tea (cup)									
Coffee, instant or ground (cup)									
Coffee, decaffeinated (cup)									
Coffee whitener, eg. Coffee-mate (teaspoon)									
Cocoa, hot chocolate (cup)									
Horlicks, Ovaltine (cup)									
Wine (glass)									
Beer, lager or cider (half pint)									
Port, sherry, vermouth, liqueurs (glass)									
Spirits, eg. gin, brandy, whisky, vodka (single)									
Low calorie or diet fizzy soft drinks (glass)									
Fizzy soft drinks, eg. Coca cola, lemonade (glass)									
Pure fruit juice (100%) eg. orange, apple juice (glass)									
Fruit squash or cordial (glass)									
FRUIT **For seasonal fruits marked *, please estimate your average use when the fruit is in season**									
Apples (1 fruit)									
Pears (1 fruit)									
Oranges, satsumas, mandarins (1 fruit)									
Grapefruit (half)									
Bananas (1 fruit)									
Grapes (medium serving)									
Melon (1 slice)									
* Peaches, plums, apricots (1 fruit)									
* Strawberries, raspberries, kiwi fruit (medium serving)									
Tinned fruit (medium serving)									
Dried fruit, eg. raisins, prunes (medium serving)									
	Never or less than once/month	1-3 per month	Once a week	2-4 per week	5-6 per week	Once a day	2-3 per day	4-5 per day	6+ per day

Please check that you have a tick (✓) on EVERY line

PLEASE PUT A TICK (✓) ON EVERY LINE

FOODS AND AMOUNTS	AVERAGE USE LAST YEAR								
VEGETABLES Fresh, frozen or tinned (medium serving)	Never or less than once/month	1-3 per month	Once a week	2-4 per week	5-6 per week	Once a day	2-3 per day	4-5 per day	6+ per day
Carrots									
Spinach									
Broccoli, spring greens, kale									
Brussels sprouts									
Cabbage									
Peas									
Green beans, broad beans, runner beans									
Marrow, courgettes									
Cauliflower									
Parsnips, turnips, swedes									
Leeks									
Onions									
Garlic									
Mushrooms									
Sweet peppers									
Beansprouts									
Green salad, lettuce, cucumber, celery									
Watercress									
Tomatoes									
Sweetcorn									
Beetroot									
Coleslaw									
Avocado									
Baked beans									
Dried lentils, beans, peas									
Tofu , soya meat, TVP, Vegeburger									
	Never or less than once/month	1-3 per month	Once a week	2-4 per week	5-6 per week	Once a day	2-3 per day	4-5 per day	6+ per day

Please check that you have a tick (✓) on EVERY line

YOUR DIET LAST YEAR, continued

2. Are there any **OTHER** foods which you ate more than once a week? Yes ☐ No ☐

If yes, please list below

Food	Usual serving size	Number of times eaten each week

3. What type of milk did you most often use?

Select one only

Full cream, silver ☐ Semi-skimmed, red/white ☐
Skimmed/blue ☐ Channel Islands, gold ☐
Dried milk ☐ Soya ☐
Other, *specify* ☐ None ☐

4. How much milk did you drink each day, including milk with tea, coffee, cereals etc?

None ☐ Three quarters of a pint ☐
Quarter of a pint ☐ One pint ☐
Half a pint ☐ More than one pint ☐

5. Did you usually eat breakfast cereal (excluding porridge and Ready Brek mentioned earlier)? Yes ☐ No ☐

If yes, which brand and type of breakfast cereal, including muesli, did you usually eat?
List the one or two types most often used

Brand *e.g. Kellogg's*	Type *e.g. cornflakes*

6. What kind of fat did you most often use for frying, roasting, grilling etc?

Select one only

Butter ☐ Solid vegetable fat ☐
Lard/dripping ☐ Margarine ☐
Vegetable oil ☐ None ☐

If you used vegetable oil, please give type eg. corn, sunflower ☐

7. What kind of fat did you most often use for baking cakes etc?

Select one only

Butter ☐ Solid vegetable fat ☐
Lard/dripping ☐ Margarine ☐
Vegetable oil ☐ None ☐

If you used margarine, please give name or type eg. Flora, Stork ☐

8. How often did you eat food that was fried at home?

Daily ☐ 1-3 times a week ☐ 4-6 times a week ☐
Less than once a week ☐ Never ☐

9. How often did you eat fried food away from home?

Daily ☐ 1-3 times a week ☐ 4-6 times a week ☐
Less than once a week ☐ Never ☐

10. What did you do with the visible fat on your meat?

Ate most of the fat ☐ Ate as little as possible ☐
Ate some of the fat ☐ Did not eat meat ☐

11. How often did you eat grilled or roast meat? ☐☐ times a week

12. How well cooked did you usually have grilled or roast meat?

Well done /dark brown ☐ Lightly cooked/rare ☐
Medium ☐ Did not eat meat ☐

13. How often did you add salt to food while cooking?

Always ☐ Rarely ☐
Usually ☐ Never ☐
Sometimes ☐

14. How often did you add salt to any food at the table?

Always ☐ Rarely ☐
Usually ☐ Never ☐
Sometimes ☐

15. Did you regularly use a salt substitute (eg LoSalt)? Yes ☐ No ☐

If yes, which brand? ☐

16. During the course of last year, on average, how many times a week did you eat the following foods?

Food type	**Times/week**	**Portion size**
Vegetables (not including potatoes)	☐☐	medium serving
Salads	☐☐	medium serving
Fruit and fruit products (not including fruit juice)	☐☐	medium serving or 1 fruit
Fish and fish products	☐☐	medium serving
Meat, meat products and meat dishes (including bacon, ham and chicken)	☐☐	medium serving

17. Have you taken any vitamins, minerals, fish oils, fibre or other food supplements during the past year? Yes ☐ No ☐ Don't know ☐

If yes, please complete the table below. If you have taken more than 5 types of supplement please put the most frequently consumed brands first.

Vitamin supplements	**Average frequency** Tick **one** box per line to show how often on average you consumed supplements									
Name and brand Please list full name, **brand** and strength	**Dose** Please state number of pills, capsules or teaspoons consumed	Never or less than once a month	1-3 per month	Once a week	2-4 per week	5-6 per week	Once a day	2-3 per day	4-5 per day	6+ per day

8.4.1.2 IPAQ questionnaire

Below if the questionnaire used to assess physical activity levels in the TwinsUK cohort.

INTERNATIONAL PHYSICAL ACTIVITY QUESTIONNAIRE

We are interested in finding out about the kinds of physical activities that people do as part of their everyday lives. The questions will ask you about the time you spent being physically active in the **last 7 days**. Please answer each question even if you do not consider yourself to be an active person. Please think about the activities you do at work, as part of your house and yard work, to get from place to place, and in your spare time for recreation, exercise or sport.

Think about all the **vigorous** activities that you did in the **last 7 days**. **Vigorous** physical activities refer to activities that take hard physical effort and make you breathe much harder than normal. Think *only* about those physical activities that you did for at least 10 minutes at a time.

1. During the **last 7 days**, on how many days did you do **vigorous** physical activities like heavy lifting, digging, aerobics, or fast bicycling?

   _____ **days per week**

   ☐ No vigorous physical activities → ***Skip to question 3***

2. How much time did you usually spend doing **vigorous** physical activities on one of those days?

   _____ **hours per day**

   _____ **minutes per day**

   ☐ Don't know/Not sure

Think about all the **moderate** activities that you did in the **last 7 days**. **Moderate** activities refer to activities that take moderate physical effort and make you breathe somewhat harder than normal. Think only about those physical activities that you did for at least 10 minutes at a time.

3. During the **last 7 days**, on how many days did you do **moderate** physical activities like carrying light loads, bicycling at a regular pace, or doubles tennis? Do not include walking.

   _____ **days per week**

   ☐ No moderate physical activities → ***Skip to question 5***

SHORT LAST 7 DAYS SELF-ADMINISTERED version of the IPAQ. Revised August 2002.

8.4.2 Results

8.4.2.1 Assessing normality, heteroscedasticity and the presence of outliers in lifestyle variables

Frequency distribution, residual vs fitted, quantile-quantile (Q-Q), scale-location and residual vs leverage plots of the residuals obtained from the correlation between Kcal and PAL (**Figure 85**), HEI and PAL (**Figure 86**) and IPAQ and PAL (**Figure 87**).

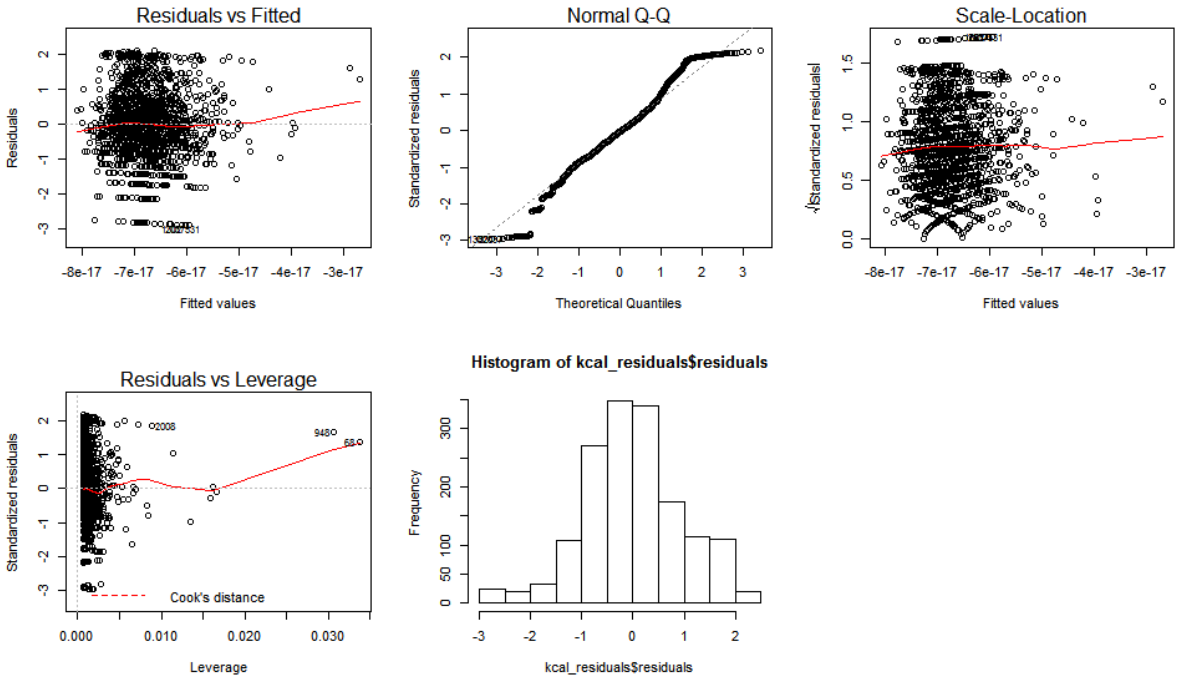

Figure 85 - Frequency distribution, residual vs fitted, quantile-quantile (Q-Q), scale-location and residual vs leverage plots of the residuals obtained from the correlation between Kcal and Paired Associates Learning (PAL)

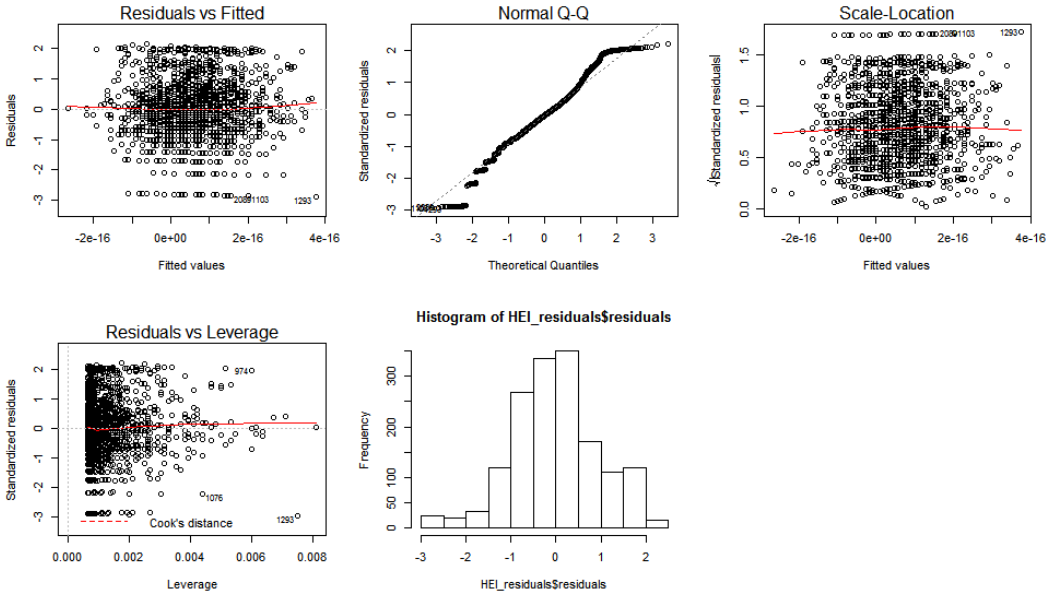

Figure 86 - Frequency distribution, residual vs fitted, quantile-quantile (Q-Q), scale-location and residual vs leverage plots of the residuals obtained from the correlation between healthy eating and Paired Associates Learning (PAL)

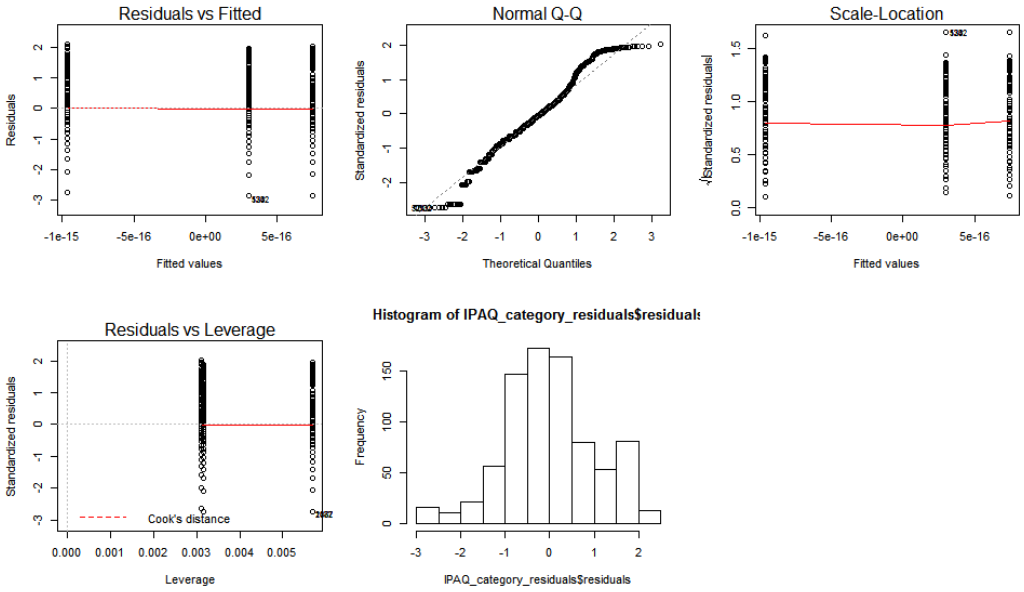

Figure 87 - Frequency distribution, residual vs fitted, quantile-quantile (Q-Q), scale-location and residual vs leverage plots of the residuals obtained from the correlation between physical activity and Paired Associates Learning (PAL)

8.4.2.2 Tag SNPs

All raw and selected tag SNPs are reported in an excel file that can be found at:

https://drive.google.com/open?id=1vjZzFTSciEYpeIvuPGpNqCl8Gv40S5uY

8.4.2.3 Results of associations between 482 tag SNPs and paired associates learning

All results from the association between the 482 tag SNPs and PAL can be found at:

https://drive.google.com/open?id=1SU_Skzh6-a4Vw1ee-N33isxZD74uGxNg

8.4.2.4 Sensitivity analysis to compare methodologies

Below are the results of the analyses used as sensitivity analysis to select the cluster method to account for relatedness within our cohort. **Table 44** shows the 5 most significant SNPs when the analysis was carried out after averaging the values of each MZ twin pair and **Table 45** shows the results of the analysis when only one of each MZ twin pair was used in the analysis. For both tables, the 2 significant SNPs highlighted by the analysis carried out in section 5.3.5 are in bold. In both other methods, similar SNPs are highlighted suggesting all methods are valid, the cluster method was selected as it provided more power.

SNP	β coefficient	L95	U95	p value	n
rs497849 (SIRT1)	0.18	0.10	0.26	0.00002	992
rs2343401 (IGF2r)	-0.14	-0.22	-0.06	0.0004	835
rs782431 (ABTB1)	0.13	0.06	0.20	0.0005	984
rs7358173 (PTEN)	0.13	0.06	0.21	0.0007	842
rs9700237 (mTOR)	-0.16	-0.25	-0.07	0.0008	663

T**able 44 - Table showing the results for the model testing SNPs for association to PAL errors after averaging of all datapoints of each Mz twin pair.** β coefficient, lower (L95) and upper (U95) confidence intervals, unadjusted p value, number of people (n) and adjusted p value (adjusted p) following Benjamini-Hochberg correction for each linear model are reported. The candidate gene closest to the SNP being tested is reported in brackets in the first column.

SNP	β coefficient	L95	U95	p value	n
rs497849 (SIRT1)	0.16	0.08	0.25	0.000188	992
rs782431 (ABTB1)	0.13	0.06	0.21	0.00054	984
rs7072702 (PTEN)	0.13	0.05	0.21	0.000869	992
rs2594290(mTOR)	0.23	0.09	0.37	0.001184	971
rs2720231 (ABTB1)	0.12	0.05	0.20	0.001542	975

Table 45 - Table showing the results for the model testing SNPs for association to PAL errors after one twin from each MZ twin pair. β coefficient, lower (L95) and upper (U95) confidence intervals, unadjusted p value, number of people (n) and adjusted p value (adjusted p) following Benjamini-Hochberg correction for each linear model are reported. The candidate gene closest to the SNP being tested is reported in brackets in the first column.

8.4.2.5 No association between genotype and lifestyle factors

As discussed in section 5.3.6, there were no significant interactions between genotype and healthy eating or genotype and calorie intake. Below are the 5 SNPs with the most significant interaction with healthy eating (Table 46) and calorie intake (**Table 47)** though as shown, none survived correction for multiple testing.

SNP * HEI	β coefficient	p value	n	Adjusted p
rs75033338 (GRB10)	0.02	0.00121	1158	0.582
rs2044859 (GRB10)	-0.01	0.00448	1161	0.617
rs4947968 (GRB10)	0.01	0.00584	1161	0.617
rs220722 (IGF2R)	-0.02	0.01073	1165	0.617
rs3120821 (mTOR)	-0.01	0.01294	1114	0.617

Table 46 - Table showing the interaction results between healthy eating and genotype on PAL score effect. β coefficient, unadjusted p value, number of people (n) and adjusted p value (adjusted p) following Benjamini-Hochberg correction for the 5 most significant interactions are reported. The candidate gene closest to the SNP being tested is reported in brackets in the first column.

SNP * KCAL	β coefficient	p value	n	Adjusted p
rs61560478 (mTOR)	-0.00023	0.00139	1138	0.492
rs7635934 (ABTB1)	0.00021	0.00293	1165	0.492
rs3758932 (UCP2)	0.00020	0.00515	1151	0.492
rs10953493 (NAMPT)	-0.00016	0.0065	1133	0.492
rs3773155 (ABTB1)	0.00021	0.00738	1163	0.492

Table 47 - Table showing the interaction results between calorie intake and genotype on PAL score effect. β coefficient, unadjusted p value, number of people (n) and adjusted p value (adjusted p) following Benjamini-Hochberg correction for the 5 most significant interactions are reported. The candidate gene closest to the SNP being tested is reported in brackets in the first column